ENERGYPLUS™

EnergyPlus Engineering Document

The Reference to EnergyPlus Calculations

(in case you want or need to know)

Date: November 13, 2002

TABLE OF CONTENTS

TABLE OF CONTENTS

TABLE OF CONTENTS

TABLE OF CONTENTS

TABLE OF CONTENTS

TABLE OF CONTENTS

TABLE OF CONTENTS

TABLE OF CONTENTS

TABLE OF CONTENTS

TABLE OF CONTENTS

TABLE OF CONTENTS

TABLE OF CONTENTS

TABLE OF CONTENTS

TABLE OF CONTENTS

TABLE OF CONTENTS

TABLE OF CONTENTS

TABLE OF CONTENTS

Overview

The EnergyPlus program is a collection of many program modules that work together to calculate the energy required for heating and cooling a building using a variety of systems and energy sources. It does this by simulating the building and associated energy systems when they are exposed to different environmental and operating conditions. The core of the simulation is a model of the building that is based on fundamental heat balance principles. Since it is relatively meaningless to state: "based on fundamental heat balance principles", the model will be described in greater detail in later sections of this document in concert with the FORTRAN code which is used to describe the model. It turns out that the model itself is relatively simple compared with the data organization and control that is needed to simulate the great many combinations of system types, primary energy plant arrangements, schedules, and environments. The next section shows this overall organization in schematic form. Later sections will expand on the details within the blocks of the schematic.
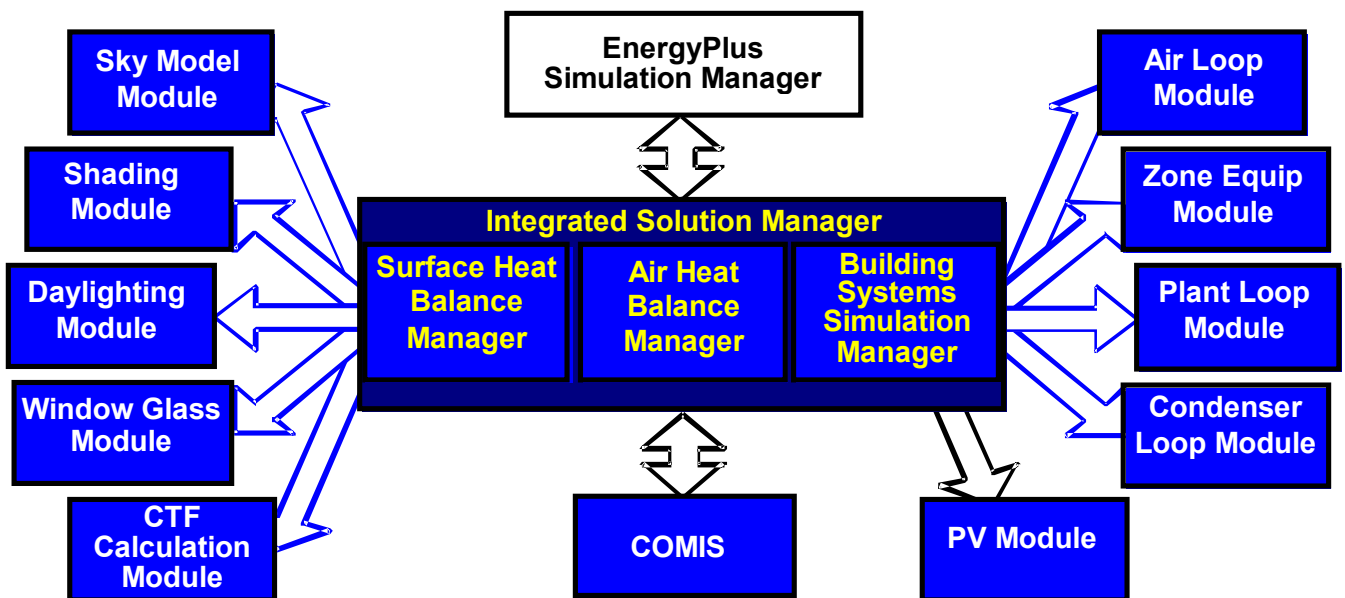
Figure 1. EnergyPlus Program Schematic.

Simulation Manager

The simulation manager of EnergyPlus is contained in a single module. The main subroutine is shown below. Flow within the entire program is managed using a series of flags. These paired flags, in order (from the highest to the lowest) are:

Table 1. Simulation Flags

Begin SimulationFlag	End SimulationFlag
BeginEnvironmentFlag	EndEnvironmentFlag(one to many days)
BeginDayFlag	EndDayFlag
BeginHourFlag	EndHourFlag
BeginTimeStepFlag	EndTimeStepFlag

There is also a WarmupFlag to signal that the program is in warmup state.

The operation of these flags can be seen in the subroutine. The advantage of using the flag system is that any subroutine throughout the code can determine the exact state of the simulation by checking the status of the flags.

```
*********************************************
SUBROUTINE ManageSimulation     ! Main driver routine for this module
BeginSimFlag = .TRUE.
  EndSimFlag = .FALSE.
  CALL OpenOutputFiles
  CALL GetProjectData
  CALL GetEnvironmentInfo                 ! Get the number and type of Environments
  CALL SetupTimePointers('Zone',TimeStepZone)  ! Set up Time pointer for HB/Zone Simulation
  Call SetupTimePointers('HVAC',TimeStepSys)
  DO Envrn = 1, NumOfEnvrn        ! Begin environment loop ...
    BeginEnvrnFlag = .TRUE.
    EndEnvrnFlag   = .FALSE.
    WarmupFlag     = .TRUE.
    DayOfSim       =  0
      DO WHILE ((DayOfSim.LT.NumOfDayInEnvrn).OR.(WarmupFlag))  ! Begin day loop ...

      DayOfSim     = DayOfSim + 1
      BeginDayFlag = .TRUE.
      EndDayFlag   = .FALSE.
      IF (WarmupFlag) THEN
        CALL DisplayString('Warming up')
      ELSE ! (.NOT.WarmupFlag)
        IF (DayOfSim.EQ.1)   CALL DisplayString('Performing Simulation')
      END IF
      DO HourOfDay = 1, 24      ! Begin hour loop ...
        BeginHourFlag = .TRUE.
        EndHourFlag   = .FALSE.
          DO TimeStep = 1, NumOfTimeStepInHour  ! Begin time step (TINC) loop ...
          BeginTimeStepFlag = .TRUE.
          EndTimeStepFlag   = .FALSE.
          ! Set the End__Flag variables to true if necessary.  Note that
          ! each flag builds on the previous level.  EndDayFlag cannot be
          ! .true. unless EndHourFlag is also .true., etc.  Note that the
          ! EndEnvrnFlag and the EndSimFlag cannot be set during warmup.
          ! Note also that BeginTimeStepFlag, EndTimeStepFlag, and the
          ! SubTimeStepFlags can/will be set/reset in the HVAC Manager.
          IF ((TimeStep.EQ.NumOfTimeStepInHour)) THEN
            EndHourFlag = .TRUE.
            IF (HourOfDay.EQ.24) THEN
              EndDayFlag = .TRUE.
              IF ((.NOT.WarmupFlag).AND.(DayOfSim.EQ.NumOfDayInEnvrn)) THEN
                EndEnvrnFlag = .TRUE.
                IF (Envrn.EQ.NumOfEnvrn) THEN
                  EndSimFlag = .TRUE.
                END IF
              END IF
            END IF
          END IF
          CALL ManageWeather

          CALL ManageHeatBalance
          BeginHourFlag  = .FALSE.
          BeginDayFlag   = .FALSE.
          BeginEnvrnFlag = .FALSE.
          BeginSimFlag   = .FALSE.
        END DO                            ! ... End time step (TINC) loop.
      END DO                    ! ... End hour loop.
    END DO                  ! ... End day loop.
  END DO                  ! ... End environment loop.
  CALL CloseOutputFiles
  RETURN
END SUBROUTINE ManageSimulation
```

Integrated Solution Manager

EnergyPlus is an integrated simulation. This means that all three of the major parts, building, system, and plant, must be solved simultaneously. In programs with sequential simulation, such as BLAST or DOE-2, the building zones, air handling systems, and central plant equipment are simulated sequentially with no feedback from one to the other. The sequential solution begins with a zone heat balance that updates the zone conditions and determines the heating/cooling loads at all time steps. This information is fed to the air handling simulation to determine the system response; but that response does not affect zone conditions. Similarly, the system information is passed to the plant simulation without feedback. This simulation technique works well when the system response is a well-defined function of the air temperature of the conditioned space. For a cooling situation, a typical supply and demand situation is shown schematically in the figure below. Here, the operating point is at the intersection of the supply and demand curves.
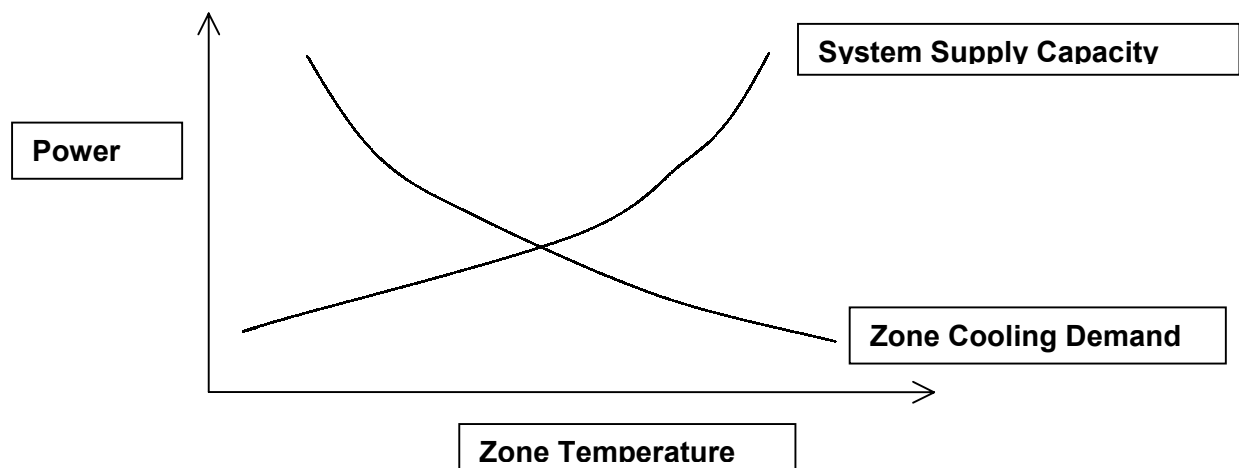
Figure 2. Sequential Simulation Supply/Demand Relationship.

However, in most situations the system capacity is dependent on outside conditions and/or other parameters of the conditioned space. The simple supply and demand situation above becomes a more complex relationship and the system curve is not fixed. The solution should move up and down the demand curve. This doesn't happen in sequential simulation methods and the lack of feedback from the system to the building can lead to nonphysical results. For example, if the system provides too much cooling to a conditioned space the excess is reported by the program as "overcooling". Other categories of unmatched loads exist and are similarly reported by the program. While this kind of reporting enables the affected system or plant components to be properly sized, the system designer would, in most cases, prefer to see the actual change in zone temperature. The same mismatches can occur between the system and plant simulations when they are simulated sequentially.

To obtain a simulation that is physically realistic, the elements have to be linked in a simultaneous solution scheme. The entire integrated program can be represented as a series of functional elements connected by fluid loops as shown in Figure "Schematic of Simultaneous Solution Scheme". In EnergyPlus all the elements are integrated and controlled by the Integrated Solution Manager. The loops are divided into supply and demand sides, and the solution scheme generally relies on successive substitution iteration to reconcile supply and demand using the Gauss-Seidell philosophy of continuous updating.
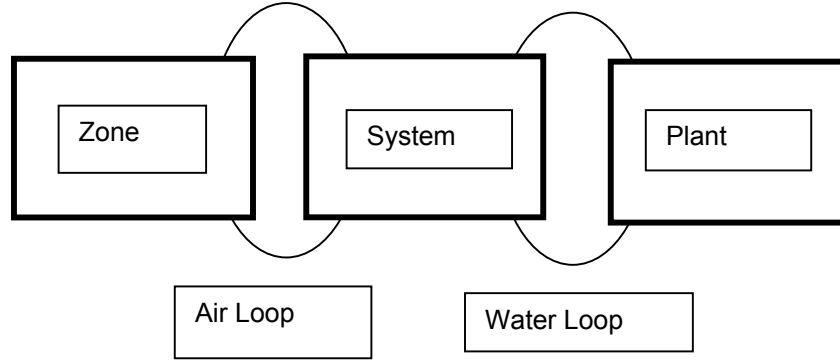
Figure 3. Schematic of Simultaneous Solution Scheme

In the sections which follow, the various individual functions of the integrated solution will be described.

Basis for the Zone and System Integration

The basis for the zone and system integration, Taylor.(1990, 1991), incorporates a shortened simulation time step, typically to between 0.1 and 0.25 hours, and uses a time-marching method having the zone conditions lagged by one time step. The error associated with this approach depends significantly on the time step. The smaller the step size the smaller the error, but the longer the computation time. To permit increasing the time step as much as possible while retaining stability, zone air capacity was also introduced into the heat balance. The resulting method is called "lagging with zone capacitance".   Although requiring substantially more time to execute than sequential simulation methods, the improved realism of the simultaneous solution of loads, systems and plants simulation is desirable.   This method was fully implemented in the program IBLAST (Integrated Building Loads Analysis and System Thermodynamics) (Taylor 1996) that was used as a basis for EnergyPlus.

The method of lagging with zone capacitance uses information from previous time steps to predict system response and update the zone temperature at the current time.   In older sequential programs, one hour is used frequently as a time step because it is convenient for record keeping purposes and it keeps computation time reasonable. But dynamic processes in the zone air can occur on a much shorter time scale than one hour. The time constant, τ , for a zone is on the order of:

$$\tau \approx \frac{\rho V c_p}{\left| \dot{Q}_{load} + \dot{Q}_{sys} \right|} \tag{1.1}$$

where the numerator is the zone air heat capacitance and the denominator is the net rate of heat energy input. Clearly, the value of τ can vary because the zone load and system output change throughout the simulation. Therefore, a variable adaptive time step shorter than one hour is used for updating the system conditions. For stability reasons it was necessary to derive an equation for the zone temperature that included the unsteady zone capacitance term and to identify methods for determining the zone conditions and system response at successive time steps. The formulation of the solution scheme starts with a heat balance on the zone.

$$C_z \frac{dT_z}{dt} = \sum_{i=1}^{N_{sl}} \dot{Q}_i + \sum_{i=1}^{N_{surfaces}} h_i A_i \left(T_{si} - T_z \right) + \sum_{i=1}^{N_{zones}} \dot{m}_i C_p \left(T_{zi} - T_z \right) + \dot{m}_{inf} C_p \left(T_\infty - T_z \right) + \dot{Q}_{sys} \tag{1.2}$$

where:

$\sum_{i=1}^{N_{sl}} \dot{Q}_i$ = sum of the convective internal loads

$\sum_{i=1}^{N_{surfaces}} h_i A_i \left(T_{si} - T_z \right)$ = convective heat transfer from the zone surfaces

$\dot{m}_{inf} C_p \left(T_\infty - T_z \right)$ = heat transfer due to infiltration of outside air

$\sum_{i=1}^{N_{zones}} \dot{m}_i C_p \left(T_{zi} - T_z \right)$ = heat transfer due to interzone air mixing

$\dot{Q}_{sys}$ = system output.

$C_z \dfrac{dT_z}{dt}$ = energy stored in zone air

If the air capacitance is neglected, the steady state system output must be:

$$\dot{Q}_{sys} = \sum_{i=1}^{N_{sl}} \dot{Q}_i + \sum_{i=1}^{N_{surfaces}} h_i A_i \left(T_{si} - T_z \right) + \sum_{i=1}^{N_{zones}} \dot{m}_i C_p \left(T_{zi} - T_z \right) + \dot{m}_{inf} C_p \left(T_\infty - T_z \right) \tag{1.3}$$

Air systems provide hot or cold air to the zones to meet heating or cooling loads. The system energy provided to the zone, $\dot{Q}_{sys}$, can thus be formulated from the difference between the supply air enthalpy and the enthalpy of the air leaving the zone as in Equation (1.4):

$$\dot{Q}_{sys} = \dot{m}_{sys} C_p \left(T_{sup} - T_z \right) \tag{1.4}$$

This equation assumes that the zone supply air mass flow rate is exactly equal to the sum of the air flow rates leaving the zone through the system return air plenum and being exhausted directly from the zone. Both air streams exit the zone at the zone mean air temperature. The result of substituting Equation (1.4) for $\dot{Q}_{sys}$ in the heat balance Equation (1.2) is shown in Equation (1.5):

$$C_z \frac{dT_z}{dt} = \sum_{i=1}^{N_{sl}} \dot{Q}_i + \sum_{i=1}^{N_{surfaces}} h_i A_i \left(T_{si} - T_z \right) + \sum_{i=1}^{N_{zones}} \dot{m}_i C_p \left(T_{zi} - T_z \right)$$
$$+ \dot{m}_{inf} C_p \left(T_\infty - T_z \right) + \dot{m}_{sys} C_p \left(T_{sup} - T_z \right) \tag{1.5}$$

The sum of zone loads and system output now equals the change in energy stored in the zone. Typically, the capacitance C_z would be that of the zone air only. However, thermal masses assumed to be in equilibrium with the zone air could be included in this term. In order to calculate the derivative term a finite difference approximation may be used, such as:

$$\frac{dT}{dt} = \left(\delta t \right)^{-1} \left(T_z^t - T_z^{t-\delta t} \right) + O\left(\delta t \right) \tag{1.6}$$

The use of numerical integration in a long time simulation is a cause for some concern due to the potential build-up of truncation error over many time steps. In this case, the finite difference approximation is of low order which further aggravates the problem. However, the

cyclic nature of building energy simulations should cause truncation errors to cancel over each daily cycle so that no net accumulation of error occurs, even over many days of simulation (Walton, 1990). The Euler formula, Equation (1.6), was employed in Equation (1.5) to replace the derivative term. All the terms containing the zone mean air temperature were then grouped on the left hand side of the equation. Since the remaining terms are not known at the current time, they were lagged by one time step and collected on the right hand side. This manipulation resulted in Equation (1.7), the formula for updating the zone mean air temperature:

$$
C_z \frac{T_z^t - T_z^{t-\delta t}}{dt} + T_z^t \left(\sum_{i=1}^{N_{surfaces}} h_i A_i + \sum_{i=1}^{N_{zones}} \dot{m}_i C_p + \dot{m}_{inf} C_p + \dot{m}_{sys} C_p \right) =
$$

$$
\sum_{i=1}^{N_{sl}} \dot{Q}_i^t + \dot{m}_{sys} C_p T_{supply}^t + \left(\sum_{i=1}^{N_{surfaces}} h_i A_i T_{si} + \sum_{i=1}^{N_{zones}} \dot{m}_i C_p T_{zi} + \dot{m}_{inf} C_p T_\infty \right)^{t-\delta t}
\qquad (1.7)
$$

One final rearrangement was to move the lagged temperature in the derivative approximation to the right side of the equation. The explicit appearance of the zone air temperature was thus eliminated from one side of the equation. An energy balance equation that includes the effects of zone capacitance was then obtained by dividing both sides by the coefficient of T_z:

$$
T_z^t = \frac{\displaystyle\sum_{i=1}^{N_{sl}} \dot{Q}_i^t + \dot{m}_{sys} C_p T_{supply}^t + \left(C_z \frac{T_z}{\delta t} + \sum_{i=1}^{N_{surfaces}} h_i A_i T_{si} + \sum_{i=1}^{N_{zones}} \dot{m}_i C_p T_{zi} + \dot{m}_{inf} C_p T_\infty \right)^{t-\delta t}}{\dfrac{C_z}{\delta t} + \left(\displaystyle\sum_{i=1}^{N_{surfaces}} h_i A_i + \sum_{i=1}^{N_{zones}} \dot{m}_i C_p + \dot{m}_{inf} C_p + \dot{m}_{sys} C_p \right)}
\qquad (1.8)
$$

Equation (1.8) could be used to estimate zone temperatures, however it was found to severely limit the time step size under some conditions. To correct this, higher order expressions for the first derivative, with corresponding higher order truncation errors, were developed. The goal of this approach was to allow for the use of larger time steps in the simulation than would be possible using the first order Euler form, without experiencing instabilities. Approximations from second through fifth order were tried as reported by Taylor, et al (1990) with the conclusion that the third order finite difference approximation, shown below, gave the best results:

$$
\left. \frac{dT_z}{dt} \right|_t \approx \left(\delta t \right)^{-1} \left(\frac{11}{6} T_z^t - 3 T_z^{t-\delta t} + \frac{3}{2} T_z^{t-2\delta t} - \frac{1}{3} T_z^{t-3\delta t} \right) + O\left(\delta t^3 \right)
\qquad (1.9)
$$

When this form for the derivative is used, equation (1.7) changes to:

$$
C_z \left(\delta t \right)^{-1} \left(\frac{11}{6} T_z^t - 3 T_z^{t-\delta t} + \frac{3}{2} T_z^{t-2\delta t} - \frac{1}{3} T_z^{t-3\delta t} \right) =
$$

$$
\sum_{i=1}^{N_{sl}} \dot{Q}_i + \sum_{i=1}^{N_{surfaces}} h_i A_i \left(T_{si} - T_z \right) + \sum_{i=1}^{N_{zones}} \dot{m}_i C_p \left(T_{zi} - T_z \right)
$$

$$
+ \dot{m}_{inf} C_p \left(T_\infty - T_z \right) + \dot{m}_{sys} C_p \left(T_{sup} - T_z \right)
\qquad (1.10)
$$

and the zone temperature update equation becomes:

$$T_z^t = \frac{\sum_{i=1}^{N_{sl}} \dot{Q}_i + \sum_{i=1}^{N_{surfaces}} h_i A_i T_{si} + \sum_{i=1}^{N_{zones}} \dot{m}_i C_p T_{zi} + \dot{m}_{inf} C_p T_\infty + \dot{m}_{sys} C_p T_{supply} - \left(\frac{C_z}{\delta t}\right)\left(-3T_z^{t-\delta t} + \frac{3}{2}T_z^{t-2\delta t} - \frac{1}{3}T_z^{t-3\delta t}\right)}{\left(\frac{11}{6}\right)\frac{C_z}{\delta t} + \sum_{i=1}^{N_{surfaces}} h_i A + \sum_{i=1}^{N_{zones}} \dot{m}_i C_p + \dot{m}_{inf} C_p + \dot{m}_{sys} C} \quad (1.11)$$

This is the form currently used in EnergyPlus. Since the load on the zone drives the entire process, that load is used as a starting point to give a demand to the system. Then a simulation of the system provides the actual supply capability and the zone temperature is adjusted if necessary. This process in EnergyPlus is referred to as a Predictor/Corrector process. It is summarized below.

> Code Reference: the **ZoneTempPredictorCorrector** module performs the calculations.

Summary of Predictor-Corrector Procedure

The predictor-corrector scheme can be summarized as follows:

- Using equation (1.3), an estimate is made of the system energy required to balance the equation with the zone temperature equal to the setpoint temperature.
- With that quantity as a demand, the system is simulated to determine its actual supply capability at the time of the simulation. This will include a plant simulation if necessary.
- The actual system capability is used in equation (1.11) to calculate the resulting zone temperature.

System Control

Previously, the formulation of a new heat balance equation with an unsteady zone capacitance term was discussed Equation (1.4). In this equation the updated zone temperature was calculated by removing its explicit dependence from the right hand side and lagging, by one time step, the unknown terms on that side. However, the right hand side still contains implicit dependencies on the zone temperature through the system control logic; the need for heating or cooling in the zones, is based on zone temperature. In real buildings the control system consists of one or more sensing units in the zone, such as a wall thermostat that samples the air temperature and sends signals to a control unit. The controller looks at the difference between the actual zone temperature and the desired temperature to ascertain if heating or cooling is required and then sends appropriate signals to the system components to drive the zone temperature closer to the desired value.

Although many control systems use only the zone temperature to control the system, most modern energy management systems consider many other variables, such as outside environment conditions. Simulating such controllers would seem to be relatively straightforward in a simulation especially since some of the more complex control problems, such as managing duct pressures and flow rates, are not modeled. However, real controllers have an advantage because they can sample zone conditions, and thus update system response, on a time scale much shorter than any characteristic time of the system or zone. Thus the feedback between zone and system usually results in steady or, at worst, slowly oscillating zone conditions and system operation unless the system is grossly oversized. On the other hand, the numerical model is only able to sample zone conditions at discrete time intervals. In the interest of minimizing computation time, these intervals need to be as long as possible. Frequently, they are of the order of, or longer than, the characteristic times of the system and zones, except in the case of small system capacity in relation to zone capacitance. This situation has the potential for unstable feedback between zone and system, resulting in an oscillatory or diverging solution.

Prior to implementing the new heat balance method in IBLAST, several system control strategies were considered. The primary objective was selection of a control method that would: be numerically stable over a reasonable range of conditions, realistic from the

standpoint of looking and operating like an actual system controller, and flexible enough to be applied to all current and projected systems. The method actually implemented in IBLAST, and later EnergyPlus, took advantage of the computational model's "knowledge" of how much energy enters or leaves the zone as a function of zone temperature i.e., the zone load. The real controller, on the other hand, does not have this information. The net zone load is given by Equation (1.12):

$$\dot{Q}_{load} = \sum_{i=1}^{N_{sl}} \dot{Q}_i + \sum_{i=1}^{N_{surfaces}} h_i A_i \left(T_{si} - T_z \right) + \sum_{i=1}^{N_{zones}} \dot{m}_i C_p \left(T_{zi} - T_z \right) + \dot{m}_{\inf} C_p \left(T_{\infty} - T_z \right) \tag{1.12}$$

This is Equation (1.4) without the term due to the system. In addition, T_Z is now the *desired* zone temperature as defined by the control system setpoints that must be specified for each zone. An assumption was made that if the system has sufficient capacity (based on the desired zone temperature) to meet the zone conditioning requirements (i.e. $\dot{Q}_{sys}$ = $\dot{Q}_{load}$) at the desired zone temperature then those requirements will be met. On the other hand, if the system can not provide enough conditioning to the zone to maintain the desired temperature, then the system provides its maximum output to the zone and the zone temperature is allowed to "float." Equation (1.12) was used to calculate the system output required to maintain the desired zone temperature; the actual zone temperature update was accomplished using Equation (1.8). This method was called *predictive system energy balance*. It has many characteristics of a predictor-corrector method since the system response is first approximated based on a predicted zone temperature and then the actual change in zone temperature is determined from that system response. The predictive system energy balance method required that the system controls on air mass flow rate, supply air temperature, etc., be formulated as a function of the zone temperature. However, this was not a serious drawback. The first example considered was a single zone draw through system. Typically, such systems have a cooling coil and heating coil in series, and constant air volume flow rate. Single zone draw through systems run at maximum capacity when turned on so the only way to regulate net system output and keep the zone temperature within the desired range is to turn the system on and off. A simplified schematic of this system type is shown in Figure "Simplified single zone draw through system".
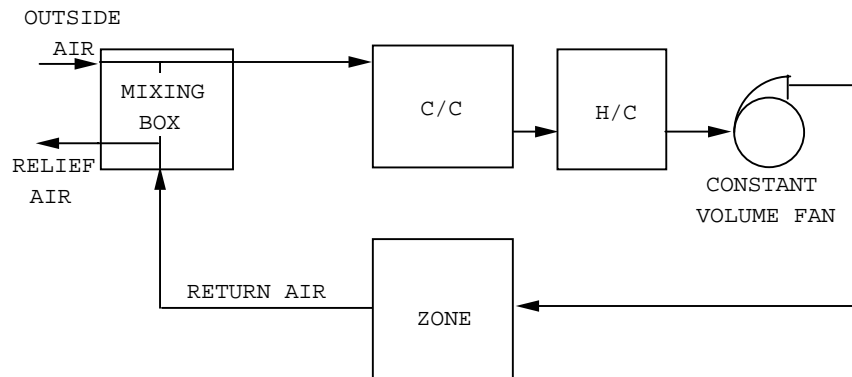
Figure 4. Simplified single zone draw through system

The amount of heating or cooling provided by the system in relation to the desired zone temperature is given by:

$$\dot{Q}_{sys} = \dot{m}_{sys} C_p \eta \left(T_{\sup} - T_{z,desired} \right) \tag{1.13}$$

where η is the fraction of the time step that the system is turned on and varies between 0 and 1. The supply air temperature is also implicitly limited by the effectiveness of the coils and

the operating parameters of the central plant components. These interactions are discussed later.

A far more complex, though again simplified, system is the variable air volume (VAV) system, shown in Figure "Simplified Variable Volume System. In VAV systems, the supply air temperature as well as the supply air volume are continuous functions of zone temperature. As shown in Figure "Idealized variable volume system operation., when the zone temperature is between T_{cl} and T_{cu}, cooling is required and the system varies the supply air flow rate while maintaining a constant supply air temperature. When the zone temperature is between T_{hl} and T_{hu}, heating is required and air is supplied at a constant minimum flow rate while the supply air temperature is varied.
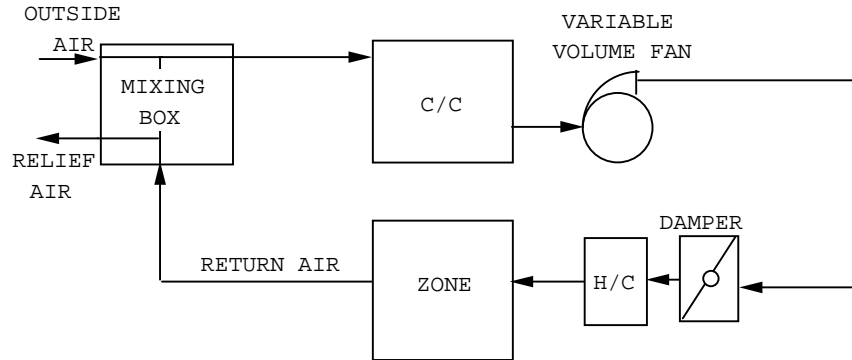
Figure 5. Simplified Variable Volume System.

The next figure (Idealized variable volume system operation) shows idealized behavior of a VAV system; in practice, the air flow rate and temperature are not exact linear functions of zone temperature.
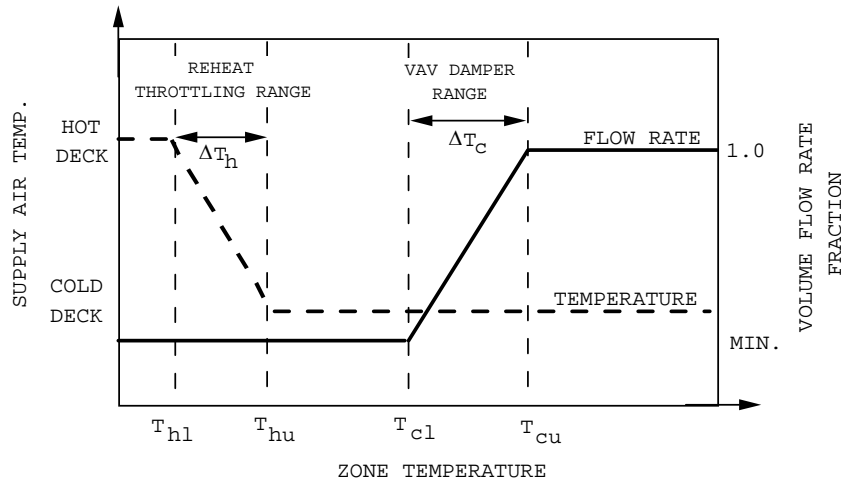
Figure 6. Idealized variable volume system operation.

As long as a VAV system has sufficient capacity, the zone temperatures can be expected to vary within the limits defining the range of operation of the air damper, when cooling, or the throttling range of the reheat coil, when the system is heating. This means that the desired zone temperature, used to predict the system response, is variable and must be calculated in order to determine the system output. For the purposes of this calculation, the following definitions were found useful:

$$\dot{Q}_0 = \sum_{i=1}^{N_{sl}} \dot{Q}_i + \sum_{i=1}^{N_{surfaces}} h_i A_i T_{si} + \sum_{i=1}^{N_{zones}} \dot{m}_i C_p T_{zi} + \dot{m}_{inf} C_p T_{\infty} \tag{1.14}$$

$$\dot{Q}_{slope} = \sum_{i=1}^{N_{surfaces}} h_i A_i + \sum_{i=1}^{N_{zones}} \dot{m}_i C_p + \dot{m}_{inf} C_p \tag{1.15}$$

Equations (1.14) and (1.15) are derived, respectively, from the numerator and denominator of Equation (1.11) ???2-3 but with the system related terms omitted. Also excluded from these expressions are the effects of zone capacitance.

When a zone requires cooling, the VAV system is designed to provide air to that zone at a constant supply air temperature. The amount of cooling is matched to the load by dampers in the supply air duct that vary the air volume flow rate of being supplied to the zone. Assuming that the volume flow rate varies linearly with zone temperature, the volume flow rate of supply air normalized to the maximum flow rate, or supply air fraction, is given by:

$$\eta_c = \eta_{c,min} + \left(1 - \eta_{c,min}\right) \left(\frac{T_z - T_{c,lower}}{T_{c,upper} - T_{c,lower}} \right); \eta_{c,min} \le \eta_c \le 1.0 \tag{1.16}$$

Normally, the minimum supply air fraction $\eta_{c,min}$ must be greater than zero to ensure a supply of fresh air sufficient to eliminate contaminants from the zone.

Conversely, when heating is required in a zone, the VAV system becomes a constant volume flow rate system with a variable supply air temperature. The dampers are set to provide air to the zone at the minimum supply air fraction. The supply air temperature is modulated by throttling the hot water supply to the reheat coil which effectively alters the coil's heating capacity. Again assuming the heat energy output varies linearly with zone temperature and normalizing with respect to the maximum coil output gives the following result:

$$\eta_h = \left(\frac{T_{h,upper} - T_z}{T_{h,upper} - T_{h,lower}} \right); 0 \le \eta_h \le 1.0 \tag{1.17}$$

Observe that when η_h is equal to zero, the zone is supplied with air at the cooling coil outlet temperature at the minimum air fraction. Because the control strategies of the VAV system are different whether the system is heating or cooling, two equations are necessary to describe the system output in terms of η_h and η_c. These expressions are as shown in Equations (1.18) and (1.19):

$$\dot{Q}_{sys,h} = \eta_h \dot{Q}_{h/c,max} + C_p \rho \dot{V}_{min} \left(T_{c/c} - T_{z,pred,heat} \right) \tag{1.18}$$

$$\dot{Q}_{sys,c} = C_p \rho \left(\eta_c \dot{V}_{max} \right) \left(T_{c/c} - T_{z,pred,cool} \right) \tag{1.19}$$

Equation (1.18) is valid for zone temperatures below $T_{h,upper}$, while Equation (1.19) is valid for all temperatures above this value. Equating the system output to the zone load, as given by Equation (1.12), the definitions of η_c and η_h were then used to develop expressions for the predicted zone temperature in the cases of heating and cooling:

$$T_{z,pred,heat} = \frac{\dot{Q}_{h/c,\max} T_{h,upper}}{T_{h,upper} - T_{h,lower}} + \dot{Q}_0 + \frac{C_p \rho \dot{V}_{\min} T_{c/c}}{\frac{\dot{Q}_{h/c,\max}}{T_{h,upper} - T_{h,lower}} + C_p \rho \dot{V}_{\min} + \dot{Q}_{slope}}$$ (1.20)

$$T_{z,pred,cool} = \frac{B_1 + \sqrt{B_1^2 + B_2}}{2}$$ (1.21)

where,

$$B_1 = T_{c/c} + T_{c,lower} - \frac{\eta_{c,\min} - C_2}{C_1}$$ (1.22)

$$B_2 = 4\left(\frac{C_3}{C_1} + T_{c/c}\left(\frac{\eta_{c,\min}}{C_1} - T_{c,lower} \right) \right)$$ (1.23)

and,

$$C_1 = \frac{1 - \eta_{c,\min}}{T_{c,upper} - T_{c,lower}}$$ (1.24)

$$C_2 = \frac{\dot{Q}_{slope}}{C_p \rho \dot{V}_{\max}}$$ (1.25)

$$C_3 = \frac{\dot{Q}_0}{C_p \rho \dot{V}_{\max}}$$ (1.26)

Once the predicted zone temperature has been calculated from Equations (1.20) and (1.21), the system response may be determined. When a zone requires cooling the system supply air temperature is constant at the cooling coil outlet temperature and the volume flow rate is given by:

$$\dot{V}_{supply} = \eta_c \dot{V}_{\max}$$ (1.27)

where the supply air fraction η_c is computed from Equation (1.16). When heating is required by the zone the system provides air at the minimum volume flow rate and at a temperature given by:

$$T_{supply} = T_{c/c} + \frac{\eta_h \dot{Q}_{h/c,\max}}{C_p \rho \dot{V}_{\min}}$$ (1.28)

The reheat coil capacity fraction η_h is determined by using Equation (1.17). Once Equation (1.27) or (1.28), has been used, the supply air flow rate and temperature are known. These values are then used in Equation (1.8) to calculate the updated zone temperature. The equations describing VAV system operation may be solved without iteration if the cooling coil

outlet temperature is constant, i.e. if the coil has infinite capacity, and if the reheat coil capacity varies linearly with zone temperature. This is not the case, either in practice or in simulations, when realistic coil models are used. Therefore, an iteration scheme was developed that solved these equations simultaneously with the coil performance models.

Moisture Predictor-Corrector

To preserve the stability of the calculation of the zone humidity ratio, a similar methodology was used for the mass balance as was used by temperature in the heat balance as explained above in the Summary of Predictor-Corrector Procedure. The third order differential approximation derived by a Taylor Series was used in the calculation of the next time steps zone air temperature

This idea was applied to predict and correct, or update, the zone humidity ratio. Writing the transient mass balance equation with the change in the zone humidity ratio = sum of internal scheduled latent loads + infiltration + system in & out + convection to the zone surfaces in the equation below.

$$\rho_{air} V_z \frac{dW_z}{dt} = \sum kg_{mass_{Sched\,Loads}} + \dot{m}_{inf}\left(W_\infty - W_z\right) + \dot{m}_{sys}W_{sys_{in}} - \dot{m}_{sys_{out}}W_z$$

$$+ \sum_{i=1}^{surfs} A_i h_{mi} \rho_{air_z}\left(W_{surfs_i} - W_z\right)$$

Then the third order derivative derived from a Taylor Series expansion is defined as:

$$\left.\frac{dW_z}{dt}\right|_t \approx \frac{\left(\frac{11}{6}W_z^t - 3W_z^{t-\delta t} + \frac{3}{2}W_z^{t-2\delta t} - \frac{1}{3}W_z^{t-3\delta t}\right)}{\delta t} + O\left(\delta t^3\right).$$

The coefficients of the approximated derivative are very close to the coefficients of the analogous Adams-Bashforth algorithm. Then the approximated derivative is substituted into the mass balance and the terms with the humidity ratio at past time steps are all put on the right hand side of the equation. This third order derivative zone humidity ratio update increases the number of previous time steps that are used in calculating the new zone humidity ratio, and decreases the dependence on the most recent. The higher order derivative approximations have the potential to allow the use of larger time steps by smoothing transitions through sudden changes in zone operating conditions.

$$\frac{\rho_{air} V_z}{\delta t}\left(\tfrac{11}{6}\right)W_z^t + \dot{m}_{inf}W_z^t + \dot{m}_{sys_{out}}W_z^t + \sum_{i=1}^{surfs} A_i h_{mi}\rho_{air_z}W_z^t =$$

$$\sum kg_{mass_{Sched\,Loads}} + \dot{m}_{inf}W_\infty + \dot{m}_{sys}W_{sys_{in}} + \sum_{i=1}^{surfs} A_i h_{mi}\rho_{air_z}W_{surfs_i}$$

$$-\frac{\rho_{air}V_z}{\delta t}\left(-3W_z^{t-\delta t} + \tfrac{3}{2}W_z^{t-2\delta t} - \tfrac{1}{3}W_z^{t-3\delta t}\right)$$

This gives us the basic mass balance equation that will be solved two different ways, one way for the predict step and one way for the correct step.

Moisture Prediction

For the moisture prediction case the equation is solved for the anticipated system response as shown below.

$$PredictedSystemLoad = \dot{m}_{sys_{out}} W_z^t - \dot{m}_{sys} W_{sys_{in}}$$

Massflow * HumRat = kg air/sec * kgWater/kg Air = kgWater/sec

Then solving the mass balance for the predicted system load or response is:

$$PredictedSystemLoad \ [kgWater/\sec] = \left[\frac{\rho_{air} \forall_z}{\delta t}\left(\tfrac{11}{6}\right) + \dot{m}_{inf} + \sum_{i=1}^{surfs} A_i h_{mi} \rho_{air_z} \right] * W_z^t -$$

$$\left[\sum kg_{mass_{Sched\,Loads}} + \dot{m}_{inf} W_\infty + \sum_{i=1}^{surfs} A_i h_{mi} \rho_{air_z} W_{surfs_i} + \frac{\rho_{air} \forall_z}{\delta t}\left(3 W_z^{t-\delta t} - \tfrac{3}{2} W_z^{t-2\delta t} + \tfrac{1}{3} W_z^{t-3\delta t}\right) \right]$$

Then using the following substitutions the mass balance equation becomes:

$$A = \dot{m}_{inf} + \sum_{i=1}^{surfs} A_i h_{mi} \rho_{air_z}$$

$$B = \sum kg_{mass_{Sched\,Loads}} + \dot{m}_{inf} W_\infty + \sum_{i=1}^{surfs} A_i h_{mi} \rho_{air_z} W_{surfs_i}$$

$$C = \frac{\rho_{air} \forall_z}{\delta t}$$

$$PredictedSystemLoad \ [kgWater/\sec] = \left[\left(\tfrac{11}{6}\right) * C + A\right] * W_{SetPoint} -$$

$$\left[B + C * \left(3 W_z^{t-\delta t} - \tfrac{3}{2} W_z^{t-2\delta t} + \tfrac{1}{3} W_z^{t-3\delta t}\right) \right]$$

At the prediction point in the simulation the system mass flows are not known, therefore the system response is approximated. The predicted system moisture load is then he used in the system simulation to achieve the best results possible. The system simulation components that have moisture control will try to meet this predicted moisture load. For example, humidifiers will look for positive moisture loads and add moisture at the specified rate to achieve the relative humidity set point. Likewise, dehumidification processes will try to remove moisture at the specified negative predicted moisture load to meet the relative humidity set point.

After the system simulation is completed the actual response from the system is used in the moisture correction of step, which is shown next.

Moisture Correction

For the correct step you solve the expanded mass balance equation for the final zone humidity ratio at the current time step. When the system is operating the mass flow for the system out includes the infiltration mass flow rate, therefore the infiltration mass flow rate is not included as a separate term in the mass balance equation. But when the system is off, the infiltration mass flow in is then exhausted out of the zone directly.

For system operating $\dot{m}_{sys_{out}} = \dot{m}_{inf} + \dot{m}_{sys_{in}}$. This ensures that the mass and energy brought into the zone due to infiltration is conditioned by the coils and is part of their load.

$$W_z^t = \left[\frac{\begin{array}{l} \sum kg_{mass_{\text{Sched Loads}}} + \dot{m}_{\text{inf}} W_\infty + \dot{m}_{sys} W_{sys_{in}} \\[2mm] + \sum_{i=1}^{surfs} A_i h_{mi} \rho_{air_z} W_{surfs_i} + \frac{\rho_{air} V_z}{\delta t} \left(3W_z^{t-\delta t} - \frac{3}{2} W_z^{t-2\delta t} + \frac{1}{3} W_z^{t-3\delta t} \right) \end{array}}{\frac{\rho_{air} V_z}{\delta t} \left(\frac{11}{6} \right) + \dot{m}_{sys_{out}} + \sum_{i=1}^{surfs} A_i h_{mi} \rho_{air_z}} \right]$$

For system off, the mass flow in due to infiltration is exhausted from the zone. Therefore if the system is shut down for a longer time, then the zone should stabilize at the outside air humidity ratio and upon system startup the added mass and heat in the zone air is handled by the system.

$$W_z^t = \left[\frac{\begin{array}{l} \sum kg_{mass_{\text{Sched Loads}}} + \dot{m}_{\text{inf}} W_\infty + \sum_{i=1}^{surfs} A_i h_{mi} \rho_{air_z} W_{surfs_i} \\[2mm] + \frac{\rho_{air} V_z}{\delta t} \left(3W_z^{t-\delta t} - \frac{3}{2} W_z^{t-2\delta t} + \frac{1}{3} W_z^{t-3\delta t} \right) \end{array}}{\frac{\rho_{air} V_z}{\delta t} \left(\frac{11}{6} \right) + \dot{m}_{\text{inf}} + \sum_{i=1}^{surfs} A_i h_{mi} \rho_{air_z}} \right]$$

and then using the same A, B, and C parameters from the prediction step modified with actual zone mass flows with the system ON and OFF:

If (ZoneMassFlowRate > 0.0) **Then**

$$B = \sum kg_{mass_{\text{Sched Loads}}} + \dot{m}_{\text{inf}} W_\infty + \dot{m}_{sys_{in}} W_{sys} + \sum_{i=1}^{surfs} A_i h_{mi} \rho_{air_z} W_{surfs_i}$$

$$A = \dot{m}_{\text{inf}} + \dot{m}_{sys_{out}} + \sum_{i=1}^{surfs} A_i h_{mi} \rho_{air_z}$$

$$C = \frac{\rho_{air} V_z}{\delta t}$$

Else If (ZoneMassFlowRate <= 0.0) **Then**

$$B = \sum kg_{mass_{\text{Sched Loads}}} + \left(\dot{m}_{\text{inf}} + \dot{m}_{Exhaust} \right) W_\infty + \sum_{i=1}^{surfs} A_i h_{mi} \rho_{air_z} W_{surfs_i}$$

$$A = \dot{m}_{\text{inf}} + \dot{m}_{Exhaust} + \sum_{i=1}^{surfs} A_i h_{mi} \rho_{air_z}$$

$$C = \frac{\rho_{air} V_z}{\delta t}$$

End If

Then inserting them in the mass balance equation, it simplifies to:

$$W_z^t = \left[\frac{B + C * \left(3W_z^{t-\delta t} - \frac{3}{2} W_z^{t-2\delta t} + \frac{1}{3} W_z^{t-3\delta t} \right)}{\left(\frac{11}{6} \right) * C + A} \right]$$

This is implemented in the Correct Zone Air Humidity Ratio step in EnergyPlus. This moisture update equation is used for the Conduction Transfer Function (CTF) case in EnergyPlus, in addition to the moisture cases. The equations are identical except that the convection to the zone surfaces is non-zero for the moisture cases. This moisture update allows both methods to be updated in the same way, and the only difference will be the additional moisture capacitance of the zone surfaces for the Moisture Transfer Function (MTF) case.

Zone Update Method

A zone is not necessarily a single room but is usually defined as a region of the building or a collection of rooms subject to the same type of thermal control and having similar internal load profiles that, subsequently, can be grouped together. Zones can interact with each other thermally through adjacent surfaces and by intermixing of zone air. In EnergyPlus, the conditions in each zone are updated by Equation (1.8), which uses previously calculated values of the zone conditions. This means that EnergyPlus does not have to iterate to find a self consistent solution of the updated zone conditions. However, because heat transfer through each zone's surfaces and interzone mixing of air still occur, the new space temperatures must be computed at the same simulation time and on the same time step in all zones, even though conditions in one zone may be changing much more rapidly than conditions in the other zones. We have previously documented the method used to update the zone temperature at each time step. This method, called the predictor corrector method, has proved to be satisfactory over a wide range of conditions.

Variable Time Step

Prior to the integration of the central plant simulation in IBLAST, a time step Δt for the zone temperature update of 0.25 hours (15 minutes) was found to give stable results without a large increase in computation time. The first step in integrating the plants was to implement the detailed coil models and coil control strategies without actually adding the plant models themselves. This meant that the user had to specify the coil water inlet temperature and the maximum coil inlet water flow rate to run the simulation. The real life analogy would be a chiller of very large, though not infinite, capacity. The coil capacity was controlled by adjusting the water flow rate, but the effect of the plant on the chilled water temperature was eliminated. After implementation of this step, experience with the program showed that updating the zone temperatures on a fixed time step frequently resulted in instabilities unless a very short time step was used. However, as the time step got shorter the time required to execute the program got prohibitively high.

Clearly, an adaptive time step was required. This would shorten the time step to maintain stability of the zone air energy balance calculation when zone conditions were changing rapidly and   expand it to speed computation when zone conditions were relatively unchanging. But, the adaptive time step could not be applied easily to the surface heat transfer calculations, even using interpolation methods to determine new temperature and flux histories. The problem of updating the zone temperature was resolved by using a two time step approach in which the zone air temperature is updated using an adaptive time step

that ensures stability. In this two time level scheme, the contributions to the zone loads from the surfaces, infiltration, mixing, and user specified internal loads are updated at the default or user specified time step which is constant. A second variable time step is used to update the system response and the zone mean air temperature. This time step is selected by first calculating the system response and updating the zone temperature using the user specified time step Δt. The maximum temperature change experienced by a zone is then evaluated on a system by system basis. If the maximum zone temperature change is more than a preset maximum of 1°C the system and zone updates are performed using a new time step Δt. This adaptive time step is initially set to $\Delta t/2$ and is successively halved until the maximum zone temperature change is less than the allowable maximum change.   This approach can be justified because the internal loads, surface temperatures, infiltration and mixing vary on a different and longer time scale than the system response and the zone air temperature. The zone temperature update was made using Equation (1.29) for each adaptive time step, which is just a different form of Equation (1.8):

$$
T_z^t = \frac{\left(\sum \dot{Q}_c + \sum_{i=1}^{\#surf.} h_i A_i T_{si} + \sum_{j=1}^{\#zones} \dot{m}_j C_p T_{zj} + \dot{m}_{\inf} C_p T_\infty \right)^{(t-\Delta t)} + \left(\dfrac{C_z}{\delta t} T_z + \dot{m}_{sys} C_p T_{\sup ply} \right)^{(t-\delta t)}}{\left(\sum_{i=1}^{\#surf.} h_i A_i + \sum_{j=1}^{\#zones} \dot{m}_j C_p + \dot{m}_{\inf} C_p \right)^{(t-\Delta t)} + \left(\dfrac{C_z}{\delta t} + \dot{m}_{sys} C_p \right)^{(t-\delta t)}}
$$
(1.29)

In Equation (1.29), Δt is the user specified time step and Δt is the adaptive time step that is always less than or equal to Δt.

Simultaneous Solution of Plant/System Water Loop

Simultaneous solution of the system and plant operating parameters required that the temperature of the water entering the coils must be the same as the temperature leaving the chillers or boilers. In addition, the temperature of the return water from the coils must be equal to the chiller or boiler entering water temperature. In practice so long as the plant is not out of capacity the leaving water temperature from chillers and boilers is constant and equal to the design value. No iteration was required to match system and plant boundary conditions. However, if either the chiller or boiler plant was overloaded then the temperature of the water leaving the plant was not equal to the design value and the maximum output of the plant could change because of the off-design conditions. An iterative scheme using the secant method to predict successive updates to the plant leaving water conditions was therefore employed to solve for the water loop conditions with the plant operating at its maximum capacity. The simulation of the system and plant loops is described in greater detail in the later sections.

References

Surface Heat Balance Manager / Processes

Conduction Through The Walls

Conduction Transfer Function Module

The most basic time series solution is the response factor equation which relates the flux at one surface of an element to an infinite series of temperature histories at both sides as shown by Equation (1.30):

$$q_{ko}''(t) = \sum_{j=0}^{\infty} X_j T_{o,t-j\delta} - \sum_{j=0}^{\infty} Y_j T_{i,t-j\delta} \tag{1.30}$$

where q" is heat flux, T is temperature, i signifies the inside of the building element, o signifies the outside of the building element, t represents the current time step, and X and Y are the response factors.

While in most cases the terms in the series decay fairly rapidly, the infinite number of terms needed for an exact response factor solution makes it less than desirable. Fortunately, the similarity of higher order terms can be used to replace them with flux history terms. The new solution contains elements that are called conduction transfer functions (CTFs). The basic form of a conduction transfer function solution is shown by the following equation:

$$q_{ki}''(t) = -Z_o T_{i,t} - \sum_{j=1}^{nz} Z_j T_{i,t-j\delta} + Y_o T_{o,t} + \sum_{j=1}^{nz} Y_j T_{o,t-j\delta} + \sum_{j=1}^{nq} \Phi_j q_{ki,t-j\delta}'' \tag{1.31}$$

for the inside heat flux, and

$$q_{ko}''(t) = -Y_o T_{i,t} - \sum_{j=1}^{nz} Y_j T_{i,t-j\delta} + X_o T_{o,t} + \sum_{j=1}^{nz} X_j T_{o,t-j\delta} + \sum_{j=1}^{nq} \Phi_j q_{ko,t-j\delta}'' \tag{1.32}$$

for the outside heat flux (q″=q/A)

where:

X_j = Outside CTF coefficient, j= 0,1,...nz.

Y_j = Cross CTF coefficient, j= 0,1,...nz.

Z_j = Inside CTF coefficient, j= 0,1,...nz.

Φ_φ = Flux CTF coefficient, j = 1,2,...nq.

T_i = Inside face temperature

T_o = Outside face temperature

q_{ko}'' = Conduction heat flux on outside face

q'' = Conduction heat flux on inside face

The subscript following the comma indicates the time period for the quantity in terms of the time step δ. Note that the first terms in the series (those with subscript 0) have been separated from the rest in order to facilitate solving for the current temperature in the solution scheme. These equations state that the heat flux at either face of the surface of any generic building element is linearly related to the current and some of the previous temperatures at both the interior and exterior surface as well as some of the previous flux values at the interior surface.

The final CTF solution form reveals why it is so elegant and powerful. With a single, relatively simple, linear equation with constant coefficients, the conduction heat transfer through an element can be calculated. The coefficients (CTFs) in the equation are constants that only need to be determined once for each construction type. The only storage of data required are the CTFs themselves and a limited number of temperature and flux terms. The formulation is valid for any surface type and does not require the calculation or storage of element interior temperatures.

Calculation of Conduction Transfer Functions

The basic method used in EnergyPlus for CTF calculations is known as the state space method (Ceylan and Myers 1980; Seem 1987; Ouyang and Haghighat 1991). Another common, older method used Laplace transformations to reach the solution; the Laplace method was used in BLAST (Hittle, 1979; Hittle & Bishop, 1983). The basic state space system is defined by the following linear matrix equations:

$$\frac{d[\mathbf{x}]}{dt} = [\mathbf{A}][\mathbf{x}] + [\mathbf{B}][\mathbf{u}]$$

$$[\mathbf{y}] = [\mathbf{C}][\mathbf{x}] + [\mathbf{D}][\mathbf{u}]$$

where x is a vector of state variables, u is a vector of inputs, y is the output vector, t is time, and A, B, C, and D are coefficient matrices. Through the use of matrix algebra, the vector of state variables (x) can be eliminated from the system of equations, and the output vector (y) can be related directly to the input vector (u) and time histories of the input and output vectors.

This formulation can be used to solve the transient heat conduction equation by enforcing a finite difference grid over the various layers in the building element being analyzed. In this case, the state variables are the nodal temperatures, the environmental temperatures (interior and exterior) are the inputs, and the resulting heat fluxes at both surfaces are the outputs. Thus, the state space representation with finite difference variables would take the following form:

$$\frac{d\begin{bmatrix} T_1 \\ \vdots \\ T_n \end{bmatrix}}{dt} = [\mathbf{A}]\begin{bmatrix} T_1 \\ \vdots \\ T_n \end{bmatrix} + [\mathbf{B}]\begin{bmatrix} T_i \\ T_o \end{bmatrix}$$

$$\begin{bmatrix} q''_i \\ q''_o \end{bmatrix} = [\mathbf{C}]\begin{bmatrix} T_1 \\ \vdots \\ T_n \end{bmatrix} + [\mathbf{D}]\begin{bmatrix} T_i \\ T_o \end{bmatrix}$$

where T_1, T_2, ..., T_{n-1}, T_n are the finite difference nodal temperatures, n is the number of nodes, T_i and T_o are the interior and exterior environmental temperatures, and q''_i and q''_o are the heat fluxes (desired output).

Seem (1987) shows that for a simple one layer slab with two interior nodes as in Figure 7 and convection at both sides the resulting finite difference equations are given by:

$$C\frac{dT_1}{dt} = hA(T_o - T_1) + \frac{T_2 - T_1}{R}$$

$$C\frac{dT_2}{dt} = hA(T_i - T_2) + \frac{T_1 - T_2}{R}$$

$$q''_i = h(T_i - T_2)$$

$$q''_o = h(T_1 - T_o)$$

where:

$$R = \frac{\ell}{kA},$$

$$C = \frac{\rho c_p \ell A}{2}, \text{ and}$$

A is the area of the surface exposed to the environmental temperatures.

In matrix format:

$$\begin{bmatrix} \dfrac{dT_1}{dt} \\ \dfrac{dT_2}{dt} \end{bmatrix} = \begin{bmatrix} -\dfrac{1}{RC} - \dfrac{hA}{C} & \dfrac{1}{RC} \\ \dfrac{1}{RC} & -\dfrac{1}{RC} - \dfrac{hA}{C} \end{bmatrix} \begin{bmatrix} T_1 \\ T_2 \end{bmatrix} + \begin{bmatrix} \dfrac{hA}{C} & 0 \\ 0 & \dfrac{hA}{C} \end{bmatrix} \begin{bmatrix} T_o \\ T_i \end{bmatrix}$$

$$\begin{bmatrix} q''_o \\ q''_i \end{bmatrix} = \begin{bmatrix} 0 & -h \\ h & 0 \end{bmatrix} \begin{bmatrix} T_1 \\ T_2 \end{bmatrix} + \begin{bmatrix} 0 & h \\ -h & 0 \end{bmatrix} \begin{bmatrix} T_o \\ T_i \end{bmatrix}$$
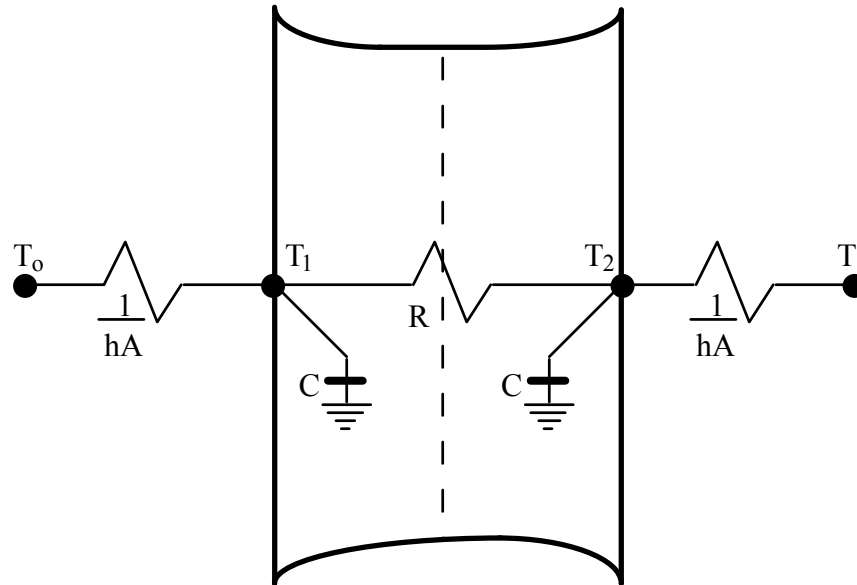
Figure 7. Two Node State Space Example.

The important aspect of the state space technique is that through the use of matrix algebra the state space variables (nodal temperatures) can be eliminated to arrive at a matrix equation which gives the outputs (heat fluxes) as a function of the inputs (environmental temperatures) only. This eliminates the need to solve for roots in the Laplace domain. In addition, the resulting matrix form has more physical meaning than complex functions required by the Laplace transform method.

The accuracy of the state space method of calculating CTFs has been addressed in the literature. Ceylan and Myers (1980) compared the response predicted by the state space method to various other solution techniques including an analytical solution. Their results showed that for an adequate number of nodes the state space method computed a heat flux at the surface of a simple one layer slab within 1% of the analytical solution. Ouyang and Haghighat (1991) made a direct comparison between the Laplace and state space methods. For a wall composed of insulation between two layers of concrete, they found almost no difference in the response factors calculated by each method.

Seem (1987) summarizes the steps required to obtain the CTF coefficients from the A, B, C, and D matrices. While more time consuming than calculating CTFs using the Laplace Transform method, the matrix algebra (including the calculation of an inverse and exponential matrix for A) is easier to follow than root find algorithms. Another difference between the Laplace and State Space methods is the number of coefficients required for a solution. In general, the State Space method requires more coefficients. In addition, the number of temperature and flux history terms is identical ($nz=nq$). Note that as with the Laplace method that the actual number of terms will vary from construction to construction.

Two distinct advantages of the State Space method over the Laplace method that are of interest when applying a CTF solution for conduction through a building element are the ability to obtain CTFs for much shorter time steps and the ability to obtain 2- and 3-D conduction transfer functions. While not implemented in the Toolkit, both Seem (1987) and Strand (1995) have demonstrated the effectiveness of the State Space method in handling these situations that can have important applications in buildings.

EnergyPlus CTF Calculations

Conduction transfer functions are an efficient method to compute surface heat fluxes because they eliminate the need to know temperatures and fluxes within the surface. However, conduction transfer function series become progressively more unstable as the

time step decreases.   This became a problem as investigations into short time step computational methods for the zone/system interactions progressed because, eventually, this instability caused the entire simulation to diverge. This phenomenon was most apparent for thermally massive constructions with long characteristic times and, correspondingly, requiring a large number of terms in the CTF series. This indicates that the problem is related to round-off and truncation error and is in no way an indictment of the CTF method itself. Methods that develop CTF series from finite difference approximations to the heat conduction equation (Meyers, 1980; Seem, 1987) were considered to address this problem. Seem's method did give better accuracy and stability at short time steps than the current BLAST technique but, the method still had difficulty computing stable CTF series for time steps of less than 1/4 hour for the heaviest constructions in the BLAST library.

The zone heat gains consist of specified internal heat gains, air exchange between zones, air exchange with the outside environment, and convective heat transfer from the zone surfaces. Of these, the surface convection load requires the most complicated calculations because a detailed energy balance is required at the inside and outside surface of each wall, floor, and roof. In addition, the transient heat conduction in the material between the surfaces must be solved. This solution gives the inside and outside temperatures and heat fluxes that must be known in order to calculate the convection component to the zone load for each zone surface. BLAST uses a conduction transfer function CTF method attributed to Hittle (1980) to solve the transient conduction problem for each surface. The method results in a time series of weighting factors that, when multiplied by previous values of the surface temperatures and fluxes and the current inside and outside surface temperatures, gives the current inside and outside heat flux.   The method is easily applied to multilayered constructions for which analytical solutions are unavailable. In addition, determining the series of CTF coefficients is a one time calculation, making the method much faster than finite difference calculations.

A problem with CTF methods is that the series time step is fixed; that is, a CTF series computed for a one hour time step takes information at t-1 hours, t-2 hours, etc. and computes conditions at the current time t. As time advances the oldest term in the input series is dropped and the data moved back one time step to allow the newest value to be added to the series. For convenience, the time step used to determine the CTF series should be the same as the time step used to update the zone mean air temperature in the zone energy balance. But, as the time step used to calculate the CTF series gets shorter, the number of terms in the series grows. Eventually, with enough terms, the series becomes unstable due to truncation and round-off error. Heavy constructions, such as slab-on-grade floors (12" heavyweight concrete over 18" dirt), have accuracy and stability problems at time steps as large as 0.5 hours when modeled by Hittle's CTF method.   In an attempt to overcome this problem, Hittle's method was replaced by Seem's method (1987) in IBLAST. This resulted in some improvement in stability at shorter time steps, but not enough to allow IBLAST to run at a 0.1 hour time step without restricting the types of surfaces that could be used.

Even though CTF methods require that values of the surface temperatures and fluxes be stored for only a few specific times before the current time, the temperature and flux histories are, actually, continuous functions between those discrete points. However, there is no way to calculate information at these intermediate times once a series has been initialized. The terms in the temperature and flux histories are out of phase with these points. However, they can be calculated by shifting the phase of the temperature and flux histories by only a fraction of a time step. This procedure would allow a CTF series computed for a time step Δt, to be used to compute information at times $t+\Delta t/2$, $t+\Delta t/3$, $t+\Delta t/4$, or any other arbitrary fraction of the time step, so long as the surface temperatures and flux values were still Δt apart. Several ways of doing this are described below.

The method shown in the Figure 8 maintains two sets of histories out of phase with each other. The figure shows how this would work for two sets of histories out of phase by one half of a time step. More sets of temperature and flux histories could be used, allowing the simulation time step to take on values: 1/3, 1/4, 1/5, etc., of the minimum time step allowed for the CTF calculations.   The time step between inputs to the CTF series would be the

smallest convenient interval at which the CTF series is stable. This scenario is illustrated in this figure for two separate sets of temperature and flux histories. Cycling through each history, in order, allowed calculations of the zone energy balance to be performed with updated surface information at a shorter time step than one CTF history series would otherwise allow. This method required no interpolation between the series once each set of histories was initialized. However, if the smallest time step for a stable CTF series was large compared to the zone temperature update time step, significant memory was required to store all the sets of histories.
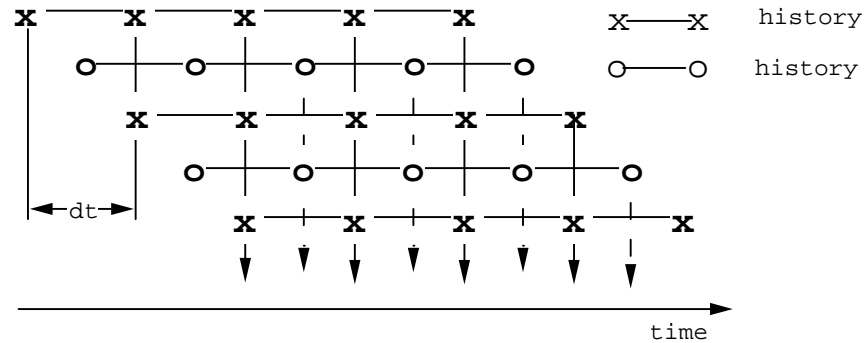
Figure 8. Multiple, staggered time history scheme

Another method is shown in Figure "Sequential interpolation of new histories" that uses successive interpolations to determine the next set of temperature and flux histories. The current history is interpolated directly from the previous history set using the required time phase shift between the two. This method required permanent storage for only one set of temperature and flux histories at a time, but smoothed out temperature and flux data as more interpolations were performed. As a result, at concurrent simulation times current values of history terms were different form previous "in phase" history terms. This was unacceptable from, a physical point of view, because it allowed current information to change data from a previous time.
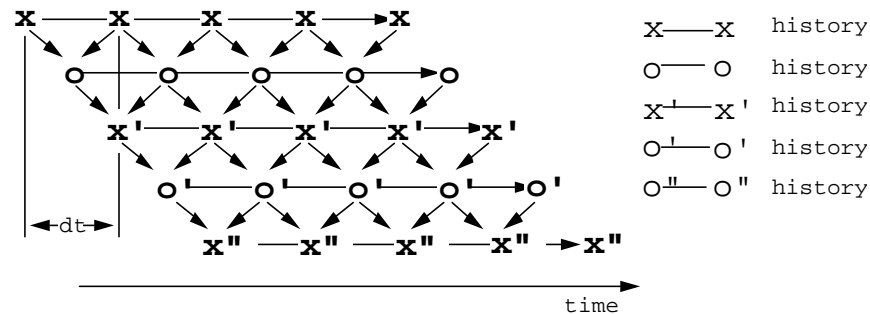
Figure 9. Sequential interpolation of new histories

A final method, shown in Figure "Master history with interpolation", was something of a hybrid of the previous two methods. One "master" history set was maintained and updated for all time; this solved the problem of current events propagating information backwards in time. When surface fluxes needed to be calculated at times out of phase with this master history a new, temporary history was interpolated from the master values. This method proved to be the best of the three options described because it eliminated propagation of information backwards in time and only required concurrent storage of two sets of temperature and flux histories. This method was subsequently incorporated into the IBLAST program in conjunction with Seem's procedure for calculating the coefficients of the CTF series.
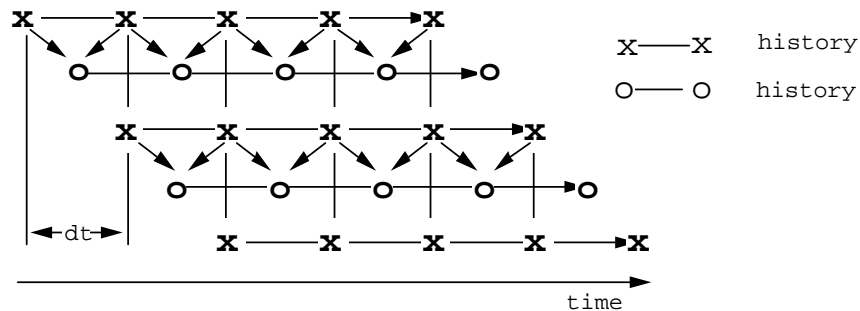
Figure 10. Master history with interpolation

References

Ceylan, H. T., and G. E. Myers. 1980. Long-time Solutions to Heat Conduction Transients with Time-Dependent Inputs. ASME Journal of Heat Transfer, Volume 102, No. 1, pp. 115-120.

Hittle, D. C. 1979. Calculating Building Heating and Cooling Loads Using the Frequency Response of Multilayered Slabs, Ph.D. Thesis, University of Illinois, Urbana, IL.

Hittle, D. C., and R. Bishop. 1983. An Improved Root-Finding Procedure for Use in Calculating Transient Heat Flow Through Multilayered Slabs. International Journal of Heat and Mass Transfer, Vol. 26, No. 11, pp. 1685-1693.

Ouyang, K., and F. Haghighat. 1991. A Procedure for Calculating Thermal Response Factors of Multi-layered Walls--State Space mMethod. Building and Environment, Vol. 26, No. 2, pp. 173-177.

Seem, J. E. 1987. Modeling of Heat Transfer in Buildings, Ph.D. Thesis, University of Wisconsin, Madison, WI.

Strand, R. K. 1995. Heat Source Transfer Functions and Their Application to Low Temperature Radiant Heating Systems, Ph.D. Thesis, University of Illinois, Urbana, IL.

Taylor, R. D., C.O. Pedersen, D.E. Fisher, R. J. Liesen, L.K. Lawrie, *Simultaneous Simulation of Buildings and Mechanical Systems in Heat Balance Based Energy Analysis Programs*, Proceedings of the 3rd International Conference on System Simulation in Buildings, Liege, Belgium, December 3-5, 1990.

Taylor, R.D., C.O. Pedersen, D.E. Fisher, R. J. Liesen, L.K. Lawrie, Impact of Simultaneous Simulation of Buildings and Mechanical Systems in Heat Balance Based Energy Analysis Programs on System Response and Control, Conference Proceedings IBPSA Building Simulation '91, Nice, France, August 20-22, 1991.

Moisture Transfer Material Properties

Moisture transfer properties are non-linear over the entire range from dry to saturated. Almost all material properties change over a large enough range of physical conditions, even thermal conductivity, density, and specific heat, and they are all functions of moisture content. With heat transfer only solutions, we frequently accept this simplification, even though the thermal properties change as a function of moisture content. The problem is that the additional material properties needed for the mass transfer equations are even stronger functions of temperature and moisture content. The additional material properties needed are the porosity, water vapor diffusivity, and coefficients to represent the moisture capacitance; the amount of moisture in the material for that amount of material [kg moisture/kg dry solid] and is dimensionless. The moisture capacitance coefficients are the most non-linear, and are mainly functions of vapor density and temperature.

Typical Masonry Moisture Capacitance

The next 2 figures are curves for two groups of major construction materials used in buildings, masonry and wood. Investigating these typical curves show that there are linear planes in these curves that can be used, as appropriate, for a building simulation. Building elements with a typical diurnal cycle for the outside boundary conditions and typical thermostat settings for the inside boundary conditions can stay within these linear planes over a period of time.
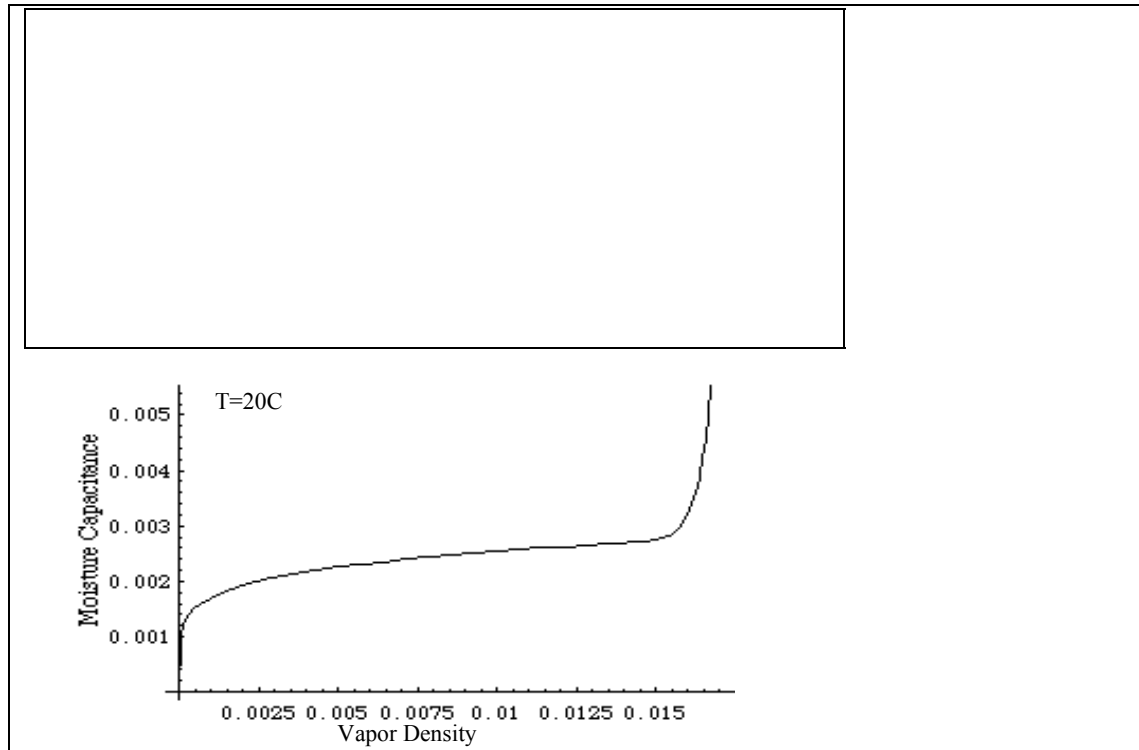
Figure 11. Masonary Moisture Capacitance Curves

The figure above shows us that there are some linear planes in the moisture capacitance curves. There are normally 3 distinct regions: funicular state, high moisture content with continuous threads of moisture in the pores; pendular state, the micropore surface is covered with thin molecular layers of moisture and intraporous capillary liquid bodies have reduced in significance; and the dry state, where the layer of moisture in the pores is essentially gone and all the moisture is in vapor. Most buildings are in the pendular state. The graph above shows there is a large linear plane that is in the pendular state. The bottom part of the figure above also shows a 2-D moisture isotherm from the 3-D graph. In the 2-D graph it is clear that there is a large portion in the pendular state where a transfer function analysis would be valid. The moisture capacitance coefficients that are used in the MTF formulation are a numerical fit of the linear plane in the 3-D graph for that material.

Typical Wood Moisture Capacitance
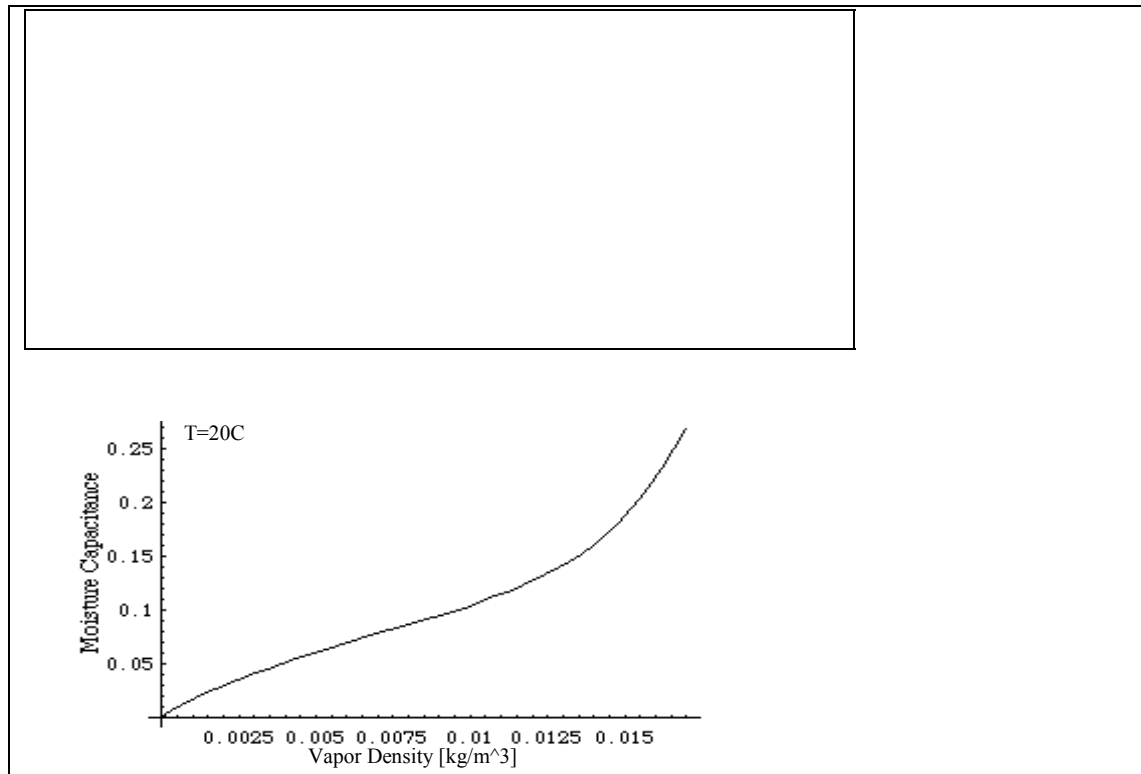
Figure 12. Wood Moisture Capacitance Curve

The same linear plane can be seen for wood in the pendular state in the figure above. Again, here it is very clear that there is a linear portion in the pendular state where a transfer function analysis would be valid. A linear fit of the plane in the pendular state is determined and the coefficients are used in a simulation. The example in the next section illustrates this assumption.

Linear Material Properties Example

The example is for an exterior wall building element with an exterior bricklayer, then fiberglass insulation, and finally a gypsum interior layer. The weather environment used for this example was an Atlanta Summer Design Day. First the environment weather extremes must be determined. In this case, the outside temperature ranges from 21.69°C to 33.25°C, while the inside ranges from 22.7°C to 24.3°C. The vapor densities range from 0.0162 to 0.01685 kg moisture/m^3 of air on the outside and 0.0123 to 0.0167 kg moisture/m^3 of air on the inside. The complete table for all the layer interfaces is shown in the table below, as determined from the simulation.

Table 2. Max & Min Temperatures and Vapor Densities for Atlanta Summer Design Day Simulation

	Outside	Out-Brick	Brick-Insul	Insul-Gyp	Gyp-Inside	Inside
Max Temperature	33.245834	47.63116	40.315024	26.014503	25.417565	24.316999
Min Temperature	21.695833	23.902025	26.034845	23.755466	23.633353	22.689005
Max Vapor Density	0.01685	0.016816	0.020962	0.018213	0.016458	0.016768
Min Vapor Density	0.016215	0.016281	0.01051	0.012284	0.012621	0.012331

From the Table above we can roughly determine the endpoints of the path that the moisture material properties traveled on the moisture capacitance curve.

Out = Interface facing the outdoors; In = Interface facing the zone interior
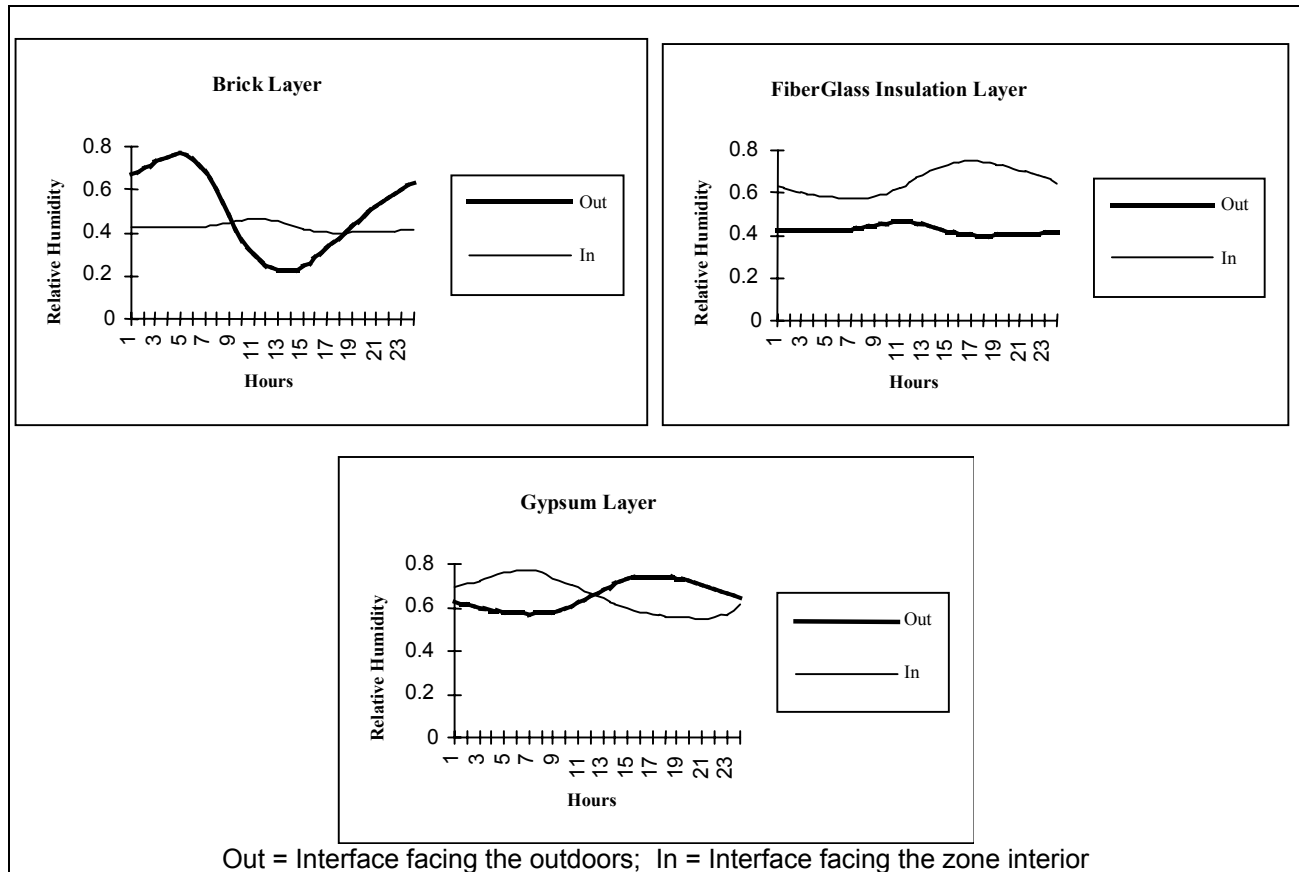
Figure 13. Relative Humidity Curves at Wall Element Interfaces

The figure above shows that none of the interfaces were above RH = 1.0 (100%), which means no condensation took place in this example. A rough straight-line path can be determined on the moisture capacitance curves. The dark dashed line shows a linear path between the 2 endpoints for each layer for the wall of Brick, Fiberglass Insulation, and Gypsum Drywall in the figures shown below. This linear path is obviously not the actual path, but the actual path should be in a band around the linear path. As determined from the simulation data, the actual path did not enter the invalid region of RH > 1.0 (100%); the actual interface relative humidity is never greater than 0.8 (80%), as shown in the figure above.
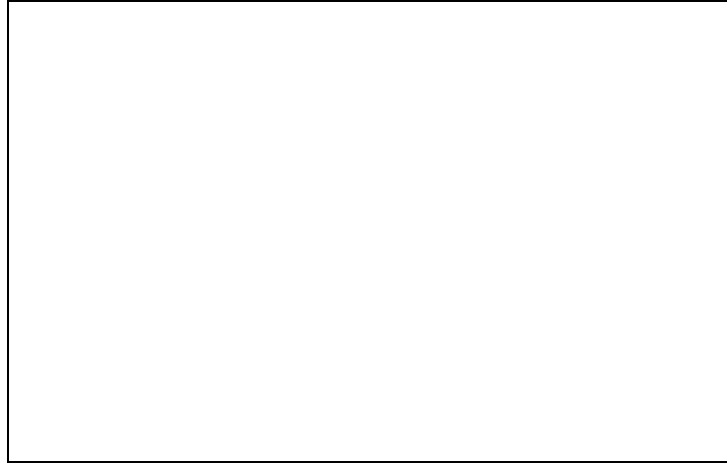
Figure 14. Moisture Capacitance Curve for Face Brick Layer

The approximate paths for all the wall materials are in or at the upper edges of the large linear plane that encompasses the pendular state, and further justifies the appropriateness of the linear assumptions for building analysis. Engineering judgment will have to be used when the temperature and vapor density conditions approach the upper and lower edges of the pendular state. Also, the upper right hand corner of each moisture capacitance curve corresponds to RH > 1.0 (100%), and is an invalid region. It should be noticed that the pendular state contains the majority of the moisture capacitance curves except as conditions approach RH = 1 (100%) and RH = 0 (0%), or the wet and dry extremes.

Figure 15. Moisture Capacitance for Fiber Glass Layer
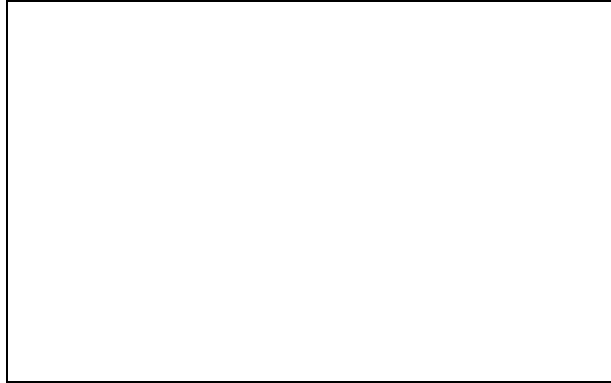
Figure 16. Moisture Capacitance for Gypsum Drywall

This example shows that, with proper selection, the linear sections of the moisture capacitance curve can be used in building simulations and a simulation using these moisture extensions can be a useful tool to examine many moisture problems. With the current implementation, it is difficult to use the MTF simulation approach for annual simulations without careful consideration of the moisture capacitance coefficients due to the moisture non-linearities.

References

Liesen, R.J., "Development of a Response Factor Approach For Modeling The Energy Effects of Combined Heat And Mass Transfer With Vapor Adsorption In Building Elements," Ph.D. Thesis, Department of Mechanical and Industrial Engineering, University of Illinois at Urbana-Champaign, 1994.

Liesen, R.J. and Pedersen, C.O., "Modeling the Energy Effects of Combined Heat and Mass Transfer in Building Elements; Part 1, Theory", ASHRAE Transactions, 1999

Outside Surface Heat Balance
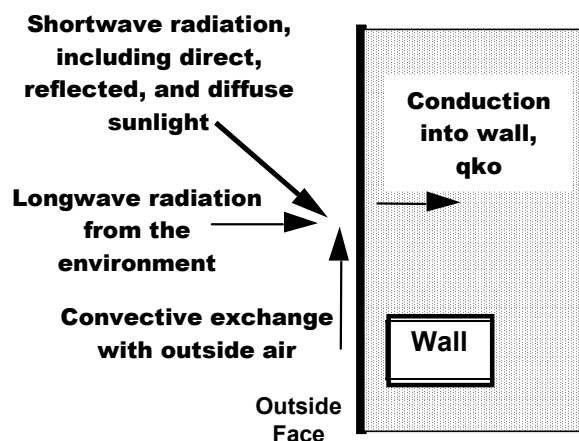
Figure 17. Outside Heat Balance Control Volume Diagram

The heat balance on the outside face is:

$$q''_{\alpha sol} + q''_{LWR} + q''_{conv} - q''_{ko} = 0 \tag{1.33}$$

where:

$q''_{\alpha sol}$ = Absorbed direct and diffuse solar (short wavelength) radiation heat flux.

q''_{LWR} = Net long wavelength (thermal) radiation flux exchange with the air and surroundings.

q''_{conv} = Convective flux exchange with outside air.

q''_{ko} = Conduction heat flux (q/A) into the wall.

All terms are positive for net flux to the face except the conduction term, which is traditionally taken to be positive in the direction from outside to inside of the wall. Simplified procedures generally combine the first three terms by using the concept of a *sol-air temperature*. Each of these heat balance components is introduced briefly below.

External SW Radiation

$q''_{\alpha sol}$ is calculated using procedures presented later in this manual and includes both direct and diffuse incident solar radiation absorbed by the surface face. This is influenced by location, surface facing angle and tilt, surface face material properties, weather conditions, etc..

External LW Radiation

q''_{LWR} is a standard radiation exchange formulation between the surface, the sky, and the ground. The radiation heat flux is calculated from the surface absorptivity, surface temperature, sky and ground temperatures, and sky and ground view factors.

External Convection

Convection is modeled using the classical formulation: q''_{conv} = h$_{co}$(T$_{air}$ - T$_{o}$) where h$_{co}$, is the convection coefficient. Several different methods are available for determining h$_{co}$. They will be discussed in more detail in a later section.

Conduction

The conduction term, q''_{ko}, can in theory be calculated using a wide variety of heat conduction formulations. In EnergyPlus, a Conduction Transfer Function (CTF) method is used. This model is described later ().

Inside Heat Balance

The heart of the heat balance method is the internal heat balance involving the inside faces of the zone surfaces. This heat balance is generally modeled with four coupled heat transfer components: 1) conduction through the building element, 2) convection to the air, 3) short wave radiation absorption and reflectance and 4) long wave radiant interchange. The incident short wave radiation is from the solar radiation entering the zone through windows and emittance from internal sources such as lights. The long wave radiation interchange includes the absorption and emittance of low temperature radiation sources, such as all other zone surfaces, equipment, and people.

The heat balance on the inside face can be written as follows:

$$q''_{LWX} + q''_{SW} + q''_{LWS} + q''_{ki} + q''_{sol} + q''_{conv} = 0 \qquad (1.34)$$

where:

q''_{LWX} = Net long wave radiant exchange flux between zone surfaces.

q''_{SW} = Net short wave radiation flux to surface from lights.

q''_{LWS} = Long wave radiation flux from equipment in zone.

q''_{ki} = Conduction flux through the wall.

q''_{sol} = Transmitted solar radiation flux absorbed at surface.

q''_{conv} = Convective heat flux to zone air.

Each of these heat balance components is introduced briefly below.
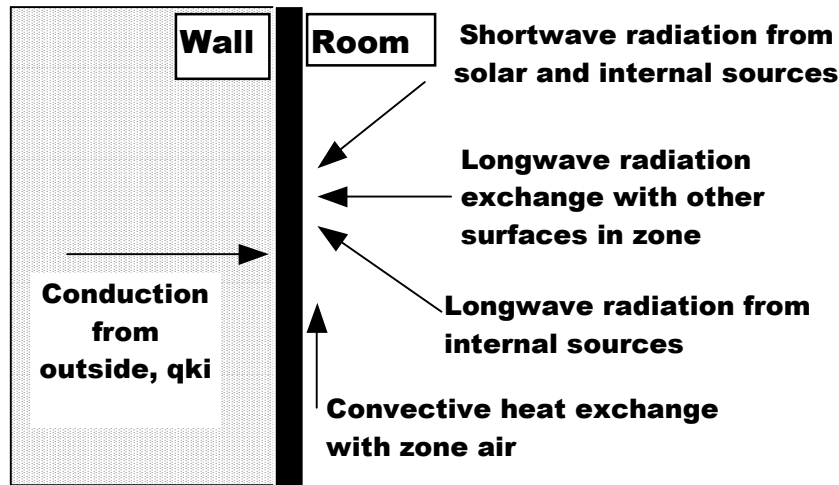
Figure 18. Inside Heat Balance Control Volume Diagram

Internal LW Radiation Exchange

LW Radiation Exchange Among Zone Surfaces

There are two limiting cases for internal LW radiation exchange that are easily modeled:

■   The zone air is completely transparent to LW radiation.

■   The zone air completely absorbs LW radiation from the surfaces within the zone.

The limiting case of completely absorbing air has been used for load calculations and also in some energy analysis calculations. This model is attractive because it can be formulated simply using a combined radiation and convection heat transfer coefficient from each surface to the zone air. However, it oversimplifies the zone surface exchange problem, and as a result, the heat balance formulation in EnergyPlus treats air as completely transparent. This means that it does not participate in the LW radiation exchange among the surfaces in the zone. The model, which considers room air to be completely transparent, is reasonable physically because of the low water vapor concentrations and the short mean path lengths. It also permits separating the radiant and convective parts of the heat transfer at the surface, which is an important attribute of the heat balance method.

Thermal Mass and Furniture

Furniture in a zone has the effect of increasing the amount of surface area that can participate in the radiation and convection heat exchanges. It also adds participating thermal mass to the zone. These two changes both affect the response to temperature changes in the zone and also affect the heat extraction characteristics.

The proper modeling of furniture is an area that needs further research, but the heat balance formulation allows the effect to be modeled in a realistic manner by including the furniture surface area and thermal mass in the heat exchange process.

LW Radiation From Internal Sources

The traditional model for this source is to define a radiative/convective split for the heat introduced into a zone from equipment. The radiative part is then distributed over the surfaces within the zone in some prescribed manner. This, of course, is not a completely realistic model, and it departs from the heat balance principles. However, it is virtually impossible to treat this source in any more detail since the alternative would require knowledge of the placement and surface temperatures of all equipment.

Internal SW Radiation

SW Radiation from Lights

The short wavelength radiation from lights is distributed over the surfaces in the zone in some prescribed manner.

Transmitted Solar

Transmitted solar radiation is also distributed over the surfaces in the zone in a prescribed manner. It would be possible to calculate the actual position of beam solar radiation, but that would involve partial surface irradiation, which is inconsistent with the rest of the zone model that assumes uniform conditions over an entire surface. The current procedures incorporate a set of prescribed distributions. Since the heat balance approach can deal with any distribution function, it is possible to change the distribution function if it seems appropriate.

Convection to Zone Air

The convection flux is calculated using the heat transfer coefficients as follows:

$$q''_{conv} = h_c \left(T_a - T_s \right) \tag{1.35}$$

The inside convection coefficients (h_c) can be calculated using one of several models. Currently the implementation uses coefficients based on natural convection correlations (3 options) and mixed and forced convection (1 option).

Conduction

This contribution to the inside surface heat balance is the wall conduction term, q''_{ki} shown in Equation (1.31). This represents the heat transfer to the inside face of the building element. Again, a CTF formulation is used to determine this heat flux.

Interior Convection

Four inside convection models are included in EnergyPlus: two natural convection models, a mixed / forced convection model, and a trombe wall convection model. Reference "Inside Convection Algorithm" object in the Input Output Reference document and the inside convection field for each zone. An overall default for the simulation is selected in the "Inside Convection Algorithm" object and can be overridden by selecting a different option in a zone description. These models are explained in the following sections.

Detailed Natural Convection Algorithm

The detailed natural convection model, which is based on flat plate experiments, correlates the convective heat transfer coefficient to the surface orientation and the difference between the surface and zone air temperatures (where $\Delta T =$ Surface Temp. – Air Temp.). The following algorithm is used:

For no temperature difference OR a vertical surface the following correlation is used.

$$h = 1.31 |\Delta T|^{\frac{1}{3}} \tag{1.36}$$

For (ΔT < 0.0 AND an upward facing surface) OR (ΔT > 0.0 AND an downward facing surface) an enhanced convection correlation is used.

$$h = \frac{9.482|\Delta T|^{\frac{1}{3}}}{7.283 - |\cos\Sigma|} \tag{1.37}$$

where Σ is the surface tilt angle.

For (ΔT > 0.0 AND an upward facing surface) OR (ΔT < 0.0 AND an downward facing surface) a reduced convection correlation is used.

$$h = \frac{1.810|\Delta T|^{\frac{1}{3}}}{1.382 + |\cos\Sigma|} \tag{1.38}$$

where Σ is the surface tilt angle.

Simple Natural Convection Algorithm

The simple convection model uses constant coefficients for each of three heat transfer configurations as follows. The model uses a criteria similar to the detailed model criteria to calculate reduced and enhanced convection scenarios, then assigns heat transfer coefficients as follows:

For a horizontal surface with reduced convection

$h = 0.948$

For a horizontal surface with enhanced convection

$h = 4.040$

For a vertical surface:

$h = 3.076$

For a Tilted surface with Reduced Convection

$h = 2.281$

For a Tilted surface with Enhanced Convection

$h = 3.870$

Ceiling Diffuser Algorithm

The ceiling algorithm is based on a room outlet temperature reference. The correlations shown in the figures below.

For Floors:

$$h = 3.873 + 0.082 * ACH^{0.98} \tag{1.39}$$

The correlation for floors is illustrated in the following figure:
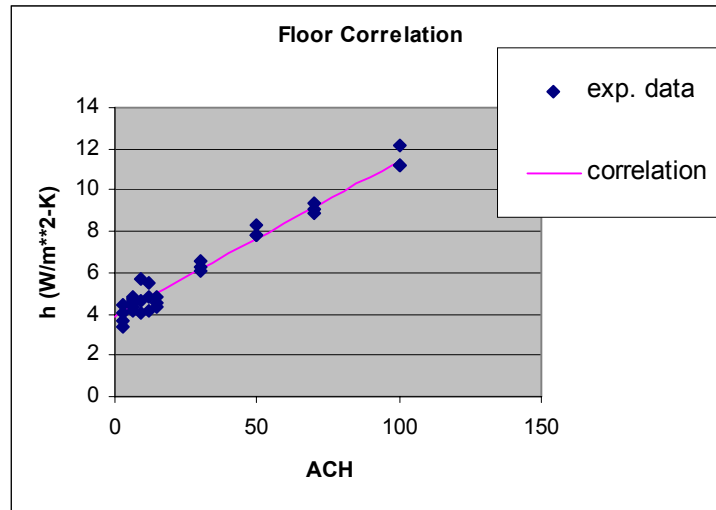
Figure 19. Ceiling Diffuser Correction for Floors

For ceilings:

$$h = 2.234 + 4.099 * ACH^{0.503}$$

(1.40)

The correlation for ceilings is illustrated in the following figure:
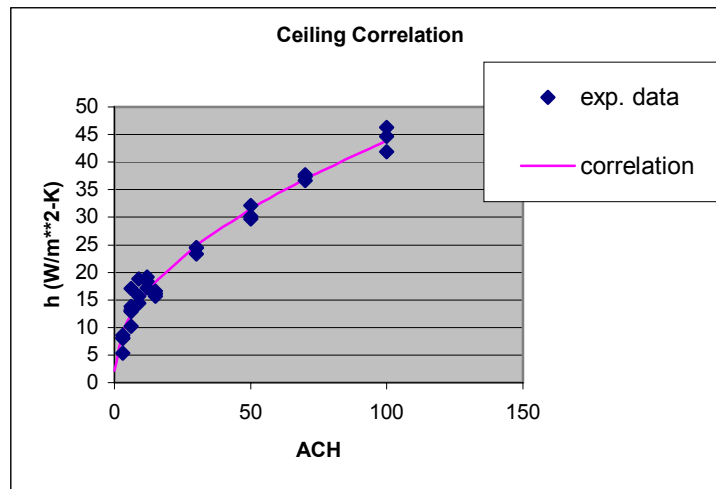
Figure 20. Ceiling Diffuser Correlation for Ceilings

For Walls:

$$h = 1.208 + 1.012 * ACH^{0.604}$$

(1.41)

The correlation for walls is illustrated in the following figure:
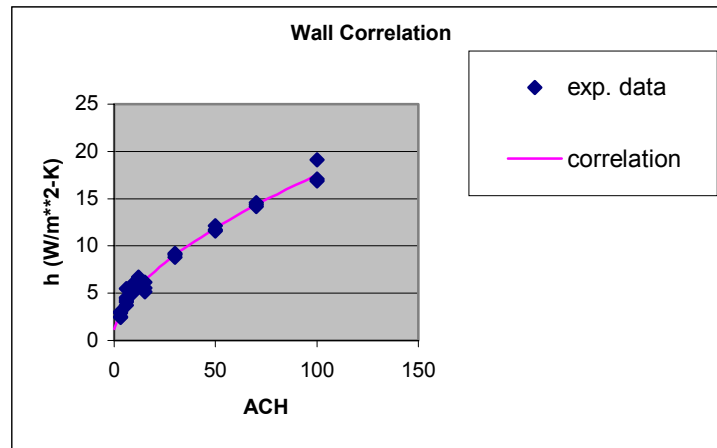
Figure 21. Ceiling Diffuser Correlation for Walls

Trombe Wall Algorithm

The Trombe wall algorithm is used to model convection in a "Trombe wall zone", i.e. the air space between the storage wall surface and the exterior glazing. (See the later sections on Passive and Active Trombe Walls below for more information about Trombe walls.)   The algorithm is identical to the convection model (based on ISO 15099) used in Window5 for convection between glazing layers in multi-pane window systems. Validation of this model for use with a Trombe wall has not yet been completed.

Exterior Convection

Substantial research has gone into the formulation of models for estimating the exterior surface convective heat transfer coefficient. Since the 1930's there have been many different methods published for calculating this coefficient, with much disparity between them (Cole and Sturrock 1977; Yazdanian and Klems 1994).   EnergyPlus can use two flavors of algorithms: detailed and simple.   Reference "Outside Convection Algorithm" object in the Input Output Reference document.

> Note that in either case (simple or detailed), when the outside environment indicates that it is raining, the exterior surfaces (exposed to wind) are assumed to be wet. The convection coefficient is set to a very high number (1000) so that the outside temperature used for the surface will be the wet bulb temperature. (If you choose to report this variable, you will see 1000 as its value.

Detailed Algorithm

Table 3. Fortran and Mathematical Variable Names for Convection calculations

Mathematical variables	Descriptions	Units	Ranges	FORTRAN variables
A	Surface area of the surface	m^2	/= 0	Surface%Area
h_c	Surface exterior convective heat transfer coefficient	$W/(m^2 K)$	-	HcOut
H_f	Forced convective heat transfer coefficient	$W/(m^2 K)$	-	Hf

H_n	Natural convective heat transfer coefficient	W/(m^{2}K)	-	Hn
P	Perimeter of surface	m	-	Perimeter
R_f	Surface roughness multiplier	-	-	RoughnessMultiplier
T_{air}	Environmental air temperature	°C	-	OutdoorDryBulb
T_{so}	Outside surface temperature	°C	-	TsOut
ΔT	Temperature difference between the surface and air,	°C	-	DeltaT
V_o	Wind speed at standard conditions	m/s	-	WindSpeed
V_{az}	Windspeed modified for height above ground	m/s	-	ModWindspeed
W_f	Wind direction modifier	-	-	WindDirectionModifier
z	Surface height above ground	M	/= 0	Surface%Height
z_o	height at which standard wind speed measurements are taken	M	= 10	StandardHeight
ϕ	Angle between the ground outward normal and the surface outward normal	degree	-	Tilt
α	Terrain-dependent coefficients	-	1~3	Terrain
α	Terrain-dependent coefficients	-	>0	Alpha
roughness index	Surface roughness index (6=very smooth, 5=smooth, 4=medium smooth, 3=medium rough, 2=rough, 1=very rough)	-	1~6	Surface%Roughness

In the detailed convection model, convection is split into forced and natural components (Walton 1981). The total convection coefficient is the sum of these components.

$$h_c = h_f + h_n \qquad (1.42)$$

The forced convection component is based on a correlation by Sparrow, Ramsey, and Mass (1979):

$$h_f = 2.537 \cdot W_f R_f \sqrt{\frac{PV_{az}}{A}} \qquad\qquad (1.43)$$

where

    W_f = 1.0 for windward surfaces

or

    W_f = 0.5 for leeward surfaces $\qquad\qquad (1.44)$

Leeward is defined as greater than 100 degrees from normal incidence (Walton 1981).

The surface roughness multiplier R_f is based on the ASHRAE graph of surface conductance (ASHRAE 1981) and may be obtained from the following table:

Table 4. Surface Roughness Multipliers (Walton 1981).

Roughness Index	R_f	Example Material
1 (Very Rough)	2.17	Stucco
2 (Rough)	1.67	Brick
3 (Medium Rough)	1.52	Concrete
4 (Medium Smooth)	1.13	Clear pine
5 (Smooth)	1.11	Smooth Plaster
6 (Very Smooth)	1.00	Glass

The wind speed is modified from the wind speed at standard conditions by the equation

$$V_{az} = V_o \cdot \left(z/10 \right)^{1/\alpha} \qquad\qquad (1.45)$$

The terrain-dependent coefficient α is given in the following table:

Table 5. Terrain Dependent Coefficients (Walton 1981).

Class	Description	α
1	Flat, open country	7.0
2	Rough, wooded country	3.5
3	Towns and cities	2.5

Based on the ASHRAE Handbook of Fundamentals (ASHRAE 1993), the natural convection component h_n (W/(m^2 K)) is

$$h_n = 9.482 \cdot \frac{\sqrt[3]{|\Delta T|}}{7.238 - |\cos\phi|} \quad \text{(for upward heat flow)} \qquad\qquad (1.46)$$

or

$$h_n = 1.810 \cdot \frac{\sqrt[3]{|\Delta T|}}{1.382 + |\cos\phi|} \quad \text{(while the heat flow is down)} \qquad (1.47)$$

Note that Equations (1.46) and (1.47) are equivalent when the wall is vertical.

Simple Algorithm

The simple algorithm uses roughness (a different correlation than above) and windspeed to calculate the exterior convection coefficient. The basic equation used is:

$$D_{roughness} + E_{roughness} \bullet WindSpeed + F_{roughness} \bullet Windspeed^2$$

The roughness correlation is taken from Figure 1, Page 22.4, ASHRAE Handbook of Fundamentals (ASHRAE 1989). Specifically, the D, E, and F coefficients are shown in the following table:

Table 6. Simple Exterior Convection Coefficients (D, E, F)

Roughness Index	D	E	F	Example Material
1 (Very Rough)	11.58	5.894	0.0	Stucco
2 (Rough)	12.49	4.065	0.028	Brick
3 (Medium Rough)	10.79	4.192	0.0	Concrete
4 (Medium Smooth)	8.23	4.0	-0.057	Clear pine
5 (Smooth)	10.22	3.1	0.0	Smooth Plaster
6 (Very Smooth)	8.23	3.33	-0.036	Glass

References

ASHRAE. 1981. 1981 ASHRAE Handbook – Fundamentals, Atlanta: American Society of Heating, Refrigerating, and Air-Conditioning Engineers, Inc.

ASHRAE. 1989. 1989 ASHRAE Handbook – Fundamentals, Atlanta: American Society of Heating, Refrigerating, and Air-Conditioning Engineers, Inc.

ASHRAE. 1993. 1993 ASHRAE Handbook – Fundamentals, Chapter 3, Heat Transfer, I-P & S-I Editions, Atlanta: American Society of Heating, Refrigerating, and Air-Conditioning Engineers, Inc.

Cole, R. J., and N. S. Sturrock. 1977. The Convective Heat Exchange at the External Surface of Buildings. Building and Environment, Vol. 12, p. 207.

Sparrow, E. M., J. W. Ramsey, and E. A. Mass. 1979. Effect of Finite Width on Heat Transfer and Fluid Flow about an Inclined Rectangular Plate. Journal of Heat Transfer, Vol. 101, p. 204.

Walton, G. N. 1981. Passive Solar Extension of the Building Loads Analysis and System Thermodynamics (BLAST) Program, Technical Report, United States Army Construction Engineering Research Laboratory, Champaign, IL.

Yazdanian, M. and J. H. Klems. 1994. Measurement of the Exterior Convective Film Coefficient for Windows in Low-Rise Buildings. ASHRAE Transactions, Vol. 100, Part 1, p. 1087.

Sky and Solar/Shading Calculations

Sky Radiance Model

In EnergyPlus the calculation of diffuse solar radiation from the sky incident on an exterior surface takes into account the anisotropic radiance distribution of the sky. This calculation is done when the user has chosen the anisotropic sky radiance option in BUILDING input (SkyRadianceDistribution = 1). In this case the diffuse sky irradiance on a surface is given by

AnisoSkyMult(SurfNum) * DifSolarRad

where DifSolarRad is the diffuse solar irradiance from the sky on the ground and SurfNum is the number of the surface.

AnisoSkyMult is determined by surface orientation and sky radiance distribution, and accounts for the effects of shading of sky diffuse radiation by shadowing surfaces such as overhangs. It does not account for *reflection* of sky diffuse radiation from shadowing surfaces.

The sky radiance distribution is based on an empirical model based on radiance measurements of real skies, as described in Perez et al., 1990. In this model the radiance of the sky is determined by three distributions that are superimposed (see Figure 22)

 (1) An isotropic distribution that covers the entire sky dome;

 (2) A circumsolar brightening centered at the position of the sun;

 (3) A horizon brightening.
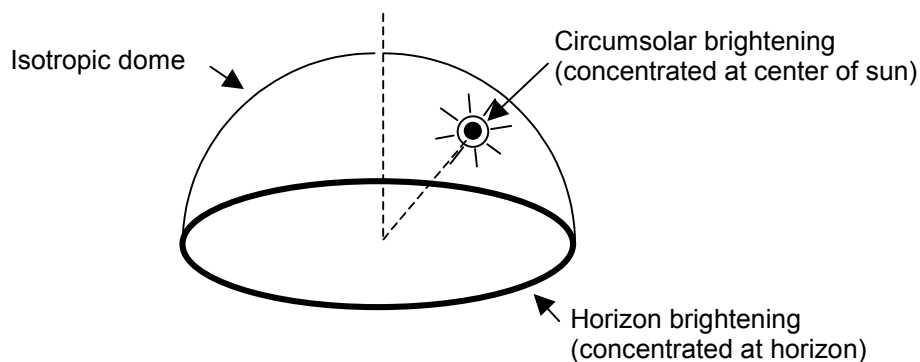
Figure 22. Schematic view of sky showing solar radiance distribution as a superposition of three components: dome with isotropic radiance, circumsolar brightening represented as a point source at the sun, and horizon brightening represented as a line source at the horizon.

The proportions of these distributions depend on the sky condition, which is characterized by two quantities, *clearness factor* and *brightness factor*, defined below, which are determined from sun position and solar quantities from the weather file.

The *circumsolar brightening* is assumed to be concentrated at a point source at the center of the sun although this region actually begins at the periphery of the solar disk and falls off in intensity with increasing angular distance from the periphery.

The *horizon brightening* is assumed to be a linear source at the horizon and to be independent of azimuth. In actuality, for clear skies, the horizon brightening is highest at the horizon and decreases in intensity away from the horizon. For overcast skies the horizon brightening has a negative value since for such skies the sky radiance increases rather than decreases away from the horizon.

Table 7. Variables in Anisotropic Sky Model and Shadowing of Sky Diffuse Radiation

Mathematical variable	Description	Units	FORTRAN variable
I_{sky}	Solar irradiance on surface from sky	W/m^2	-
$I_{horizon}$	Solar irradiance on surface from sky horizon	W/m^2	-
I_{dome}	Solar irradiance on surface from sky dome	W/m^2	-
$I_{circumsolar}$	Solar irradiance on surface from circumsolar region	W/m^2	-
I_h	Horizontal solar irradiance	W/m^2	-
S	Surface tilt	radians	Surface(SurfNum)%Tilt*DegTo Radians
a, b	intermediate variables	-	-
F_1, F_2	Circumsolar and horizon brightening coefficients	-	F1, F2
α	Incidence angle of sun on surface	radians	IncAng
Z	Solar zenith angle	radians	ZenithAng
Δ	Sky brightness factor	-	Delta
ε	Sky clearness factor	-	Epsilon
m	relative optical air mass	-	AirMass
I_O	Extraterrestrial solar irradiance	W/m^2	-
I	Direct normal solar irradiance	W/m^2	Material%Thickness
κ	constant = 1.041 for Z in radians	radians^{-3}	-
F_{ij}	Brightening coefficient factors	-	F11R, F12R, etc.
$R_{circumsolar}$	Shadowing factor for circumsolar radiation	-	SunLitFrac
R_{dome}	Shadowing factor for sky dome radiation	-	DifShdgRatioIsoSky
$R_{horizon}$	Shadowing factor for horizon radiation	-	DifShdgRatioHoriz
E	Sky radiance	W/m^2	-
θ	Azimuth angle of point in sky	radians	Theta
φ	Altitude angle of point in sky	radians	Phi
I_i	Irradiance on surface from a horizon element	W/m^2	-
I_{ij}	Irradiance on surface from a sky dome element	W/m^2	-
SF	Sunlit fraction	-	FracIlluminated

I'	Sky solar irradiance on surface with shadowing	W/m^2	-

Sky Diffuse Solar Radiation on a Tilted Surface

The following calculations are done in subroutine AnisoSkyViewFactors in the SolarShading module.

In the absence of shadowing, the sky formulation described above gives the following expression for sky diffuse irradiance, I_{sky}, on a tilted surface:

$$I_{sky} = I_{horizon} + I_{dome} + I_{circumsolar}$$

where

$$I_{horizon} = \text{irradiance on surface from sky horizon} = I_h F_2 \sin S$$
$$I_{dome} = \text{irradiance on surface from sky dome} = I_h (1 - F_1)(1 + \cos S)/2$$
$$I_{circumsolar} = \text{irradiance on surface from circumsolar region} = I_h F_1 a / b$$

AnisoSkyMult is then I_{sky}/DifSolarRad.

In the above equations:

I_h = horizontal solar irradiance (W/m^2)

S = surface tilt (radians)

a = max(0,cosα)

b = max(0.087, cos$Z$)

F_1 = circumsolar brightening coefficient

F_2 = horizon brightening coefficient

where

α = incidence angle of sun on the surface (radians)

Z = solar zenith angle (radians).

The brightening coefficients are a function of sky conditions; they are given by

$$F_1 = F_{11}(\varepsilon) + F_{12}(\varepsilon)\Delta + F_{13}(\varepsilon)Z$$
$$F_2 = F_{21}(\varepsilon) + F_{22}(\varepsilon)\Delta + F_{23}(\varepsilon)Z$$

Here the sky brightness factor is

$$\Delta = I_h m / I_o$$

where

m = relative optical air mass

I_o = extraterrestrial irradiance (taken to have an average annual value of 1353 W/m^2);

and the sky *clearness factor* is

$$\varepsilon = \frac{(I_h + I)/I_h + \kappa Z^3}{1 + \kappa Z^3}$$

where

I = direct normal solar irradiance

κ = 1.041 for Z in radians

The factors F_{ij} are shown in the following table.[1]

Table 8. F_{ij} Factors as a Function of Sky Clearness Range.

ε Range	1.000-1.065	1.065-1.230	1.230-1.500	1.500-1.950	1.950-2.800	2.800-4.500	4.500-6.200	> 6.200
F_{11}	-0.0083117	0.1299457	0.3296958	0.5682053	0.8730280	1.1326077	1.0601591	0.6777470
F_{12}	0.5877285	0.6825954	0.4868735	0.1874525	-0.3920403	-1.2367284	-1.5999137	-0.3272588
F_{13}	-0.0620636	-0.1513752	-0.2210958	-0.2951290	-0.3616149	-0.4118494	-0.3589221	-0.2504286
F_{21}	-0.0596012	-0.0189325	0.0554140	0.1088631	0.2255647	0.2877813	0.2642124	0.1561313
F_{22}	0.0721249	0.0659650	-0.0639588	-0.1519229	-0.4620442	-0.8230357	-1.1272340	-1.3765031
F_{23}	-0.0220216	-0.0288748	-0.0260542	-0.0139754	0.0012448	0.0558651	0.1310694	0.2506212

Shadowing of Sky Diffuse Solar Radiation

Sky diffuse solar shadowing on an exterior surface is calculated as follows in subroutine SkyDifSolarShading in the SolarShading module. The sky is assumed to be a superposition of the three Perez sky components described above.

For the horizon source the following ratio is calculated by dividing the horizon line into 24 intervals of equal length:

$$R_{horiz} = \frac{\text{Irradiance from horizon with obstructions}}{\text{Irradiance from horizon without obstructions}} = \frac{\sum_{i=1}^{24} I_i SF_i}{\sum_{i=1}^{24} I_i}$$

where I_i is the unobstructed irradiance on the surface from the ith interval, SF_i is the sunlit fraction from radiation coming from the ith interval, and the sums are over intervals whose center lies in front of the surface. SF_i is calculated using the beam solar shadowing method as though the sun were located at the ith horizon point. Here

$$I_i = E(\theta_i) d\theta \cos\alpha_i$$

where

$E(\theta_i)$ = radiance of horizon band (independent of θ)

$d\theta$ = $2\pi/24$ = azimuthal extent of horizon interval (radians)

θ_i = 0°, 15°, … , 345°

α_i = incidence angle on surface of radiation from θ_i

The corresponding ratio for the isotropic sky dome is given by

$$R_{dome} = \frac{\text{Irradiance from dome with obstructions}}{\text{Irradiance from dome without obstructions}} = \frac{\sum_{i=1}^{24}\sum_{j=1}^{6} I_{ij} SF_{ij}}{\sum_{i=1}^{24}\sum_{j=1}^{6} I_{ij}}$$

---

[1] The F_{ij} values in this table were provided by R. Perez, private communication, 5/21/99. These values have higher precision than those listed in Table 6 of Perez et al., 1990.

where (*i,j*) is a grid of 144 points (6 in altitude by 24 in azimuth) covering the sky dome, I_{ij} is the unobstructed irradiance on the surface from the sky element at the ij^{th} point, SF_{ij} is the sunlit fraction for radiation coming from the ij^{th} element, and the sum is over points lying in front of the surface. Here

$$I_{ij} = E(\theta_i, \phi_j) \cos\phi_j d\theta \, d\phi \, \cos\alpha_{ij}$$

where

$E(\theta_i, \varphi_j)$ = sky radiance (independent of θ and φ for isotropic dome)

$d\theta$ = 2π/24 = azimuthal extent of sky element (radians)

$d\varphi$ = (π/2)/6 = altitude extent of sky element (radians)

θ_i = 0°, 15°, … , 345°

φ_j = 7.5°, 22.5°, … , 82.5°

α_{ij} = incidence angle on surface of radiation from (θ_i, φ_j)

Because the circumsolar region is assumed to be concentrated at the solar disk, the circumsolar ratio is

$$R_{circumsolar} = \frac{\text{Irradiance from circumsolar region with obstructions}}{\text{Irradiance from circumsolar without obstructions}} = SF_{sun}$$

where SF_{sun} is the beam sunlit fraction. The total sky diffuse irradiance on the surface with shadowing is then

$$I'_{sky} = R_{horizon}I_{horizon} + R_{dome}I_{dome} + R_{circumsolar}I_{circumsolar}$$

$R_{horizon}$ and R_{dome} are calculated once for each surface since they are independent of sun position.

With shadowing we then have:

AnisoSkyMult = I'_{sky} /DifSolarRad.

Shadowing of Sky Long-Wave Radiation

EnergyPlus calculates the sky long-wave radiation incident on exterior surfaces assuming that the sky long-wave radiance distribution is isotropic. If obstructions such as overhangs are present the sky long-wave incident on a surface is multiplied by the isotropic shading factor, R_{dome}, described above. The long-wave radiation from these obstructions is added to the long-wave radiation from the ground; in this calculation both obstructions and ground are assumed to be at the outside air temperature and to have an emissivity of 0.9.

Shading Module

Shading and Sunlit Area Calculations

When assessing heat gains in buildings due to solar radiation, it is necessary to know how much of each part of the building is shaded and how much is in direct sunlight. As an example, the figure below shows a flat roofed, L-shaped structure with a window in each of the visible sides. The sun is to the right so that walls 1 and 3 and windows a and c are completely shaded, and wall 4 and window d are completely sunlit. Wall 2 and window b are partially shaded. The sunlit area of each surface changes as the position of the sun changes during the day. The purpose of the EnergyPlus shadow algorithm is to compute such sunlit

areas. Predecessors to the EnergyPlus shadowing concepts include the BLAST and TARP shadowing algorithms.

The shadow algorithm is based on coordinate transformation methods similar to Groth and Lokmanhekim and the shadow overlap method of Walton.
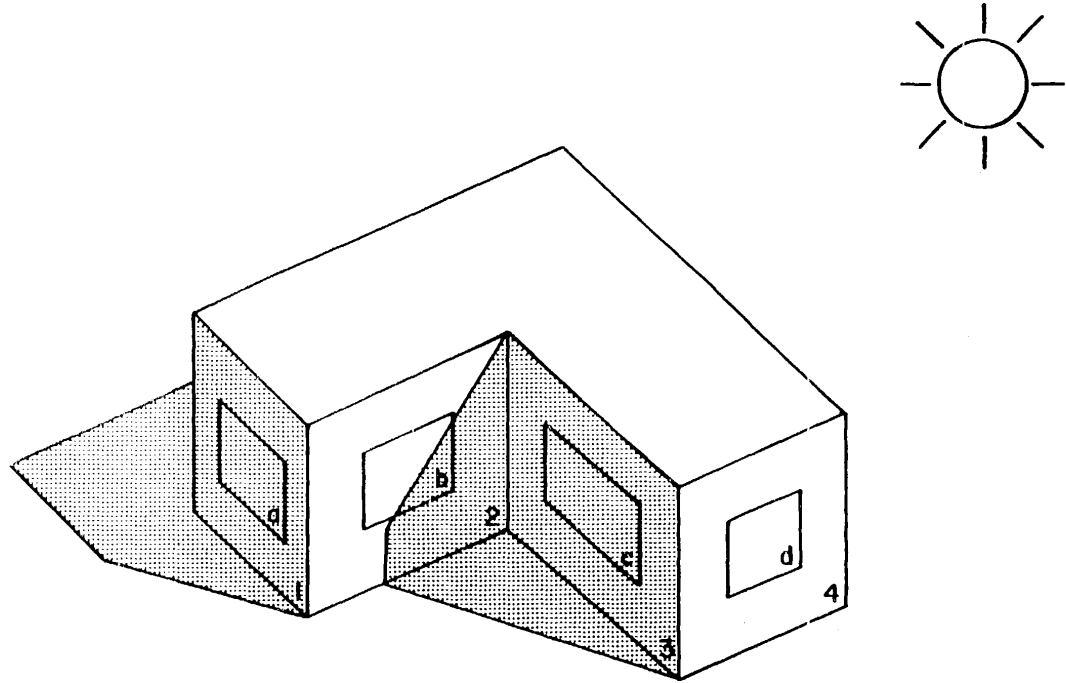
Figure 23. Overall Shadowing Scheme Depiction

Solar Position

Current solar position is described in terms of three direction cosines that are convenient for determining the angle of incidence of the sun's rays on a building surface. The following procedure is used to determine the direction cosines. The values of the solar declination angle, δ, and the equation of time, ε, are based on *Astronomical Algorithms*, Meeus. Solar declination is a function of local/site latitude.

The fractional year is calculated, in radians:

$$\gamma = \frac{2\pi}{366}(day\_of\_year)$$

From this fractional year, the equation of time and solar declination angle are calculated. For each time step (time value = fractional hour), the hour angle is calculated from:

$$HourAngle = \left(15 \bullet \left(12 - \left(TimeValue + EquationOfTime\right)\right) + \left(TimeZoneMeridian - Longitude\right)\right)$$

TimeZoneMeridian is the standard meridian for the location's time zone {GMT +/-}.

Solar HourAngle (*H*) gives the apparent solar time for the current time period (degrees); HourAngle is positive before noon, negative after noon. It is common astronomical practice to express the hour angle in hours, minutes and seconds of time rather than in degrees. You can convert the hour angle displayed from EnergyPlus to time by dividing by 15. (Note that 1

hour is equivalent to 15 degrees; 360° of the Earth's rotation takes place every 24 hours.) The relationship of angles in degrees to time is shown in the following table:

Table 9. Relationship of Angles (degrees) to Time

Unit of Angle	Equivalent time
1 radian	3.819719 hours
1 degree	4 minutes
1 arcmin	4 seconds
1 arcsec	0.066667 seconds

The Solar Altitude Angle (β) is the angle of the sun above the horizontal (degrees). The Solar Azimuth Angle (ϕ) is measured from the North (clockwise) and is expressed in degrees. This is shown more clearly in the following figure.
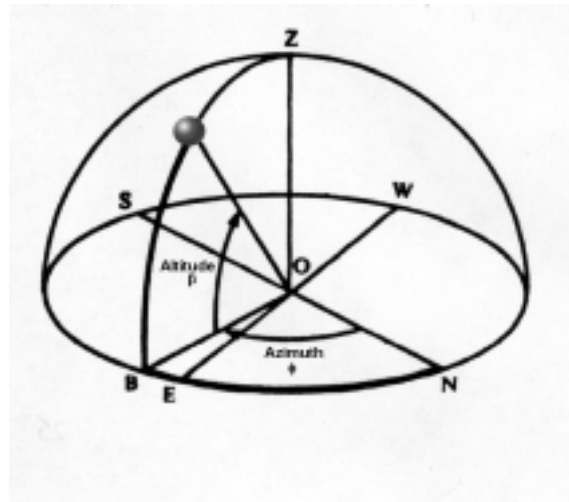
Figure 24. Solar Position Illustration

Surface Geometry

Shadow calculations first require that the building surfaces be described geometrically. Surfaces are described by the coordinates of their vertices in a three dimensional Cartesian coordinate system. This Right-hand coordinate system has the X-axis pointing east, the Y-axis pointing north, and the Z-axis pointing up (see figure below). The azimuth angle (ψ) of a surface is the angle from the north axis to the projection onto the X-Y plane of a normal to the surface (clockwise positive). The surface tilt angle (ϕ) is the angle between the Z-axis and the normal to the surface. The vertices are recorded in counter-clockwise sequence (as the surface is viewed from outside its zone).
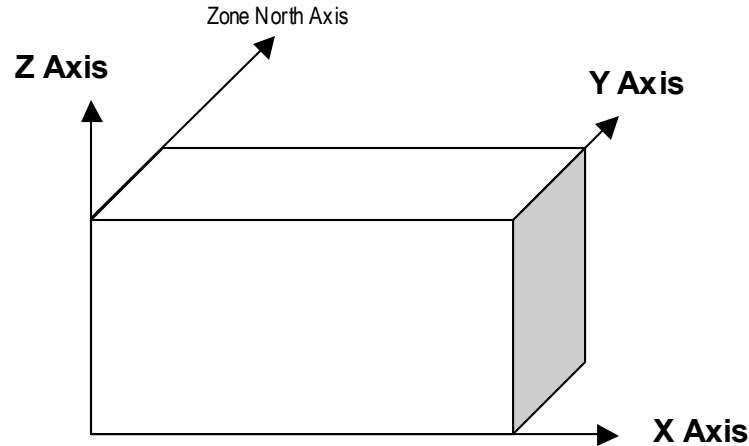
Figure 25. EnergyPlus Coordinate System

The SurfaceGeometry object specifies to EnergyPlus how the surface vertices will be presented in the input file. Of pertinent interest here is that the user may specify the vertices in either "relative" or "world" coordinates. Regardless of input specifications, when vertices are reported, they are reported in world coordinates, starting at the upper-left-corner (4-sided surface) and are listed counter-clockwise.

Relative Coordinate Transformation

When vertices are specified in "relative" coordinates, there can be a "building" north axis as well as a "zone" north axis. The building north axis/coordinate system is a rotation of ψ_b degrees from the global/world coordinate system. The global coordinates of zone origins are related to the building relative coordinates by:

$$X_{zo} = X_{br} \cdot \cos\psi_b - Y_{br} \cdot \sin\psi_b \tag{1.48}$$

$$Y_{zo} = Y_{br} \cdot \sin\psi_b - Y_{br} \cdot \cos\psi_b \tag{1.49}$$

$$Z_{zo} = Z_{br} \tag{1.50}$$

Where

zo – represents Zone Origin

br – represents the Zone Origin as input (relative to building origin)

The zone may also be rotated ψ_z degrees relative to the building coordinates. Origins of zone surfaces are then given relative to the zone coordinate system. The global coordinates of the surface origins are calculated by:

$$X_{so} = X_{zo} + X_{zr} \cdot \cos\psi_z - Y_{zr} \cdot \sin\psi_z \tag{1.51}$$

$$Y_{so} = Y_{zo} + X_{zr} \cdot \sin\psi_z - Y_{zr} \cdot \cos\psi_z \tag{1.52}$$

$$X_{so} = X_{zo} + X_{zr} \cdot \cos\psi_z - Y_{zr} \cdot \sin\psi_z \tag{1.53}$$

A surface azimuth angle relative to the zone coordinate system (ψ_s) is converted to a global azimuth by:

$$\psi = \psi_s + \psi_z + \psi_b \tag{1.54}$$

The surface tilt angle (ϕ) is not changed by these rotations about the Z-axis.

The coordinates of the surface vertices are given in a coordinate system in the plane of the surface relative to the second vertex as shown for surfaces in Figure 25. The X-axis of the surface coordinate system is a horizontal line through the second vertex. The global coordinates of the surface vertices are given by:

$$X = X_{so} + X_{sr} \bullet \cos\psi - Y_{sr} \bullet \sin\psi \bullet \cos\phi \tag{1.55}$$

$$Y = Y_{so} + X_{sr} \bullet \sin\psi - Y_{sr} \bullet \cos\psi \bullet \cos\phi \tag{1.56}$$

$$Z = Z_{so} + Y_{sr} \bullet \sin\phi \tag{1.57}$$

World Coordinates ➔ Relative Coordinates

Vertices in the global coordinate system can be transformed to the coordinate system relative to a given surface by

$$X' = X - X_{so} \tag{1.58}$$

$$Y' = Y - Y_{so} \tag{1.59}$$

$$Z' = Z - Z_{so} \tag{1.60}$$

$$X_{sr} = -X' \bullet \cos\psi + Y' \bullet \sin\psi \tag{1.61}$$

$$Y_{sr} = -X' \bullet \sin\psi \bullet \cos\phi + Y' \bullet \cos\psi \bullet \cos\phi + Z' \bullet \sin\phi \tag{1.62}$$

$$Z_{sr} = -X' \bullet \sin\psi \bullet \sin\phi + Y' \bullet \cos\psi \bullet \sin\phi + Z' \bullet \cos\phi \tag{1.63}$$

Shadow Projection

All architectural forms are represented by plane polygons. This can give good accuracy even for curved surfaces: a sphere can be approximated by the 20 nodes of an icosohedron with only 3 percent error in the shadow area cast by the sphere. Consider how a solid object, which is composed of a set of enclosing plane polygons, casts a shadow. Figure 26 shows a box shaped structure on a horizontal surface. The structure consists of a top (surface 1) and four vertical surfaces (2 and 3 visible to the observer and 4 and 5 not visible). The sun is positioned behind and to the right of the structure and a shadow is cast onto the horizontal surface (the ground).

Surfaces 1, 4, and 5 are in sunlight; 2 and 3 are in shade. It is possible to think of the structure's shadow as the combination of shadows cast by surfaces 1, 2, 3, 4 and 5 or by 1, 4 and 5, or by surfaces 2 and 3. This last combination of shadow casting surfaces is the simplest. In the EnergyPlus shadow algorithm every surface is considered to be one of the

surfaces that enclose a solid, and only those surfaces that are not sunlit at a given hour are considered shadowing surfaces.
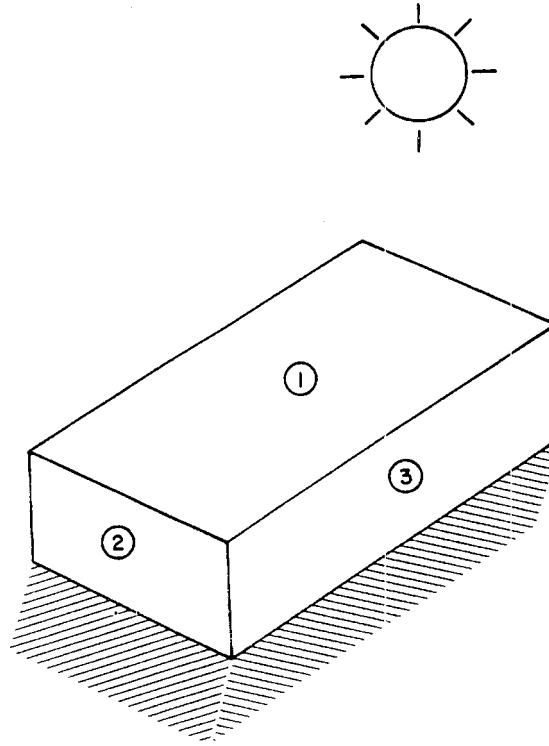
Figure 26. Basic shadowing concept structure

The expressions in equation (1.63) are the direction cosines of the surface:

$$CW_1 = \sin\psi \cdot \cos\phi \tag{1.64}$$

$$CW_2 = \cos\psi \cdot \sin\phi \tag{1.65}$$

$$CW_3 = \cos\phi \tag{1.66}$$

The cosine of the angle of incidence of the sun's rays on the surface are given by the dot product of surface and sun direction cosines.

$$\cos\theta = CS_1 \cdot CW_1 + CS_2 \cdot CW_2 + CS_3 \cdot CW_3 \tag{1.67}$$

If $\cos\theta$ is less than zero, the sun is behind the surface.

A shadow is projected from the vertices of the shadowing polygon (SP) along the direction of the sun's rays to the plane of the shadow receiving polygon (RP). If any vertices of the SP are below the plane of the RP (z < 0), a false shadow is cast as in Figure 27. The "submerged" portion of the SP must be clipped off before projection.
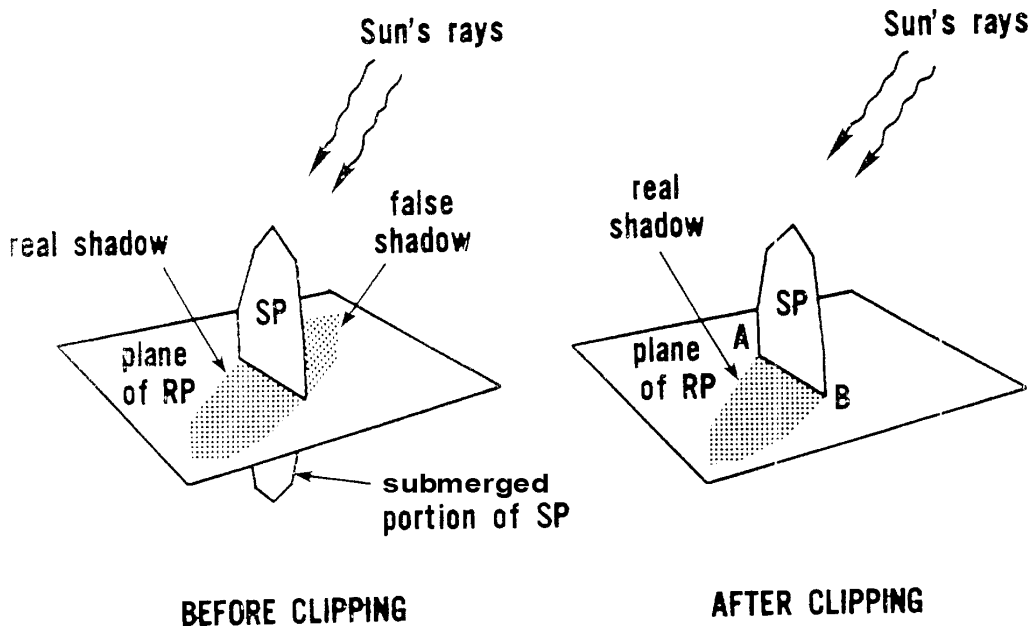
Figure 27. Illustration of Shadow Clipping

This is done by finding, through linear interpolation, the points on the perimeter of the SP, which intersect the plane of the RP. These points become new vertices of the SP, which together with the other positive vertices define a clipped SP that casts only a real shadow.

A vertex located at (x, y, z) relative to the RP coordinate system casts a shadow to a point in the plane of the RP given by

$$x^{'} = x - \frac{z \cdot a}{\cos\theta} \qquad\qquad (1.68)$$

$$y^{'} = y - \frac{z \cdot b}{\cos\theta} \qquad\qquad (1.69)$$

where

$$a = \sin\psi \cdot CS_1 - \cos\psi \cdot CS_2$$

and

$$b = -\cos\psi \cdot \cos\phi \cdot CS_1 - \sin\psi \cdot \cos\phi \cdot CS_2 + \sin\phi \cdot CS_3$$

Homogeneous Coordinates

Two-dimensional homogeneous coordinate techniques are used to determine the vertices of shadow overlaps. In homogeneous coordinates, points and lines are represented by a single form that allows simple vector operations between those forms [Newman-Sproul]. A point (X, Y) is represented by a three element vector (x, y, w) where x = w*X, y = w*Y, and w is any real number except zero. A line is also represented by a three element vector (a, b, c). The directed line (a, b, c) from point (x_1, y_1, w_1) to point (x_2, y_2, w_2) is given by:

$$(a, b, c) = (x_1, y_1, z_1) \otimes (x_2, y_2, z_2) \qquad\qquad (1.70)$$

The sequence in the cross product is a convention to determine sign. The condition that a point (x, y, w) lie on a line (a, b, c) is that

$$(a,b,c) \bullet (x, y, w) = 0 \tag{1.71}$$

The point is normalized by dividing by w. Then if

$$(a,b,c) \bullet (x/w, y/w, 1) > 0 \tag{1.72}$$

the point is to the left of the line. If it is less than zero, the point is to the right of the line. The intercept (x, y, w) of line (a_1, b_1, c_1) and line (a_2, b_2, c_2) is given by:

$$(x, y, w) = (a_1, b_1, c_1) \otimes (a_2, b_2, c_2) \tag{1.73}$$

Note that the use of homogeneous coordinates as outlined above provides a consistent method and notation for defining points and lines, for determining intercepts, and for determining whether a point lies to the left, to the right, or on a line. Normalization provides the means for transforming to and from homogeneous notation and Cartesian coordinates. Thus, if (X, Y) is a Cartesian coordinate pair, its homogeneous coordinates are (X, Y, 1). Similarly, the homogeneous coordinates (x, y, w) can be transformed to the Cartesian point with coordinates (x/w, y/w).

Overlapping Shadows

After transforming the shadows onto the plane of the receiving surface, the basic job of the shadow algorithm is to determine the area of the overlap between the polygons representing the shadows and the polygon representing the receiving surface.

There is considerable simplification if only convex (no interior angle > 180) polygons are considered. The overlap between two convex polygons is another convex polygon. Coordinate and projection transformations of a convex polygon produce another convex polygon. Any non-convex polygon can be constructed as a sum of convex ones.

The vertices that define the overlap between two convex polygons, A and B, consist of:

1) the vertices of A enclosed by B

2)   the vertices of B enclosed by A

3) and the intercepts of the sides of A with the sides of B

In Figure 28, point a is the result of rule 1, point c is the result of rule 2, and points b and d result from rule 3. The overlap of A and B is the polygon a-b-c-d. Figure 29 shows an overlap where all of the vertices of B are enclosed by A. Figure 30 shows an overlap defined only by the intercepts of A and B. Figure 31 shows a more complex overlap.
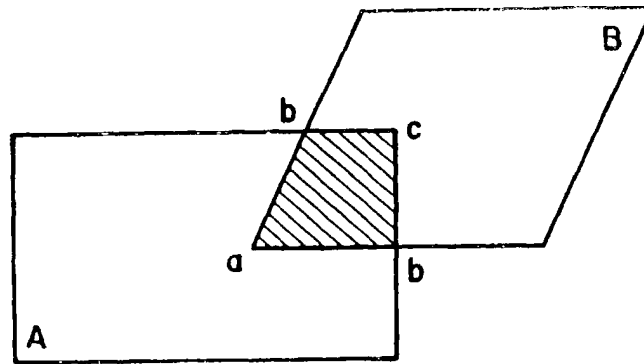
Figure 28. Point a – vertex of A enclosed by B

Coordinate transformation retains the order of the vertices of a polygon, while a projection reverses the order. The sequence of vertices of the receiving polygons should be reversed so it and all shadow polygons will have the same sequence.
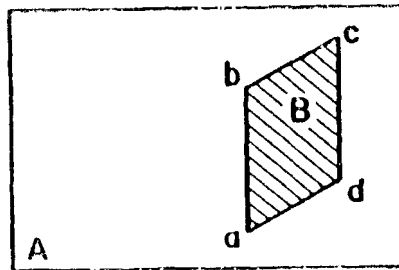
Figure 29. Surface A totally overlaps Surface B.

A point is enclosed by a clockwise, convex polygon if the point lies to the right of all sides (or does not lie to the left of any side) of the polygon. The intercept of two sides may not lie beyond the ends of either side. These are "line segments" rather than "lines". It is possible to tell if line segments A and B intercept within their end points by noting that the ends of A must lie on both sides of B, and the ends of B must lie on both sides of A. This should be done before the intercept is calculated.
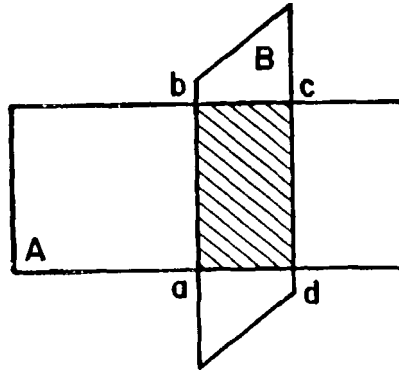
Figure 30. Figure formed from Intercept Overlaps between A and B

Once the vertices are determined, they must be sorted into clockwiseorder for the area to be computed. Given a closed, planar polygon of n sequential vertices (x_1, y_1), (x_2, Y_2) …, (x_n, Y_n), its **area** is given:

$$Area = \tfrac{1}{2}\sum_{i=1}^{n}(x_i y_{i+1} - x_{i+1} y_i)$$

(1.74)

where $(x_{n+1}, y_{n+1}) = (x_1, y_1)$

The area is positive if the vertices are counter-clockwise and negative if they are clockwise.
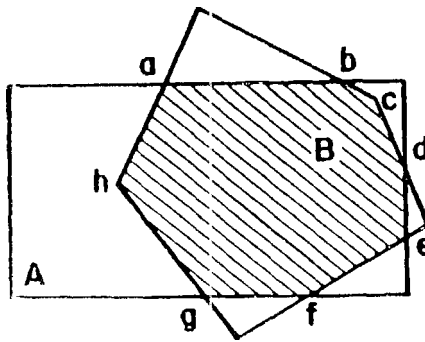
Figure 31. Complex overlapping condition

If two shadows overlap the receiving surface, they may also overlap each other as in Figure 32. The vertices of this overlap can be computed. The areas of all overlaps can be computed. The total sunlit area can be expressed as the sum of all polygon areas given a proper sign on each of the areas.

The following convention was adopted:

Surface Characteristic	Area Convention
receiving surface	positive (A)
overlap between shadow and receiving	negative (B & C)
overlap between two shadows	positive (D)

and so on through multiple overlaps where the sign of the overlap area is the product of the signs of the overlapping areas.
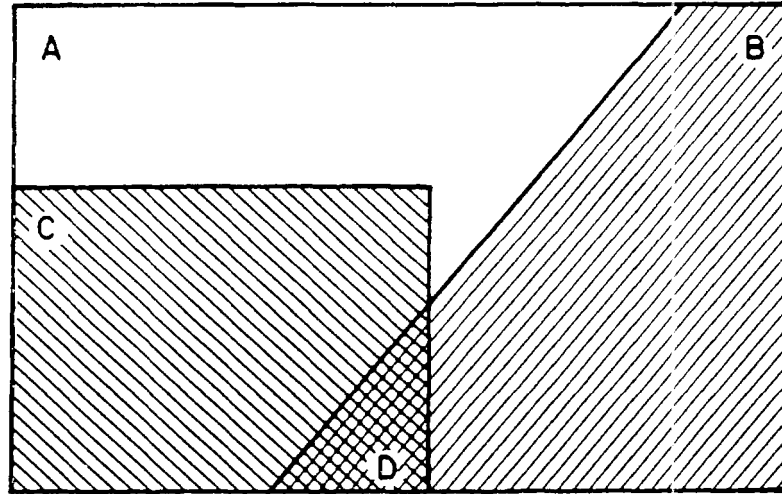
Figure 32. Multiple Shadow Overlaps

Partially transparent shadowing surfaces can also be modeled by giving a transparency (τ) to every shadowing polygon. Let τ of the receiving polygon be one. Then the τ of every overlap of polygons i and j is the product of τ_i and τ_j The shaded area is then computed by summing $A_i \bullet (1 - \tau_i)$ for all overlap polygons.

It is easy to determine the sunlit area of a window once all the shadow and overlap vertices on the wall have been computed. Consider wall 2 of figure E.1. First the wall is considered a simple rectangle and the window on it is ignored. The shadow overlapping is performed and the sunlit portion of the gross wall area is computed. Then the window rectangle is overlapped with the shadow to determine its sunlit area. The sunlit area of the window is subtracted from the gross wall sunlit area to determine the net wall sunlit area. During this calculation it is not necessary to recompute the shadows, because they were precisely determined on the wall.

Solar Gains

The total solar gain on any exterior surface is a combination of the absorption of direct and diffuse solar radiation given by

$$Q_{so} = \alpha \bullet \left(\frac{I_b \bullet \cos\theta \bullet S_s}{S + I_s \bullet F_{ss} + I_g \bullet F_{sg}} \right) \qquad (1.75)$$

where

a =solar absorptance of the surface

A =angle of incidence of the sun's rays

S =area of the surface

S_s = sunlit area

I_b =intensity of beam (direct) radiation

I_s =intensity of sky diffuse radiation

I_g =intensity of ground reflected diffuse radiation

F_{ss} = angle factor between the surface and the sky

F_{sg} = angle factor between the surface and the ground

For the surface of a building located on a featureless plain

$$F_{ss} = \frac{1 + \cos\phi}{2}$$
(1.76)

and

$$F_{sg} = \frac{1 - \cos\phi}{2}$$
(1.77)

If the surface is shaded the program modifies F_{ss} by a correction factor that takes into account the radiance distribution of the sky (see "Shadowing of Sky Diffuse Solar Radiation").

Shading of ground diffuse solar radiation is not calculated by the program. It is up to the user to estimate the effect of this shading and modify the input value of F_{sg} accordingly.

Solar Distribution

As discussed in the Input Output Reference (Object:Building), the solar distribution field value determines how EnergyPlus will treat beam solar radiation entering a zone through exterior windows. There are three choices: **MinimalShadowing**, **FullExterior** and **FullInteriorAndExterior**.

MinimalShadowing

In this case, there is no exterior shadowing except from window and door reveals. All beam solar radiation entering the zone is assumed to fall on the floor, where it is absorbed according to the floor's solar absorptance. Any reflected by the floor is added to the transmitted diffuse radiation, which is assumed to be uniformly distributed on all interior surfaces. If no floor is present in the zone, the incident beam solar radiation is absorbed on all interior surfaces according to their absorptances. The zone heat balance is then applied at each surface and on the zone's air with the absorbed radiation being treated as a flux on the surface.

FullExterior

In this case, shadow patterns on exterior surfaces caused by detached shading, wings, overhangs, and exterior surfaces of all zones are computed. As for MinimalShadowing, shadowing by window and door reveals is also calculated. Beam solar radiation entering the zone is treated as for MinimalShadowing.

FullInteriorAndExterior

This is the same as FullExterior except that instead of assuming all transmitted beam solar falls on the floor the program calculates the amount of beam radiation falling on each surface in the zone, including floor, walls and windows, by projecting the sun's rays through the exterior windows, taking into account the effect of exterior shadowing surfaces and window shading devices.

If this option is used, you should be sure that the surfaces of the zone totally enclose a space. This can be determined by viewing the **eplusout.dxf** file with a program like AutoDesk's Volo View Express. You should also be sure that the zone is **convex**. Examples of convex and non-convex zones are shown in the figure below. The most common non-convex zone is an L-shaped zone. (A formal definition of convex is that any straight line

passing through the zone intercepts at most two surfaces.) If the zone's surfaces do not enclose a space or if the zone is not convex you should use Solar Distribution = **FullExterior** instead of **FullInteriorAndExterior**.

If you use **FullInteriorAndExterior** the program will calculate how much beam radiation falling on an interior window is absorbed by the window, how much is reflected back into the zone, and how much is transmitted into the adjacent zone. (Interior windows are assumed to have no shading device). Note, however, that daylighting through interior windows is not calculated.

If you use **FullInteriorAndExterior** the program will also calculate how much beam radiation falling on the inside of an exterior window (from other windows in the zone) is absorbed by the window, how much is reflected back into the zone, and how much is transmitted to the outside. In this calculation the effect of an interior or exterior shading device, if present, is accounted for.

Convex zones   Non-Convex zones
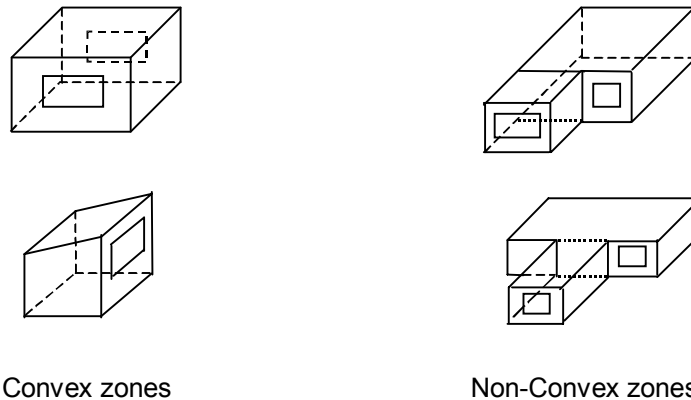
Figure 33. Illustration of Convex and Non-convex Zones

References

Groth, C. C., and Lokmanhekim, M., "Shadow - A New Technique for the Calculation of Shadow Shapes and Areas by Digital Computer," Second Hawaii International Conference on System Sciences, (Honolulu, HI, January 22-24, 1969).

Walton, G.N., "The Thermal Analysis Research Program Reference Manual Program (TARP)", National Bureau of Standards (now National Institute of Standards and Technology), Febrary 1983.

Walton, G. N., "The Application of Homogeneous Coordinates to Shadowing Calculations", ASHRAE Transactions, Vol 84 (ASHRAE, 1978), Part I.

Meeus, Jean, Astronomical Algorithms, (Willmann-Bell, 2000).

Newman, M. W., and Sproul, R. F., Principles of Interactive Computer Graphics, (McGraw-Hill, 1973).

Polygon area derived from Green's Theorem. Graphic Gems repository.

Daylighting and Window Calculations

Daylighting Calculations

The EnergyPlus daylighting model, in conjunction with the thermal analysis, determines the energy impact of daylighting strategies based on analysis of daylight availability, site conditions, window management in response to solar gain and glare, and various lighting control strategies.

The daylighting calculation has three main steps:

(1) *Daylight factors*, which are ratios of interior illuminance or luminance to exterior horizontal illuminance, are calculated and stored. The user specifies the coordinates of one or two reference points in each daylit zone. EnergyPlus then integrates over the area of each exterior window in the zone to obtain the contribution of direct light from the window to the illuminance at the reference points, and the contribution of light that reflects from the walls, floor and ceiling before reaching the reference points. Window luminance and window background luminance, which are used to determine glare, are also calculated. Taken into account are such factors as sky luminance distribution, window size and orientation, glazing transmittance, inside surface reflectances, sun control devices such as movable window shades, and external obstructions. Dividing daylight illuminance or luminance by exterior illuminance yields daylight factors. These factors are calculated for the hourly sun positions on sun-paths for representative days of the run period.

(2) A daylighting calculation is performed each heat-balance time step when the sun is up. In this calculation the illuminance at the reference points in each zone is found by interpolating the stored daylight factors using the current time step's sun position and sky condition, then multiplying by the exterior horizontal illuminance. If glare control has been specified, the program will automatically deploy window shading, if available, to decrease glare below a specified comfort level. A similar option uses window shades to automatically control solar gain.

(3) The electric lighting control system is simulated to determine the lighting energy needed to make up the difference between the daylighting illuminance level and the design illuminance. Finally, the zone lighting electric reduction factor is passed to the thermal calculation, which uses this factor to reduce the heat gain from lights.

The EnergyPlus daylighting calculation is derived from the daylighting calculation in DOE-2.1E, which is described in [Winkelmann, 1983] and [Winkelmann and Selkowitz, 1985]. There are two major differences between the two implementations: (1) In EnergyPlus daylight factors are calculated for four different sky types—clear, clear turbid, intermediate, and overcast; in DOE-2 only two sky types are used—clear and overcast. (2) In EnergyPlus the clear-sky daylight factors are calculated for hourly sun-path sun positions several times a year whereas in DOE-2 these daylight factors are calculated for a set of 20 sun positions that span the annual range of sun positions for a given geographical location.

Daylight Factor Calculation

Table 10. Variables in Daylighting Calculations

Mathematical variable	Description	Units	FORTRAN variable
$E_{h,sky}$	Exterior horizontal illuminance due to light from the sky	lux	GILSK

$E_{h,sun}$	Exterior horizontal illuminance due to light from the sun	lux	GILSU
d_{sky}, d_{sun}	Interior illuminance factor due to sky, sun related light	-	DFACSK, DFACSU
w_{sky}, w_{sun}	Window luminance factor due to sky, sun related light	cd/lm	SFACSK, SFACSU
b_{sky}, b_{sun}	Window background luminance factor due to sky, sun related light	cd/lm	BFACSK, BFACSU
N	Number of exterior windows in a zone	-	NWD
θ_{sky}, φ_{sky}	Azimuth and altitude angles of a point in the sky	radians	THSKY, PHSKY
ψ_{cs}	Clear sky luminance distribution	cd/m^2	-
ψ_{ts}	Clear turbid sky luminance distribution	cd/m^2	-
ψ_{is}	Intermediate sky luminance distribution	cd/m^2	-
ψ_{os}	Overcast sky luminance distribution	cd/m^2	-
φ_{sun}	Altitude angle of the sun	radians or degrees	PHSUN
γ	Angle between point in the sky and the sun; or angle between vertical and ray from reference point to window element	radians	G
L_z	Sky zenith luminance	cd/m^2	ZENL
m	Optical air mass of the atmosphere	m	AM
h	Building altitude	m	Elevation
$E_{h,k}$	Exterior horizontal illuminance for sky type k	lux	-
N_θ, N_φ	Number of azimuth, altitude steps for sky integration		NTH, NPH
$\vec{R}_{ref}$	Vector from zone origin to reference point	m	RREF
$\vec{R}_{win}$	Vector from zone origin to window element	m	RWIN
$d\Omega$	Solid angle subtended by window element	steradians	DOMEGA
L_w	Luminance of a window element as seen from reference point	cd/m^2	WLUMSK, WLUMSU
$L_{w,shade}$	Luminance of window element with shade in place	cd/m^2	WLUMSK, WLUMSU

dE_h	Horizontal illuminance at reference point from window element	lux	-
dx, dy	Size of window element	m	DWX, DWY
D	Distance from reference point to window element	m	DIS
B	Angle between window element's outward normal and ray from reference point to window element	radians	-
$\hat{R}_{ray}$	Unit vector from reference point to window element	-	RAY
$\hat{W}_n$	Unit vector normal to window element, pointing away from zone	-	WNORM
$\hat{W}_{21}$	Unit vector along window y-axis	-	W21
$\hat{W}_{23}$	Unit vector along window x-axis	-	W23
τ_{vis}	Glass visible transmittance	-	TVISB
L	Luminance of sky or obstruction	cd/m^2	ELUM, -
Φ_{FW}	Downgoing luminous flux from a window	lm	FLFW--
Φ_{CW}	Upgoing luminous flux from a window	lm	FLCW--
F_1	First-reflected flux	lm	-
ρ_{FW}	Area-weighted reflectance of floor and upper part of walls	-	SurfaceWindow%RhoFloorWall
ρ_{CW}	Area-weighted reflectance of ceiling and upper part of walls	-	SurfaceWindow%RhoCeilingWall
E_r	Average internally-reflected illuminance	lux	EINTSK, EINTSU
A	Total inside surface area of a zone	m^2	ATOT
ρ	Area-weighted average reflectance of zone interior surfaces	-	ZoneDaylight%AveVisDiffReflect
θ, φ	Azimuth and altitude angle of a sky or ground element	radians	TH, PH
$L(\theta,\varphi)$	Luminance of sky or ground element at (θ,φ)	cd/m^2	HitPointLum--
A_w	Area of glazed part of window	m^2	Surface%Area
β	Angle of incidence, at center of window, of light from a sky or ground element	radians	-
$T(\beta)$	Glazing visible transmittance at incidence angle β		TVISBR

$d\Phi_{inc}$	Luminous flux incident on window from sky or ground element	lm	-
$d\Phi$	Luminous flux from sky or ground element transmitted through window	lm	-
$d\Phi_{FW}$, $d\Phi_{CW}$	Luminous flux from sky or ground element transmitted through window and goind downwar, upward	lm	-
θ_{min}, θ_{max}	Azimuth angle integration limits	radians	THMIN, THMAX
φ_w	Window normal altitude angle	radians	-
Φ_{sh}, Φ_{unsh},	Transmitted flux through window with shade, without shade	lm	-
$\Phi_{CW,sh}$, $\Phi_{FW,sh}$	Upgoing and downgoing portions of transmitted flux through window with shade	lm	-
$\Phi_{CW,unsh}$, $\Phi_{FW,unsh}$	Upgoing and downgoing portions of transmitted flux through window without shade	lm	-
f	Fraction of hemisphere seen by the inside of window that lies above the window midplane	-	SurfaceWindow%FractionUpgoing
Φ_{inc}	Flux incident on glazing from direct sun	lm	-
f_{sunlit}	Fraction of glazing that is sunlit	-	SunLitFrac
Φ	Transmitted flux from direct sun	-	-
L_{sh}	Luminance of window with shade	cd/m^2	-
L_b	Window background luminance	cd/m^2	BLUM
G	Discomfort glare constant	-	GTOT
G_i	Discomfort glare constant from window i	-	-
ω	Solid angle subtended by window with respect to reference point	steradians	SolidAngAtRefPt
Ω	Solid angle subtended by window with respect to reference point, modified to take direction of occupant view into account	steradians	SolidAngAtRefPtWtd

N_x, N_y	Number of elements in x and y direction that window is divided into for glare calculation	-	NWX, NWY
$p(x_R, y_R)$	Position factor for horizontal and vertical displacement ratios x_R and y_R	-	DayltgGlarePositionFactor
p_H	Hopkinson position factor	-	DayltgGlarePositionFactor
L_b	Window background luminance	cd/m^2	BLUM
E_b	Illuminance on window background	lm	-
E_r	Total internally-reflected component of daylight illuminance	lm	-
E_s	Illuminance setpoint	lm	IllumSetPoint
G_I	Glare index	-	GLINDX

Overview

There are three types of daylight factors: interior illuminance factors, window luminance factors, and window background luminance factors. To calculate these factors the following steps are carried out for each hourly sun position on the sun paths for the design days and for representative days[2] during the simulation run period:

(1) Calculate exterior horizontal daylight illuminance from sky and sun for standard (CIE) clear and overcast skies.

(2) Calculate interior illuminance, window luminance and window background luminance for each window/reference-point combination, for bare and for shaded window conditions (if a shading device has been specified), for overcast sky and for standard clear sky.

(3) Divide by exterior horizontal illuminance to obtain daylight factors.

Interior Illuminance Components

To calculate daylight factors, daylight incident on a window is separated into two components: (1) light that originates from the *sky* and reaches the window directly or by reflection from exterior surfaces; and (2) light that originates from the *sun* and reaches the window directly or by reflection from exterior surfaces. Light from the window reaches the workplane directly or via reflection from the interior surfaces of the room.

For fixed sun position, sky condition (clear or overcast) and room geometry, the sky-related interior daylight will be proportional to the exterior horizontal illuminance, $E_{h,sky}$, due to light from the sky. Similarly, the sun-related interior daylight will be proportional to the exterior horizontal solar illuminance, $E_{h,sun}$.

Daylight Factors

The following daylight factors are calculated:

$$d_{sky} = \frac{\text{Illuminance at reference point due to sky-related light}}{E_{h,sky}}$$

---

[2] The sun positions for which the daylight factors are calculated are the same as those for which the solar shadowing calculations are done.

$$d_{sun} = \frac{\text{Illuminance at reference point due to sun-related light}}{E_{h,sun}}$$

$$w_{sky} = \frac{\text{Average window luminance due to sky-related light}}{E_{h,sky}}$$

$$w_{sun} = \frac{\text{Average window luminance due to sun-related light}}{E_{h,sun}}$$

$$b_{sky} = \frac{\text{Window background luminance due to sky-related light}}{E_{h,sky}}$$

$$b_{sun} = \frac{\text{Window background luminance due to sun-related light}}{E_{h,sun}}$$

For a daylit zone with N windows these six daylight factors are calculated for each of the following combinations of reference point, window, sky-condition/sun-position and shading device:

$$
\begin{bmatrix} \text{Ref. pt. \#1} \\ \text{Ref. pt. \#2} \end{bmatrix}
\begin{bmatrix} \text{Window \#1} \\ \text{Window \#2} \\ ... \\ \text{Window \#N} \end{bmatrix}
\begin{bmatrix} \text{Clear sky, first sun-up hour} \\ \text{Clear/turbid sky, first sun-up hour} \\ \text{Intermediate sky, first sun-up hour} \\ \text{Overcast sky, first sun-up hour} \\ ... \\ \text{Clear sky, last sun-up hour} \\ \text{Clear/turbid sky, last sun-up hour} \\ \text{Intermediate sky, last sun-up hour} \\ \text{Overcast sky, last sun-up hour} \end{bmatrix}
\begin{bmatrix} \text{Unshaded window} \\ \text{Shaded window} \\ \text{(if shade assigned)} \end{bmatrix}
$$

Sky Luminance Distributions

The luminance distribution of the sky is represented as a superposition of four standard CIE skies using the approach described in [Perez et al., 1990]. The standard skies are as follows.

Clear Sky

The clear sky luminance distribution has the form [Kittler, 1965; CIE, 1973]

$$\psi_{cs}(\theta_{sky}, \phi_{sky}) = L_z \frac{(0.91 + 10e^{-3\gamma} + 0.45\cos^2\gamma)(1 - e^{-0.32\operatorname{cosec}\phi_{sky}})}{0.27385(0.91 + 10e^{-3(\frac{\pi}{2} - \phi_{sun})} + 0.45\sin^2\phi_{sun})}$$

Here, L_z is the zenith luminance (i.e., the luminance of the sky at a point directly overhead). In the calculation of daylight factors, which are ratios of interior and exterior illumination quantities that are both proportional to L_z, the zenith luminance cancels out. For this reason we will use L_z = 1.0 for all sky luminance distributions.

The various angles, which are defined in the building coordinate system, are shown in Figure 34. The angle, γ, between sun and sky element is given by

$$\gamma = \cos^{-1}\left[\sin\phi_{sky} \sin\phi_{sun} + \cos\phi_{sky} \cos\phi_{sun} \cos(\theta_{sky} - \theta_{sun}) \right]$$

The general characteristics of the clear-sky luminance distribution are a large peak near the sun; a minimum at a point on the other side of the zenith from the sun, in the vertical plane containing the sun; and an increase in luminance as the horizon is approached.

Clear Turbid Sky

The clear turbid sky luminance distribution has the form [Matsuura, 1987]

$$\psi_{ts}(\theta_{sky}, \phi_{sky}) = L_z \frac{(0.856 + 16e^{-3\gamma} + 0.3\cos^2\gamma)(1 - e^{-0.32\operatorname{cosec}\phi_{sky}})}{0.27385(0.856 + 10e^{-3(\frac{\pi}{2} - \phi_{sun})} + 0.3\sin^2\phi_{sun})}$$

Intermediate Sky

The intermediate sky luminance distribution has the form [Matsuura, 1987]

$$\psi_{is}(\theta_{sky}, \phi_{sky}) = L_z Z_1 Z_2 / (Z_3 Z_4)$$

where

$$Z_1 = \left[1.35(\sin(3.59\phi_{sky} - 0.009) + 2.31)\sin(2.6\phi_{sun} + 0.316) + \phi_{sky} + 4.799\right] / 2.326$$

$$Z_2 = \exp\left[-0.563\gamma\{(\phi_{sun} - 0.008)(\phi_{sky} + 1.059) + 0.812\}\right]$$

$$Z_3 = 0.99224\sin(2.6\phi_{sun} + 0.316) + 2.73852$$

$$Z_4 = \exp\left[-0.563(\tfrac{\pi}{2} - \phi_{sun})\{2.6298(\phi_{sun} - 0.008) + 0.812\}\right]$$
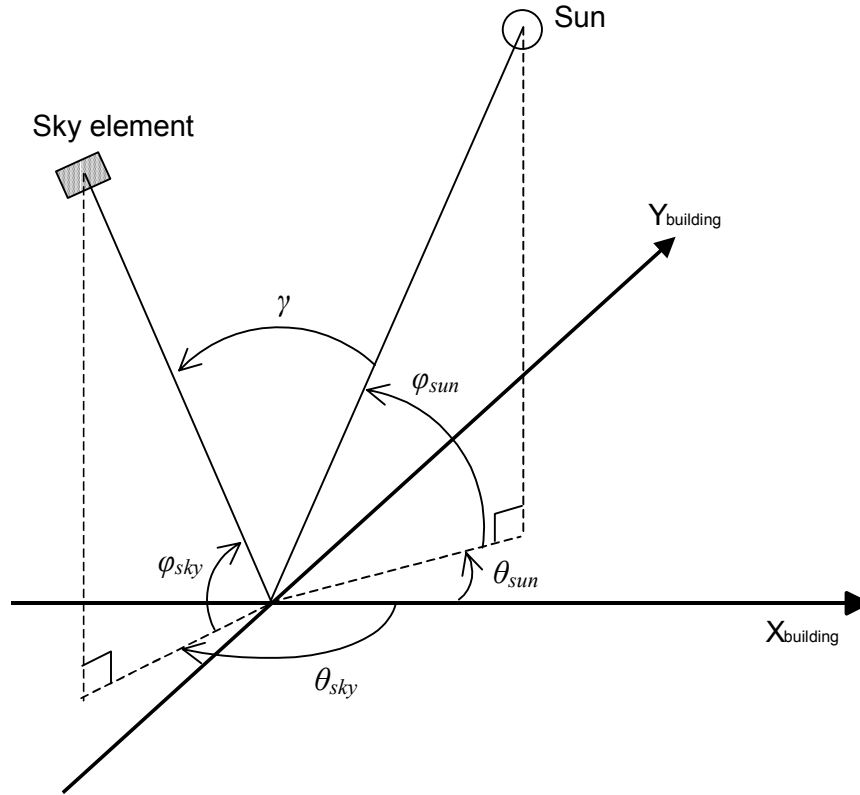
Figure 34. Angles appearing in the expression for the clear-sky luminance distribution.

Overcast Sky

The overcast sky luminance distribution has the form [Moon & Spencer, 1942]

$$\psi_{os}(\phi_{sky}) = L_z \frac{1 + 2\sin\phi_{sky}}{3}$$

Unlike the clear sky case, the overcast sky distribution does not depend on the solar azimuth or the sky azimuth. Note that at fixed solar altitude the zenith ($\phi_{sky} = \pi/2$) is three times brighter than the horizon ($\phi_{sky} = 0$).

Direct Normal Solar Illuminance

For purposes of calculating daylight factors associated with beam solar illuminance, the direct normal solar illuminance is taken to be 1.0 W/m^2. The actual direct normal solar illuminance, determined from direct normal solar irradiance from the weather file and empirically-determined luminious efficacy, is used in the time-step calculation.

Exterior Horizontal Illuminance

The illuminance on an unobstructed horizontal plane due to diffuse radiation from the sky is calculated for each of the four sky types by integrating over the appropriate sky luminance distribution:

$$E_{h,k} = \int\limits_{0}^{2\pi} \int\limits_{0}^{\pi/2} \psi_k(\theta_{sky}, \phi_{sky}) \sin\phi_{sky} \cos\phi_{sky} d\theta_{sky} d\phi_{sky}$$

where $k = cs$, ts, is or os. The integral is evaluated as a double summation:

$$E_{h,k} = \sum_{i=1}^{N_\theta} \sum_{j=1}^{N_\phi} \psi_k \left(\theta_{sky}(i), \phi_{sky}(j) \right) \sin\phi_{sky}(j) \cos\phi_{sky}(j) \Delta\theta_{sky} \Delta\phi_{sky}$$

where

$$\theta_{sky}(i) = (i - 1/2)\Delta\theta_{sky}$$

$$\phi_{sky}(j) = (j - 1/2)\Delta\phi_{sky}$$

$$\Delta\theta_{sky} = 2\pi / N_\theta$$

$$\Delta\phi_{sky} = \pi / 2N_\phi$$

$N_\theta = 18$ and $N_\phi = 8$ were found to give a $\pm 1\%$ accuracy in the calculation of $E_{h,k}$.

Direct Component of Interior Daylight Illuminance

The direct daylight illuminance at a reference point from a particular window is determined by dividing the window into an x-y grid and finding the flux reaching the reference point from each grid element. The geometry involved is shown in Figure 35. The horizontal illuminance at the reference point, $\vec{R}_{ref}$, due to a window element is

$$dE_h = L_w d\Omega \cos\gamma$$

where L_w is the luminance of the window element as seen from the reference point.
The subtended solid angle is approximated by

$$d\Omega = \frac{dxdy}{D^2} \cos B \tag{1.78}$$

where

$$D = \left| \bar{R}_{win} - \bar{R}_{ref} \right|$$

$CosB$ is found from

$$\cos B = \hat{R}_{ray} \cdot \hat{W}_n$$

where

$$\vec{R}_{ray} = (\vec{R}_{win} - \vec{R}_{ref}) / D$$

$$\hat{W}_n = \text{ window outward normal } = \hat{W}_{21} \times \hat{W}_{23}$$

$$= \frac{\vec{W}_1 - \vec{W}_2}{\left|\vec{W}_1 - \vec{W}_2\right|} \times \frac{\vec{W}_3 - \vec{W}_2}{\left|\vec{W}_3 - \vec{W}_2\right|}$$

Equation (1.78) becomes exact as dx/D and $dy/D \to 0$ and is accurate to better than about 1% for $dx \le D/4$ and $dy \le D/4$.

The net illuminance from the window is obtained by summing the contributions from all the window elements:

$$E_h = \sum_{\substack{window \\ elements}} L_w d\Omega \cos\gamma \tag{1.79}$$

In performing the summation, window elements that lie below the workplane ($\cos\gamma < 0$) are omitted since light from these elements cannot reach the workplane directly.
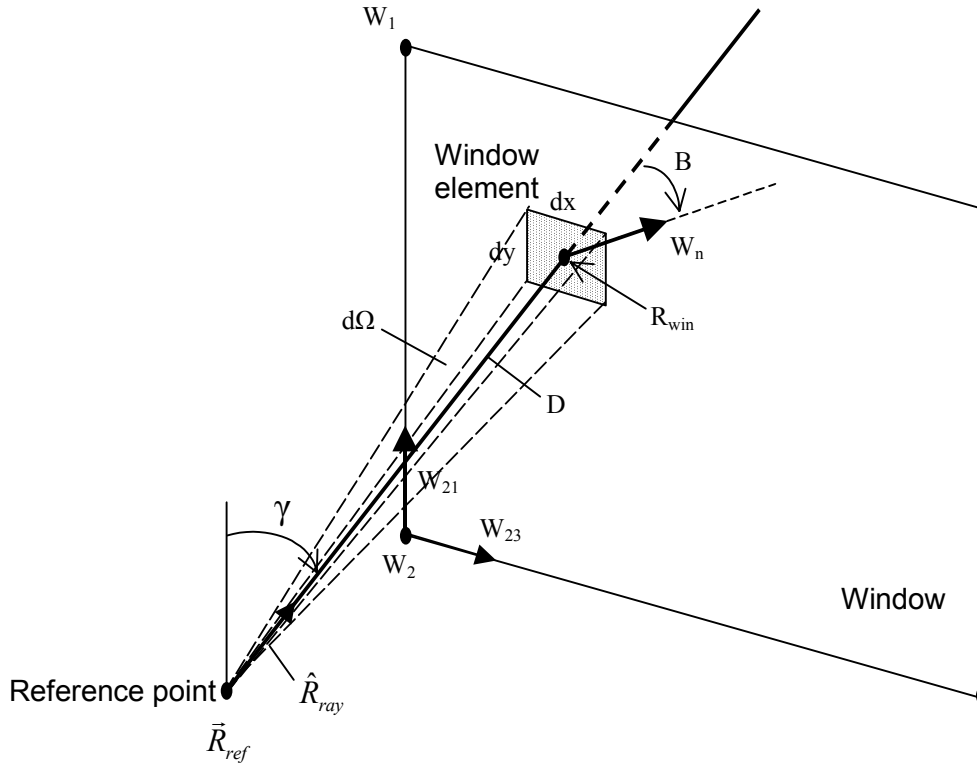
Figure 35.   Geometry for calculation of direct component of daylight illuminance at a reference point. Vectors R_{ref}, W_1, W_2, W_3 and R_{win} are in the building coordinate system.

Unshaded Window

For the unshaded window case, the luminance of the window element is found by projecting the ray from reference point to window element and determining whether it intersects the sky or an exterior obstruction such as an overhang. It is assumed that there are no internal

obstructions. If L is the corresponding luminance of the sky or obstruction[3], the window luminance is

$$L_w = L\tau_{vis}(\cos B)$$

where τ_{vis} is the visible transmittance of the glass for incidence angle B.

Shaded Window

For the window-plus-shade case the shade is assumed to be a perfect diffuser, i.e., the luminance of the shade is independent of angle of emission of light, position on shade, and angle of incidence of solar radiation falling on the shade. Closely-woven drapery fabric and translucent roller shades are closer to being perfect diffusers than Venetian blinds or other slatted devices, which usually have non-uniform luminance characteristics.

The calculation of the window luminance with the shade in place, $L_{w,sh}$, is described in [Winkelmann, 1983]. The illuminance contribution at the reference point from a shaded window element is then given by Eq. (1.79) with $L_w = L_{w,sh}$.

Internally-Reflected Component of Interior Daylight Illuminance

Daylight reaching a reference point after reflection from interior surfaces is calculated using the *split-flux* method [Hopkinson et al., 1954], [Lynes, 1968]. In this method the daylight transmitted by the window is split into two parts—a downward-going flux, Φ_{FW} (lumens), which falls on the floor and portions of the walls below the imaginary horizontal plane passing through the center of the window (*window midplane*), and an upward-going flux, Φ_{CW}, that strikes the ceiling and portions of the walls above the window midplane. A fraction of these fluxes is absorbed by the room surfaces. The remainder, the first-reflected flux, F_1, is approximated by

$$F_1 = \Phi_{FW}\rho_{FW} + \Phi_{CW}\rho_{CW}$$

where ρ_{FW} is the area-weighted average reflectance of the floor and those parts of the walls below the window midplane, and ρ_{CW} is the area-weighted average reflectance of the ceiling and those parts of the walls above the window midplane.

To find the final average internally-reflected illuminance, E_r, on the room surfaces (which in this method is uniform throughout the room) a flux balance is used. The total reflected flux absorbed by the room surfaces (or lost through the windows) is $AE_r(1-\rho)$, where A is the total inside surface area of the floor, walls, ceiling and windows in the room, and ρ is the area-weighted average reflectance of the room surfaces, including windows. From conservation of energy

$$AE_r(1-\rho) = F_1$$

or

$$E_r = \frac{\Phi_{FW}\rho_{FW} + \Phi_{CW}\rho_{CW}}{A(1-\rho)}$$

---

[3] Currently, obstructions are assumed to be black, i.e., have zero luminance.

This procedure assumes that the room behaves like an integrating sphere with perfectly diffusing interior surfaces and with no internal obstructions. It therefore works best for rooms that are close to cubical in shape, have matte surfaces (which is usually the case), and have no internal partitions. Deviations from these conditions, such as would be the case for rooms whose depth measured from the window-wall is more than three times greater than ceiling height, can lead to substantial inaccuracies in the split-flux calculation.

Transmitted Flux from Sky and Ground

The luminous flux incident on the center of the window from a luminous element of sky or ground at angular position (θ, ϕ), of luminance $L(\theta, \phi)$, and subtending a solid angle $\cos\phi \, d\theta \, d\phi$ is

$$d\Phi_{inc} = A_w L(\theta, \phi) \cos\beta \, \cos\phi \, d\theta \, d\phi$$

The transmitted flux is

$$d\Phi = d\Phi_{inc} T(\beta)$$

where $T(\beta)$ is the window transmittance for light at incidence angle β. This transmittance depends on whether or not the window has a shade.

For an unshaded window the total downgoing transmitted flux is obtained by integrating over the part of the exterior hemisphere seen by the window that lies above the window midplane. This gives

$$\Phi_{FW,unshaded} = A_w \int_{\theta_{min}}^{\theta_{max}} \int_{0}^{\pi/2} L(\theta, \phi) T(\beta) \cos\beta \, \cos\phi \, d\theta \, d\phi \qquad (1.80)$$

The upgoing flux is obtained similarly by integrating over the part of the exterior hemisphere that lies below the window midplane:

$$\Phi_{CW,unshaded} = A_w \int_{\theta_{min}}^{\theta_{max}} \int_{\pi/2-\phi_w}^{0} L(\theta, \phi) T(\beta) \cos\beta \, \cos\phi \, d\theta \, d\phi \qquad (1.81)$$

where ϕ_w is the angle the window outward normal makes with the horizontal plane.

For a window with a diffusing shade the total transmitted flux is

$$\Phi_{sh} = A_w \int_{\theta_{min}}^{\theta_{max}} \int_{\pi/2-\phi_w}^{\pi/2} L(\theta, \phi) T(\beta) \cos\beta \, \cos\phi \, d\theta \, d\phi \qquad (1.82)$$

The downgoing and upgoing portions of this flux are

$$\Phi_{FW,sh} = \Phi(1-f)$$
$$\Phi_{CW,sh} = \Phi f$$

where f, the fraction of the hemisphere seen by the inside of the window that lies above the window midplane, is given by

$$f = 0.5 - \phi_w / \pi$$

For a vertical window ($\phi_w = 0$) the up- and down-going transmitted fluxes are equal:

$$\Phi_{FW,sh} = \Phi_{CW,sh} = \Phi / 2 \, .$$

For a horizontal skylight ($\phi_w = \pi / 2$):

$$\Phi_{FW,sh} = \Phi, \Phi_{CW,sh} = 0$$

The limits of integration of θ in Eqs. (1.80), (1.81) and (1.82) depend on ϕ. From Fig. 12 in [Winkelmann, 1983] we have

$$\sin \alpha = \sin(A - \pi / 2) = \frac{\sin \phi \tan \phi_w}{\cos \phi}$$

which gives

$$A = \cos^{-1}(\tan \phi \tan \phi_w)$$

Thus

$$\theta_{\min} = - \left| \cos^{-1}(- \tan \phi \tan \phi_w) \right|$$
$$\theta_{\max} = \left| \cos^{-1}(- \tan \phi \tan \phi_w) \right|$$

Transmitted Flux from Direct Sun

The flux incident on the window from direct sun is

$$\Phi_{inc} = A_w E_{DN} \cos \beta \, f_{sunlit}$$

The transmitted flux is

$$\Phi = T(\beta) \Phi_{inc}$$

where T is the net transmittance of the window glazing (plus shade, if present).

For an unshaded window all of the transmitted flux is downward since the sun always lies above the window midplane. Therefore

$$\Phi_{FW,unsh} = \Phi$$
$$\Phi_{CW,unsh} = 0$$

For a window with a diffusing shade

$$\Phi_{FW,sh} = \Phi(1-f)$$

$$\Phi_{CW,sh} = \Phi f$$

Luminance of Shaded Window

The luminance of a shaded window is determined at the same time that the transmitted flux is calculated. It is given by

$$L_{sh} = \frac{1}{\pi} \int_{\theta_{min}}^{\theta_{max}} \int_{\pi/2-\phi_w}^{\pi/2} L(\theta,\phi)T(\beta)\cos\beta\,\cos\phi\,d\theta\,d\phi$$

Daylight Discomfort Glare

The discomfort glare at a reference point due to luminance contrast between a window and the interior surfaces surrounding the window is given by [Hopkinson, 1970] and [Hopkinson, 1972]:

$$G = \frac{L_w^{1.6}\Omega^{0.8}}{L_b + 0.07\omega^{0.5}L_w}$$

where

G = discomfort glare constant

L_w = average luminance of the window as seen from the reference point

Ω = solid angle subtended by window, modified to take direction of occupant view into account

L_b = luminance of the background area surrounding the window

By dividing the window into N_x by N_y rectangular elements, as is done for calculating the direct component of interior illuminance, we have

$$L_w = \frac{\displaystyle\sum_{j=1}^{N_y}\sum_{i=1}^{N_x} L_w(i,j)}{N_x N_y}$$

where $L_w(i,j)$ is the luminance of element (i,j) as seen from the reference point.
Similarly,

$$\omega = \sum_{j=1}^{N_y}\sum_{i=1}^{N_x} d\omega(i,j)$$

where $d\omega(i,j)$ is the solid angle subtended by element (i,j) with respect to the reference point.
The modified solid angle is

$$\Omega = \sum_{j=1}^{N_y}\sum_{i=1}^{N_x} d\omega(i,j)p(x_R,y_R)$$

where p is a "position factor" [Petherbridge & Longmore, 1954] that accounts for the decrease in visual excitation as the luminous element moves away from the line of sight. This factor depends on the horizontal and vertical displacement ratios, x_R and y_R (Figure 36), given by

$$x_R(i,j) = \frac{\left|A^2 - (YD)^2\right|^{1/2}}{RR}$$

$$y_R(i,j) = \left|YD/RR\right|$$

where

$$RR = D(\hat{R}_{ray} \cdot \hat{v}_{view})$$

$$A^2 = D^2 - (RR)^2$$

$$YD = R_{win}(3) - R_{ref}(3)$$

$$\hat{R}_{ray}$$

Figure 36. Geometry for calculation of displacement ratios used in the glare formula.

The factor p can be obtained from graphs given in [Petherbridge & Longmore, 1954] or it can be calculated from tabulated values of p_H, the Hopkinson position factor [Hopkinson, 1966], since $p = p_H^{1.25}$. The values resulting from the latter approach are given in Table 11. Interpolation of this table is used in EnergyPlus to evaluate p at intermediate values of x_R and y_R.

Table 11. Position factor for glare calculation

		x_R: Horizontal Displacement Factor							
		0	0.5	1.0	1.5	2.0	2.5	3.0	>3.0
y_R: Vertical Displacement Factor	0	1.00	0.492	0.226	0.128	0.081	0.061	0.057	0
	0.5	0.123	0.119	0.065	0.043	0.029	0.026	0.023	0
	1.0	0.019	0.026	0.019	0.016	0.014	0.011	0.011	0
	1.5	0.008	0.008	0.008	0.008	0.008	0.006	0.006	0
	2.0	0	0	0.003	0.003	0.003	0.003	0.003	0
	>2.0	0	0	0	0	0	0	0	0

The background luminance is

$$L_b = E_b \rho_b$$

where ρ_b is approximated by the average interior surface reflectance of the entire room and

$$E_b = \max(E_r, E_s)$$

where E_r is the total internally-reflected component of daylight illuminance produced by all the windows in the room and E_s is the illuminance set point at the reference point at which

glare is being calculated. A precise calculation of E_b is not required since the glare index (see next section) is logarithmic. A factor of two variation in E_b generally produces a change of only 0.5 to 1.0 in the glare index.

Glare Index

The net daylight glare at a reference point due to all of the windows in a room is expressed in terms of a *glare index* given by

$$G_I = 10\log_{10} \sum_{i=1}^{\substack{\text{number of} \\ \text{windows}}} G_i$$

where G_i is the glare constant at the reference point due to the ith window

Time-Step Daylighting Calculation

Overview

A daylighting calculation is performed each time step that the sun is up for each zone that has one or two daylighting reference points specified. The exterior horizontal illuminance from the sun and sky is determined from solar irradiance data from the weather file. The interior illuminance at each reference point is found for each window by interpolating the daylight illuminance factors for the current sun position, then, for sky-related interior illuminance, multiplying by the exterior horizontal illuminance from the appropriate sky types that time step, and, for sun-related interior illuminance, multiplying by the exterior horizontal solar illuminance that time step. By summation, the net illuminance and glare due to all of the windows in a zone are found. If glare control has been specified window shading (by movable shading devices or switchable glazing) is deployed to reduce glare. Finally the illuminance at each reference point for the final window and shade configuration is used by the lighting control system simulation to determine the electric lighting power required to meet the illuminance set point at each reference point.

Table 12. Variables in Time-Step Calculations

Mathematical variable	Description	Units	FORTRAN variable
$S_{norm,dir}$	Direct normal solar irradiance	W/m^2	BeamSolarRad
$S_{h,dif}$	Exterior diffuse horizontal solar irradiance	W/m^2	SDIFH, DifSolarRad
$S_{h,dir}$	Exterior direct horizontal solar irradiance	W/m^2	SDIRH
Z	Solar zenith angle	radians	Zeta
m	Relative optical air mass	-	AirMass
Δ	Sky brightness	-	SkyBrightness
ε	Sky clearness	-	SkyClearness
k, k'	Sky type index	-	ISky
$s_{k,k'}$	Interpolation factor for skies k and k'	-	SkyWeight
$\Psi_{k,k'}$	Sky luminance distribution formed from linear interpolation of skies k and k'	cd/m^2	-

f_k	Fraction of sky that is type k	-	-
$E_{h,k}$	Horizontal illuminance from sky type k	cd/m^2	HorIllSky
$E_{h,sky}$	Exterior horizontal illuminance from sky	lux	HISKF
$E_{h,sun}$	Exterior horizontal illuminance from sun	lux	HISUNF
η_{dif}, η_{dir}	Luminous efficacy of diffuse and direct solar radiation	lm/W	DiffLumEff, DirLumEff
I_{win}	Interior illuminance from a window	lux	DayllIlum
S_{win}	Window luminance	cd/m^2	SourceLumFromWinAtRefPt
B_{win}	Window background luminance	cd/m^2	BACLUM
d_{sun}, $d_{sky,k}$	Interior illuminance factor for sun, for sky of type k	-	DaylIllFacSun, DFSUHR, DaylIllFacSky, DFSUHR
w_{sun}, $w_{sky,k}$	Window luminance factor for sun, for sky of type k	-	DaylSourceFacSun, SFSUHR, DaylSourceFacSky, SFSKHR
b_{sun}, $b_{sky,k}$	Window background luminance factor for sun, for sky of type k	-	DaylBackFacSun, BFSUHR, DaylBackFacSky, BFSKHR
w_j	Weighting factor for time step interpolation	-	WeightNow
i_L	Reference point index	-	IL
i_S	Window shade index	-	IS
I_{tot}	Total daylight illuminance at reference point	lux	DayllIlum
B_{tot}, B	Total window background luminance	cd/m^2	BLUM
I_{set}	Illuminance setpoint	lux	ZoneDaylight%IllumSetPoint
f_L	Fractional electric lighting output	-	FL
f_P	Fractional electric lighting input power	-	FP
N_L	Number of steps in a stepped control system	-	LightControlSteps
M_P	Lighting power multiplier	-	ZonePowerReductionFactor

Time-Step Sky Luminance

The sky luminance distribution, ψ, for a particular time step is expressed as a linear interpolation of two of the four standard skies — ψ_{cs}, ψ_{ts}, ψ_{is} and ψ_{os} — described above under "Sky Luminance Distributions." The two sky types that are interpolated depend on the value of the sky clearness. The interpolation factors are a function of sky clearness and sky brightness [Perez et al., 1990]. Sky clearness is given by

$$\varepsilon = \frac{\dfrac{S_{h,dif} + S_{norm,dir}}{S_{h,dif}} + \kappa\, Z^3}{1 + \kappa\, Z^3}$$

where $S_{h,dif}$ is the diffuse horizontal solar irradiance, $S_{norm,dir}$ is the direct normal solar irradiance, Z is the solar zenith angle and κ is a constant equal to 1.041 for Z in radians. Sky brightness is given by

$$\Delta = S_{h,dif}\, m\, /\, S_{norm,dir}^{ext}$$

where m is the relative optical air mass and $S_{norm,dir}^{ext}$ is the extraterrestrial direct normal solar irradiance.

If $\varepsilon \le 1.2$

$$\psi_{is,os} = s_{is,os}\psi_{is} + (1 - s_{is,os})\psi_{os}$$

where ψ_{is} is the intermediate sky luminance distribution, ψ_{os} is the overcast sky luminance distribution, and

$$s_{is,os} = \min\left\{1, \max[0, (\varepsilon - 1)/0.2, (\Delta - 0.05)/4]\right\}$$

If $1.2 < \varepsilon \le 3$

$$\psi_{ts,is} = s_{ts,is}\psi_{ts} + (1 - s_{ts,is})\psi_{is}$$

where ψ_{ts} is the clear turbid sky luminance distribution and

$$s_{ts,is} = (\varepsilon - 1.2)/1.8$$

If $\varepsilon > 3$

$$\psi_{cs,ts} = s_{cs,ts}\psi_{cs} + (1 - s_{cs,ts})\psi_{ts}$$

where ψ_{cs} is the clear sky luminance distribution and

$$s_{cs,ts} = \min[1, (\varepsilon - 3)/3]$$

Interior Illuminance

For each time step the interior illuminance, I_{win}, from a window is calculated as follows by multiplying daylight factors and exterior illuminance.

First, the sun- and sky-related daylight illuminance factors for the time step are determined by interpolation of the hourly factors:

$$\overline{d}_{sun}(i_L, i_S) = w_j d_{sun}(i_L, i_S, i_h) + (1 - w_j) d_{sun}(i_L, i_S, i_h + 1)$$

$$\overline{d}_{sky,k}(i_L, i_S) = w_j d_{sky,k}(i_L, i_S, i_h) + (1 - w_j) d_{sky,k}(i_L, i_S, i_h + 1)$$

where i_L is the reference point index (1 or 2), i_S is the window shade index (1 for unshaded window, 2 for shaded window), i_h is the hour number, and k is the sky type index. For the j th time step in an hour, the time-step interpolation weight is given by

$$w_j = 1 - \min[1, j / N_t]$$

where N_t is the number of time steps per hour.

The interior illuminance from a window is calculated as

$$I_{win}(i_L, i_S) = \overline{d}_{sun} E_{h,sun} + [\overline{d}_{sky,k}(i_L, i_S) f_k + \overline{d}_{sky,k'}(i_L, i_S) f_{k'}] E_{h,sky}$$

where $E_{h,sun}$ and $E_{h,sky}$ are the exterior horizontal illuminance from the sun and sky, respectively, and f_k and $f_{k'}$ are the fraction of the exterior horizontal illuminance from the sky that is due to sky type k and k', respectively.

The horizontal illuminance from sun and sky are given by

$$E_{h,sun} = \eta_{dir} S_{norm,dir} \cos Z$$
$$E_{h,sky} = \eta_{dif} S_{h,dir}$$

where Z is the solar zenith angle, η_{dif} is the luminous efficacy (in lumens/Watt) of diffuse solar radiation from the sky and η_{dir} is the luminous efficacy of direct radiation from the sun. The efficacies are calculated from direct and global solar irradiance using a method described in [Perez et al, 1990].)

The fractions f_k and $f_{k'}$ are given by

$$f_k = \frac{s_{k,k'} E_{h,k}}{s_{k,k'} E_{h,k} + (1 - s_{k,k'}) E_{h,k'}}$$

$$f_{k'} = \frac{(1 - s_{k,k'}) E_{h,k'}}{s_{k,k'} E_{h,k} + (1 - s_{k,k'}) E_{h,k'}}$$

where $E_{h,k}$ and $E_{h,k'}$ are the horizontal illuminances from skies k and k', respectively (see "Exterior Horizontal Luminance," above), and $s_{k,k'}$ is the interpolation factor for skies k and k' (see "Time-Step Sky Luminance," above). For example, if $\varepsilon > 3$, $k = cs$ (clear sky), $k' = ts$ (clear turbid sky) and

$$s_{k,k'} = s_{cs,ts} = \min[1,(\varepsilon - 3)/3]$$

Similarly, the window source luminance, S_{win}, and window background luminance, B_{win}, for a window are calculated from

$$S_{win}(i_L, i_S) = \overline{w}_{sun} E_{h,sun} + [\overline{w}_{sky,k}(i_L, i_S) f_k + \overline{w}_{sky,k'}(i_L, i_S) f_{k'}] E_{h,sky}$$

$$B_{win}(i_L, i_S) = \overline{b}_{sun} E_{h,sun} + [\overline{b}_{sky,k}(i_L, i_S) f_k + \overline{b}_{sky,k'}(i_L, i_S) f_{k'}] E_{h,sky}$$

The total illuminance at a reference point from all of the exterior windows in a zone is

$$I_{tot}(i_L) = \sum_{\substack{windows \\ in\ zone}} I_{win}(i_s, i_L)$$

where i_S = 1 if the window is unshaded and i_S = 2 if the window is shaded that time step. (Before the illuminance calculation is done the window shading control will have been simulated to determine whether or not the window is shaded.)

Similarly, the total background luminance is calculated:

$$B_{tot}(i_L) = \sum_{\substack{windows \\ in\ zone}} B_{win}(i_s, i_L)$$

Glare Index

The net glare index at each reference point is calculated as

$$G_I(i_L) = 10\log_{10} \sum_{\substack{windows \\ in\ zone}} \frac{S_{win}(i_L, i_S)^{1.6} \Omega(i_L)^{0.8}}{B(i_L) + 0.07\omega(i_L)^{0.5} S_{win}(i_L, i_S)}$$

where

$$B(i_L) = \max(B_{win}(i_L), \rho_b I_{set}(i_L))$$

In the last relationship, the background luminance is approximated as the larger of the background luminance from daylight and the average background luminance that would be produced by the electric lighting at full power if the illuminance on the room surfaces were equal to the setpoint illuminance. In a more detailed calculation, where the luminance of each room surface is separately determined, $B(i_L)$ would be better approximated as an area-weighted luminance of the surfaces surrounding a window, taking into account the luminance contribution from the electric lights.

Glare Control Logic

If glare control has been specified and the glare index at either reference point exceeds a user-specified maximum value, $G_{I,max}$, then the windows in the zone are shaded one by one in attempt to bring the glare at both points below $G_{I,max}$. (Each time a window is shaded the glare and illuminance at each reference point is recalculated.) The following logic is used:

(1) If there is only one reference point, shade a window if it is unshaded and shading it decreases the glare, even if it does not decrease the glare below $G_{I,max}$. Note that if a window has already been shaded, say to control solar gain, it will be left in the shaded state.

(2) If there are two reference points, then:

    (a) If glare is too high at both points, shade the window if it decreases glare at both points.

    (b) If glare is too high only at the first point, shade the window if the glare at the first point decreases, and the glare at the second point stays below $G_{I,max}$.

    (c) If glare is too high only at the second point, shade the window if the glare at the second point decreases, and the glare at the first point stays below $G_{I,max}$.

(3) Shades are closed in the order of window input until glare at both points is below $G_{I,max}$, or until there are no more windows left to shade.

Lighting Control System Simulation

Once the final daylight illuminance value at each reference point has been determined, the electric lighting control is simulated. The fractional electric lighting output, f_L, required to meet the setpoint at reference point i_L is given by

$$f_L(i_L) = \max\left[0, \frac{I_{set}(i_L) - I_{tot}(i_L)}{I_{set}(i_L)}\right]$$

Here, I_{set} is the illuminance setpoint and I_{tot} is the daylight illuminance at the reference point. This relationship assumes that the electric lights at full power produce an illuminance equal to I_{set} at the reference point.

The fractional electric lighting input power, f_P, corresponding to f_L is then calculated. The relationship between f_P and f_L depends on the lighting control type.

Continuous Dimming Control

For a continuously-dimmable control system, it is assumed that f_P is constant and equal to $f_{P,min}$ for $f_L < f_{L,min}$ and that f_P increases linearly from $f_{P,min}$ to 1.0 as f_L increases from $f_{L,min}$ to 1.0 (Figure 37). This gives

$$f_P = \begin{cases} f_{P,\min} & \text{for } f_L < f_{L,\min} \\ \dfrac{f_L + (1 - f_L)f_{P,\min} - f_{L,\min}}{1 - f_{L,\min}} & \text{for } f_{L,\min} \leq f_L \leq 1 \end{cases}$$
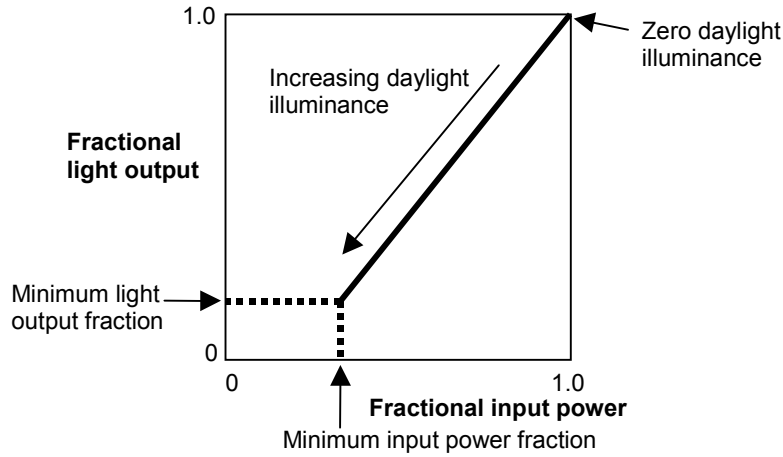
Figure 37. Control action for a continuous dimming system.

Continuous/Off Dimming Control

A "continuous/off" dimming system has the same behavior as a continuous dimming system except that the lights switch off for $f_L < f_{L,min}$ rather than staying at $f_{P,min}$.

Stepped Control

For a stepped control system, f_P takes on discrete values depending on the range of f_L and the number of steps, N_L (Figure 38). This gives

$$f_P = \begin{cases} 0, & \text{if} f_L = 0 \\ \dfrac{\text{int}(N_L f_L) + 1}{N_L}, & \text{for } 0 < f_L < 1 \\ 1, & \text{if} f_L = 1 \end{cases}$$

If a lighting control probability, p_L, is specified, f_P is set one level higher a fraction of the time equal to $1-p_L$. Specifically, if $f_P < 1$, $f_P \rightarrow f_P + 1/N_L$ if a random number between 0 and 1 exceeds p_L. This can be used to simulate the uncertainty associated with manual switching of lights.
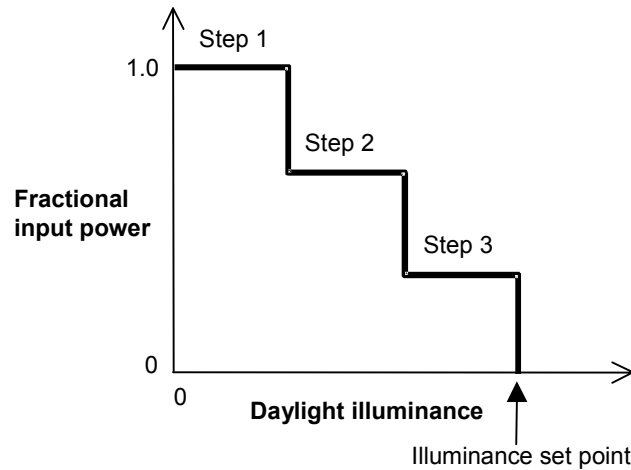
Figure 38. Stepped lighting control with three steps.

Lighting Power Reduction

Using the value of f_P at each reference point and the fraction f_Z of the zone controlled by the reference point, the net lighting power multiplier, M_P, for the entire zone is calculated; this value multiplies the lighting power output without daylighting.

$$M_P = \sum_{i_L=1}^{2} f_P(i_L) f_Z(i_L) + \left(1 - \sum_{i_L=1}^{2} f_Z(i_L)\right)$$

In this expression, the term to the right in the parentheses corresponds to the fraction of the zone not controlled by either reference point. For this fraction the electric lighting is unaffected and the power multiplier is 1.0.

References

CIE Technical Committee 4.2. Standardization of the Luminance Distribution on Clear Skies. CIE Pub. No. 22, Commission Internationale d'Eclairage, Paris, 1973.

Hopkinson, R.G., J. Longmore and P. Petherbridge. An Empirical Formula for the Computation of the Indirect Component of Daylight Factors. Trans. Illum. Eng. Soc. (London) 19, 201 (1954).

Hopkinson, R.G., P. Petherbridge and J. Longmore. Daylighting. Heinnemann, London, 1966, p. 322.

Hopkinson, R.G. Glare from Windows. Construction Research and Development Journal 2, 98 (1970).

Hopkinson, R.G. Glare from Daylighting in Buildings. Applied Ergonomics 3, 206 (1972).

Kittler, R. Standardization of Outdoor Conditions for the Calculation of the Daylight Factor with Clear Skies. Proc. CIE Inter-Session Meeting on Sunlight, Newcastle-Upon-Tyne, 1965.

Lynes, J.A. Principles of Natural Lighting. Applied Science Publishers, Ltd., London, 1968, p. 129.

Matsuura, K. Luminance Distributions of Various Reference Skies. CIE Technical Report of TC 3-09 (1987).

Moon, P. and D. Spencer, Illumination from a Nonuniform Sky. Illuminating Engineering 37, 707-726 (1942).

Perez, R., P. Ineichen, R. Seals, J. Michalsky and R. Stewart. Modeling Daylight Availability and Irradiance Components from Direct and Global Irradiance. Solar Energy 44, 271-289 (1990).

Petherbridge, P. and J. Longmore. Solid Angles Applied to Visual Comfort Problems. Light and Lighting 47,173 (1954)

Winkelmann, F.C. Daylighting Calculation in DOE-2. Lawrence Berkeley Laboratory report no. LBL-11353, Jan. 1983.

Winkelmann, F.C. and S. Selkowitz. Daylighting Simulation in the DOE-2 Building Energy Analysis Program. Energy and Buildings 8, 271-286 (1985)

Window Calculations Module(s)

In EnergyPlus a window is considered to be composed of the following four components, only the first of which, glazing, is required to be present:

1) *Glazing*, which consists of one or more plane/parallel glass layers. If there are two or more glass layers, the layers are separated by gaps filled with air or another gas. The glazing optical and thermal calculations are based on algorithms from the WINDOW 4 and WINDOW 5 programs [Arasteh et al., 1989], [Finlayson et al., 1993].

2) *Frame*, which surrounds the glazing on four sides.

3) *Divider*, which consists of horizontal and/or vertical elements that divide the glazing into individual lites.

4) *Shading device*, which is a separate layer, such as drapery, roller shade or blind, on the inside or outside of the glazing, whose purpose is to reduce solar gain, reduce heat loss (movable insulation) or control daylight glare.

In the following, the description of glazing algorithms is based on material from Finlayson et al., 1993. The frame and divider thermal model, and the shading device optical and thermal models, are new to EnergyPlus.

Optical Properties of Glazing

The solar radiation transmitted by a system of glass layers and the solar radiation absorbed in each layer depend on the solar transmittance, reflectance and absorptance properties of the individual layers. The absorbed solar radiation enters the glazing heat balance calculation that determines the inside surface temperature and, therefore, the heat gain to the zone from the glazing (see "Window Heat Balance Calculation"). The transmitted solar radiation is absorbed by interior zone surfaces and, therefore, contributes to the zone heat balance. In addition, the visible transmittance of the glazing is an important factor in the calculation of interior daylight illuminance from the glazing.

Table 13. Variables in Window Calculations

Mathematical variable	Description	Units	FORTRAN variable
T	Transmittance	-	-
R	Reflectance	-	-
R^f, R^b	Front reflectance, back reflectance	-	-
$T_{i,j}$	Transmittance through glass layers i to j	-	-
T^{dir}_{gl}	Direct transmittance of glazing	-	-

$R^f_{i,j}$, $R^b_{i,j}$	Front reflectance, back reflectance from glass layers i to j	-	-
$R^{dir}_{gl,f}$, $R^{dir}_{gl,b}$	Direct front and back reflectance of glazing	-	-
A^f_i, A^b_i	Front absorptance, back absorptance of layer i	-	-
N	Number of glass layers	-	nlayer
λ	Wavelength	microns	wle
$E_s(\lambda)$	Solar spectral irradiance function	W/m^2-micron	e
$R(\lambda)$	Photopic response function of the eye	-	y30
φ	Angle of incidence (angle between surface normal and direction of incident beam radiation)	-	Phi
τ	Transmittivity or transmittance	-	tf0
ρ	Reflectivity or reflectance	-	rf0, rb0
α	Spectral absorption coefficient	m^{-1}	-
d	Glass thickness	m	Material%Thickness
n	Index of refraction	-	ngf, ngb
κ	Extinction coefficient	-	-
β	Intermediate variable	-	betaf, betab
P, p	A general property, such as transmittance	-	-
τ_{sh}	Shade transmittance	-	Material%Trans
ρ_{sh}	Shade reflectance	-	-
α_{sh}	Shade absorptance	-	Material%AbsorpSolar
τ_{bl}, ρ_{bl}, α_{bl}	Blind transmittance, reflectance, absorptance	-	-
Q, G, J	Source, irradiance and radiosity for blind optical properties calculation	W/m^2	-
F_{ij}	View factor between segments i and j	-	-
f_{switch}	Switching factor	-	SwitchFac
T	Transmittance	-	-
R	Reflectance	-	-
R^f, R^b	Front reflectance, back reflectance	-	-
$T_{i,j}$	Transmittance through glass layers i to j	-	-

$R^f_{i,j}$, $R^b_{i,j}$	Front reflectance, back reflectance from glass layers i to j	-	-
A^f_i, A^b_i	Front absorptance, back absorptance of layer i	-	-
N	Number of glass layers	-	nlayer
λ	Wavelength	microns	wle
$E_s(\lambda)$	Solar spectral irradiance function	W/m^2-micron	e
$R(\lambda)$	Photopic response function of the eye	-	y30
φ	Angle of incidence (angle between surface normal and direction of incident beam radiation)	-	Phi
τ	Transmittivity or transmittance	-	tf0
ρ	Reflectivity or reflectance	-	rf0, rb0
A	Spectral absorption coefficient	m^{-1}	-
D	Glass thickness	m	Material%Thickness
N	Index of refraction	-	ngf, ngb
K	Extinction coefficient	-	-
B	Intermediate variable	-	betaf, betab
P, p	A general property, such as transmittance	-	-
τ_{sh}	Shade transmittance	-	Material%Trans
ρ_{sh}	Shade reflectance	-	-
α_{sh}	Shade absorptance	-	Material%AbsorpSolar
f_{switch}	Switching factor	-	SwitchFac

Glass Layer Properties

In EnergyPlus, the optical properties of individual glass layers are given by the following quantities at normal incidence as a function of wavelength:

Transmittance, T

Front reflectance, R^f

Back reflectance, R^b

Here "front" refers to radiation incident on the side of the glass closest to the outside environment, and "back" refers to radiant incident on the side of the glass closest to the inside environment. For glazing in exterior walls, "front" is therefore the side closest to the outside air and "back" is the side closest to the zone air. For glazing in interior (i.e., interzone) walls, "back" is the side closest to the zone in which the wall is defined in and "front" is the side closest to the adjacent zone.

Glazing System Properties

The optical properties of a glazing system consisting of N glass layers separated by nonabsorbing gas layers (Figure 39. Schematic of transmission, reflection and absorption of solar radiation within a multi-layer glazing system.) are determined by solving the following recursion relations for $T_{i,j}$, the transmittance through layers i to j; $R^f_{i,j}$ and $R^b_{i,j}$, the front and back reflectance, respectively, from layers i to j; and A_j , the absorption in layer j. Here layer 1 is the outermost layer and layer N is the innermost layer. These relations account for multiple internal reflections within the glazing system. Each of the variables is a function of wavelength.

$$T_{i,j} = \frac{T_{i,j-1}T_{j,j}}{1 - R^f_{j,j}R^b_{j-1,i}} \qquad (1.83)$$

$$R^f_{i,j} = R^f_{i,j-1} + \frac{T^2_{i,j-1}R^f_{j,j}}{1 - R^f_{j,j}R^b_{j-1,i}} \qquad (1.84)$$

$$R^b_{j,i} = R^b_{j,j} + \frac{T^2_{j,j}R^b_{j-1,i}}{1 - R^b_{j-1,i}R^f_{j,j}} \qquad (1.85)$$

$$A^f_j = \frac{T_{1,j-1}(1 - T_{j,j} - R^f_{j,j})}{1 - R^f_{j,N}R^b_{j-1,1}} + \frac{T_{1,j}R^f_{j+1,N}(1 - T_{j,j} - R^b_{j,j})}{1 - R^f_{j,N}R^b_{j-1,1}} \qquad (1.86)$$

In Eq. (1.86) $T_{i,j}$ = 1 and $R_{i,j}$ = 0 if $i<0$ or $j>N$.
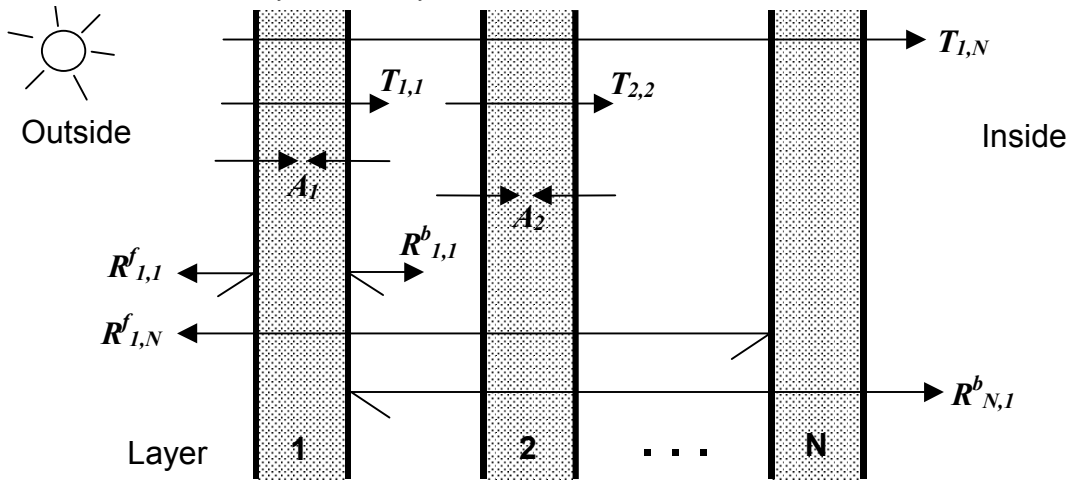
Figure 39. Schematic of transmission, reflection and absorption of solar radiation within a multi-layer glazing system.

As an example, for double glazing (N=2) these equations reduce to

$$T_{1,2} = \frac{T_{1,1}T_{2,2}}{1 - R^f_{2,2}R^b_{1,1}}$$

$$R_{1,2}^f = R_{1,1}^f + \frac{T_{1,1}^2 R_{2,2}^f}{1 - R_{2,2}^f R_{1,1}^b}$$

$$R_{2,1}^b = R_{2,2}^b + \frac{T_{2,2}^2 R_{1,1}^b}{1 - R_{1,1}^b R_{2,2}^f}$$

$$A_1^f = (1 - T_{1,1} - R_{1,1}^f) + \frac{T_{1,1} R_{2,2}^f (1 - T_{1,1} - R_{1,1}^b)}{1 - R_{2,2}^f R_{1,1}^b}$$

$$A_2^f = \frac{T_{1,1}(1 - T_{2,2} - R_{2,2}^f)}{1 - R_{2,2}^f R_{1,1}^b}$$

If the above transmittance and reflectance properties are input as a function of wavelength, EnergyPlus calculates "spectral average" values of the above glazing system properties by integrating over wavelength:

The spectral-average solar property is

$$P_s = \frac{\int P(\lambda) E_s(\lambda) d\lambda}{\int E_s(\lambda) d\lambda}$$

The spectral-average visible property is

$$P_v = \frac{\int P(\lambda) E_s(\lambda) R(\lambda) d\lambda}{\int E_s(\lambda) R(\lambda) d\lambda}$$

where $E_s(\lambda)$ is the solar spectral irradiance function and $R(\lambda)$ is the photopic response function of the eye. These functions are shown in Table 14 and Table 15. They are expressed as a set of values followed by the corresponding wavelengths for values.

If a glazing layer has optical properties that are roughly constant with wavelength, the wavelength-dependent values of $T_{i,i}$, $R^f_{i,i}$ and $R^b_{i,i}$ in Eqs. (1.83) to (1.86) can be replaced with constant values for that layer.

Table 14: Solar spectral irradiance function.

Air mass 1.5 terrestrial solar global spectral irradiance values (W/m²-micron) on a 37° tilted surface. Corresponds to wavelengths in following data block. Based on ISO 9845-1 and ASTM E 892; derived from Optics5 data file ISO-9845GlobalNorm.std, 10-14-99.

```
    0.0,    9.5,   42.3,  107.8,  181.0,  246.0,  395.3,  390.1,  435.3,  438.9,
  483.7,  520.3,  666.2,  712.5,  720.7,1013.1,1158.2,1184.0,1071.9,1302.0,
 1526.0,1599.6,1581.0,1628.3,1539.2,1548.7,1586.5,1484.9,1572.4,1550.7,
 1561.5,1501.5,1395.5,1485.3,1434.1,1419.9,1392.3,1130.0,1316.7,1010.3,
 1043.2,1211.2,1193.9,1175.5,  643.1,1030.7,1131.1,1081.6,  849.2,  785.0,
  916.4,  959.9,  978.9,  933.2,  748.5,  667.5,  690.3,  403.6,  258.3,  313.6,
  526.8,  646.4,  746.8,  690.5,  637.5,  412.6,  108.9,  189.1,  132.2,  339.0,
  460.0,  423.6,  480.5,  413.1,  250.2,   32.5,    1.6,   55.7,  105.1,  105.5,
```

``` 182.1, 262.2, 274.2, 275.0, 244.6, 247.4, 228.7, 244.5, 234.8, 220.5, 171.5, 30.7,   2.0,   1.2, 21.2, 91.1, 26.8, 99.5, 60.4, 89.1, 82.2, 71.5, 70.2, 62.0, 21.2, 18.5,   3.2 ```
Wavelengths (microns) corresponding to above data block
``` 0.3000,0.3050,0.3100,0.3150,0.3200,0.3250,0.3300,0.3350,0.3400,0.3450, 0.3500,0.3600,0.3700,0.3800,0.3900,0.4000,0.4100,0.4200,0.4300,0.4400, 0.4500,0.4600,0.4700,0.4800,0.4900,0.5000,0.5100,0.5200,0.5300,0.5400, 0.5500,0.5700,0.5900,0.6100,0.6300,0.6500,0.6700,0.6900,0.7100,0.7180, 0.7244,0.7400,0.7525,0.7575,0.7625,0.7675,0.7800,0.8000,0.8160,0.8237, 0.8315,0.8400,0.8600,0.8800,0.9050,0.9150,0.9250,0.9300,0.9370,0.9480, 0.9650,0.9800,0.9935,1.0400,1.0700,1.1000,1.1200,1.1300,1.1370,1.1610, 1.1800,1.2000,1.2350,1.2900,1.3200,1.3500,1.3950,1.4425,1.4625,1.4770, 1.4970,1.5200,1.5390,1.5580,1.5780,1.5920,1.6100,1.6300,1.6460,1.6780, 1.7400,1.8000,1.8600,1.9200,1.9600,1.9850,2.0050,2.0350,2.0650,2.1000, 2.1480,2.1980,2.2700,2.3600,2.4500,2.4940,2.5370 ```

Table 15: Photopic response function.

Photopic response function values corresponding to wavelengths in following data block. Based on CIE 1931 observer; ISO/CIE 10527, CIE Standard Calorimetric Observers; derived from Optics5 data file "CIE 1931 Color Match from E308.txt", which is the same as WINDOW4 file Cie31t.dat.
``` 0.0000,0.0001,0.0001,0.0002,0.0004,0.0006,0.0012,0.0022,0.0040,0.0073, 0.0116,0.0168,0.0230,0.0298,0.0380,0.0480,0.0600,0.0739,0.0910,0.1126, 0.1390,0.1693,0.2080,0.2586,0.3230,0.4073,0.5030,0.6082,0.7100,0.7932, 0.8620,0.9149,0.9540,0.9803,0.9950,1.0000,0.9950,0.9786,0.9520,0.9154, 0.8700,0.8163,0.7570,0.6949,0.6310,0.5668,0.5030,0.4412,0.3810,0.3210, 0.2650,0.2170,0.1750,0.1382,0.1070,0.0816,0.0610,0.0446,0.0320,0.0232, 0.0170,0.0119,0.0082,0.0158,0.0041,0.0029,0.0021,0.0015,0.0010,0.0007, 0.0005,0.0004,0.0002,0.0002,0.0001,0.0001,0.0001,0.0000,0.0000,0.0000, 0.0000 / ```
Wavelengths (microns) corresponding to above data block
``` .380,.385,.390,.395,.400,.405,.410,.415,.420,.425, .430,.435,.440,.445,.450,.455,.460,.465,.470,.475, .480,.485,.490,.495,.500,.505,.510,.515,.520,.525, .530,.535,.540,.545,.550,.555,.560,.565,.570,.575, .580,.585,.590,.595,.600,.605,.610,.615,.620,.625, .630,.635,.640,.645,.650,.655,.660,.665,.670,.675, .680,.685,.690,.695,.700,.705,.710,.715,.720,.725, .730,.735,.740,.745,.750,.755,.760,.765,.770,.775, .780 ```

Calculation of Angular Properties

Calculation of optical properties is divided into two categories: uncoated glass and coated glass.

Angular Properties for Uncoated Glass

The following discussion assumes that optical quantities such as transmittivity, reflectvity, absorptivity and index of refraction are a function of wavelength, λ. If there are no spectral data the angular dependence is calculated based on the single values for transmittance and reflectance in the visible and solar range. In the visible range an average wavelength of 0.575

microns is used in the calculations. In the solar range an average wavelength of 0.898 microns is used.

The spectral data include the transmittance, T, and the reflectance, R. For uncoated glass the reflectance is the same for the front and back surfaces. For angle of incidence, ϕ, the transmittance and reflectance are related to the transmissivity, τ, and reflectivity, ρ, by the following relationships:

$$T(\phi) = \frac{\tau(\phi)^2 e^{-\alpha d/\cos\phi'}}{1 - \rho(\phi)^2 e^{-2\alpha d/\cos\phi'}}$$ (1.87)

$$R(\phi) = \rho(\phi)\left(1 + T(\phi)e^{-\alpha d/\cos\phi'}\right)$$ (1.88)

The spectral reflectivity is calculated from Fresnel's equation assuming unpolarized incident radiation:

$$\rho(\phi) = \frac{1}{2}\left(\left(\frac{n\cos\phi - \cos\phi'}{n\cos\phi + \cos\phi'}\right)^2 + \left(\frac{n\cos\phi' - \cos\phi}{n\cos\phi' + \cos\phi}\right)^2\right)$$ (1.89)

The spectral transmittivity is given by

$$\tau(\phi) = 1 - \rho(\phi)$$ (1.90)

The spectral absorption coefficient is defined as

$$\alpha = 4\pi\kappa/\lambda$$ (1.91)

where κ is the dimensionless spectrally-dependent extinction coefficient and λ is the wavelength expressed in the same units as the sample thickness.

Solving Eq. (1.89) at normal incidence gives

$$n = \frac{1 + \sqrt{\rho(0)}}{1 - \sqrt{\rho(0)}}$$ (1.92)

Evaluating Eq. (1.88) at normal incidence gives the following expression for κ

$$\kappa = -\frac{\lambda}{4\pi d}\ln\frac{R(0) - \rho(0)}{\rho(0)T(0)}$$ (1.93)

Eliminating the exponential in Eqs. (1.87) and (1.88) gives the reflectivity at normal incidence:

$$\rho(0) = \frac{\beta - \sqrt{\beta^2 - 4(2 - R(0))R(0)}}{2(2 - R(0))}$$ (1.94)

where

$$\beta = T(0)^2 - R(0)^2 + 2R(0) + 1 \tag{1.95}$$

The value for the reflectivity, $\rho(0)$, from Eq. (1.94) is substituted into Eqs. (1.92) and (1.93). The result from Eq. (1.93) is used to calculate the absorption coefficient in Eq. (1.91). The index of refraction is used to calculate the reflectivity in Eq. (1.89) which is then used to calculate the transmittivity in Eq. (1.90). The reflectivity, transmissivity and absorption coefficient are then substituted into Eqs. (1.87) and (1.88) to obtain the angular values of the reflectance and transmittance.

Angular Properties for Coated Glass

A regression fit is used to calculate the angular properties of coated glass from properties at normal incidence. If the transmittance of the coated glass is > 0.645, the angular dependence of uncoated clear glass is used. If the transmittance of the coated glass is ≤ 0.645, the angular dependence of uncoated bronze glass is used. The values for the angular functions for the transmittance and reflectance of both clear glass $(\overline{\tau}_{clr}, \overline{\rho}_{clr})$ and bronze glass $(\overline{\tau}_{bnz}, \overline{\rho}_{bnz})$ are determined from a fourth-order polynomial regression:

$$\overline{\tau}(\phi) = \overline{\tau}_0 + \overline{\tau}_1 \cos(\phi) + \overline{\tau}_2 \cos^2(\phi) + \overline{\tau}_3 \cos^3(\phi) + \overline{\tau}_4 \cos^4(\phi)$$

and

$$\overline{\rho}(\phi) = \overline{\rho}_0 + \overline{\rho}_1 \cos(\phi) + \overline{\rho}_2 \cos^2(\phi) + \overline{\rho}_3 \cos^3(\phi) + \overline{\rho}_4 \cos^4(\phi) - \overline{\tau}(\phi)$$

The polynomial coefficients are given in Table 16.

Table 16: Polynomial coefficients used to determine angular properties of coated glass.

	0	**1**	**2**	**3**	**4**
$\overline{\tau}_{clr}$	-0.0015	3.355	-3.840	1.460	0.0288
$\overline{\rho}_{clr}$	0.999	-0.563	2.043	-2.532	1.054
$\overline{\tau}_{bnz}$	-0.002	2.813	-2.341	-0.05725	0.599
$\overline{\rho}_{bnz}$	0.997	-1.868	6.513	-7.862	3.225

These factors are used as follows to calculate the angular transmittance and reflectance:

For $T(0) > 0.645$:

$$T(\phi) = T(0)\overline{\tau}_{clr}(\phi)$$

$$R(\phi) = R(0)(1 - \overline{\rho}_{clr}(\phi)) + \overline{\rho}_{clr}(\phi)$$

For $T(0) \leq 0.645$:

$$T(\phi) = T(0)\overline{\tau}_{bnz}(\phi)$$

$$R(\phi) = R(0)(1 - \overline{\rho}_{bnz}(\phi)) + \overline{\rho}_{bnz}(\phi)$$

Calculation of Hemispherical Values

The hemispherical value of a property is determined from the following integral:

$$P_{hemispherical} = 2\int_0^{\frac{\pi}{2}} P(\phi)\cos(\phi)\sin(\phi)d\phi$$

The integral is evaluated by Simpson's rule for property values at angles of incidence from 0 to 90 degrees in 10-degree increments.

Optical Properties of Window Shading Devices

Shading devices affect the system transmittance and glass layer absorptance for short-wave radiation and for long-wave (thermal) radiation. The effect depends on the shade position (exterior or interior), its transmittance, and the amount of inter-reflection between the shading device and the glazing. Also of interest is the amount of radiation absorbed by the shading device.

In EnergyPlus, shading devices are divided into three categories, "shades," 'blinds," and "switchable glazing." "Shades" are assumed to be perfect diffusers. This means that direct radiation incident on the shade is reflected and transmitted as hemispherically uniform diffuse radiation: there is no direct component of transmitted radiation. It is also assumed that the transmittance, τ_{sh}, reflectance, ρ_{sh}, and absorptance, α_{sh}, are the same for the front and back of the shade and are independent of angle of incidence. Many types of drapery and pull-down roller devices are close to being perfect diffusers and can be categorized as "shades."

"Blinds" in EnergyPlus are slat-type devices such as venetian blinds. Unlike shades, the optical properties of blinds are strongly dependent on angle of incidence. Also, depending on slat angle and the profile angle of incident direct radiation, some of the direct radiation may pass between the slats, giving a direct component of transmitted radiation.

With "Switchable glazing" shading is achieved making the glazing more absorbing or more reflecting, usually by an electrical or chemical mechanism. An example is electrochromic glazing where the application of an electrical voltage or current causes the glazing to switch from light to dark.

Shades and blinds can be either fixed or moveable. If moveable, they can be deployed according to a schedule or according to a trigger variable, such as solar radiation incident on the window.

Shades

Shade/Glazing System Properties for Short-Wave Radiation

Short-wave radiation includes

(1) Beam solar radiation from the sun and diffuse solar radiation from the sky and ground incident on the outside of the window,

(2) Solar radiation reflected from the inside zone surfaces and incident as diffuse radiation on the inside of the window,

(3) Beam solar radiation from one exterior window incident on the inside of another window in the same zone, and

(4) Short-wave radiation from electric lights incident as diffuse radiation on the inside of thewindow.

Exterior Shade

For an exterior shade we have the following expressions for the effective system transmittance, the effective glass layer absorptance, and the effective shade absorptance, taking inter-reflection between shade and glazing into account. Here, "effective" means the shade is in place. The effective properties are given in terms of the isolated shade properties

(i.e., shade properties in the absence of the glazing) and the isolated glazing properties (i.e., glazing properties in the absence of the shade).

$$T_{eff}(\phi) = T_{1,N}^{dif} \frac{\tau_{sh}}{1 - R_f^{dif} \rho_{sh}}$$

$$T_{eff}^{dif} = T_{1,N}^{dif} \frac{\tau_{sh}}{1 - R_f^{dif} \rho_{sh}}$$

$$A_{j,f}^{eff}(\phi) = A_{j,f}^{dif} \frac{\tau_{sh}}{1 - R_f \rho_{sh}}, \qquad j = 1 \text{ to } N$$

$$A_{j,f}^{dif,eff} = A_{j,f}^{dif} \frac{\tau_{sh}}{1 - R_f \rho_{sh}}, \qquad j = 1 \text{ to } N$$

$$A_{j,b}^{dif,eff} = A_{j,b}^{dif} \frac{T_{1,N}^{dif} \rho_{sh}}{1 - R_f \rho_{sh}}, \qquad j = 1 \text{ to } N$$

$$\alpha_{sh}^{eff} = \alpha_{sh} \left(1 + \frac{\tau_{sh} R_f}{1 - R_f \rho_{sh}} \right)$$

Interior Shade

The effective system properties when an interior shade is in place are the following.

$$T_{eff}(\phi) = T_{1,N}(\phi) \frac{\tau_{sh}}{1 - R_b^{dif} \rho_{sh}}$$

$$T_{eff}^{dif} = T_{1,N}^{dif} \frac{\tau_{sh}}{1 - R_b^{dif} \rho_{sh}}$$

$$A_{j,f}^{eff}(\phi) = A_{j,f}(\phi) + T_{1,N}(\phi) \frac{\rho_{sh}}{1 - R_b^{dif} \rho_{sh}} A_{j,b}^{dif}, \qquad j = 1 \text{ to } N$$

$$A_{j,f}^{dif,eff} = A_{j,f}^{dif} + T_{1,N}^{dif} \frac{\rho_{sh}}{1 - R_b^{dif} \rho_{sh}} A_{j,b}^{dif}, \qquad j = 1 \text{ to } N$$

$$A_{j,b}^{dif,eff} = \frac{\tau_{sh}}{1 - R_b^{dif} \rho_{sh}} A_{j,b}^{dif}, \qquad j = 1 \text{ to } N$$

$$\alpha_{sh}^{eff}(\phi) = T_{1,N}(\phi) \frac{\alpha_{sh}}{1 - R_b^{dif} \rho_{sh}}$$

$$\alpha_{sh}^{dif,eff} = T_{1,N}^{dif} \frac{\alpha_{sh}}{1 - R_b^{dif}\rho_{sh}}$$

Long-Wave Radiation Properties of Window Shades

Long-wave radiation includes

(1) Thermal radiation from the sky and ground incident on the outside of the window,

(2) Thermal radiation from other room surfaces incident on the inside of the window, and

(3) Thermal radiation from internal sources, such as equipment and electric lights, incident on the inside of the window.

The program calculates how much long-wave radiation is absorbed by the shade and by the adjacent glass surface. The effective emissivity (thermal absorptance) for an interior or exterior shade, taking into account reflection of long-wave radiation between the glass and shade, is given by

$$\varepsilon_{sh}^{lw,eff} = \varepsilon_{sh}^{lw}\left(1 + \frac{\tau_{sh}^{lw}\rho_{gl}^{lw}}{1 - \rho_{sh}^{lw}\rho_{gl}^{lw}}\right)$$

where ρ_{gl}^{lw} is the long-wave reflectance of the outermost glass surface for an exterior shade or the innermost glass surface for an interior shade, and it is assumed that the long-wave transmittance of the glass is zero.

The effective innermost (for interior shade) or outermost (for exterior shade) glass surface emissivity when the shade is present is

$$\varepsilon_{gl}^{lw,eff} = \varepsilon_{gl}^{lw} \frac{\tau_{sh}^{lw}}{1 - \rho_{sh}^{lw}\rho_{gl}^{lw}}$$

Switchable Glazing

For switchable glazing, such as electrochromics, the solar and visible optical properties of the glazing can switch from a light state to a dark state. The switching factor, f_{switch}, determines what state the glazing is in. An optical property, p, such as transmittance or glass layer absorptance, for this state is given by

$$p = (1 - f_{switch})p_{light} + f_{switch}p_{dark}$$

where

p_{light} is the property value for the unswitched, or light state, and p_{dark} is the property value for the fully switched, or dark state.

The value of the switching factor in a particular time step depends on what type of switching control has been specified: "schedule," "trigger," or "daylighting." If "schedule," f_{switch} = schedule value, which can be 0 or 1.

Blinds

Window blinds in EnergyPlus are defined as a series of equidistant slats that are oriented horizontally or vertically. All of the slats are assumed to have the same optical properties. The overall optical properties of the blind are determined by the slat geometry (width, separation and angle) and the slat optical properties (front-side and back-side transmittance and reflectance). Blind properties for direct radiation are also sensitive to the "profile angle," which

is the angle of incidence in a plane that is perpendicular to the window plane and to the direction of the slats. The blind optical model in EnergyPlus is based on Simmler, Fischer and Winkelmann, 1996; however, that document has numerous typographical errors and should be used with caution.

The following assumptions are made in calculating the blind optical properties:

- The slats are flat.

- The spectral dependence of inter-reflections between slats and glazing is ignored; spectral-average slat optical properties are used.

- The slats are perfect diffusers. They have a perfectly matte finish so that reflection from a slat is isotropic (hemispherically uniform) and independent of angle of incidence, i.e., the reflection has no specular component. This also means that absorption by the slats is hemispherically uniform with no incidence angle dependence. If the transmittance of a slat is non-zero, the transmitted radiation is isotropic and the transmittance is independent of angle of incidence.

- Inter-reflection between the blind and wall elements near the periphery of the blind is ignored.

The effect of the holes in the slats through which support strings pass is ignored.

Slat Optical Properties

The slat optical properties used by EnergyPlus are shown in the following table.

Table 17. Slat Optical Properties

$\tau_{dir,dif}$	Direct-to-diffuse transmittance (same for front and back of slat)
$\tau_{dif,dif}$	Diffuse-to-diffuse transmittance (same for front and back of slat)
$\rho_{dir,dif}^{f}$, $\rho_{dir,dif}^{b}$	Front and back direct-to-diffuse reflectance
$\rho_{dif,dif}^{f}$, $\rho_{dif,dif}^{b}$	Front and back diffuse-to-diffuse reflectance

It is assumed that there is no direct-to-direct transmission or reflection, so that $\tau_{dir,dir} = 0$, $\rho_{dir,dir}^{f} = 0$, and $\rho_{dir,dir}^{b} = 0$. It is further assumed that the slats are perfect diffusers, so that $\tau_{dir,dif}$, $\rho_{dir,dif}^{f}$ and $\rho_{dir,dif}^{b}$ are independent of angle of incidence.

Direct Transmittance of Blind

The direct-to-direct and direct-to-diffuse transmittance of a blind is calculated using the slat geometry shown in Figure 40 (a), which shows the side view of one of the cells of the blind. For the case shown, each slat is divided into two segments, so that the cell is bounded by a total of six segments, denoted by s_1 through s_6 (note in the following that s_i refers to both segment i and the length of the segment i).The lengths of s_1 and s_2 are equal to the slat separation, h, which is the distance between adjacent slat faces. s_3 and s_4 are the segments illuminated by direct radiation. In the case shown in Figure 40 (a) the cell receives radiation by reflection of the direct radiation incident on s_4 and, if the slats have non-zero transmittance, by transmission through s_3, which is illuminated from above.

The goal of the blind direct transmission calculation is to determine the direct and diffuse radiation leaving the cell through s_2 for unit direct radiation entering the cell through s_1.
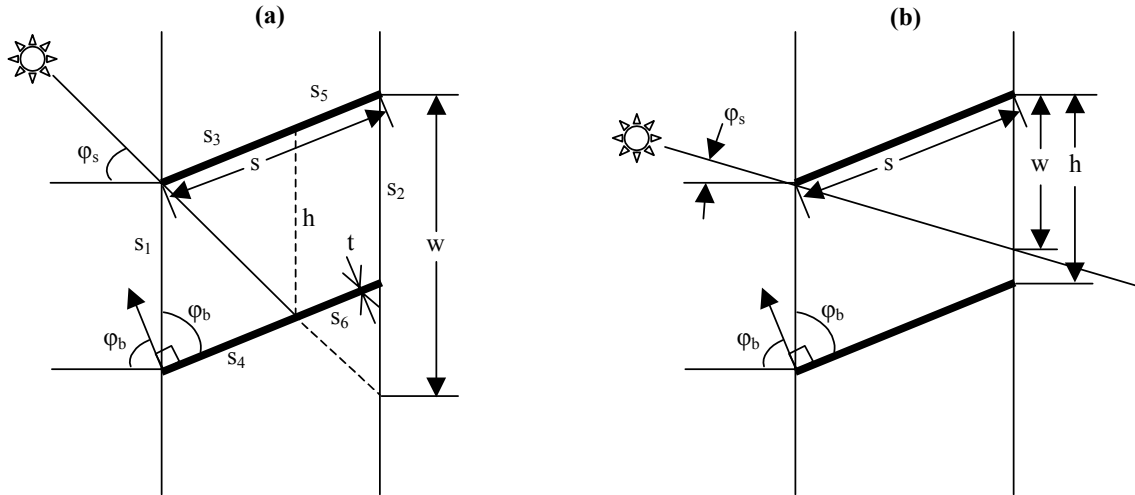
Figure 40. (a) Side view of a cell formed by adjacent slats showing how the cell is divided into segments for the calculation of direct solar transmittance; (b) side view of a cell showing case where some of the direct solar passes between adjacent slats without touching either of them. In this figure φ_s is the profile angle and φ_b is the slat angle.

Direct-to-Direct Blind Transmittance

Figure 40 (b) shows the case where some of the direct radiation passes through the cell without hitting the slats. From the geometry in this figure we see that
where

$$ w = s\frac{\cos(\varphi_b - \varphi_s)}{\cos\varphi_s} $$

Note that we are assuming that the slat thickness is zero. A correction for non-zero slat thickness is described later.

Direct-to-Diffuse Blind Transmittance, Reflectance and Absorptance

The direct-to-diffuse and transmittance and reflectance of the blind are calculated using a radiosity method that involves the following three vector quantities:

J_i = the radiosity of segment s_i, i.e., the total radiant flux into the cell from s_i

G_i = the irradiance on the cell side of s_i

Q_i = the source flux from the cell side of s$_i$

Based on these definitions we have the following equations that relate J, G and Q for the different segments:

$$ J_1 = Q_1 $$
$$ J_2 = Q_2 $$
$$ J_3 = Q_3 + \rho_{dif,dif}^b G_3 + \tau_{dif,dif} G_4 $$
$$ J_4 = Q_4 + \tau_{dif,dif} G_3 + \rho_{dif,dif}^f G_4 $$
$$ J_5 = Q_5 + \rho_{dif,dif}^b G_5 + \tau_{dif,dif} G_6 $$
$$ J_6 = Q_6 + \tau_{dif,dif} G_5 + \rho_{dif,dif}^f G_6 $$

In addition we have the following equation relating G and J:

$$G_i = \sum_{j=1}^{6} J_j F_{ji}, \quad i = 1, 6$$

where F_{ji} is the view factor between s_j and s_i, i.e., F_{ji} is the fraction of radiation leaving s_j that is intercepted by s_i.

Using $J_1 = Q_1 = 0$ and $J_2 = Q_2 = 0$ and combining the above equations gives the following equation set relating J and Q:

$$J_3 - \rho_{dif,dif}^b \sum_{j=3}^{6} J_j F_{j3} - \tau_{dif,dif} \sum_{j=3}^{6} J_j F_{j4} = Q_3$$

$$J_4 - \tau_{dif,dif} \sum_{j=3}^{6} J_j F_{j3} - \rho_{dif,dif}^f \sum_{j=3}^{6} J_j F_{j4} = Q_4$$

$$J_5 - \rho_{dif,dif}^b \sum_{j=3}^{6} J_j F_{j5} - \tau_{dif,dif} \sum_{j=3}^{6} J_j F_{j6} = Q_5$$

$$J_6 - \tau_{dif,dif} \sum_{j=3}^{6} J_j F_{j3} - \rho_{dif,dif}^f \sum_{j=3}^{6} J_j F_{j6} = Q_6$$

This can be written in the form

$$XJ' = Q' \qquad\qquad (1.96)$$

where X is a 4x4 matrix and

$$J' = \begin{bmatrix} J_3 \\ J_4 \\ J_5 \\ J_6 \end{bmatrix} \qquad Q' = \begin{bmatrix} Q_3 \\ Q_4 \\ Q_5 \\ Q_6 \end{bmatrix}$$

We then obtain J' from

$$J' = X^{-1} Q'$$

The view factors, F_{ij}, are obtained as follows. The cell we are dealing with is a convex polygon with n sides. In such a polygon the view factors must satisfy the following constraints:

$$\sum_{j=1}^{n} F_{ij} = 1, \quad i = 1, n$$

$$s_i F_{ij} = s_j F_{ji}, \quad i = 1, n; \ j = 1, n$$

$$F_{ii} = 0, \quad i = 1, n$$

These constraints lead to simple equations for the view factors for $n = 3$ and 4. For $n = 3$, we have the following geometry and view factor expression:
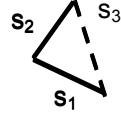
$$F_{12} = \frac{s_1 + s_2 - s_3}{2s_1}$$

For $n = 4$ we have:
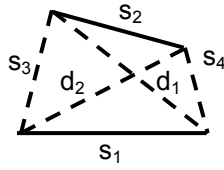
$$F_{12} = \frac{d_1 + d_2 - (s_3 + s_4)}{2s_1}$$

Applying these to the slat cell shown in Figure 41 we have the following:

$$F_{12} = \frac{d_1 + d_2 - 2s}{2h}$$

$$F_{13} = \frac{h + s_3 - d_3}{2h} \ , \quad \text{etc.}$$
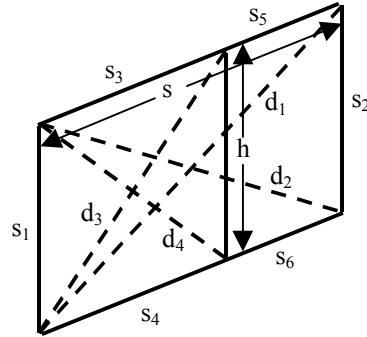
Figure 41. Slat cell showing geometry for calculation of view factors between the segments of the cell.

The sources for the direct-to-diffuse transmittance calculation are:

$$Q_1 = Q_2 = Q_5 = Q_6 = 0 \ \text{ (and therefore } J_1 = J_2 = 0)$$

$$\left. \begin{array}{l} Q_3 = \tau_{dir,dif} \\ Q_4 = \rho_{dir,dif}^f \end{array} \right\} \ \varphi_b \leq \varphi_s + \frac{\pi}{2} \ \text{ (beam hits front of slats)}$$

$$
\left.\begin{array}{l}
Q_3 = \rho_{dir,dif}^{b} \\[2mm]
Q_4 = \tau_{dir,dif}
\end{array}\right\} \quad \varphi_b > \varphi_s + \frac{\pi}{2} \quad \text{(beam hits back of slats)}
$$

For unit incident direct flux, the front direct-to-diffuse transmittance and reflectance of the blind are:

$$
\tau_{bl,f}^{dir,dif} = G_2
$$

$$
\rho_{bl,f}^{dir,dif} = G_1
$$

where

$$
G_2 = \sum_{j=3}^{6} J_j F_{j2}
$$

$$
G_1 = \sum_{j=3}^{6} J_j F_{j1}
$$

and J_3 to J_6 are given by Eq. (1.96).

The front direct absorptance of the blind is then

$$
\alpha_{bl,f}^{dir} = 1 - \tau_{bl,f}^{dir,dif} - \tau_{bl,f}^{dir,dir} - \rho_{bl,f}^{dir,dif}
$$

The direct-to-diffuse calculations are performed separately for solar and visible slat properties to get the corresponding solar and visible blind properties.

Dependence on Profile Angle

The direct-to-direct and direct-to-diffuse blind properties are calculated for direct radiation profile angles (see Figure 40) ranging from –90$^{\text{O}}$ to +90$^{\text{O}}$ in 5$^{\text{O}}$ increments. (The "profile angle" is the angle of incidence in a plane that is perpendicular to the window *and* perpendicular to the slat direction.) In the time step loop the blind properties for a particular profile angle are obtained by interpolation.

Dependence on Slat Angle

All blind properties are calculated for slat angles ranging from –90$^{\text{O}}$ to +90$^{\text{O}}$ in 10$^{\text{O}}$ increments. In the time-step loop the slat angle is determined by the slat-angle control mechanism and then the blind properties at that slat angle are determined by interpolation. Three slat-angle controls are available: (1) slat angle is adjusted to just block beam solar incident on the window; (2) slat angle is determined by a schedule; and (3) slat angle is fixed.

Diffuse-to-Diffuse Transmittance and Reflectance of Blind

To calculate the diffuse-to-diffuse properties each slat bounding the cell is divided into two segments of equal length (Figure 42), i.e., $s_3 = s_4$ and $s_5 = s_6$. For front-side properties we have a unit source, $Q_1 = 1$. All the other Q_i are zero. Using this source value, we apply the methodology described above to obtain G_2 and G_1. We then have

$$
\tau_{bl,f}^{dif,dif} = G_2
$$

$$
\rho_{bl,f}^{dif,dif} = G_1
$$

$$
\alpha_{bl,f}^{dif} = 1 - \tau_{bl,f}^{dif,dif} - \rho_{bl,f}^{dif,dif}
$$

The back-side properties are calculated in a similar way by setting $Q_2 = 1$ with the other Q_i equal to zero.

The diffuse-to-diffuse calculations are performed separately for solar, visible and IR slat properties to get the corresponding solar, visible and IR blind properties.
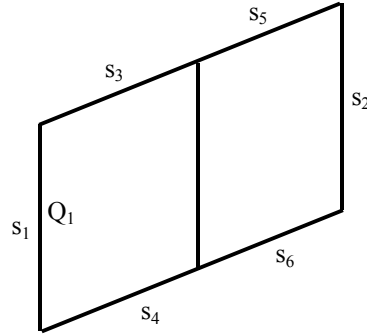
Figure 42. Slat cell showing arrangement of segments and location of source for calculation of diffuse-to-diffuse optical properties.

Correction Factor for Slat Thickness

A correction has to be made to the blind transmittance, reflectance and absorptance properties to account for the amount of radiation incident on a blind that is reflected and absorbed by the slat edges (the slats are assumed to be opaque to radiation striking the slat edges). This is illustrated in Figure 43 for the case of direct radiation incident on the blind. The slat cross-section is assumed to be rectangular. The quantity of interest is the fraction, f_{edge}, of direct radiation incident on the blind that strikes the slat edges. Based on the geometry shown in Figure 43 we see that

$$f_{edge} = \frac{t\cos\gamma}{\left(h+\dfrac{t}{\cos\xi}\right)\cos\varphi_s} = \frac{t\cos(\varphi_s-\xi)}{\left(h+\dfrac{t}{\cos\xi}\right)\cos\varphi_s} = \frac{t\sin(\varphi_b-\varphi_s)}{\left(h+\dfrac{t}{\sin\varphi_b}\right)\cos\varphi_s}$$

The edge correction factor for diffuse incident radiation is calculated by averaging this value of f_{edge} over profile angles, φ_s, from -90° to $+90^O$.

As an example of how the edge correction factor is applied, the following two equations show how blind front diffuse transmittance and reflectance calculated assuming zero slat thickness are modified by the edge correction factor. It is assumed that the edge transmittance is zero and that the edge reflectance is the same as the slat front reflectance, ρ_f.

$$\tau_{bl,f}^{dif} \to \tau_{bl,f}^{dif}\left(1-f_{edge}\right)$$

$$\rho_{bl,f}^{dif} \to \rho_{bl,f}^{dif}\left(1-f_{edge}\right)+f_{edge}\rho_f$$
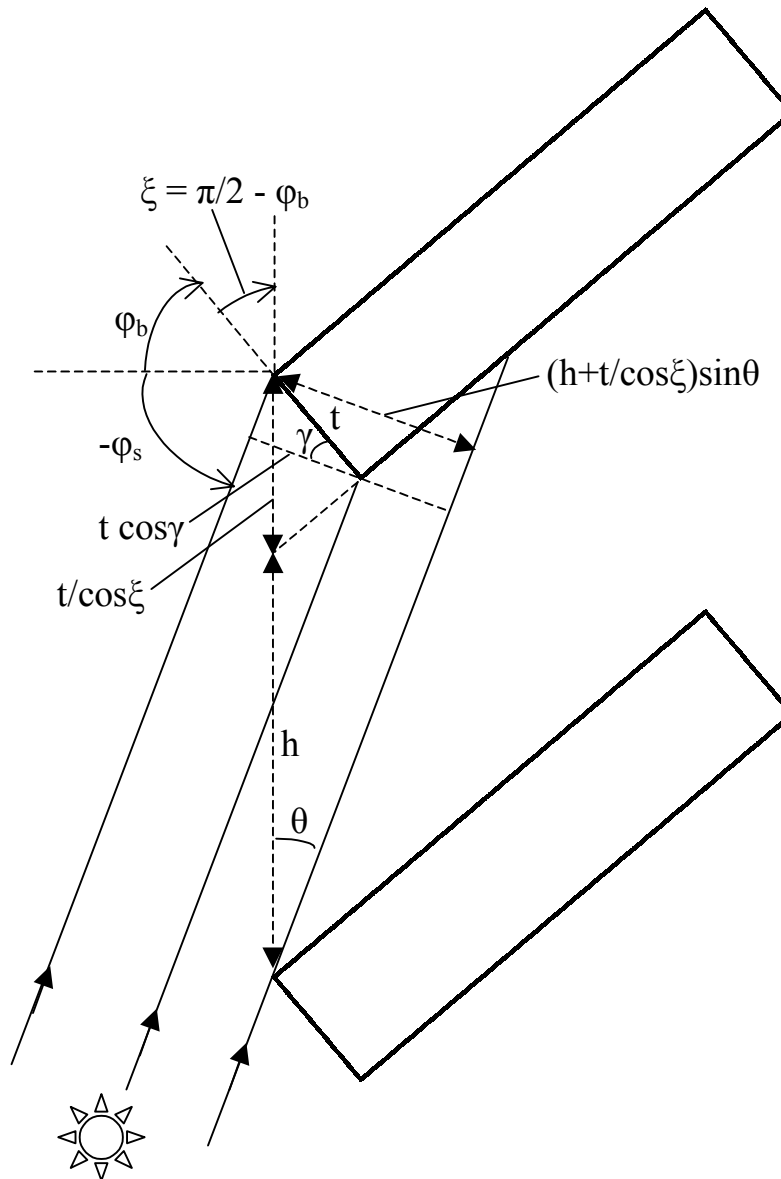
Figure 43. Side view of slats showing geometry for calculation of slat edge correction factor for incident direct radiation.

Comparison with ISO 15099 Calculation of Blind Optical Properties

Table 18 compares EnergyPlus and ISO 15099 [2001] calculations of blind optical properties for a variety of profile angles, slat angles and slat optical properties. The ISO 15099 calculation method is similar to that used in EnergyPlus, except that the slats are divided into five equal segments. The ISO 15099 and EnergyPlus results agree to within 12%, except for the solar transmittances for the 10-degree slat angle case. Here the transmittances are small (from 1% to about 5%) but differ by about a factor of up to two between ISO 15099 and EnergyPlus. This indicates that the slats should be divided into more than two segments at small slat angles.

Table 18. Comparison of blind optical properties calculated with the EnergyPlus and ISO 15099 methods. EnergyPlus values that differ by more than 12% from ISO 15099 values are shown in bold italics.

Slat properties

Separation (m)	0.012		0.012		0.012		0.012		0.012	
Width (m)	0.016		0.016		0.016		0.016		0.016	
Angle (deg)	45		45		45		10		45	
IR transmittance	0.0		0.0		0.0		0.0		0.4	
IR emissivity, front side	0.9		0.9		0.9		0.9		0.55	
IR emissivity, back side	0.9		0.9		0.9		0.9		0.55	
Solar transmittance	0.0		0.0		0.0		0.0		0.4	
Solar reflectance, front side	0.70		0.55		0.70		0.70		0.50	
Solar reflectance, back side	0.70		0.55		0.40		0.40		0.50	
Solar Profile angle (deg)	0	60	0	60	0	60	0	60	0	60
Calculated blind properties (first row = ISO 15099 calculation, second row (in italics) = EnergyPlus calculation)										
Front solar transmittance, direct to direct	0.057 *0.057*	0.0 *0.0*	0.057 *0.057*	0.0 *0.0*	0.057 *0.057*	0.0 *0.0*	0.0 *0.0*	0.0 *0.0*	0.057 *0.057*	0.0 *0.0*
Back solar transmittance, direct to direct	0.057 *0.057*	0.310 *0.309*	0.057 *0.057*	0.310 *0.309*	0.057 *0.057*	0.310 *0.309*	0.0 *0.0*	0.088 *0.087*	0.057 *0.057*	0.310 *0.309*
Front solar transmittance, direct to diffuse	0.141 *0.155*	0.073 *0.074*	0.090 *0.100*	0.047 *0.048*	0.096 *0.104*	0.051 *0.051*	0.012 ***0.019***	0.005 ***0.006***	0.373 *0.375*	0.277 *0.275*
Back solar transmittance, direct to diffuse	0.141 *0.155*	0.288 *0.284*	0.090 *0.100*	0.216 *0.214*	0.076 *0.085*	0.271 *0.269*	0.011 ***0.019***	0.027 ***0.052***	0.373 *0.375*	0.306 *0.304*
Front solar reflectance, direct to diffuse	0.394 *0.389*	0.558 *0.558*	0.295 *0.293*	0.430 *0.431*	0.371 *0.368*	0.544 *0.546*	0.622 *0.636*	0.678 *0.679*	0.418 *0.416*	0.567 *0.568*
Back solar reflectance, direct to diffuse	0.394 *0.389*	0.103 *0.115*	0.295 *0.293*	0.066 *0.074*	0.216 *0.214*	0.070 *0.077*	0.356 *0.363*	0.273 *0.272*	0.418 *0.416*	0.273 *0.275*
Front solar transmittance, diffuse to diffuse	0.332 *0.338*		0.294 *0.298*		0.291 *0.295*		0.038 ***0.053***		0.495 *0.502*	
Back solar transmittance, diffuse to diffuse	0.332 *0.338*		0.294 *0.298*		0.291 *0.295*		0.038 ***0.053***		0.495 *0.502*	
Front IR transmittance	0.227 *0.227*		0.227 *0.227*		0.227 *0.227*		0.0245 *0.025*		0.385 *0.387*	
Back IR transmittance	0.227 *0.227*		0.227 *0.227*		0.227 *0.227*		0.0245 *0.025*		0.385 *0.387*	
Front IR emissivity	0.729 *0.730*		0.729 *0.730*		0.729 *0.730*		0.890 *0.895*		0.536 *0.534*	
Back IR emissivity	0.729 *0.730*		0.729 *0.730*		0.729 *0.730*		0.890 *0.895*		0.536 *0.534*	

Blind/Glazing System Properties for Short-Wave Radiation

When a blind is in place we have the following expressions for the effective system transmittance, the effective glass layer absorptance, and the effective blind absorptance, taking inter-reflection between blind and glazing into account. The effective properties are given in terms of the isolated blind properties (i.e., blind properties in the absence of the

glazing) and the isolated glazing properties (i.e., glazing properties in the absence of the blind).

Interior Blind

The effective system properties when an interior blind is in place are the following:

$$
T_{f,eff}^{dir,all}(\phi,\phi_s) = T_{gl}^{dir}(\phi)\left(\tau_{bl,f}^{dir,dir}(\phi_s) + \tau_{bl,f}^{dir,dif}(\phi_s) + \frac{\tau_{bl,f}^{dif}\rho_{bl,f}^{dir,dif}(\phi_s)R_{gl,b}^{dif}}{1-\rho_{bl,f}^{dif}R_{gl,b}^{dif}} \right)
$$

$$
A_{gl,j,f}^{dir,eff}(\phi,\phi_s) = A_{gl,j,f}^{dir}(\phi) + \frac{T_{gl}^{dir}(\phi)\alpha_{gl,j,b}^{dif}\rho_{bl,f}^{dir}(\phi_s)}{1-\rho_{bl,f}^{dir}(\phi_s)R_{gl,b}^{dif}}, \quad j = 1,N
$$

$$
\alpha_{bl,f}^{dir,eff}(\phi,\phi_s) = T_{gl}^{dir}(\phi)\left(\alpha_{bl,f}^{dir}(\phi_s) + \frac{\rho_{bl,f}^{dir}(\phi_s)R_{gl,b}^{dif}\alpha_{bl,f}^{dif}}{1-\rho_{bl,f}^{dif}R_{gl,b}^{dif}} \right)
$$

Exterior Blind

The effective system properties when an exterior blind is in place are the following:

$$
T_{f,eff}^{dir,all}(\phi,\phi_s) = \tau_{bl,f}^{dir,dir}(\phi_s)\left(T_{gl}^{dir}(\phi) + \frac{T_{gl}^{dif}R_{gl,f}^{dir}\rho_{bl,b}^{dir,dif}}{1-R_{gl,f}^{dif}\rho_{bl,b}^{dif}} \right) + \frac{\tau_{bl}^{dir,dif}(\phi_s)T_{gl}^{dif}}{1-R_{gl,f}^{dif}\rho_{bl,b}^{dif}}
$$

$$
A_{gl,j,f}^{eff}(\phi,\phi_s) = \tau_{bl,f}^{dir,dir}(\phi_s)A_{gl,j,f}^{dir}(\phi) +
$$
$$
\frac{\left(\tau_{bl,f}^{dir,dir}(\phi_s)R_{gl}^{dir}(\phi)\rho_{bl,b}^{dir}(\phi_s) + \tau_{bl,f}^{dir,dif}(\phi_s) \right)A_{gl,j,f}^{dif}}{1-R_{gl,f}^{dif}\rho_{bl,b}^{dif}}, \quad j = 1,N
$$

$$
\alpha_{bl,f}^{dir,eff}(\phi,\phi_s) = \alpha_{bl,f}^{dir}(\phi_s) + \alpha_{bl,b}^{dir}(\phi_s)R_{gl,f}^{dir}(\phi)\tau_{bl,f}^{dir,dir}(\phi_s) +
$$
$$
\frac{\alpha_{bl,b}^{dif}R_{gl,f}^{dif}}{1-\rho_{bl,b}^{dif}R_{gl,f}^{dif}}\left(R_{gl,f}^{dir}(\phi)\tau_{bl,f}^{dir,dir}(\phi_s)\rho_{bl,b}^{dir}(\phi_s) + \tau_{bl,f}^{dir,dif}(\phi_s) \right)
$$

__Blind/Glazing System Properties for Long-Wave Radiation__

The program calculates how much long-wave radiation is absorbed by the blind and by the adjacent glass surface. The effective emissivity (long-wave absorptance) of an interior or exterior blind, taking into account reflection of long-wave radiation between the glass and blind, is given by

$$
\varepsilon_{bl}^{lw,eff} = \varepsilon_{bl}^{lw}\left(1 + \frac{\tau_{bl}^{lw}\rho_{gl}^{lw}}{1-\rho_{bl}^{lw}\rho_{gl}^{lw}} \right)
$$

where ρ_{gl}^{lw} is the long-wave reflectance of the outermost glass surface for an exterior blind or the innermost glass surface for an interior blind, and it is assumed that the long-wave transmittance of the glass is zero.

The effective innermost (for interior blind) or outermost (for exterior blind) glass surface emissivity when the blind is present is

$$\varepsilon_{gl}^{lw,eff} = \varepsilon_{gl}^{lw} \frac{\tau_{bl}^{lw}}{1 - \rho_{bl}^{lw} \rho_{gl}^{lw}}$$

The effective inside surface emissivity is the sum of the effective blind and effective glass emissivities:

$$\varepsilon_{ins}^{lw,eff} = \varepsilon_{bl}^{lw,eff} + \varepsilon_{gl}^{lw,eff}$$

The effective temperature of the blind/glazing combination that is used to calculate the window's contribution to the zone's mean radiant temperature (MRT) is given by

$$T^{eff} = \frac{\varepsilon_{bl}^{lw,eff} T_{bl} + \varepsilon_{gl}^{lw,eff} T_{gl}}{\varepsilon_{bl}^{lw,eff} + \varepsilon_{gl}^{lw,eff}}$$

Window Heat Balance Calculation

Table 19. Fortran Variables used in Window Heat Balance Calculations

Mathematical variable	Description	Units	FORTRAN variable
N	Number of glass layers	-	nlayer
σ	Stefan-Boltzmann constant		sigma
ε_i	Emissivity of face i	-	emis
k_i	Conductance of glass layer i	W/m²-K	scon
h_o, h_i	Outside, inside air film convective conductance	W/m²-K	hcout, hcout
h_j	Conductance of gap j	W/m²-K	hgap
T_o, T_i	Outside and inside air temperature	K	tout, tin
E_o, E_i	Exterior, interior long-wave radiation incident on window	W/m²	outir, rmir
θ_i	Temperature of face i	K	thetas
S_i	Radiation (short-wave, and long-wave from zone internal sources) absorbed by face i	W/m²	AbsRadGlassFace
I_{bm}^{ext}	Exterior beam normal solar intensity	W/m²	BeamSolarRad
I_{dif}^{ext}	Exterior diffuse solar intensity on glazing	W/m²	-
I_{sw}^{int}	Interior short-wave radiation (from lights and from reflected diffuse solar) incident on glazing from inside	W/m²	QS

I^{int}_{lw}	Long-wave radiation from lights and equipment incident on glazing from inside	W/m^2	QL
φ	Angle of incidence	radians	-
A^f_j	Front beam solar absorptance of glass layer j	-	-
$A_j^{f,dif}$, $A_j^{b,dif}$	Front and back diffuse solar absorptance of glass layer j	-	AbsDiff, AbsDiffBack
A, B	Matrices used to solve glazing heat balance equations	W/m^2, W/m^2-K	Aface, Bface
$h_{r,i}$	Radiative conductance for face i	W/m^2-K	hr(i)
$Δθ_i$	Difference in temperature of face i between successive iterations	K	-

The Glazing Heat Balance Equations

The window glass face temperatures are determined by solving the heat balance equations on each face every time step. For a window with N glass layers there are $2N$ faces and therefore $2N$ equations to solve. Figure 44 shows the variables used for double glazing (N=2).
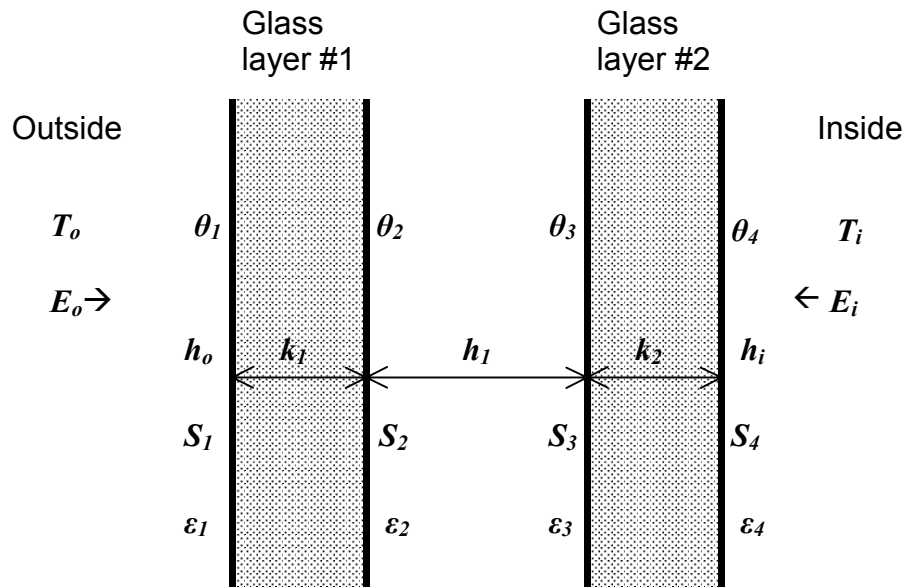
Figure 44. Glazing system with two glass layers showing variables used in heat balance equations.

The following assumptions are made in deriving the heat balance equations:

1) The glass layers are thin enough (a few millimeters) that heat storage in the glass can be neglected; therefore, there are no heat capacity terms in the equations.

2) The heat flow is perpendicular to the glass faces and is one dimensional. See "Edge of Glass Corrections," below, for adjustments to the gap conduction in multi-pane glazing to

account for 2-D conduction effects across the pane separators at the boundaries of the glazing.

3) The glass layers are opaque to IR. This is true for most glass products. For thin plastic suspended films this is not a good assumption, so the heat balance equations would have to be modified to handle this case.

4) The glass faces are isothermal. This is generally a good assumption since glass conductivity is very high.

5) The short wave radiation absorbed in a glass layer can be apportioned equally to the two faces of the layer.

The four equations for double-glazing are as follows. The equations for single glazing (N=1) and for N=3 and N=4 are analogous and are not shown.

$$E_o \varepsilon_1 - \varepsilon_1 \sigma \theta_1^4 + k_1 (\theta_2 - \theta_1) + h_o (T_o - \theta_1) + S_1 = 0 \tag{1.97}$$

$$k_1 (\theta_1 - \theta_2) + h_1 (\theta_3 - \theta_2) + \sigma \frac{\varepsilon_2 \varepsilon_3}{1 - (1 - \varepsilon_2)(1 - \varepsilon_3)} (\theta_3^4 - \theta_2^4) + S_2 = 0 \tag{1.98}$$

$$h_1 (\theta_2 - \theta_3) + k_2 (\theta_4 - \theta_3) + \sigma \frac{\varepsilon_2 \varepsilon_3}{1 - (1 - \varepsilon_2)(1 - \varepsilon_3)} (\theta_2^4 - \theta_3^4) + S_3 = 0 \tag{1.99}$$

$$E_i \varepsilon_4 - \varepsilon_4 \sigma \theta_4^4 + k_2 (\theta_3 - \theta_4) + h_i (T_i - \theta_4) + S_4 = 0 \tag{1.100}$$

Absorbed Radiation

S_i in Eqs. (1.97) to (1.100) is the radiation (short-wave and long-wave from zone lights and equipment) absorbed on the ith face. Short-wave radiation (solar and short-wave from lights) is assumed to be absorbed uniformly along a glass layer, so for the purposes of the heat balance calculation it is split equally between the two faces of a layer. Glass layers are assumed to be opaque to IR so that the thermal radiation from lights and equipment is assigned only to the inside (room-side) face of the inside glass layer. For N glass layers S_i is given by

$$S_{2j-1} = S_{2j} = \frac{1}{2} \left(I_{bm}^{ext} \cos\phi \, A_j^f(\phi) + I_{dif}^{ext} A_j^{f,dif} + I_{sw}^{int} A_j^{b,dif} \right), \quad j = 1 \text{ to } N$$

$$S_{2N} = S_{2N} + \varepsilon_{2N} I_{lw}^{int}$$

Here

I_{bm}^{ext} = exterior beam normal solar intensity

I_{dif}^{ext} = exterior diffuse solar incident on glazing from outside

I_{sw}^{int} = interior short-wave radiation (from lights and from reflected diffuse solar) incident on glazing from inside

I_{lw}^{int} = long-wave radiation from lights and equipment incident on glazing from inside

ε_{2N} = emissivity (thermal absorptance) of the room-side face of the inside glass layer

Solving the Glazing Heat Balance Equations

The equations are solved as follows:

1) Linearize the equations by defining $h_{r,i} = \varepsilon_i \sigma \theta_i^3$. For example, Eq. (1.97) becomes

$$E_o \varepsilon_1 - h_{r,1}\theta_1 + k_1(\theta_2 - \theta_1) + h_o(T_o - \theta_1) + S_1 = 0$$

2) Write the equations in the matrix form $A\theta = B$.

3) Use previous time step values of θ_i to calculate starting values for the $h_{r,i}$.

4) Find the solution $\theta = A^{-1}B$ by LU decomposition.

5) Re-evaluate the $h_{r,i}$ using the new θ_i.

6) Re-calculate $\theta = A^{-1}B$ using the new $h_{r,i}$.

Repeat steps 4,5 and 6 until the difference, $\Delta\theta_i$, between values of the θ_i in successive iterations is less than some tolerance value. Currently, the test is

$$\frac{1}{2N}\sum_{i=1}^{2N}|\Delta\theta_i| \ < 0.01K$$

This method converges in 6-8 iterations. Convergence in 2-4 iterations is obtained by relaxation on $h_{r,i}$, i.e.,

$$\left(h_{r,i}\right)_{new} \rightarrow 0.5[\left(h_{r,i}\right)_{new} + \left(h_{r,i}\right)_{previous}]$$

The value of the inside face temperature, θ_{2N}, determined in this way participates in the zone heat balance solution (see Inside Heat Balance).

Edge-Of-Glass Effects

Table 20. Fortran Variables used in Edge of Glass calculations

Mathematical variable	Description	Units	FORTRAN variable
$\bar{h}$	Area-weighted net conductance of glazing including edge-of-glass effects	W/m²-K	-
A_{cg}	Area of center-of-glass region	m²	CenterGlArea
A_{fe}	Area of frame edge region	m²	FrameEdgeArea
A_{de}	Area of divider edge region	m²	DividerEdgeArea
A_{tot}	Total glazing area	m²	Surface%Area
h_{cg}	Conductance of center-of-glass region (without air films)	W/m²-K	-
h_{fe}	Conductance of frame edge region (without air films)	W/m²-K	-

h_{de}	Conductance of divider edge region (without air films)	W/m^2-K	-
h_{ck}	Convective conductance of gap k	W/m^2-K	-
h_{rk}	Radiative conductance of gap k	W/m^2-K	-
η	Area ratio	-	-
α	Conductance ratio	-	FrEdgeToCenterGlCondRatio, DivEdgeToCenterGlCondRatio

Because of thermal bridging across the spacer separating the glass layers in multi-pane glazing, the conductance of the glazing near the frame and divider, where the spacers are located, is higher than it is in the center of the glass. The area-weighted net conductance (without inside and outside air films) of the glazing in this case can be written

$$\overline{h} = \left(A_{cg} h_{cg} + A_{fe} h_{fe} + A_{de} h_{de} \right) / A_{tot} \tag{1.101}$$

where

h_{cg} = conductance of center-of-glass region (without air films)

h_{fe} = conductance of frame edge region (without air films)

h_{de} = conductance of divider edge region (without air films)

A_{cg} = area of center-of-glass region

A_{fe} = area of frame edge region

A_{de} = area of divider edge region

A_{tot} = total glazing area = $A_{cg} + A_{fe} + A_{de}$

The different regions are shown in Figure 45:
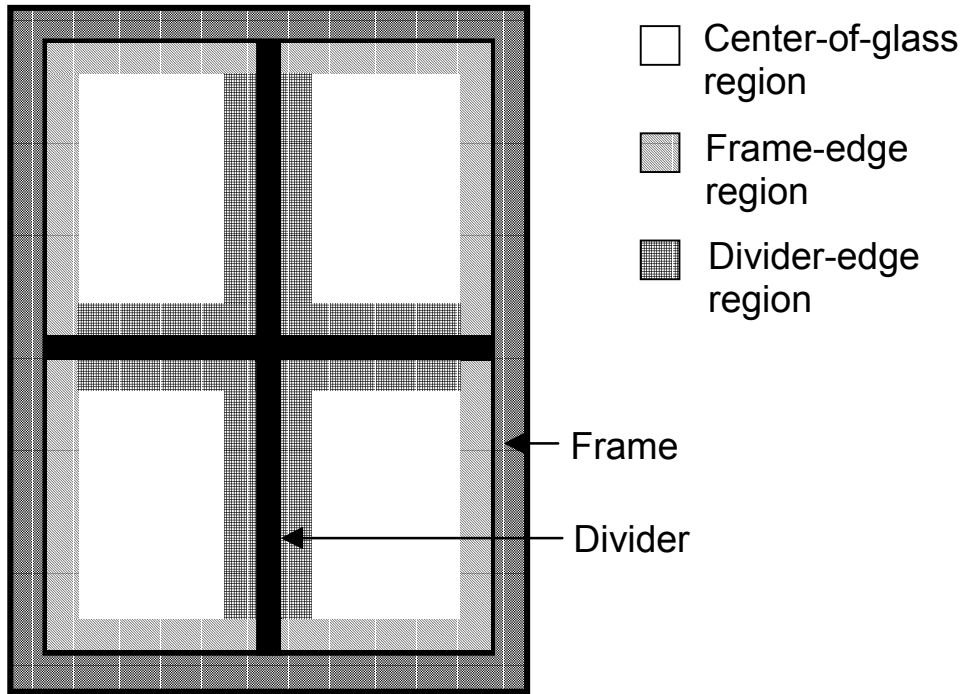
Figure 45: Different types of glass regions.

Equation (1.101) can be rewritten as

$$\overline{h} = h_{cg}\left(\eta_{cg} + \alpha_{fe}\eta_{fe} + \alpha_{de}\eta_{de}\right)$$ (1.102)

where

$$\eta_{cg} = A_{cg} / A_{tot}$$

$$\eta_{fe} = A_{fe} / A_{tot}$$

$$\eta_{de} = A_{de} / A_{tot}$$

$$\alpha_{fe} = h_{fe} / h_{cg}$$

$$\alpha_{de} = h_{de} / h_{cg}$$

The conductance ratios α_{fe} and α_{de} are user inputs obtained from Window 5. They depend on the glazing construction as well as the spacer type, gap width, and frame and divider type.

In the EnergyPlus glazing heat balance calculation effective gap convective conductances are used to account for the edge-of-glass effects. These effective conductances are determined as follows for the case with two gaps (triple glazing). The approach for other numbers of gaps is analogous.

Neglecting the very small resistance of the glass layers, the center-of-glass conductance (without inside and outside air films) can be written as

$$h_{cg} = \left(\left(h_{r,1} + h_{c,1}\right)^{-1} + \left(h_{r,2} + h_{c,2}\right)^{-1}\right)^{-1}$$

where

$h_{c,k} =$ convective conductance of the kth gap

$h_{r,k} =$ radiative conductance of the kth gap

$$= \frac{1}{2} \sigma \frac{\varepsilon_i \varepsilon_j}{1-\left(1-\varepsilon_i\right)\left(1-\varepsilon_j\right)} \left(\theta_i + \theta_j\right)^3$$

$\varepsilon_i, \varepsilon_j =$ emissivity of the faces bounding the gap

$\theta_i, \theta_j =$ temperature of faces bounding the gap (K)

Equation (1.102) then becomes

$$\overline{h} = \left(\eta_{cg} + \alpha_{fe}\eta_{fe} + \alpha_{de}\eta_{de}\right)\left(\left(h_{r,1} + h_{c,1}\right)^{-1} + \left(h_{r,2} + h_{c,2}\right)^{-1}\right)^{-1} \tag{1.103}$$

We can also write $\overline{h}$ in terms of effective convective conductances of the gaps as

$$\overline{h} = \left(\left(h_{r,1} + \overline{h}_{c,1}\right)^{-1} + \left(h_{r,2} + \overline{h}_{c,2}\right)^{-1}\right)^{-1} \tag{1.104}$$

Comparing Eqs. (1.103) and (1.104) we obtain

$$h_{r,k} + \overline{h}_{c,k} = \left(\eta_{cg} + \alpha_{fe}\eta_{fe} + \alpha_{de}\eta_{de}\right)\left(h_{r,k} + h_{c,k}\right)$$

Using $\eta_{cg} = 1 - \eta_{fe} - \eta_{de}$ gives

$$\overline{h}_{c,k} = h_{r,k}\left(\eta_{fe}\left(\alpha_{fe} - 1\right) + \eta_{de}\left(\alpha_{de} - 1\right)\right) + h_{c,k}\left(1 + \eta_{fe}\left(\alpha_{fe} - 1\right) + \eta_{de}\left(\alpha_{de} - 1\right)\right)$$

This is the expression used by EnergyPlus for the gap convective conductance when a frame or divider is present.

Apportioning of Absorbed Short-Wave Radiation in Shading Device Layers

If a shading device has a non-zero short-wave transmittance then absorption takes place throughout the shading device layer. The following algorithm is used to apportion the absorbed short-wave radiation to the two faces of the layer. Here f_1 is the fraction assigned to the face closest to the incident radiation and f_2 is the fraction assigned to the face furthest from the incident radiation.

$f_1 = 1, f_2 = 0$ if $\tau_{sh} = 0$

Otherwise

$$f_1 = 0, f_2 = 0 \quad \text{if } \alpha_{sh} \leq 0.01$$

$$f_1 = 1, f_2 = 0 \quad \text{if } \alpha_{sh} > 0.999$$

$$\left. \begin{array}{l} f_1 = \dfrac{1 - e^{\frac{1}{2}\ln(1-\alpha_{sh})}}{\alpha_{sh}} \\[4mm] f_2 = 1 - f_1 \end{array} \right\} \; 0.01 < \alpha_{sh} \leq 0.999$$

Window Frame and Divider Calculation

For the zone heat balance calculation the inside surface temperature of the frame and that of the divider are needed. These temperatures are determined by solving the heat balance equations on the inside and outside surfaces of the frame and divider.

Table 21. Fortran Variables used in Window/Frame and Divider calculations

Mathematical variable	Description	Units	FORTRAN variable
$Q_{ExtIR,abs}$	IR from the exterior surround absorbed by outside frame surfaces	W	-
$Q_{IR,emitted}$	IR emitted by outside frame surfaces	W	-
Q_{conv}	Convection from outside air to outside frame surfaces	W	-
Q_{cond}	Conduction through frame from inside frame surfaces to outside frame surfaces	W	-
Q_{abs}	Solar radiation plus outside glass IR absorbed by outside of frame	W	-
$Q^{dif}_{abs,sol}$	Diffuse solar absorbed by outside frame surfaces, per unit frame face area	W/ m^2	-
$Q^{bm}_{abs,sol}$	Beam solar absorbed by outside frame surfaces, per unit frame face area	W/ m^2	-
I^{dif}_{ext}	Diffuse solar incident on window	W/ m^2	-
I^{bm}_{ext}	Direct normal solar irradiance	W/ m^2	-
α^{fr}_{sol}	Solar absorptance of frame	-	FrameSolAbsorp
$R_{gl}^{f,dif}$	Front diffuse solar reflectance of glazing	-	
$R_{gl}^{f,bm}$	Front beam solar reflectance of glazing	-	
$\cos(\beta_{face})$	Cosine of angle of incidence of beam solar on frame outside face		CosIncAng

$\text{Cos}(\beta_h)$	Cosine of angle of incidence of beam solar on frame projection parallel to window x-axis	-	CosIncAngHorProj
$\text{Cos}(\beta_v)$	Cosine of angle of incidence of beam solar on frame projection parallel to window y-axis	-	CosIncAngVertProj
f_{sunlit}	Fraction of window that is sunlit	-	SunlitFrac
A_f	Area of frame's outside face (same as area of frame's inside face)	m^2	-
A_{p1}, A_{p2}	Area of frame's outside and inside projection faces	m^2	-
F_f	Form factor of frame's outside or inside face for IR	-	-
F_{p1}, F_{p2}	Form factor of frame outside projection for exterior IR; form factor of frame inside projection for interior IR	-	-
E_o	Exterior IR incident on window plane	W/m^2	outir
E_i	Interior IR incident on window plane	W/m^2	SurroundIRfromParentZone
$\varepsilon_1, \varepsilon_2$	Outside, inside frame surface emissivity	-	FrameEmis
θ_1, θ_2	Frame outside, inside surface temperature	K	FrameTempSurfOut, FrameTempSurfIn
T_o, T_i	Outside and inside air temperature	K	tout, tin
$h_{o,c}, h_{i,c}$	Frame outside and inside air film convectinve conductance	W/m2-K	HOutConv, HInConv
k	Effective inside-surface to outside-surface conductance of frame per unit area of frame projected onto window plane	W/m^2-K	FrameConductance, FrameCon
S_1	Q_{abs}/A_f	W/m^2-K	FrameQRadOutAbs
S_2	Interior short-wave radiation plus interior IR from internal sources absorbed by inside of frame divided by A_f	W/m^2-K	FrameQRadInAbs
η_1, η_2	$A_{p1}/A_f, A_{p2}/A_f$	-	-
H	Height of glazed portion of window	m	Surface%Height
W	Width of glazed portion of window	m	Surface%Width
w_f, w_d	Frame width, divider width	m	FrameWidth, DividerWidth

p_{f1}, p_{f2}	Frame outside, inside projection	m	FrameProjectionOut, FrameProjectionIn
N_h, N_v	Number of horizontal, vertical dividers	-	HorDividers, VertDividers
$T_{o,r}$, $T_{i,r}$	Frame outside, inside radiative temperature	K	TOutRadFr, TInRadFr
$h_{o,r}$, $h_{i,r}$	Frame outside, inside surface radiative conductance	W/m^2-K	HOutRad, HInRad
A	Intermediate variable in frame heat balance solution	K	Afac
C	Intermediate variable in frame heat balance solution	-	Efac
B, D	Intermediate variables in frame heat balance solution	-	Bfac, Dfac

Frame Temperature Calculation

Figure 46 shows a cross section through a window showing frame and divider. The outside and inside frame and divider surfaces are assumed to be isothermal. The frame and divider profiles are approximated as rectangular since this simplifies calculating heat gains and losses (see "Error Due to Assuming a Rectangular Profile," below).
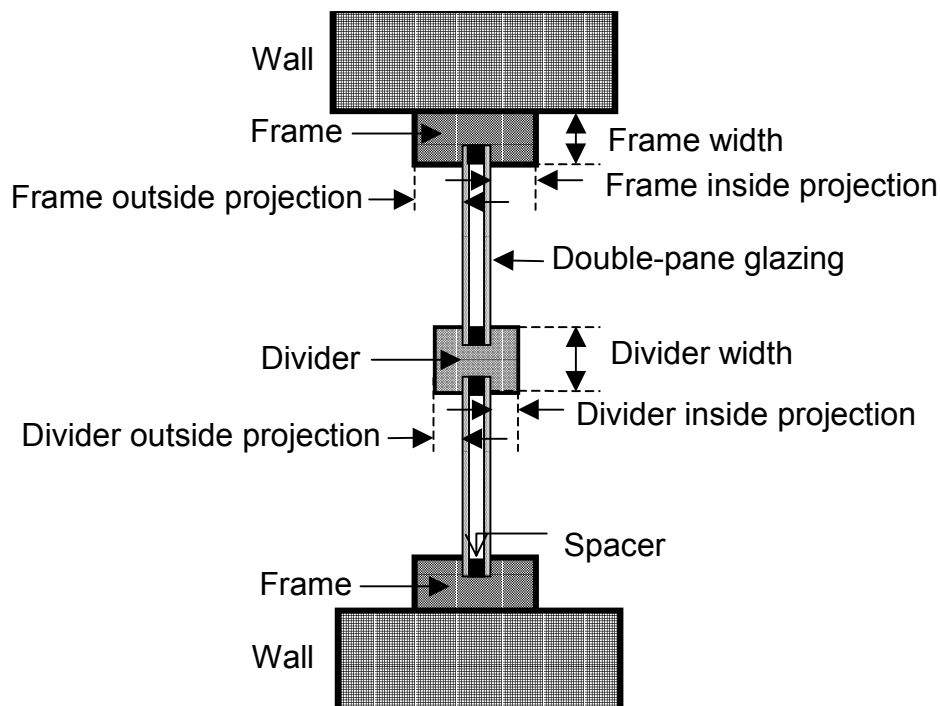
Figure 46. Cross section through a window showing frame and divider (exaggerated horizontally).

Frame Outside Surface Heat Balance

The outside surface heat balance equation is

$$Q_{ExtIR,abs} - Q_{IR,emitted} + Q_{conv} + Q_{cond} + Q_{abs} = 0$$

where

$Q_{ExtIR,abs}$ = IR from the exterior surround (sky and ground) absorbed by outside frame surfaces

$Q_{IR,emitted}$ = IR emitted by outside frame surfaces

Q_{conv} = convection from outside air to outside frame surfaces

Q_{cond} = conduction through frame from inside frame surfaces to outside frame surfaces

Q_{abs} = solar radiation (from sun, sky and ground) plus IR from outside window surface absorbed by outside frame surfaces (see "Calculation of Absorbed Solar Radiation," below).

The first term can be written as the sum of the exterior IR absorbed by the outside face of the frame and the exterior IR absorbed by the frame's outside projection surfaces.

$$Q_{ExtIR,abs} = \varepsilon_1 E_o A_f F_f + \varepsilon_1 E_o A_{p1} F_{p1}$$

where ε_1 is the outside surface emissivity.

The exterior IR incident on the plane of the window, E_o, is the sum of the IR from the sky, ground and obstructions. For the purposes of the frame heat balance calculation it is assumed to be isotropic. For isotropic incident IR, F_f = 1.0 and F_{p1} = 0.5, which gives

$$Q_{ExtIR,abs} = \varepsilon_1 E_o (A_f + \frac{1}{2} A_{p1})$$

The IR emitted by the outside frame surfaces is

$$Q_{ExtIR,emitted} = \varepsilon_1 \sigma (A_f + A_{p1}) \theta_1^4$$

The convective heat flow from the outside air to the outside frame surfaces is

$$Q_{conv} = h_{o,c} (A_f + A_{p1})(T_o - \theta_1)$$

The conduction through the frame from inside to outside is

$$Q_{cond} = k A_f (\theta_2 - \theta_1)$$

Note that A_f is used here since the conductance, k, is, by definition, per unit area of frame projected onto the plane of the window.

Adding these expressions for the Q terms and dividing by A_f gives

$$E_0 \varepsilon_1 \left(1 + \frac{1}{2}\eta_1\right) - \varepsilon_1 \left(1 + \eta_1\right)\theta_1^4 + h_{o,c}\left(1 + \eta_1\right)\left(T_0 - \theta_1\right) + k\left(\theta_2 - \theta_1\right) + S_1 = 0 \qquad (1.105)$$

where S_1 = Q_{abs}/A_f and

$$\eta_1 = \frac{A_{p1}}{A_f} = \left(\frac{p_{f,1}}{w_f}\right) \frac{H + W - (N_h + N_v)w_d}{H + W + 2w_f}$$

We linearize Eq. (1.105) as follows.
Write the first two terms as

$$\varepsilon_1(1 + \eta_1)[E_o(1 + \frac{1}{2}\eta_1)/(1 + \eta_1) - \theta_1^4]$$

and define a radiative temperature

$$T_{o,r} = [E_o(1 + \frac{1}{2}\eta_1)/(1 + \eta_1)]^{1/4}$$

This gives

$$\varepsilon_1(1 + \eta_1)[T_{o,r}^4 - \theta_1^4]$$

which, within a few percent, equals

$$\varepsilon_1(1 + \eta_1)\frac{(T_{o,r} + \theta_1)^3}{2}(T_{o,r} - \theta_1)$$

Defining an outside surface radiative conductance as follows

$$h_{o,r} = \varepsilon_1(1 + \eta_1)\frac{(T_{o,r} + \theta_1)^3}{2}$$

then gives

$$h_{o,r}(T_{o,r} - \theta_1)$$

The final outside surface heat balance equation in linearized form is then

$$h_{o,r}(T_{o,r} - \theta_1) + h_{o,c}(1 + \eta_1)(T_o - \theta_1) + k(\theta_2 - \theta_1) + S_1 = 0 \qquad (1.106)$$

Frame Inside Surface Heat Balance

A similar approach can be used to obtain the following linearized *inside* surface heat balance equation:

$$h_{i,r}(T_{i,r} - \theta_2) + h_{i,c}(1 + \eta_2)(T_i - \theta_2) + k(\theta_1 - \theta_2) + S_2 = 0 \qquad (1.107)$$

where

$$T_{i,r} = [E_i(1 + \frac{1}{2}\eta_2)/(1 + \eta_2)]^{1/4}$$

$$\eta_2 = \frac{A_{p2}}{A_f} = \left(\frac{p_{f,2}}{w_f}\right) \frac{H + W - (N_h + N_v)w_d}{H + W + 2w_f}$$

and E_i is the interior IR intensity incident on the plane of the window.

Solving Eqs. (1.106) and (1.107) simultaneously gives

$$\theta_2 = \frac{D + CA}{1 - CB}$$

with

$$A = \frac{h_{o,r}T_{o,r} + h_{o,c}T_o + S_1}{h_{o,r} + k + h_{o,c}}$$

$$B = \frac{k}{h_{o,r} + k + h_{o,c}}$$

$$C = \frac{k}{h_{i,r} + k + h_{i,c}}$$

$$D = \frac{h_{i,r}T_{i,r} + h_{i,c}T_i + S_2}{h_{i,r} + k + h_{i,c}}$$

Calculation of Solar Radiation Absorbed by Frame

The frame outside face and outside projections and inside projections absorb beam solar radiation (if sunlight is striking the window) and diffuse solar radiation from the sky and ground. For the outside surfaces of the frame, the absorbed diffuse solar per unit frame face area is

$$Q_{abs,sol}^{dif} = I_{ext}^{dif}\alpha_{fr,sol}\left(A_f + F_{p1}A_{p1}\right)/A_f = I_{ext}^{dif}\alpha_{fr,sol}\left(1 + 0.5\frac{A_{p1}}{A_f}\right)$$

If there is no exterior window shade, I^{dif}_{ext} includes the effect of diffuse solar reflecting off of the glazing onto the outside frame projection, i.e.,

$$I_{ext}^{dif} \to I_{ext}^{dif}\left(1 + R_{gl}^{f,dif}\right)$$

The beam solar absorbed by the outside face of the frame, per unit frame face area is

$$Q_{abs,sol}^{bm,face} = I_{ext}^{bm}\alpha_{fr,sol}\cos\beta_{face}f_{sunlit}$$

The beam solar absorbed by the frame outside projection parallel to the window x-axis is

$$Q_{abs,sol}^{bm,h} = I_{ext}^{bm}\alpha_{fr,sol}\cos\beta_h p_{f1}\left(W - N_v w_d\right)f_{sunlit}/A_f$$

Here it is assumed that the sunlit fraction, f_{sunlit}, for the window can be applied to the window frame. Note that at any given time beam solar can strike only one of the two projection surfaces that are parallel to the window x-axis. If there is no exterior window shade, I^{bm}_{ext} includes the effect of beam solar reflecting off of the glazing onto the outside frame projection, i.e.,

$$I^{bm}_{ext} \rightarrow I^{bm}_{ext}\left(1 + R^{f,bm}_{gl}\right)$$

The beam solar absorbed by the frame outside projection parallel to the window y-axis is

$$Q^{bm,v}_{abs,sol} = I^{bm}_{ext}\alpha_{fr,sol} \cos \beta_v p_{f1}\left(H - N_h w_d\right)f_{sunlit} / A_f$$

Using a similar approach, the beam and diffuse solar absorbed by the *inside* frame projections is calculated, taking the transmittance of the glazing into account.

Error Due to Assuming a Rectangular Profile

Assuming that the inside and outside frame profile is rectangular introduces an error in the surface heat transfer calculation if the profile is non-rectangular. The percent error in the calculation of convection and emitted IR is approximately $100\left|L_{profile,rect} - L_{profile,actual}\right| / L_{profile,rect}$, where $L_{profile,rect}$ is the profile length for a rectangular profile ($w_f + p_{f1}$ for outside of frame or $w_f + p_{f2}$ for inside of frame) and $L_{profile,actual}$ is the actual profile length. For example, for a circular profile *vs* a square profile the error is about 22%. The error in the calculation of absorbed beam radiation is close to zero since the beam radiation intercepted by the profile is insensitive to the shape of the profile. The error in the absorbed diffuse radiation and absorbed IR depends on details of the shape of the profile. For example, for a circular profile vs. a square profile the error is about 15%.

Divider Temperature Calculation

The divider inside and outside surface temperatures are determined by a heat balance calculation that is analogous to the frame heat balance calculation described above.

Beam Solar Reflection from Window Reveal Surfaces

This section describes how beam solar radiation that is reflected from window reveal surfaces is calculated. Reflection from outside reveal surfaces—which are associated with the setback of the glazing from the outside surface of the window's parent wall—increases the solar gain through the glazing. Reflection from inside reveal surfaces—which are associated with the setback of the glazing from the inside surface of the window's parent wall—decreases the solar gain to the zone because some of this radiation is reflected back out of the window.

The amount of beam solar reflected from reveal surfaces depends, among other things, on the extent to which reveal surfaces are shadowed by other reveal surfaces. An example of this shadowing is shown in Figure 47. In this case the sun is positioned such that the top reveal surfaces shadow the left and bottom reveal surfaces. And the right reveal surfaces shadow the bottom reveal surfaces. The result is that the left/outside, bottom/outside, left/inside and bottom/inside reveal surfaces each have sunlit areas. Note that the top and right reveal surfaces are facing away from the sun in this example so their sunlit areas are zero.
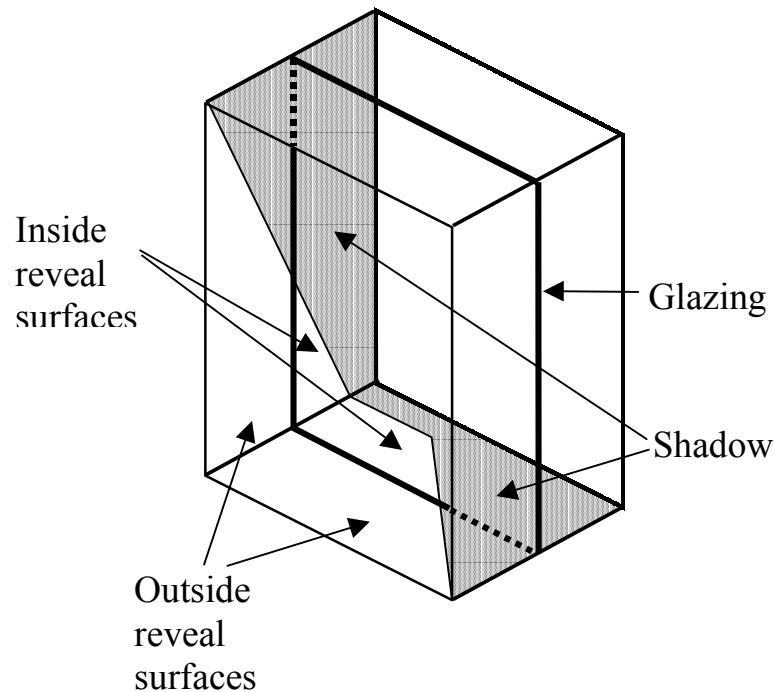
Figure 47. Example of shadowing of reveal surfaces by other reveal surfaces.

The size of the shadowed areas, and the size of the corresponding illuminated areas, depends on the following factors:

- The sun position relative to the window
- The height and width of the window
- The depth of the outside and inside reveal surfaces

We will assume that the reveal surfaces are perpendicular to the window plane and that the window is rectangular. Then the above factors determine a unique shadow pattern. From the geometry of the pattern the shadowed areas and corresponding illuminated areas can be determined.   This   calculation   is   done   in   subroutine CalcBeamSolarReflectedFromWinRevealSurface in the SolarShading module. The window reveal input data is specified in the WindowFrameAndDivider object expect for the depth of the outside reveal, which is determined from the vertex locations of the window and its parent wall.

If an exterior shading device (shade or blind) is in place it is assumed that it blocks beam solar before it reaches outside or inside reveal surfaces. Correspondingly, it is assumed that an interior shading device blocks beam solar before it reaches inside reveal surfaces.

Representative shadow patterns are shown in Figure 48 for a window with no shading device, and without and with a frame. The case with a frame has to be considered separately because the frame can cast an additional shadow on the inside reveal surfaces.

The patterns shown apply to both vertical and horizontal reveal surfaces. It is important to keep in mind that, for a window of arbitrary tilt, if the left reveal surfaces are illuminated the right surfaces will not be, and vice versa. And if the bottom reveal surfaces are illuminated the top surfaces will not be, and vice versa. (Of course, for a vertical window, the top reveal surfaces will never be illuminated by beam solar if the reveal surfaces are perpendicular to the glazing, as is being assumed.

For each shadow pattern in Figure 48, equations are given for the shadowed areas $A_{1,sh}$ and $A_{2,sh}$ of the outside and inside reveal surfaces, respectively. The variables in these equations are the following (see also Figure 49):

d_1 = depth of outside reveal, measured from the outside plane of the glazing to the edge of the reveal, plus one half of the glazing thickness.

d_2 = depth of inside reveal (or, for illumination on bottom reveal surfaces, inside sill depth), measured from the inside plane of the glazing to the edge of the reveal or the sill, plus one half of the glazing thickness.

L = window height for vertical reveal surfaces or window width for horizontal reveal surfaces

α = vertical solar profile angle for shadowing on vertical reveal surfaces or horizontal solar profile angle for shadowing on horizontal reveal surfaces.
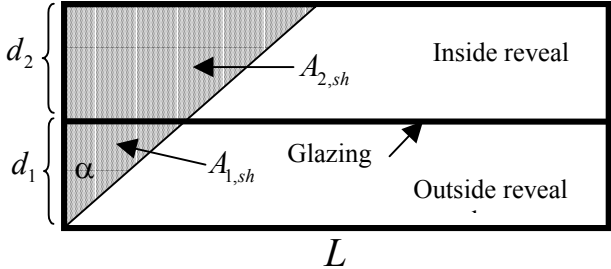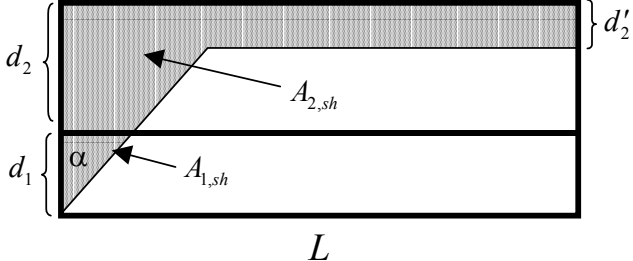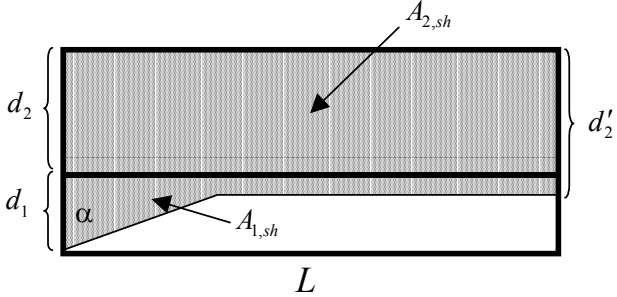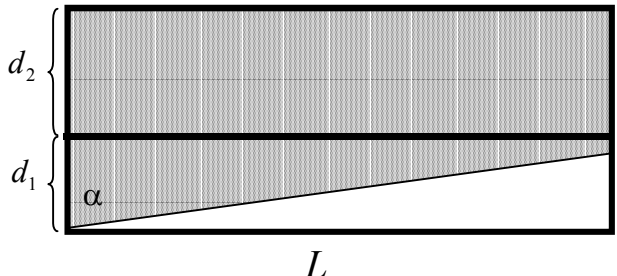
$p_1(p_2)$ = distance from outside (inside) surface of frame to glazing midplane.
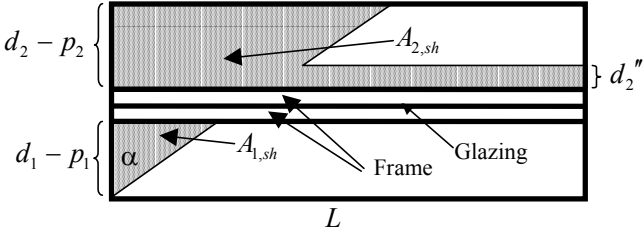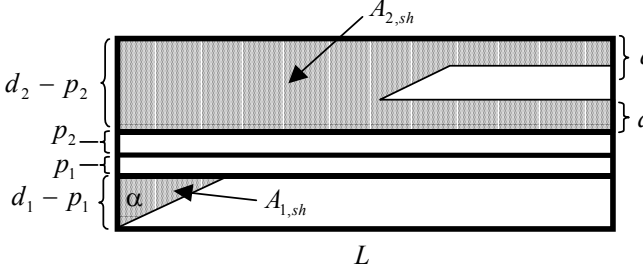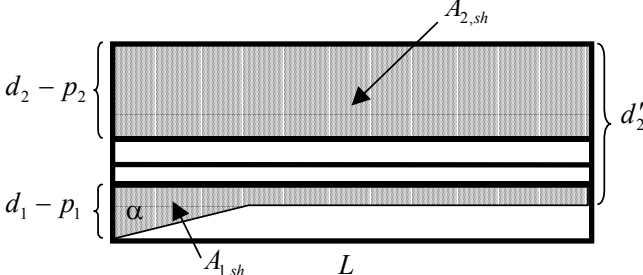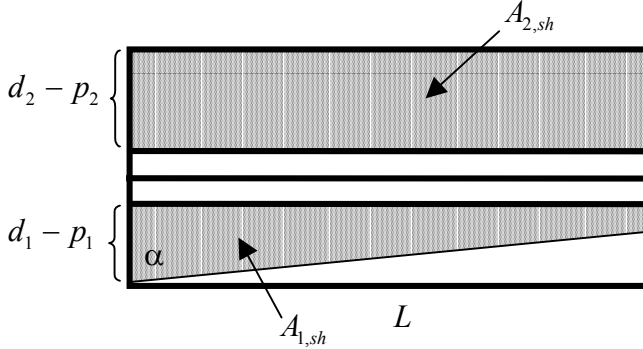
$d_2{}'$ = depth of shadow cast by top reveal on bottom reveal, or by left reveal on right reveal, or by right reveal on left reveal.

$d_2{}''$ = depth of shadow cast by frame.

For simplicity it is assumed that, for the case without a frame, the shadowed and illuminated areas extend into the glazing region. For this reason, d_1 and d_2 are measured from the midplane of the glazing. For the case with a frame, the beam solar absorbed by the surfaces formed by the frame outside and inside projections perpendicular to the glazing is calculated as described in "Window Frame and Divider Calculation: Calculation of Solar Radiation Absorbed by Frame."

Figure 48. Expression for area of shaded regions for different shadow patterns: (a) window without frame, (b) window with frame

(b)

Row 1:

$$A_{1,sh} = \frac{1}{2}(d_1 - p_1)^2 \tan\alpha$$

$$A_{2,sh} = d_2'' L + \frac{1}{2}(d_1 + d_2)^2 \tan\alpha - $$

$$\frac{1}{2}(d_1 + p + d_2'')^2 \tan\alpha$$

Row 2:

$$A_{1,sh} = \frac{1}{2}(d_1 - p_1)^2 \tan\alpha$$

$$A_{2,sh} = d_2' L + d_2'' L + \frac{1}{2}(d_1 + d_2 - d_2')^2 \tan\alpha$$

$$-\frac{1}{2}(d_1 + p_2 + d_2'')^2 \tan\alpha$$

Row 3:

$$A_{1,sh} = \left(d_2' - (d_2 + p_1)\right)L + $$

$$\frac{1}{2}(d_1 + d_2 - d_2')^2 \tan\alpha$$

$$A_{2,sh} = (d_2 - p_2)L$$

Row 4:

$$A_{1,sh} = (d_1 - p_1)L - \frac{1}{2}\frac{L^2}{\tan\alpha}$$

$$A_{2,sh} = (d_2 - p_2)L$$
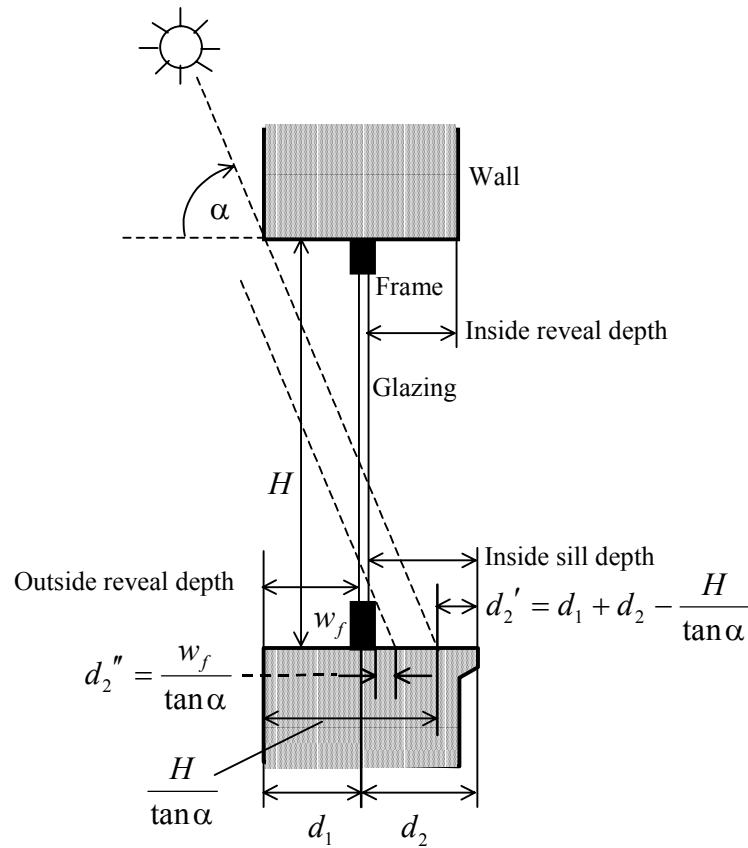
Figure 49. Vertical section through a vertical window with outside and inside reveal showing calculation of the shadows cast by the top reveal onto the inside sill and by the frame onto the inside sill.

The following logic gives expressions for the shadowed areas for all possible shadow patterns. Here:

d1 = d_1

d2 = d_2

P1 = p_1

P2 = p_2

f1 = $d_1 - p_1$

f2 = $d_2 - p_2$

d2prime = d_2'

d2prime2 = d_2''

d12 = $d_1 + d_2 - d_2'$

TanAlpha = $\tan\alpha$

A1sh = $A_{1,sh}$

A2sh = $A_{2,sh}$

L = L

L1 = average distance to frame of illuminated area of outside reveal
    (used to calculate view factor to frame).
L2 = average distance to frame of illuminated area of inside reveal
    (used to calculate view factor to frame).

```
IF(window does not have a frame) THEN
     IF(d2prime <= d2) THEN
    IF(d12*TanAlpha <= L) THEN
      A1sh = 0.5*TanAlpha*d1**2
      A2sh = d2prime*L + 0.5*TanAlpha*d12**2 - A1sh
    ELSE  ! d12*TanAlpha > L
      IF(d1*TanAlpha <= L) THEN
        A1sh = 0.5*TanAlpha*d1**2
        A2sh = d2*L - 0.5*TanAlpha*(L/TanAlpha - d1)**2
      ELSE  ! d1*TanAlpha > L
        A1sh = d1*L - (0.5/TanAlpha)*L**2
        A2sh = d2*L
      END IF
    END IF
  ELSE  ! d2prime > d2
    A2sh = d2*L
    IF(d2prime < d1+d2) THEN
      IF(d12*TanAlpha <= L) THEN
        A1sh = L*(d2prime-d2) + 0.5*TanAlpha*d12**2
      ELSE  ! d12*TanAlpha > L
        A1sh = d1*L - 0.5*L**2/TanAlpha
      END IF
    ELSE  ! d2prime >= d1+d2
      A1sh = d1*L
    END IF
  END IF
ELSE  ! Window has a frame
 f1 = d1-P1
 f2 = d2-P2
 d2prime2 = FrameWidth/TanGamma
 IF(vertical reveal) THEN  ! Vertical reveal
   IF(InsReveal+0.5*GlazingThickness <= P2) d2 = P2 + 0.001
 ELSE                      ! Horizontal
   IF(bottom reveal surfaces may be illuminated) THEN
     ! Bottom reveal surfaces may be illuminated
     IF(InsSillDepth+0.5*GlazingThickness<=P2) d2= P2 + 0.001
   ELSE
     ! Top reveal surfaces may be illuminated
     IF(InsReveal+0.5*GlazingThickness <= P2) d2 = P2 + 0.001
   END IF
 END IF
 IF(d2prime <= f) THEN
   ! Shadow from opposing reveal does not go beyond inside
   !  surface of frame
   IF(d12*TanAlpha <= L) THEN
     A1sh = 0.5*TanAlpha*f1**2
     L1   = f1*(f1*TanAlpha/(6*L)+0.5)
     IF(d2-(d2prime+d2prime2+P2) >= 0.) THEN
       A2sh = (d2prime+d2prime2)*L + &
         0.5*TanAlpha*((d1+d2-d2prime)**2-d1+p2+d2prime2)**2)
       L2   = d2prime2 + 0.5*(d2-(d2prime+d2prime2+P2))
     ELSE  ! d2-(d2prime+d2prime2+P2) < 0.
       ! Inside reveal is fully shadowed by frame and/or
       !opposing reveal
       A2sh = f2*L
```

```
        L2    = f2
      END IF
    ELSE   ! d12*TanAlpha >= L
      IF((d1+P2)*TanAlpha <= L) THEN
        A1sh = 0.5*TanAlpha*f1**2
        L1 = f1*((f1*TanAlpha)/(6*L) + 0.5)
        IF((d1+P2+d2prime2)*TanAlpha >= L) THEN
          A2sh = f2*L
          L2    = f2
        ELSE   ! (d1+P2+d2prime2)*TanAlpha < L
          A2sh = f2*L - 0.5*(L-(d1+P2)*TanAlpha)**2/TanAlpha &
            + d2prime2*(L-(d1+P2+d2prime2/2)*TanAlpha)
          L2 = d2prime2 + (L/TanAlpha - (d1+P2+d2prime2))/3
        END IF
      ELSE   ! (d1+P2)*TanAlpha > L
        L2 = f2
        A2sh = f2*L
        IF(f1*TanAlpha <= L) THEN
          A1sh = 0.5*TanAlpha*f1**2
          L1 = f1*((f1*TanAlpha)/(6*L) + 0.5)
        ELSE   ! f1*TanAlpha > L
          A1sh = f1*L - 0.5*L**2/TanAlpha
          L1 = f1-(L/TanAlpha)/3
        END IF
      END IF
    END IF
  ELSE
    ! d2prime > f2 -- Shadow from opposing reveal goes beyond
    ! inside of frame
    A2sh = f2*L
    L2 = f2
    IF(d2prime >= d1+d2) THEN
      A1sh = 0.0
      L1    = f1
    ELSE   ! d2prime < d1+d2
      IF(d2prime <= d2+P1) THEN
        IF(f1*TanAlpha <= L) THEN
          A1sh = 0.5*TanAlpha*f1**2
          L1 = f1*((f1*TanAlpha)/(6*L) + 0.5)
        ELSE   ! f1*TanAlpha > L
          A1sh = f1*L - 0.5*L**2/TanAlpha
            L1    = f1 - (L/TanAlpha)/3
          END IF
        ELSE   ! d2prime > d2+P1
          IF(d12*TanAlpha <= L) THEN
            A1sh = L*(d2prime-(d2+P1)) + 0.5*TanAlpha*d12**2
            L1    = (L*(f1-d12/2)-d12*TanAlpha* &
              (f1/2-d12/3))/(L-d12*TanAlpha/2)
          ELSE   ! d12*TanAlpha > L
            A1sh = f1*L - 0.5*L**2/TanAlpha
            L1    = f1 - (L/TanAlpha)/3
          END IF
        END IF
      END IF
    END IF
    FracToGlassOuts = 0.5*(1.0 - ATAN(FrameWidth/L1)/PiOvr2)
    FracToGlassIns  = 0.5*(1.0 - ATAN(FrameWidth/L2)/PiOvr2)
  END IF  ! End of check if window has frame
```

The beam solar reflected from a sunlit region of area A is given by

$$R = I_B A \cos \beta (1 - a)$$

where

R = reflected solar radiation [W]

I_B = beam normal irradiance [W/m^2]

A = sunlit area [m^2]

β = beam solar angle of incidence on reveal surface

a = solar absorptance of reveal surface

All reflected radiation is assumed to be isotropic diffuse. For outside reveal surfaces it is assumed that $R/2$ goes toward the window and $R/2$ goes to the exterior environment. Of the portion that goes toward the window a fraction F_1 goes toward the frame, if present, and $1-F_1$ goes toward the glazing.

The view factor F_1 to the frame calculated by assuming that the illuminated area can be considered to be a line source. Then the area-weighted average distance, L_1, of the source to the frame is calculated from the shape of the illuminated area (see above psuedo-code). Then F_1 is related as follows to the average angle subtended by the frame of width w_f:

$$F_1 = \frac{\tan^{-1}(w_f / L_1)}{\pi/2}$$

For the portion going towards the frame, $(R/2)F_1 a_f$ is absorbed by the frame (where a_f is the solar absorptance of the frame) and contributes to the frame heat conduction calculation. The rest, $(R/2)F_1(1-a_f)$, is assumed to be reflected to the exterior environment.

If the glazing has diffuse transmittance τ_{diff}, diffuse front reflectance ρ_{diff}^f, and layer front absorptance $\alpha_{l,diff}^f$, then, of the portion, $(R/2)(1-F_1)$, that goes toward the glazing, $(R/2)(1-F_1)\tau_{diff}$ is transmitted to the zone, $(R/2)(1-F_1)\alpha_{l,diff}^f$ is absorbed in glass layer l and contributes to the glazing heat balance calculation, and $(R/2)(1-F_1)\rho_{diff}^f$ is reflected to the exterior environment.

The beam solar absorbed by an outside reveal surface is added to the other solar radiation absorbed by the outside of the window's parent wall.

For inside reveal surfaces it is assumed that $R/2$ goes towards the window and $R/2$ goes into the zone. Of the portion that goes toward the window a fraction $(R/2)F_2$ goes toward the frame, if present, and $(R/2)(1-F_2)$ goes toward the glazing (F_2 is calculated using a method analogous to that used for F_1). For the portion going towards the frame, $(R/2)F_2 a_f$ is absorbed by the frame and contributes to the frame heat conduction calculation. The rest, $(R/2)F_2(1-a_f)$, is assumed to be reflected back into the zone.

If the glazing has diffuse back reflectance ρ_{diff}^b, and layer back absorptance $\alpha_{l,diff}^b$, then, of the portion $(R/2)(1-F_2)$ that goes toward the glazing, $(R/2)(1-F_2)\tau_{diff}$ is transmitted

back out the glazing, $(R/2)(1-F_2)\alpha_{l,diff}^b$ is absorbed in glass layer l and contributes to the

glazing heat balance calculation, and $(R/2)(1-F_2)\rho_{diff}^b$ is reflected into the zone.

The beam solar absorbed by an inside reveal surface is added to the other solar radiation absorbed by the inside of the window's parent wall.

Shading Device Thermal Model

The window shading device thermal model in EnergyPlus accounts for the thermal interactions between the shading layer and the adjacent glass, and between the shading layer and the room (for interior shading) or the shading layer and the outside surround (for exterior shading).

An important feature of the shading device thermal model is calculating the air flow between the shading device and glass. This flow affects the temperature of the shading device and glazing and, for interior shading, is a determinant of the convective heat gain from the shading layer and glazing to the zone air. The air flow model is based on one described in the ISO Standard 15099, "Thermal Performance of Windows, Doors and Shading Devices— Detailed Calculations" [ISO15099, 2001].

The following effects are considered by the shade thermal model:

- Long-wave radiation (IR) from surround (other zone surfaces for interior shading or sky/ground for exterior shading) absorbed by shading device, or transmitted by the shading device and absorbed by the adjacent glass.
- Inter-reflection of IR between the shading device and adjacent glass.
- Direct and diffuse solar radiation absorbed by the shading device.
- Inter-reflection of solar radiation between shading layer and glass layers.
- Convection from shading layer and glass to the air in the gap between the shading layer and adjacent glass, and convection from interior shading layer to zone air (or from exterior shading layer to outside air).
- Air flow in the gap between shading layer and adjacent glass induced by buoyancy effects, and the effect of this flow on the shading layer-to-gap and glass-to-gap convection coefficients.
- For interior shading, convective gain (or loss) to zone air from gap air flow.

In the following it is assumed that the shading device, when in place, covers the glazed part of the window (and dividers, if present) and is parallel to the glazing and separated from it by an air gap. If the window has a frame, it is assumed that the shading device does *not* cover the frame.

Heat Balance Equations for Shading Device and Adjacent Glass

If a window shading device is deployed the heat balance equation for the glass surface facing the shading layer is modified, and two new equations, one for each face of the shading layer, are added. Figure 50 illustrates the case of double glazing with an interior shading device.
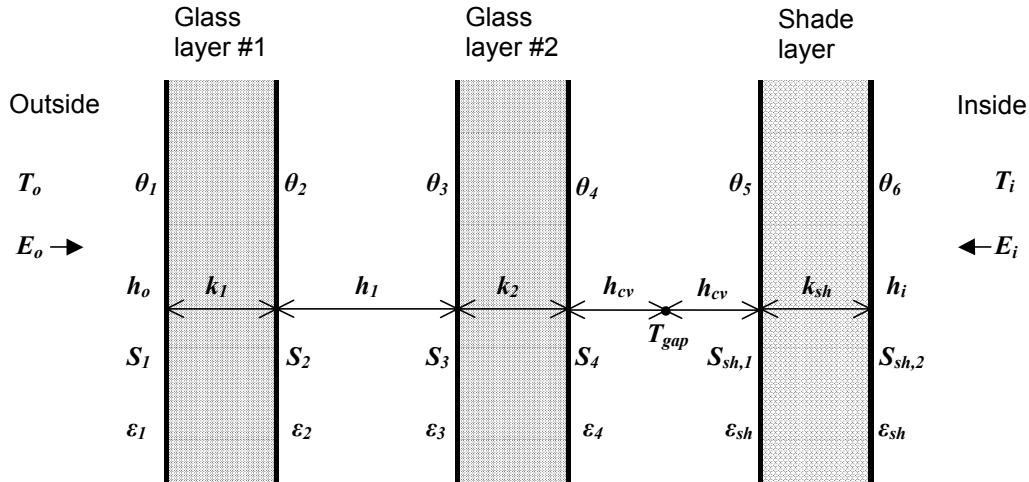
Figure 50. Glazing system with two glass layers and an interior shading layer showing variables used in heat balance equations.

The heat balance equation for the glass surface facing the gap between glass and shading layer (called in the following, "gap") is

$$\frac{E_t \varepsilon_4 \tau_{sh}}{1 - \rho_4 \rho_{sh}} + \frac{\sigma \varepsilon_4}{1 - \rho_4 \rho_{sh}} \left[\theta_5^4 \varepsilon_{sh} - \theta_4^4 (1 - \rho_{sh}) \right] + k_2 \left(\theta_3 - \theta_4 \right) + h_{cv} \left(T_{gap} - \theta_4 \right) + S_4 = 0$$

where

τ_{sh} = IR diffuse transmittance of shading device

ε_{sh} = diffuse emissivity of shading device

ρ_{sh} = IR diffuse reflectance of shading device   (assumed same on both sides) = 1 - (τ_{sh} + ε_{sh})

θ_5 = temperature of the surface of the shading layer that faces the gap (K).

The term $1 - \rho_4 \rho_{sh}$ accounts for the inter-reflection of IR radiation between glass and shading layer.

The convective heat transfer from glass layer #2 to the air in the gap is

$$q_{c,gl} = h_{cv} (\theta_4 - T_{gap})$$

where

T_{gap} = effective mean temperature of the gap air (K).

h_{cv} = convective heat transfer coefficient from glass or shading layer to gap air (W/m²K).

The corresponding heat transfer from shading layer to gap air is

$$q_{c,sh} = h_{cv} (\theta_5 - T_{gap})$$

The convective heat transfer coefficient is given by

$$h_{cv} = 2h_c + 4v$$

(1.108)

where

h_c = surface-to-surface heat transfer coefficient for non-vented (closed) cavities (W/m^{2}K)

v = mean air velocity in the gap (m/s).

The quantities h_{cv} and T_{gap} depend on the air flow velocity in the gap, which in turn depends on several factors, including height of shading layer, glass/shading layer separation (gap depth), zone air temperature for interior shading or outside air temperature for exterior shading, and shading layer and glass face temperatures. The calculation of h_{cv} and T_{gap} is described in the following sections.

The heat balance equation for the shading layer surface facing the gap is

$$\frac{E_i \tau_{sh} \rho_4 \varepsilon_{sh}}{1 - \rho_4 \rho_{sh}} + \frac{\sigma \varepsilon_{sh}}{1 - \rho_4 \rho_{sh}} \left[\varepsilon_4 \theta_4^4 - \theta_5^4 (1 - \rho_4 (\varepsilon_{sh} + \rho_{sh})) \right] +$$

$$k_{sh} \left(\theta_6 - \theta_5 \right) + h_{cv} \left(T_{gap} - \theta_5 \right) + S_{sh,1} = 0$$

where

k_{sh} = shading layer conductance (W/m^{2}K).

θ_6 = temperature of shading layer surface facing the zone air (K).

$S_{sh,1}$ = solar radiation plus short-wave radiation from lights plus IR radiation from lights and zone equipment absorbed by the gap-side face of the shading layer (W/m^{2}K).

The heat balance equation for the shading layer surface facing the zone air is

$$E_i \varepsilon_{sh} - \varepsilon_{sh} \sigma \theta_6^4 + k_{sh} \left(\theta_5 - \theta_6 \right) + h_i \left(T_i - \theta_6 \right) + S_{sh,2} = 0$$

where

$S_{sh,2}$ = solar radiation plus short-wave radiation from lights plus IR radiation from lights and zone equipment absorbed by the zone-side face of the shading layer (W/m^{2}K).

Solving for Gap Air Flow and Temperature

A pressure-balance equation is used to determine gap air velocity, gap air mean equivalent temperature and gap outlet air temperature given values of zone air temperature (or outside temperature for exterior shading), shading layer face temperatures and gap geometry. The pressure balance equates the buoyancy pressure acting on the gap air to the pressure losses associated with gap air flow between gap inlet and outlet [ISO15099, 2001]. The variables used in the following analysis of the interior shading case are shown in Figure 51.
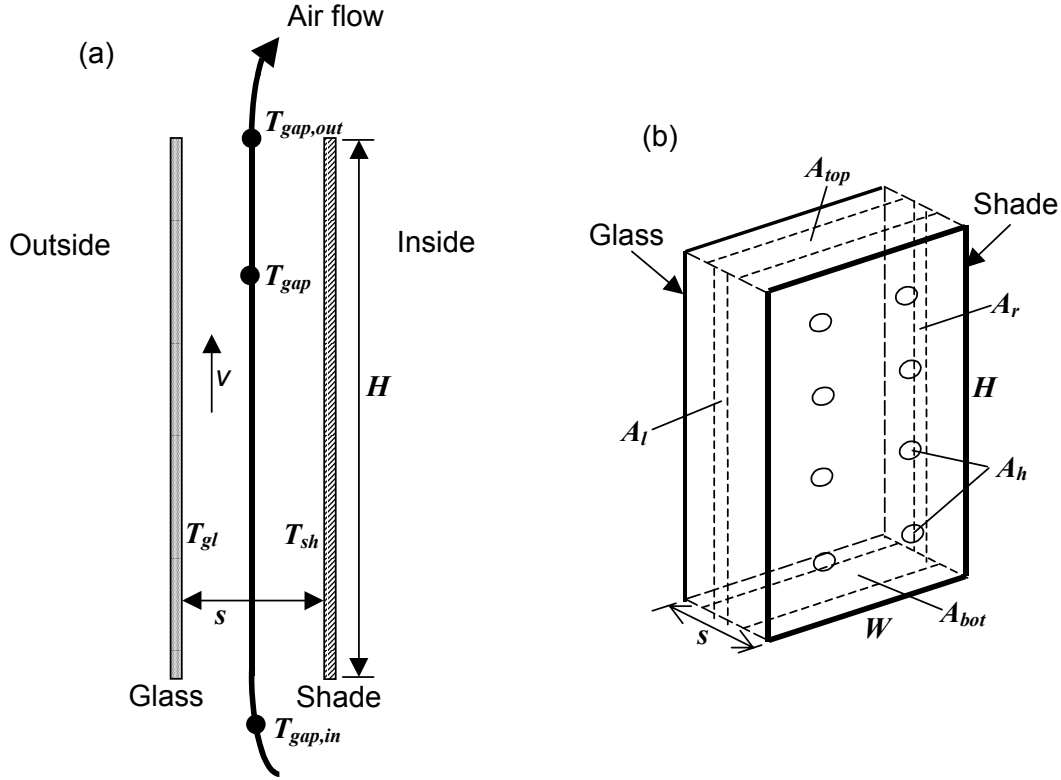
Figure 51. Vertical section (a) and perspective view (b) of glass layer and interior shading layer showing variables used in the gap air flow analysis. The opening areas A_{bot}, A_{top}, A_l, A_r and A_h are shown schematically.

Pressure Balance Equation

The pressure balance equation for air flow through the gap is

$$\Delta p_T = \Delta p_B + \Delta p_{HP} + \Delta p_Z \tag{1.109}$$

Here, Δp_T is the driving pressure difference between room air and gap air. It is given by

$$\Delta p_T = \rho_0 T_0 g H \sin\phi \frac{\left|T_{gap} - T_{gap,in}\right|}{T_{gap}T_{gap,in}}$$

where

ρ_0 = density of air at temperature T_0 (kg/m^3)

T_0 = reference temperature (283K)

g = acceleration due to gravity (m/s^2)

H = height of shading layer (m)

φ = tilt angle of window (vertical = 90°)

T_{gap} = effective mean temperature of the gap air (K)

$T_{gap,in}$ = gap inlet temperature (= zone air temperature for interior shading) (K)

The $\mathit{\Delta p}_B$ term is due to the acceleration of air to velocity v (Bernoulli's law). It is given by

$$\Delta p_B = \frac{\rho}{2} v^2 \quad \text{(Pa)}$$

where ρ is the gap air density evaluated at T_{gap} (kg/m^3).

The $\mathit{\Delta p}_{HP}$ term represents the pressure drop due to friction with the shading layer and glass surfaces as the air moves through the gap. Assuming steady laminar flow, it is given by the Hagen-Poiseuille law for flow between parallel plates [Munson et al. 1998]:

$$\Delta p_{HP} = 12\mu \frac{H}{s^2} v \quad \text{(Pa)}$$

where μ is the viscosity of air at temperature T_{gap} (Pa-s).

The $\mathit{\Delta p}_Z$ term is the sum of the pressure drops at the inlet and outlet openings:

$$\Delta p_Z = \frac{\rho v^2}{2}\left(Z_{in} + Z_{out}\right) \quad \text{(Pa)}$$

Here, the inlet pressure drop factor, Z_{in}, and the outlet pressure drop factor, Z_{out}, are given by

$$Z_{in} = \left(\frac{A_{gap}}{0.66 A_{eq,in}} - 1\right)^2$$

$$Z_{out} = \left(\frac{A_{gap}}{0.60 A_{eq,out}} - 1\right)^2$$

where

$A_{eq,in}$ = equivalent inlet opening area (m^2)

$A_{eq,out}$ = equivalent outlet opening area (m^2)

A_{gap} = cross-sectional area of the gap = sW (m^2)

If $T_{gap} > T_{gap,in}$

$$A_{eq,in} = A_{bot} + \frac{A_{top}}{2(A_{bot} + A_{top})}\left(A_l + A_r + A_h\right)$$

$$A_{eq,out} = A_{top} + \frac{A_{bot}}{2(A_{bot} + A_{top})}\left(A_l + A_r + A_h\right)$$

If $T_{gap} \leq T_{gap,in}$

$$A_{eq,in} = A_{top} + \frac{A_{bot}}{2(A_{bot} + A_{top})}\left(A_l + A_r + A_h\right)$$

$$A_{eq,out} = A_{bot} + \frac{A_{top}}{2(A_{bot} + A_{top})}\left(A_l + A_r + A_h\right)$$

Here, the area of the openings through which air flow occurs (see Figure 51 and Figure 52) are defined as follows:

A_{bot} = area of the bottom opening (m^2)

A_{top} = area of the top opening (m^2)

A_l = area of the left-side opening (m^2)

A_r = area of the right-side opening (m^2)

A_h = air permeability of the shade expressed as the total area of openings ("holes") in the shade surface (these openings are assumed to be uniformly distributed over the shade) (m^2)

Figure 52 shows examples of A_{bot}, A_{top}, A_l and A_r for different shade configurations. These areas range from zero to a maximum value equal to the associated shade-to-glass cross-sectional area; i.e., A_{bot} and $A_{top} \leq sW$, A_l and $A_r \leq sH$.
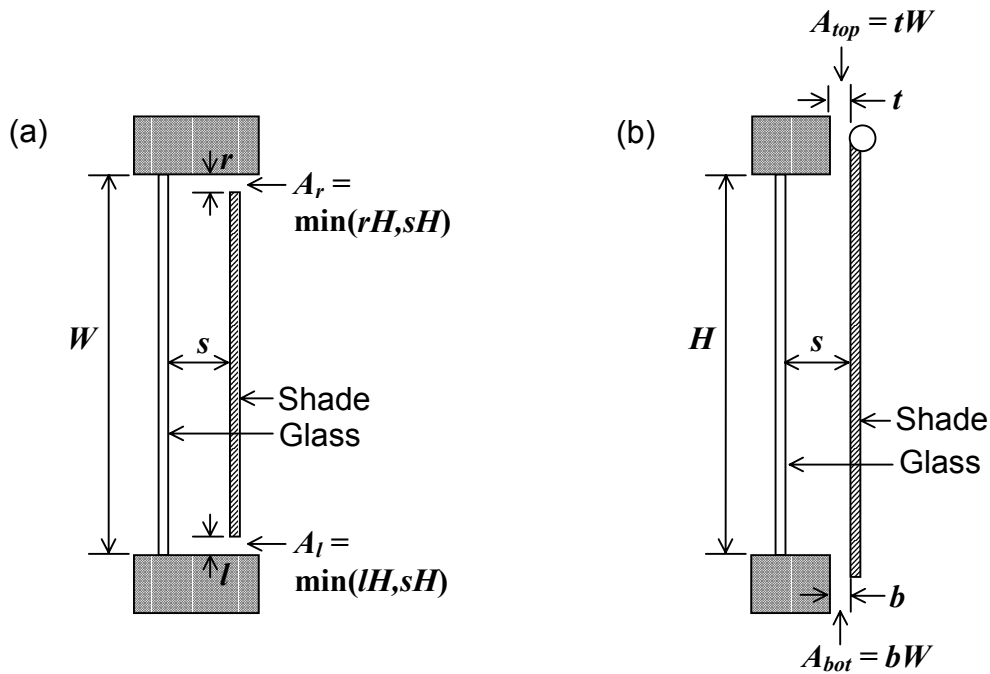
Figure 52. Examples of openings for an interior shading layer covering glass of height *H* and width *W*. Not to scale. (a) Horizontal section through shading layer with openings on the left and right sides (top view). (b) Vertical section through shading layer with openings at the top and bottom (side view).

Expression for the Gap Air Velocity

Expressing Equation (1.108) in terms of v yields the following quadratic equation:

$$\frac{\rho v^2}{2}\left(1+Z_{in}+Z_{out}\right)+\frac{12\mu H}{s^2}v-\rho_0 T_0 gH\sin\phi\frac{\left|T_{gap,in}-T_{gap}\right|}{T_{gap,in}T_{gap}}=0$$

Solving this gives

$$v=\frac{\left[\left(\frac{12\mu H}{s^2}\right)^2+\frac{2\rho^2(1+Z_{in}+Z_{out})\rho_0 T_0 gH\sin\phi\left|T_{gap,in}-T_{gap}\right|}{T_{gap,in}T_{gap}}\right]^{1/2}-\frac{12\mu H}{s^2}}{\rho(1+Z_{in}+Z_{out})} \tag{1.110}$$

The choice of the root of the quadratic equation is dictated by the requirement that $v=0$ if $T_{gap,in}=T_{gap}$.

Gap Outlet Temperature and Equivalent Mean Air Temperature

The temperature of air in the gap as a function of distance, h, from the gap inlet (Figure 53) is

$$T_{gap}(h)=T_{ave}-(T_{ave}-T_{gap,in})e^{-h/H_0}$$

where

$$T_{ave}=\frac{T_{gl}+T_{sh}}{2} \tag{1.111}$$

is the average temperature of the glass and shading layer surfaces facing the gap (K).

H_0 = characteristic height (m), given by

$$H_0=\frac{\rho C_p s}{2h_{cv}}v$$

where C_p is the heat capacity of air.

The gap outlet temperature is given by

$$T_{gap,out}=T_{ave}-(T_{ave}-T_{gap,in})e^{-H/H_0} \tag{1.112}$$

The thermal equivalent mean temperature of the gap air is

$$T_{gap}=\frac{1}{H}\int_0^H T_{gap}(h)dh=T_{ave}-\frac{H_0}{H}\left(T_{gap,out}-T_{gap,in}\right) \tag{1.113}$$
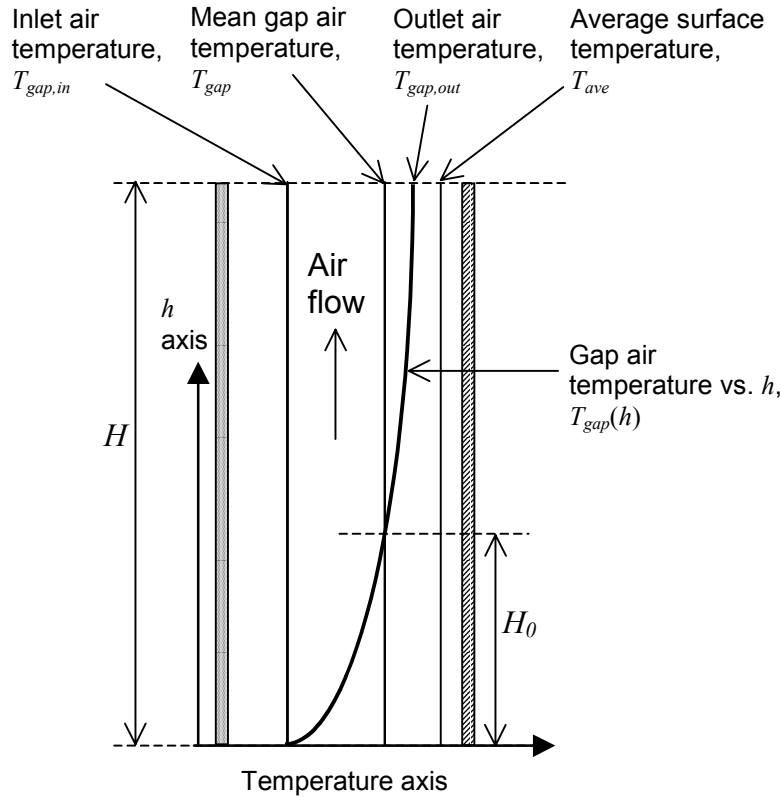
Figure 53. Variation of gap air temperature with distance from the inlet for upward flow.

Solution Sequence for Gap Air Velocity and Outlet Temperature

The routine WinShadeGapFlow is called within the glazing heat balance iterative loop in SolveForWindowTemperatures to determine v and $T_{gap,out}$. The solution sequence in WinShadeGapFlow is as follows:

- At start of iteration, guess T_{gap} as $((T_{gl} + T_{sh})/2 + T_{gap,in})/2$. Thereafter use value from previous iteration.

- Get still-air conductance, h_c, by calling WindowGasConductance and NusseltNumber.

- Get v from Equation (1.110)

- Get h_{cv} from Equation (1.108)

- Get T_{ave} from Equation (1.111)

- Get $T_{gap,out}$ from Equation (1.112)

- Get new value of T_{gap} from Equation (1.113)

The values of h_{cv} and T_{gap} so determined are then used in the window heat balance equations to find new values of the face temperatures of the glass and shading layers. These temperatures are used in turn to get new values of h_{cv} and T_{gap} until the whole iterative process converges.

Convective Heat Gain to Zone from Gap Air Flow

The heat added (or removed) from the air as it passes through the gap produces a convective gain (or loss) to the zone air given by

$$q_v = LW \left[h_{cv} \left(T_{gl} - T_{gap} \right) + h_{cv} \left(T_{sh} - T_{gap} \right) \right] = 2 h_{cv} LW \left(T_{ave} - T_{gap} \right) \quad \text{(W)}$$

This can also be expressed as

$$q_v = \dot{m} C_p \left(T_{gap,out} - T_{gap,in} \right) \quad \text{(W)}$$

where the air mass flow rate in the gap is given by

$$\dot{m} = \rho A_{gap} v \quad \text{(kg/s)}$$

References

Arasteh, D.K., M.S. Reilly and M.D. Rubin. A versatile procedure for calculating heat transfer through windows. ASHRAE Trans., Vol. 95, Pt. 2, 1989.

Finlayson, E.U., D.K. Arasteh, C. Huizenga, M.D. Rubin and M.S. Reilly. WINDOW 4.0: documentation of calculation procedures. Lawrence Berkeley National Laboratory report no. LBL-33943, 1993.

ISO15099. Thermal performance of windows, doors and shading devices—detailed calculations. Draft, July 18, 2001.

Munson, B.R, D.F. Young and T.H. Okiishi. "Fundamentals of Fluid Mechanics," Third Edition Update, John Wiley & Sons, Inc., 1998.

Simmler, H., U. Fischer and F. Winkelmann. Solar-Thermal Window Blind Model for DOE-2. Lawrence Berkeley National Laboratory, Simulation Research Group internal report, 1996 (unpublished).Air Heat Balance Manager / Processes

Air Heat Balance Manager / Processes

Convection from Surfaces

This contribution is expressed using the convective heat transfer coefficient as follows:

$$q_{conv} = \sum_{i=1}^{nsurfaces} h_{c,i} A_i \left(T_a - T_{s,i} \right) \tag{1.114}$$

The inside heat transfer coefficient is modeled from a choice of correlations.

Convection from Internal Sources

This component is the companion part of the radiant contribution from internal gains described previously. It is added directly into the air heat balance. Such a treatment also violates the tenets of the heat balance since the surface temperature of the surfaces producing the internal loads exchange heat with the zone air through normal convective processes.   However, once again, the details required to include this component in the heat balance are generally not available, and its direct inclusion into the air heat balance is a reasonable approach..

Infiltration/Ventilation

Any air that enters by way of infiltration is assumed to be immediately mixed with the zone air. The determination of the amount of infiltration air is quite complicated and subject to significant uncertainty. In the most common procedure, the infiltration quantity is converted from a number of air changes per hour (ACH) and included in the zone air heat balance using the outside temperature at the current hour.

Air Exchange

Air exchange and interchange between zones is treated as a convective gain.

Calculation of Zone Air Temperature

The zone air heat balance is the primary mechanism for linking the loads calculation to the system simulation. As such, the zone air temperature becomes the main interface variable. Its role in the integration process was described previously ("Basis for the Zone and System Integration").

COMIS

COMIS was originally developed in 1994 as a stand-alone multi-zone air flow program with its own input and output processors. In this implementation into EnergyPlus, the COMIS source code has been modified into ten modules that are called by the EnergyPlus program during each time step. At the beginning of the simulation, the Heat Balance Air Manager module generates an internal COMIS input file (comistest.cif) based on the building air flow description described in this section, and the exterior environmental conditions and internal zone temperatures. Comistest.cif can be used as input to the original COMIS program for testing and debugging purposes. COMIS, in turn, returns to the Heat Balance Air Manager the calculated air flows from the outside as infiltration, and from zone to zone as cross-mixing air flows. For each time step, the exterior and interior temperatures are updated, as well as any changes in window and door opening conditions.

The COMIS air flow building description shares many similarities to the building description used for modeling heat transfer. Both treat the building as a collection of zones that are linked to the external environment and other zones by a network of nodes. In the air flow representation, however, the nodes are the air flow properties rather than the thermal properties of the various building components such as walls, roofs, windows, doors, etc. The following table shows the general parallels between the thermal and air flow representations of a building :

Table 22. Thermal vs. Air Flow representations in Buildings

	Thermal inputs	**Air flow inputs**
Zone	Thermal Zone	COMIS Zone
Building Component	Wall, Roof or Floor Construction, Window or Door Construction	COMIS Air Flow : Crack, COMIS Air Flow : Opening
Surfaces	Surface: HeatTransfer	COMIS Surface
External Environment	Environmental Data (temperature, humidity, radiation, wind speed and direction, pressure, etc.)	Environmental Data, COMIS External Nodes, COMIS Site Wind Conditions, COMIS Cp Values

A substantial part of the information needed for the air flow modeling already exists and can be extracted or referenced from the building description for the thermal modeling, such as the volume and neutral height of the zones, the orientation and location of the building surfaces, etc. In fact, no additional inputs are needed to define an air flow zone, while a COMIS surface needs only references to the air flow type and the corresponding heat transfer surface. The COMIS model, however, does require substantially more information about the external environment.   Whereas the thermal modeling assumes the same external environment for all surfaces (except solar and wind), the air flow modeling requires differing external nodes where the pressure coefficients (Cp) by wind direction may differ.

References

More detailed discussions of their use, defaults and suggested values can be found in Feustel, H. and Smith, B. (ed.) 1998. "COMIS 3.0 User's Guide", Lawrence Berkeley National Laboratory, Berkeley CA.   This document and other information is available on the LBNL web site: http://epb1.lbl.gov/comis/

Building System Simulation System Manager / Processes

EnergyPlus uses a loop based HVAC system formulation. An example of the dual duct VAV system is shown below.

Air Loops

Figure 54. Dual Duct Schematic Diagram
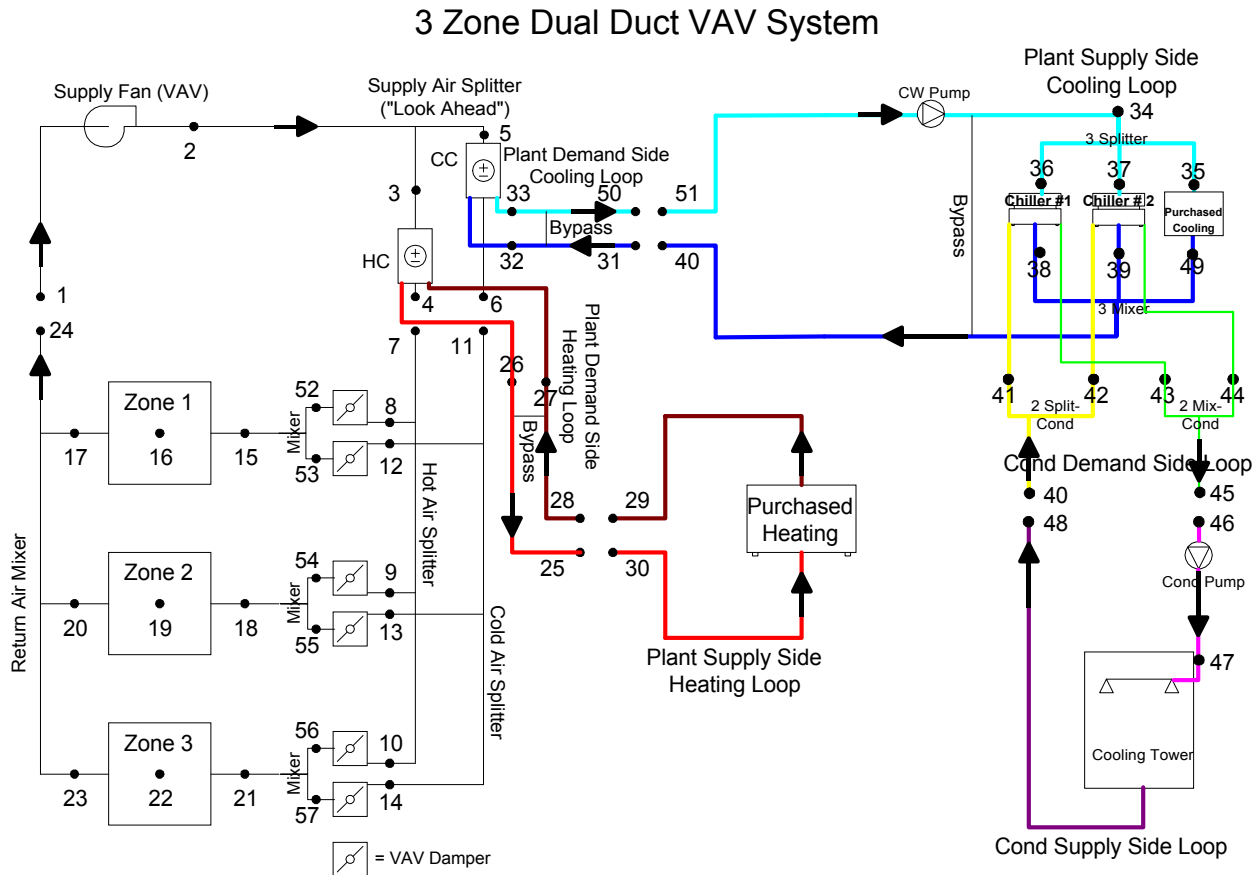
Zone Equipment Flow Resolver

Allowable Component Descriptions

For the generic flow resolver only one splitter is allowed per loop. "Nested" splitters are not supported.   The zone equipment loop typically begins with multiple branches that had their origin in a splitter on the air loop side of the interface.   The proposed zone equipment protocol will allow one splitter per branch. For consistency with existing code, the branches will be called "Supply Air Paths". Components upstream of the splitters will not be allowed. This is not a meaningful restriction since all such components can be included on the air loop side of the interface.

The dual duct shown in "Figure 54. Dual Duct Schematic Diagram" can now be described with 1 dual duct VAV box per zone as shown in the following figure. This figure shows each component connected to two supply air paths.   In general this scheme will also allow components to be connected to return air paths.   This should facilitate simulation of components such as fan powered VAV boxes that induce flow from the return air plenum.
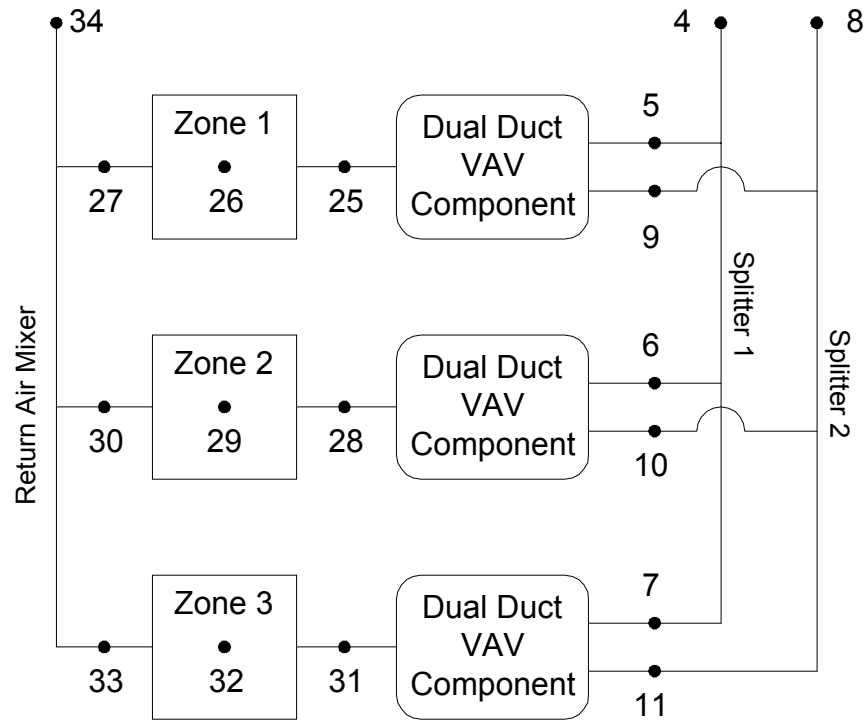
Figure 55. Dual Duct VAV Component Diagram

The Simulation Algorithm

The simulation of the zone equipment section of EnergyPlus can be viewed from many perspectives. This document is intended to only describe high level interactions (top 3) and thus will leave the details of component level simulation to other documents.

The main HVAC calling module (HVACManager) calls the other main managers based on the EnergyPlus loop scheme. In this case, we are interested in the Zone Equipment Manager. It is assumed that each zone equipment group has an overall control algorithm associated with it. This control algorithm would define which splitter (if a splitter exists such as in the Dual Duct VAV shown above) is the controlling splitter for various operating and environmental conditions. For example, the overall zone equipment group control for a dual duct VAV system might assign a priority to the splitter that is fed from the cold deck. This overall control scheme is the vital link in the simulation algorithm that follows. Note that the example which follows is specific to a Dual Duct VAV system but is applicable in general to any foreseeable EnergyPlus system since Dual Duct VAV is the most complex system available (we think).

The following algorithm is a simulation method only. Initializations and get routines are described in detail elsewhere.

1) Enter the Zone Equipment Manager.

2) Get/Initialize as appropriate for the time and iteration of the simulation.

3) Using the overall control algorithm, determine the order of priority/simulation of the different splitters. For example, in a Dual Duct VAV system during the summer, the cooling splitter might be given top priority.

4) Simulate the priority 1 splitter. This involves modeling each successive component on the first branch encountered until the "flow controlling" component is reached. The flow-controlling component will be responsible for querying the zone data module for zone loads, etc. and arriving at a desired flow rate for that branch based on it's own control algorithm.

5) Repeat the above step for every branch on the priority 1 splitter.

6) At this point, a desired flow rate for each branch coming out of the priority 1 splitter has been defined. Now, reconcile flow rates for the priority 1 splitter (inlet and outlet) and set min available/max available/actual flow rates for each individual branch coming out of the priority 1 splitter to lock in flow rates for those branches.

7) Resimulate the components between the priority 1 splitter and the flow-controlling components on each branch coming out of it (simulate splitter 1 branches with final flow rates).

8) Repeat steps 4 through 7 for all of the other splitters in order of priority defined by the control algorithm for the current conditions.

9) At this point, the flow conditions and the temperatures for all components in front of the flow controlling components have been fixed. Now, each zone branch is simulated (from the flow-controlling component to where the zone branch terminates in a return air mixer).

10) Once all the zone branches have been simulated, the return air mixer (if present) can be modeled.

Plant/Condenser Loops

Integration of System and Plant

In order to integrate the air handling system simulation with the zones simulation, methods were developed to model the system air loop and its interactions with the zones due to temperature controls and the relative difference between the zone and supply air temperatures.   A similar situation is encountered when integrating the central plant simulation. Typically, the central plant interacts with the systems via a fluid loop between the plant components and heat exchangers, called either heating or cooling coils. In EnergyPlus the performance of the systems and plant are interdependent because the simulations are combined. The plant outputs must match the system inputs and vice versa. That is, the temperature of the chilled water leaving the plant must equal the temperature of the water entering the coils, and the chilled water flow rate must satisfy mass continuity. In addition, coil controls are usually necessary to ensure that the values of chilled water flow variables entering and leaving the coil remain in a reasonable range. The specific controls vary from application to application but two common possibilities are: maintaining a constant coil leaving air temperature or limiting the water temperature rise across the coil.

Current Primary System Modeling Methodology

There are three main loops within the HVAC simulation in the new program: an air loop, a plant loop, and a condenser loop. The air loop is assumed to use air as the transport medium as part of an air handling system while the plant and condenser loops may use a fluid of the user's choosing (typically water). A user may have any number of each type of loop in a particular input file. There are no explicit limits on the number of loops within the program—the user is only limited by computer hardware. Execution speed will naturally vary with the complexity of the input file.

Main loops are further divided into "sub-loops" or "semi-loops" for organizational clarity and simulation logistics (see Figure "Connections between the Main HVAC Simulation Loops and Sub-Loops"). These sub-loops are matched pairs that consist of half of a main loop. Plant and condenser loops are broken into supply and demand sides. The plant demand loop contains equipment that places a load on the primary equipment. This might include coils, baseboards, radiant systems, etc. The load is met by primary equipment such as chillers or boilers on the plant supply loop. Each plant supply loop must be connected to a plant demand loop and vice versa. A similar breakdown is present on condenser loops where the demand side includes the water side of condensers while the supply side includes condenser equipment such as cooling towers.
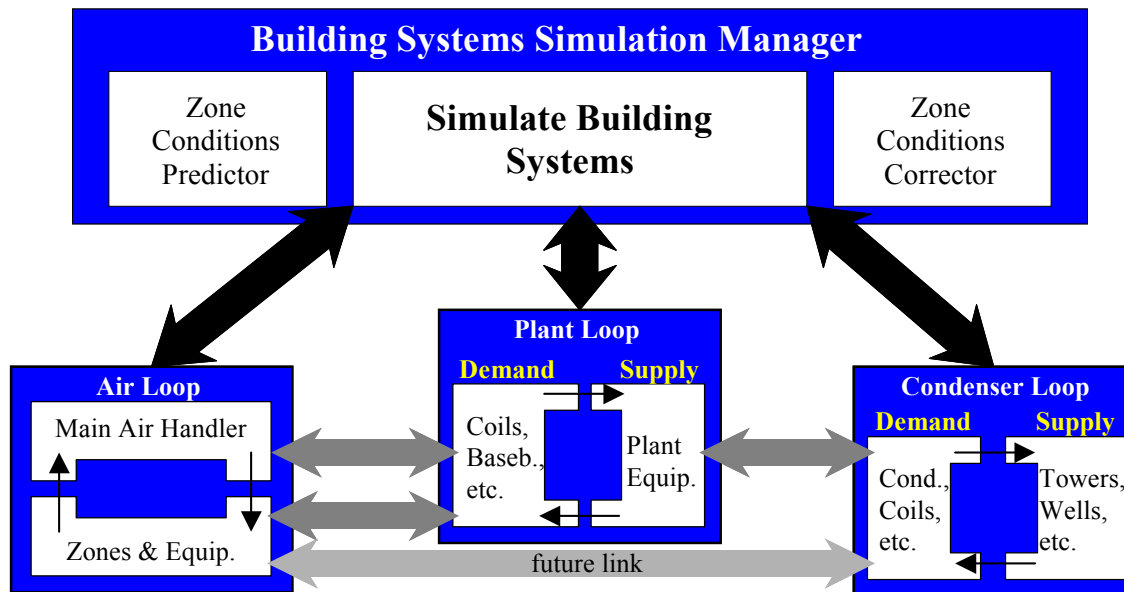
Figure 56. Connections between the Main HVAC Simulation Loops and Sub-Loops.

The breakdown into sub-loops allows for better handling and control of information and simulation flow throughout the program. Direct connections between the sub-loops of the air, plant, and condenser loops are enhanced by indirect connections between the various main loop types. For example, coils (heating or cooling) are in reality heat exchangers with an air and a water or refrigerant side. The air side of the coil is handled within the air loop where the control of the device is also maintained. The fluid side of the coil is handled within the plant demand side, which passes the energy requirements of the coil on to the plant supply side. All loops are simulated simultaneously, though sub-iteration loops are maintained between the two sides of any loop to speed convergence. Overall iterations ensure that the results for the current time step are balanced and updated information has been passed to both sides of the sub-loops as well as across to the other side of indirect connections such as coils.

Branches further divide the sub-loops into groups as they would appear within any HVAC system. Elements can be defined in series, in parallel, or both with some restrictions. Figure "Branch Layout for Individual HVAC Sub-Loops" provides an overview of a generic sub-loop representation. Branches are defined as individual legs within the loop structure. Thus, the segment between point A and point B is defined as a branch, as is the section between points E and F. There may be multiple sections (C1 to D1 through Cn to Dn) in between the splitter and mixer. Each sub-loop may only have one splitter and one mixer. Thus, equipment may be in parallel between the mixer and splitter, however, within any branch, there can only be elements in series and not in parallel. The topology rules for individual sub-loops allow a reasonable amount of flexibility without requiring a complicated solver routine to determine the actual flow and temperature conditions. Note that since plant supply and demand are broken up into two separate sub-loops chillers or boilers may be in parallel to each other in the supply side and coils may be in parallel to each other on the demand side. Thus, the restriction of only a single splitter and mixer on a particular sub-loop does not limit the normal configurations. Also, a sub-loop does not require a splitter or mixer if all equipment on the sub-loop are simply in series—this would correspond to a single branch that would define the entire sub-loop.
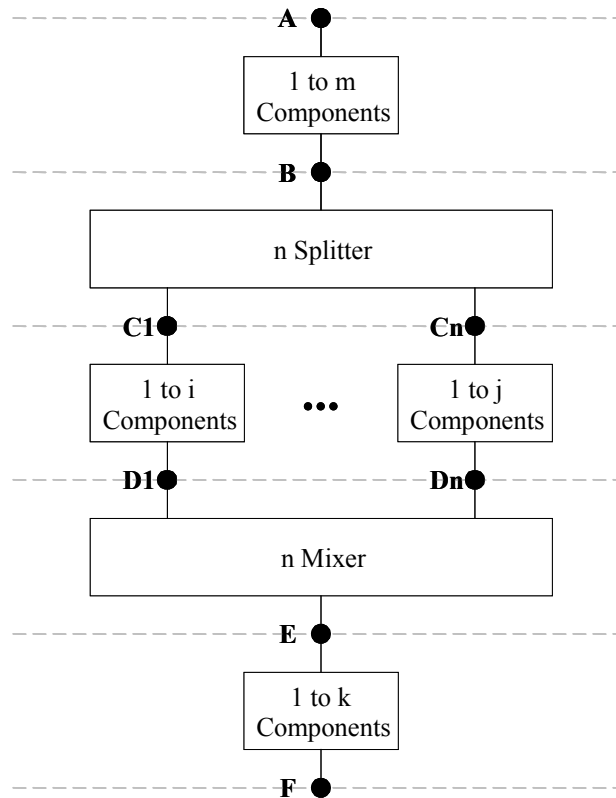
Figure 57. Branch Layout for Individual HVAC Sub-Loops

Essentially, each branch is made up of one or more components linked together in series. The branch has an information node containing properties of the loop (temperature, enthalpy, flow rate, etc.) at the beginning and end of the branch as well as between components. Components on the branch take the conditions of the node at their inlet and use that information as well as overall control information to simulate the component and write the outlet data to the node following the component. This information is then used either by the next component on the branch or establishes the outlet conditions for the branch.

Plant Flow Resolver

Overview of the Plant Flow Resolver Concept

One of the most important aspects of the solution procedure within the plant and condenser loops of the new program is the method used to solve the various sub-loops. This involves making the supply side meet a particular load based on the simulation of the demand side loops. Load distribution is an issue that must be addressed as well as how flow rates are adjusted and temperatures are updated. These issues are discussed in the next several subsections, and the algorithms described are important to how the HVAC simulation functions.

In the first step, the loop manager would call the appropriate module to simulate (in order) all of the components on each branch of the loop except for splitters and mixers. In this step, each component would set the conditions at the outlet node including temperature, flow rate, maximum allowed (design) flow rate, minimum allowed (design) flow rate, maximum available flow rate, and minimum available flow rate. This would be based purely on the component's own control scheme and thus each component would be free to request as much (or as little) flow as desired.

In the second step, the loop manager would resolve the flow at all nodes and through all branches of the local loop. The components are then simulated with the corrected flows. For this iteration, the flow resolver sets the flow rate through each loop component.

Pump Control for Plant and Condenser Loops.

The pump is quite simply the component that drives the flow. How it reacts depends on several different conditions. In total, there are three different decision variables, two of which are defined by user input. These three deciding factors are whether the pump is constant or variable speed, whether the pump operation is continuous or intermittent, and whether or not there is a load on the loop. The pump is simulated first on the supply side loop after the demand side loop has determined what the demand on the loop will be. The load is simply calculated by multiplying the requested flow rate from the demand side by the difference between the enthalpy at the supply side inlet and the enthalpy that corresponds to the current loop setpoint temperature. This setpoint temperature is the fluid temperature that one is attempting to maintain at the outlet of the supply side and can be scheduled to different values on an hourly basis.

The operation of a constant speed pump is fairly straightforward. If the user designates a constant speed pump that is operating continuously, the pump will run regardless of whether or not there is a load. This may have the net effect of adding heat to the loop if no equipment is turned on. If the pump is constant speed and operates intermittently, the pump will run at its capacity if a load is sensed and will shut off if there is no load on the loop.

A variable speed pump is defined with maximum and minimum flow rates that are the physical limits of the device. If there is no load on the loop and the pump is operating intermittently, then the pump can shutdown. For any other condition such as the loop having a load and the pump is operating intermittently or the pump is continuously operating (regardless of the loading condition), the pump will operate and select a flow somewhere between the minimum and maximum limits. In these cases where the pump is running, it will try to meet the flow request made by demand side components.

In many cases, the first estimate of flow requested by the demand side tends to be fairly accurate and the flow rate does not vary in subsequent iterations. However, because there is the possibility that the coils or some other component might request more flow in future iterations during the same time step, the program must not only set flow rates but also maintain a record of the current maximum and minimum flow rate limits. This information is important not only to the pump itself but also to other pieces of equipment which may control their flow rates and thus require knowledge of the limits within which they may work. In general, the decisions on what to set the maximum and minimum flow rates is directly related to the type of pump (constant or variable speed). For constant speed pumps, the maximum and minimum flow rate values are the same and thus if the flow requested does not match this, the other components must either deal with the flow or a bypass branch must be available to handle the excess flow. For variable speed pumps, the maximum and minimum flow rates are set by the user defined limits.

Plant/Condenser Supply Side

Component models, such as boilers, chillers, condensers and cooling towers are simulated on the supply side of the plant and condenser loops. In order to allow specification of realistic configurations, the plant and condenser supply side loop managers were designed to support parallel-serial connection of component models on the loop. In addition, loop managers were designed to support both semi-deterministic models (e.g. the parameter estimation models of the ASHRAE Primary Toolkit [Pedersen 2001]) and "demand based" models (e.g. the performance map models of BLAST and DOE2.1E). As a result, the loop manager must be able to simulate models that require the mass flow rate as an input and models that calculate the mass flow rate as an output—sometimes in the context of a single loop configuration.

In order to achieve these design criteria without resorting to a pressure based flow network solver in the HVAC portion of the code, a rules-based "flow resolver" was developed for the

EnergyPlus plant and condenser supply side managers. The flow resolver is based on the following assumptions and limitations:

- Each loop is only allowed to have a single splitter and a single mixer
- Due to the fact that there can only be one splitter and one mixer on a given loop, it follows logically that there can be at most one bypass on each loop
- No other components may be in series with a bypass, i.e., a branch that contains a bypass may have no other equipment on that branch
- Equipment may be in parallel only between the splitter and mixer component of a loop or between one of those types of equipment and the loop inlet/outlet nodes
- Equipment may be hooked together in series in each branch of the loop
- Flow rates on individual branches will be controlled using maximum and minimum available flow rate limits

The flow resolver employs a simple predictor-corrector algorithm to enforce mass continuity across the plant loop splitter as shown in the following figure.
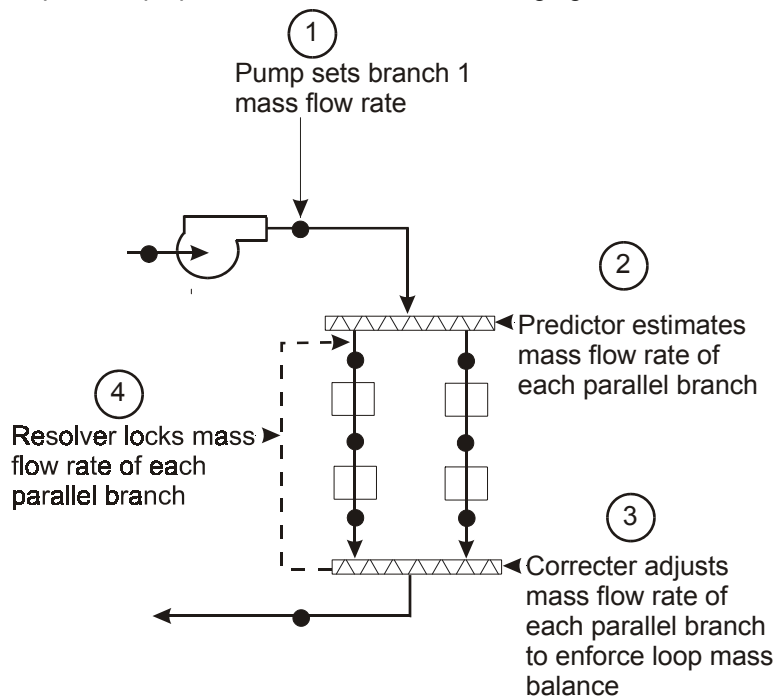
Figure 58. Plant/Condenser Supply Side Solution Scheme.

As previously discussed, the pump establishes the total loop mass flow rate by setting the flow in the first supply side branch. In the second step, a predictor algorithm polls each piece of equipment on the loop and "predicts" branch mass flow rates based on the requested flow rate for each. The loop manager calls the appropriate module to simulate (in order) all of the components on each branch of the loop except for splitters and mixers. In this step, each component sets the conditions at its outlet node including temperature, flow rate, maximum allowed (design) flow rate, minimum allowed (design) flow rate, maximum available flow rate, and minimum available flow rate.   These predicted values are based purely on the component's own control scheme and thus each component is free to request as much (or as little) flow as desired.

Each component is tagged in the user input file as an ACTIVE, PASSIVE or BYPASS type of model. An ACTIVE type describes a demand based plant model that calculates mass flow rate as an output. A PASSIVE type describes a semi-deterministic model that is simulated with the mass flow rate as an input. The BYPASS type designates a loop bypass.

The predictor algorithm first establishes the desired flow rate of each branch by searching for ACTIVE components on the branch. The first ACTIVE component in simulation order sets the desired branch flow. Branches with only PASSIVE components require a flow rate between the minimum and maximum allowable branch flow. Branches with a BYPASS component have a branch flow only when all other branches combined cannot handle the entire loop flow.

In the third step, the loop manager makes any necessary "corrections" to the requested branch flows in order to enforce overall continuity on the loop. If mass conservation allows all ACTIVE branches to be satisfied, then the remaining flow is divided between the PASSIVE branches and as a last resort, the BYPASS. If there is insufficient flow to meet the branch demand, ACTIVE branch requests are met first in the order that the branches appear in the branch list in the input file.

Plant/Condenser Demand Side

The plant and condenser demand side are simulated in a different manner than the supply sides because in reality there are no components to simulate or control. On the supply sides, there is a load management scheme and other constraints that must be resolved. On the demand sides, all of the components have already been simulated and controlled by the air loop, the zone equipment, or the plant supply side. Thus, the demand side management module only needs to resolve the actual flow rate through each section or branch of the sub-loop and also monitor the maximum and minimum flow rates that are available.

The flow rate is resolved first for each individual branch. For every branch, the program cycles through each node on the branch and determines what the flow requests and flow limits are. The most restrictive flow constraints are assumed to be valid for the entire branch regardless of component type. Since there may be several components in series on a particular branch, there is also a defined scheme for assigning priority to components that will have the ability to control the flow. The user may specify individual components as either active or passive. Active components are given highest priority for requesting a particular flow rate. If there is more than one active component on a particular branch, then it is assumed that the first active component on the branch is the highest priority and dictates the flow request.

Once all of the branches have set their flow rates and constraints, the splitter and mixer must resolve the various flow requests. In the demand side scheme, the mixer and any branch following the mixer is completely passive. Thus, all of the control happens at the splitter. The splitter first attempts to sum the maximum and minimum constraints from all of the branches coming out of the device and compares those to the constraints that are valid for the branch leading into the splitter. When there is a mismatch between the outlet constraints and the inlet constraints, the simulation will defer to the inlet constraints due to the fact that the pump is in reality controlling flow on the loop. Since the constraints of the pump would be passed across to the demand side from the supply side, an assumption is made that the coils or other demand side components must live within the bounds of the pump.

Once the flow has been resolved at the splitter, the branch flow rates and constraints between the splitter and mixer can be adjusted, if necessary. In some cases, this will be mandatory to maintain a mass balance at the splitter. When the flow rate coming out of the splitter does not match the branch requests, individual branch flow rates must be adjusted to provide for the extra flow or the "flow deficit". When there is extra flow, flow is sent through any bypass branch first and then is sent to passive branches in reverse order of their appearance in the splitter outlet list. When all of these branches have been exhausted, flow will be increased to the active branches, also in reverse order. The reverse order guarantees that the branch appearing first has the highest priority to receive the flow rate is has requested. If there is not enough flow for all of the requests, flow rates will be decreased in a similar order: passive branches first in reverse order followed by active branches in reverse order. Flow rates are increased or decreased until a mass balance at the splitter exists.

It is also necessary to monitor the flow constraints at the branches and components since once the flow rates are changed, the components must be resimulated by the controlling loop (air loop, zone equipment, or plant supply side). The controllers for these components must know if the constraints have been modified so that the simulation does not toggle between a component requesting a flow that the pump cannot meet and the pump then resetting the flow to what it can provide. Note that once a flow rate for any component has changed that this signals the need to resimulate any sub-loop to which it might have an indirect connection. Currently, this means that if a flow rate on the plant demand side changes, the simulation must recalculate the conditions on both the air loop and zone equipment sub-loops since coils and other equipment could be on either side of the main air loop. Similarly, if the condenser demand side simulation results in a change in flow rate through a chiller condenser, then the plant supply side must be triggered to perform its calculations again. Care has been taken to avoid cases where the various sub-loops might simply keep triggering the resimulation of their indirect connections in an infinite loop.

Temperature Resolution

The transition from load or energy based plant models to a loop based arrangement makes variables of both the flow rate and the fluid temperature. This means there are more degrees of freedom that must be controlled. The flow resolver concept discussed previously controls the flow rates through the components and maintains an overall mass flow balance through the loop. However, the temperatures still need to be controlled. A purely iterative procedure can be expected to converge to the appropriate loop temperatures, but the procedure can become slow to converge under conditions where the demand changes rapidly or the supply components may not have enough capacity to meet the system demand. This situation is somewhat analogous to that existing in the link between the zone and the air system. In that case, the convergence and stability of the iterative solution was greatly improved by adding the thermal capacitance of the zone air and other fast responding mass within the zone. Based on that experience, it was decided to add thermal capacitance to the plant loop and benefit from the added stability. Because the thermal capacitance in the zone/system interaction is relatively small, it was necessary to use a third order numerical solution there. Since the plant loop thermal capacitance is higher, a simple first order solution has been found to be satisfactory.

To implement the capacitance, each loop is assigned a fluid volume as user input. This is used to determine a capacitance concentrated in the supply side outlet node. If the loop setpoint cannot be maintained, this node becomes an energy storage location and its temperature reflects the current capability of the supply side. The size of the thermal capacitance affects the speed of recovery from situations where the setpoint was not maintained. The user must estimate a fluid volume based on the size of the pipes in the loop. However rough estimates seem to be sufficient. The supply side outlet node temperature and the demand side inlet temperature proceed through smooth paths from one time step to the next. No energy is lost or gained because of storage in the loop capacitance. Once setpoint temperature is reached, the storage effects are not involved.

Loop Instability Induced by the Capacitance Calculation

The demand inlet temperature, (Tdi, as shown in Figure "Demand and Supply Side Loops") is calculated at the end of each Iteration of the HVAC simulation, based on the loop mass, the calculated supply side outlet, (Tso) and the demand inlet temperature from the previous timestep.
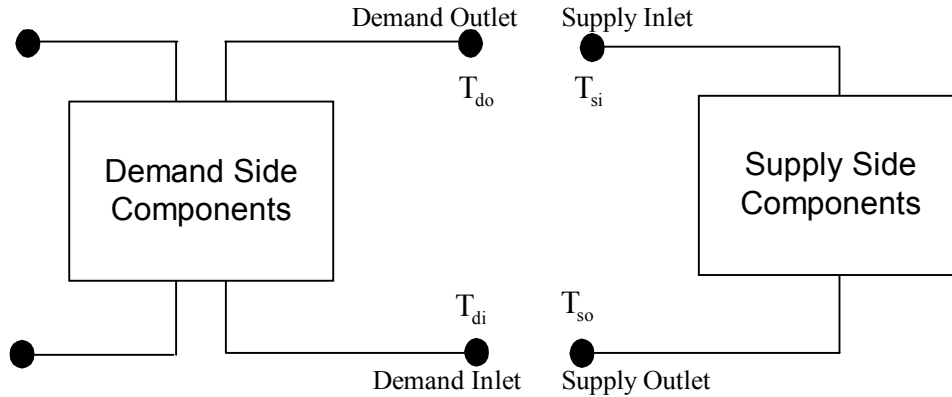
Figure 59. Demand and Supply Side Loops

The capacitance of the water in the loop is accounted for by balancing the energy added to the total mass of the water in the loop, M [kg], with the energy added during the current timestep. The formulation assumes that the water in the loop is "well mixed".

$$M\left(T_{di-new} - T_{di-old}\right) = \left(\dot{m}_s * t_{sys} * 3600\right) * \left(T_{so} - T_{di}\right)$$

Where:

T_{di-old} Previous system time-step demand inlet temperature [°C]

T_{di-new} Current demand side inlet temperature [°C]

$\dot{m}_s$ Maximum expected supply side mass flow rate [Kg/s]

t_{sys} System time step [hr]

T_{so} Supply side outlet temperature [°C]

M Mass of the water in the loop [Kg]

The new inlet temperature is calculated as shown in Equation 2. This formulation is stable as long as the mass ratio is les than one.

$$\frac{\left(\dot{m}_s * t_{sys} * 3600\right)}{M} \leq 1$$

A mass ratio greater than one implies that the water will be pumped around the loop more than once during a single system timestep. The resulting gain on the temperature calculation would lead to instability in the calculated loop water temperature.

$$T_{di-new} = T_{di-old} + \left(\frac{\left(\dot{m}_s * t_{sys} * 3600\right)}{M} * \left(T_{so} - T_{di}\right)\right)$$

There is the option of shortening the time step or increasing the mass to maintain stability. Upon entering the Loop Volume with the "autosize" option the program calculates the stable volume with the stability criteria equal to 0.8, and then converts this to a mass quantity. The program is driven top down by time step, and redefining the time step has vast implications throughout the simulation. Since the mass quantity is put in to stabilize the loop as its primary purpose this quantity is modified to retain loop stability. If the user needs to do a

study and simulating a small loop is the major criteria, then the overall simulation time step can be shortened to facilitate. The user still has the capability to enter the Loop Volume, the lower limit will be checked and larger loop volumes can still be entered to simulate large, massive systems.

Note that if a user specifies a maximum loop volumetric flow rate and loop volume that may lead to instabilities based on the above noted convergence criteria, then the program will recalculate the loop mass. Thus, users should be particularly mindful of both the maximum loop volumetric flow rate and the plant loop volume parameters in their input file. Any inconsistencies between these two parameters may lead the program to override the loop volume and lead to unexpected results.

The Plant Flow Resolver Input

The input specifically related to the flow resolver consists of the Plant BRANCH list and the Plant CONNECTOR LIST as shown in the figure below. These user defined names link the plant loop to its branches (contained in the BRANCH list) and define the loop splitters and mixers contained in the CONNECTOR LIST. The SPLITTER and MIXER syntax in turn define the relative connection of the branches to each other on the loop.

```
PLANT LOOP,
  A1 , \field Plant Loop Name
        \required-field
        \reference PlantLoops
  A2 , \field Fluid Type
        \required-field
        \type choice
        \key Water
        \default Water
  A3 , \field Plant Operation Scheme List Name
        \required-field
        \type object-list
        \object-list PlantOperationSchemes
  A4 , \field Loop Temperature Setpoint Schedule Name
        \required-field
        \type object-list
        \object-list ScheduleNames
  N1 , \field Maximum Loop Temperature
        \required-field
        \units C
  N2 , \field Minimum Loop Temperature
        \required-field
        \units C
  N3 , \field Maximum Loop Volumetric Flow Rate
        \required-field
        \units m3/s
        \autosizable
  N4 , \field Minimum Loop Volumetric Flow Rate
        \required-field
        \units m3/s
        \default 0.0
  N5, \field volume of the plant loop
        \required-field
        \units m3
        \autosizable
  A5, \field Plant Side Inlet Node Name
  A6, \field Plant Side Outlet Node Name
  A7, \field Plant Side Branch List Name
        \object-list BranchLists
  A8, \field Plant Side Connector List Name
        \object-list ConnectorLists
  A9, \field Demand Side Inlet Node Name
```

```
A10, \field Demand Side Outlet Nodes Name
A11, \field Demand Side Branch List Name
     \object-list BranchLists
A12, \field Demand Side Connector List Name
     \object-list ConnectorLists
A13; \field Load Distribution Scheme
     \type choice
     \key OPTIMAL
     \key SEQUENTIAL
     \default SEQUENTIAL
```

The BRANCH definition shown below lists in simulation and connection order all of the components on the branch. The simulation assumes that the inlet node of the first component listed on the branch is the branch inlet node and the outlet node of the last component listed on the branch is the branch outlet node. Up to ten components may be listed on the branch.

The flow control algorithm described in Section 3 to determine the flow through the loop uses the branch control types: ACTIVE, PASSIVE, and BYPASS. An ACTIVE control type describes a demand based plant model that calculates mass flow rate as an output of the model. A PASSIVE control type describes a model that is simulated with the mass flow rate as a model input. The BYPASS control type designates a loop bypass.

```
BRANCH,
   A1,  \field Branch Name
        \reference Branches
   !List components on the branch in simulation and connection order
   !Note: this should NOT include splitters or mixers which define
   !      endpoints of branches
   N1, \field Maximum Branch Flow Rate
       \units m3/sec
   A2, \field Comp1 Type
   A3, \field Comp1 Name
   A4, \field Comp1 Inlet Node Name
   A5, \field Comp1 Outlet Node Name
   A6, \field Comp1 Branch Control Type
       \type choice
       \key ACTIVE
       \key PASSIVE
       \key BYPASS
       \note for ACTIVE, Component tries to set branch flow
       \note for PASSIVE, Component does not try to set branch flow
       \note for BYPASS,  Component designates a loop bypass
```

The Plant Flow Resolver Algorithm

The flow resolver is called from the plant and condenser loop managers as shown below. All branches are simulated with desired flow rates, then the flow resolver sets the branch flows and the loops are simulated again. Finally the loop mixer is updated and the mixer outlet branch is simulated.

- Simulate Components with the flow rate "requested" to meet loop demand.
- Check Branch flows (downstream of splitter) to ensure that continuity is not being violated.
- Adjust branch flows if necessary to achieve a mass balance on the loop
- Resimulate Components with adjusted flows.

```
DO All Branches
  CALL Sim Plant Equipment
  IF (Branch is Splitter inlet ) CALL Update Splitter
END DO

CALL Solve Flow Network
```

```
DO All Branches
  CALL Sim Plant Equipment
  IF (Branch is Splitter inlet ) CALL Update Splitter
END DO

CALL Update Mixer

CALL Sim Plant Equipment on Mixer Outlet Branch
```

The flow resolver algorithm first establishes the desired flow rate of each branch by searching for ACTIVE components on the branch. The first ACTIVE component in simulation order sets the desired branch flow. Branches with only PASSIVE components require a flow rate between the minimum and maximum allowable branch flow. Branches with a BYPASS component have a branch flow only when all other branches combined cannot handle the entire loop flow.

If mass conservation allows all ACTIVE branches to be satisfied, then remaining flow is divided between the remaining PASSIVE branches and as a last resort, the BYPASS. If there is insufficient flow to meet the branch demand, ACTIVE branch requests are met first in the order that the branches appear in the branch list in input.

Primary-Secondary Loop Systems

The Plant Loop Connection Component is used to connect 2 plant loops together, typically to create a Primary-Secondary plant loop system. This system normally has multiple chillers on the primary constant volume loop, with a variable volume flow system to provide flow to multiple cooling coils. This keeps the flow through the chillers at a fixed level and allows for variable flow in the secondary systems. The hydraulic coupling is provided between the primary and secondary loop by the Plant Loop Connection Component. The Plant Loop Connection Component is a control volume around some piping and bypass valve. Its main function is to resolve mass flow between the two nested plant loops based upon the control modes entered by the user.

The Plant Loop connection component was designed to use the existing component/loop/solution structure to facilitate the simulation with the existing demand side manager and the supply side manager. The initial implementation has a constant flow primary loop (Loop with Chillers) and a variable flow secondary loop (Loop with the Coils). The connection component does the mass flow resolution between the nested loops and does the proper mixing with the bypass as necessary. This should facilitate the majority of the primary secondary systems being used today, a diagram is shown below and a sample input file is included in the test suite.
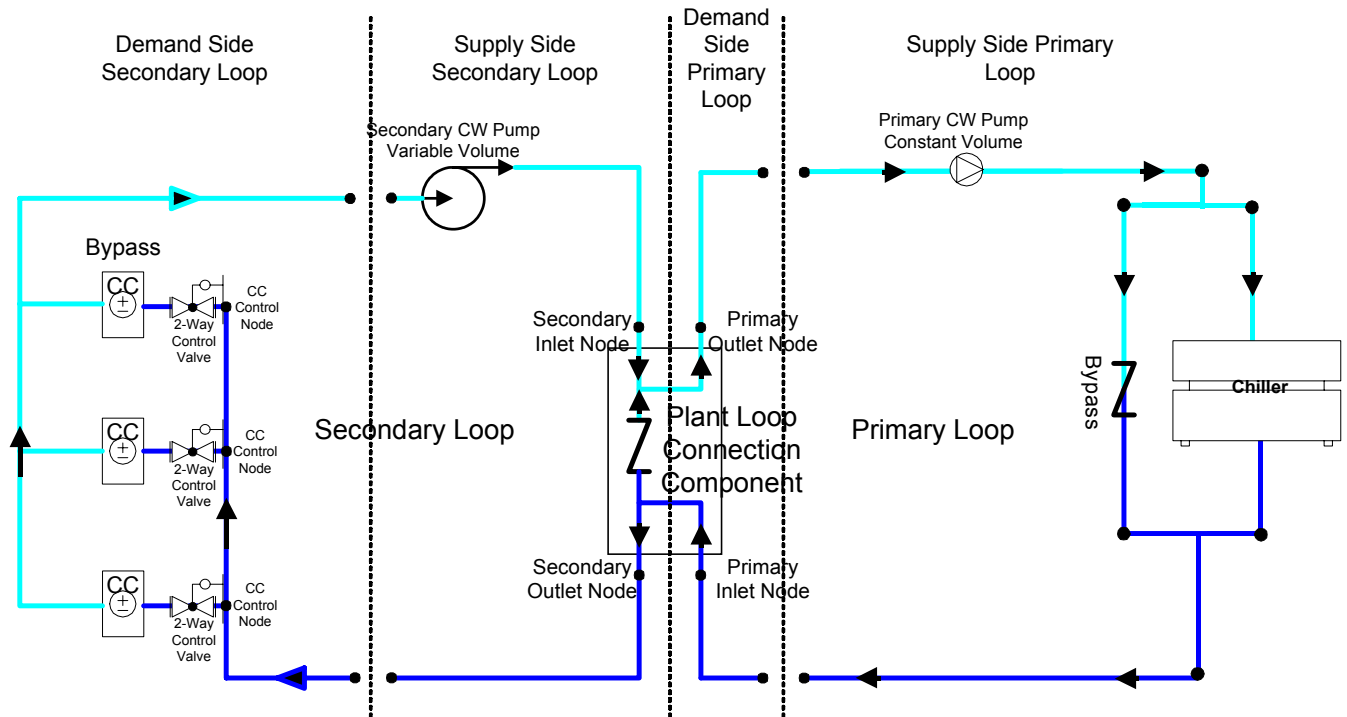
Figure 60. Example of a Primary-Secondary Nested Loop Simulation

The Plant Loop Connection Component is simulated on the Supply Side of the Secondary Loop and the results are provided to the Demand Side of the Primary Loop. Since the demand side of the primary loop is not simulated until the supply side of the secondary loop is simulated, there is an additional iteration through the demand side that is necessary. Only the Plant Loop Connection Component triggers this additional demand-side iteration. This was necessary to keep the iterated information current and to ensure that an energy balance is achieved. There are some assumptions that are necessary:

■ When the secondary side shuts down, either by no demand or the secondary pump scheduled off, the primary side will also shut down for that time step.

■ If either the secondary or primary pump is scheduled, the same scheduled needs to be applied to both of the pumps.

■ Currently, only two loops can be simulated together, i.e. only one level of nesting.

These assumptions are essential due to the fact that control information is difficult to pass between the nested loops.

Auxiliary Processes / Examples

Photovoltaic Array

Introduction

This module models the electrical performance of a photovoltaic (PV) array; it may be used in simulations involving electrical storage batteries, direct load coupling, and utility grid connections. The methodology of the module is that a user describes a PV array in the EnergyPlus input file. Prior to a RunPeriod simulation, EnergyPlus reads the description and then calls TRNSYS [1] which performs the simulation of the PV array performance before returning control to EnergyPlus.

Mathematically speaking, the EnergyPlus/TRNSYS PV module employs equations for an empirical equivalent circuit model to predict the current-voltage characteristics of a single module. This circuit consists of a DC current source, diode, and either one or two resistors. The strength of the current source is dependent on solar radiation and the IV characteristics of the diode are temperature-dependent. The results for a single module equivalent circuit are extrapolated to predict the performance of a multi-module array.

For crystalline modules (either single crystal or polycrystalline technology), the module employs a "four-parameter" equivalent circuit. The values of these parameters cannot normally be obtained directly from manufacturers' catalogs. However, the PV module will automatically calculate them from available data. A second equivalent circuit model involving five mathematical parameters is available for amorphous/thin-film PV modules. Again, the component will determine these values from manufactures' catalog data. The PV module also includes an optional incidence angle modifier correlation to calculate how the reflectance of the PV module surface varies with the angle of incidence of solar radiation.

The module determines PV current as a function of load voltage. Other OUTPUTS include current and voltage at the maximum power point along the IV curve, open-circuit voltage, and short circuit current.

Table 23. General Nomenclature for the PV model

Mathematical variable	Description
β	Slope of PV array [degrees]
γ	Empirical PV curve-fitting parameter
ε_γ	Semiconductor bandgap [eV]
η_c	Module conversion efficiency
$\mu_{I\sigma\chi}$	Temperature coefficient of short-circuit current [A/K]
$\mu_{\varsigma o\chi}$	Temperature coefficient of open-circuit voltage [V/K]
θ	Angle of incidence for solar radiation [degrees]
$\tau\alpha$	Module transmittance-absorptance product
$\tau\alpha_{normal}$	Module transmittance-absorptance product at normal incidence
FLAG	Flag for PV convergence promotion algorithm
G_T	Total radiation incident on PV array
$G_{T,beam}$	Beam component of incident radiation
$G_{T,diff}$	Diffuse component of incident radiation

$G_{T,gnd}$	Ground-reflected component of incident radiation
$G_{T,NOCT}$	Incident radiation at NOCT conditions
$G_{T,ref}$	Incident radiation at reference conditions
I	Current
I_L	Module photocurrent
$I_{L,ref}$	Module photocurrent at reference conditions
I_o	Diode reverse saturation current
$I_{o,ref}$	Diode reverse saturation current at reference conditions
I_{sc}	Short-circuit current
$I_{sc,ref}$	Short-circuit current at reference conditions
I_{mp}	Current at maximum power point along IV curve
$I_{mp,ref}$	Current at maximum power point along IV curve, reference conditions
IAM	Dimensionless incidence angle modifier
k	Boltzmann constant [J/K]
NP	Number of modules in parallel in array
NS	Number of modules in series in array
N_s	Number of individual cells in module
P	PV output power
P_{max}	PV output power at maximum power point along IV curve
q	Electron charge constant
R_s	Module series resistance [Ω]
R_{sh}	Module shunt resistance [Ω]
T_c	Module temperature [K]
$T_{c,NOCT}$	Module temperature at NOCT conditions [K]
$T_{c,ref}$	Module temperature at reference conditions [K]
U_L	Array thermal loss coefficient
V	Voltage
V_{mp}	Voltage at maximum power point along IV curve
$V_{mp,ref}$	Voltage at maximum power point along IV curve, reference conditions
V_{oc}	Open-circuit voltage
$V_{oc,ref}$	Open-circuit voltage at reference conditions [V]

PV Modeling Options

A number of simulation options are available for the Photovoltaic Array module. The first of these is the mathematical model used to predict the electrical performance of the array. The "four-parameter" model should be used to for single crystal or polycrystalline PVs. This assumes that the slope of the IV curve at short-circuit conditions is zero. The four-parameter model is enabled whenever zero or a positive value is entered for the slope of the IV curve at the short circuit reference condition. The second PV model, the "five-parameter model" is intended for amorphous or thin-film PVs. This produces a finite negative slope in the IV characteristic at the short-circuit condition. When a negative value is entered for the IV curve slope, the module takes this value to be the short-circuit IV slope and enables the five-

parameter model. PV Sections 1 and 2 of Mathematical Description address the four-parameter model and five-parameter model.

The second option is whether or not the simulation should call the "incidence angle modifier" correlation. This correlation accounts for the increased reflective losses when radiation is incident on the module at large angles. If the specified transmittance-absorptance product ($\tau\alpha$) is a positive value, EnergyPlus and TRNSYS will not call the incidence angle modifier routine. In this case, the specified $\tau\alpha$ value is used for all angles of incidence. The angle modifier correlation is enabled when a negative value is entered for the transmittance-absorptance product ($\tau\alpha$). The magnitude $\tau\alpha$ is then the $\tau\alpha$ product for normal incidence; $\tau\alpha$ for other angles are calculated based on the normal value and an empirical correlation as described in PV Section 4 of the Mathematical Description.

Finally, the user may choose to enter a value for the module series resistance R_s or to call on TYPE 94 to calculate R_s from other manufacturers' data. The EnergyPlus/TRNSYS PV module reads the series resistance directly from the idf whenever a positive value is given. A zero or a negative value indicates that the module should calculate R_s; the magnitude of the specified series resistance is irrelevant in this case.

Mathematical Description

PV Section 1: Four-Parameter Model

The four-parameter equivalent circuit model was developed largely by Townsend [1989] and is detailed by Duffie and Beckman [1991]. The model was first incorporated into a TRNSYS component by Eckstein [1990]. The module employs the Eckstein model for crystalline PV modules, using it whenever the short-circuit IV slope is set to zero or a positive value. The four parameter model assumes that the slope of the IV curve is zero at the short-circuit condition:

$$\left(\frac{dI}{dV}\right)_{v=0} = 0 \tag{1.115}$$

This is a reasonable approximation for crystalline modules. The "four parameters" in the model are $I_{L,ref}$, $I_{o,ref,}$ γ, and R_s. These are empirical values that cannot be determined directly through physical measurement.   The TRNSYS model calculates these values from manufactures' catalog data as discussed in the following section on calculating these parameters

The four-parameter equivalent circuit is shown in the following figure:
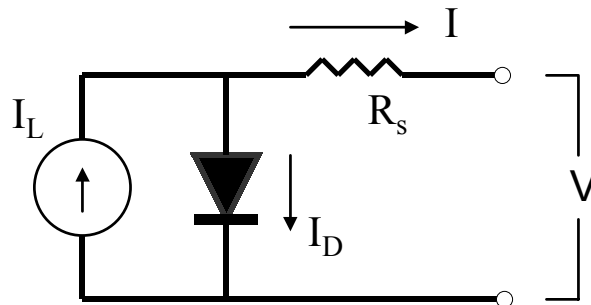
Figure 61. Equivalent circuit in the four parameter model

V is the load voltage and *I* is the current flowing through the load and PV.

Determining Performance under Operating Conditions

The IV characteristics of a PV change with both insolation and temperature. The PV model employs these environmental conditions along with the four module constants $I_{L,ref}$, $I_{o,ref}$, γ, and R_s to generate an IV curve at each timestep.

The current-voltage equation of circuit shown in the previous figure is as follows:

$$I = I_L - I_o \left[\exp\left(\frac{q}{\gamma k T_c}(V + IR_s) \right) - 1 \right]$$

(1.116)

R_s and γ are constants. The photocurrent I_L depends linearly on incident radiation:

$$I_L = I_{L,ref} \frac{G_T}{G_{T,ref}}$$

(1.117)

The reference insolation G_{ref} is nearly always defined as 1000 W/m^2. The diode reverse saturation current I_o is a temperature dependent quantity:

$$\frac{I_o}{I_{o,ref}} = \left(\frac{T_c}{T_{c,ref}} \right)^3$$

(1.118)

Equation (1.116) gives the current implicitly as a function of voltage. Once I_o and I_L are found from Eqs. (1.117)3 and (1.118)4, Newton's method is employed to calculate the PV current. In addition, an iterative search routine finds the current (I_{mp}) and voltage (V_{mp}) at the point of maximum power along the IV curve.

Calculating $I_{L,ref}$, $I_{o,ref}$, γ, and R_s

The Idf specification for the PV model include several values which must be read from manufacturers' PV module catalogs. The manufactures' values are used to determine the equivalent circuit characteristics $I_{L,ref}$, $I_{o,ref}$, γ, and R_s. These characteristics define an equivalent circuit that is employed to find the PV performance at each timestep, as described previously. This section describes the algebra and calculation algorithms used to solve for the four equivalent circuit characteristics.

Three of these values, $I_{L,ref}$, $I_{o,ref}$, γ, may be isolated algebraically. The first step is to substitute the current and voltage into Eq. (1.116) at the open-circuit, short circuit, and maximum power conditions:

$$0 = I_{L,ref} - I_{o,ref} \left[\exp\left(\frac{q}{\gamma k T_{c,ref}} V_{oc,ref} \right) - 1 \right] - \frac{V_{oc,ref}}{R_{sh}}$$

(1.119)

$$I_{sc,ref} = I_{L,ref} - I_{o,ref} \left[\exp\left(\frac{q I_{sc,ref} R_s}{\gamma k T_{c,ref}} \right) - 1 \right] - \frac{I_{sc,ref} R_s}{R_{sh}}$$

(1.120)

$$I_{mp,ref} = I_{L,ref} - I_{o,ref} \left[\exp\left(\frac{q}{\gamma k T_{c,ref}}(V_{mp,ref} + I_{mp,ref} R_s) \right) - 1 \right] - \frac{V_{mp,ref} + I_{mp,ref} R_s}{R_{sh}}$$

(1.121)

In each case the "-1" term is may be dropped to simplify the algebra. This approximation has little influence on the right side of the equations since because the magnitude of I_o is very

small, generally on the order of 10^{-6} A. Some rearrangement then yields the following three expressions which isolate $I_{L,ref}$, $I_{o,ref}$, γ:

$$I_{L,ref} \approx I_{sc,ref} \tag{1.122}$$

$$\gamma = \frac{q\left(V_{mp,ref} - V_{oc,ref} + I_{mp,ref} R_s\right)}{kT_{c,ref}\ln\left(1 - \dfrac{I_{mp,ref}}{I_{sc,ref}}\right)} \tag{1.123}$$

$$I_{o,ref} = \frac{I_{sc,ref}}{\exp\left(\dfrac{qV_{oc,ref}}{\gamma\,kT_{c,ref}}\right)} \tag{1.124}$$

At this point an additional equation is needed in order to determine the last unknown parameter. The fourth equation is derived by taking the analytical derivative of voltage with respect to temperature at the reference open-circuit condition. This analytical value is matched to the open-circuit temperature coefficient, a catalog specification:

$$\frac{\partial V_{oc}}{\partial T_c} = \mu_{voc} = \frac{\gamma k}{q}\left[\ln\left(\frac{I_{sc,ref}}{I_{o,ref}}\right) + \frac{T_c \mu_{isc}}{I_{sc,ref}} - \left(3 + \frac{q\varepsilon}{AkT_{c,ref}}\right)\right] \tag{1.125}$$

where

$$A = \frac{\gamma}{N_s}$$

The TRNSYS PV model uses an iterative search routine in these four equations to calculate the equivalent circuit characteristics. The first step is to set upper and lower bounds for the series resistance parameter R_s: physical constraints require the R_s value to lie between 0 and the value such that $\gamma = N_s$. The initial guess for R_s is midway between these bounds. γ and $I_{o,ref}$ are found from Eq. (1.123) and Eq. (1.124), while Eq. (1.122) gives a trivial solution for $I_{L,ref}$.   The model then employs Eq. (1.125) to compare the analytical and catalog values for μ_{voc}. When all other variables are held constant, the analytical value for μ_{voc} increases monotonically with series resistance [Townsend, 1989]. If the analytical voltage coefficient is less than the catalog value, the lower bound for R_s is reset to the present guess value. Likewise, the upper bound is set to the current value if the calculated μ_{voc} is too large. After resetting the upper or lower bound for R_s, a new guess value is found by averaging the bounds. This procedure repeats until R_s and γ converge. Note that for $I_{L,ref}$, $I_{o,ref}$, γ, and R_s are assumed to be constant and are calculated only on the first call in the simulation. Alternatively, the user may enter a known series resistance by entering a **positive** value in the IDF. In this case the iterative routine described above is skipped and Eqs. (1.122), (1.123), and (1.124) find $I_{L,ref}$, $I_{o,ref}$, and γ directly from the given value of R_s.

PV Section 2 : Five Parameter Model

The four-parameter model described above in the four parameter model section does not adequately describe the current-voltage characteristics of amorphous silicon or thin-film PV modules. There is one major qualitative difference between the IV curves of crystalline and amorphous PVs. The short-circuit slope of the IV curve for crystalline modules is very close

to zero, while slope for amorphous modules is generally finite and negative. The five parameter model is called whenever the short-circuit IV curve slope is set to a negative value. This slope is not generally included in the list of module catalog specifications. However, it may be obtained graphically if the manufacturer provides a module IV curve at reference conditions.

The five parameter adds a shunt resistance R_{sh} to the equivalent circuit used in the four-parameter model. This circuit is illustrated in the following figure.
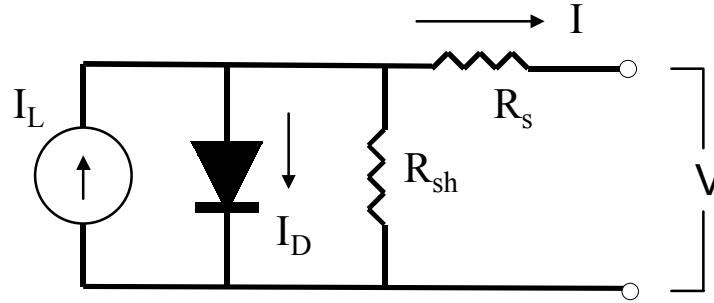
Figure 62. Equivalent circuit in the five-parameter model

The four-parameter model may be considered a special case of the five-parameter model in which R_{sh} is infinite. All the equations employed in the five-parameter model reduce to those described for the four-parameter model as the shunt resistance approaches infinity.

The current-voltage equation for the equivalent circuit in the previous figure is

$$I = I_L - I_o\left[\exp\left(\frac{q}{\gamma kT_c}(V + IR_s)\right) - 1\right] - \frac{V + IR_s}{R_{sh}}$$ (1.126)

The algorithms and behavior of the five-parameter model are discussed in detail by Fry [1999].

Determining Performance Under Operating Conditions

As in the four-parameter model, Eq. (1.127) and Eq. (1.128) define the insolation and temperature dependence of the PV module:

$$I_L = I_{L,ref}\frac{G_{T,ref}}{G_{T,ref}}$$ (1.127)

$$\frac{I_o}{I_{o,ref}} = \left(\frac{T}{T_{ref}}\right)^3$$ (1.128)

However, the five-parameter model uses different equations to find the reference values $I_{o,ref}$ and $I_{L,ref}$. These equations are discussed in the following section.

Calculating $I_{L,ref}$, $I_{o,ref}$, γ, R_{sh}, and R_s

The five-parameter model adds another equivalent circuit characteristic to the four-parameter model: the shunt resistance R_{sh}. The addition of this circuit element changes the equations used to find the other values ($I_{L,ref}$, $I_{o,ref}$, γ, and R_s) from available manufacturers' data.

Fry [1999] has shown that the negative reciprocal of the short-circuit IV slope closely approximates the shunt resistance:

$$R_{sh} \approx \frac{-1}{\left(\dfrac{dI}{dV}\right)_{V=0}} \tag{1.129}$$

This expression reduces the number of unknown quantities to four: $I_{L,ref}$, $I_{o,ref}$, γ, R_s. Rearranging Eq. (1.129) (and neglecting the "-1") at open-circuit, short-circuit, and maximum power conditions yields the following expressions for $I_{L,ref}$, $I_{o,ref}$, γ:

$$I_{L,ref} = I_{sc,ref}\left(1 + \frac{R_s}{R_{sh}}\right) \tag{1.130}$$

$$I_{o,ref} = \frac{I_{L,ref} - \dfrac{V_{oc,ref}}{R_{sh}}}{\exp\left(\dfrac{q}{k\gamma\,T_{c,ref}}V_{oc,ref}\right)} \tag{1.131}$$

$$\gamma = \frac{\left(q\left(V_{mp,ref} - V_{oc,ref} + I_{mp,ref}R_s\right)\right)}{kT_{c,ref}\ln\left(\dfrac{I_{L,ref} - I_{mp,ref} - \dfrac{V_{mp,ref} + I_{mp,ref}R_s}{R_{sh}}}{I_{sc,ref} - \dfrac{V_{oc,ref}}{R_{sh}}}\right)} \tag{1.132}$$

At this point only R_s is needed to solve the system. An iterative search routine is used to find the correct values for R_s and γ by matching the analytical value for μ_{voc} to that given in the catalog. Differentiating Eq. (1.126) with respect to temperature at the open-circuit condition yields:

$$\frac{\partial V_{oc}}{\partial T_c} = \mu_{Voc} = \frac{\mu_{Isc} - \dfrac{I_{o,ref}}{T_c}\left(3 + \dfrac{q\varepsilon}{AkT}\right)\exp\left(\dfrac{q}{k\lambda T_{c,ref}}\right)}{\dfrac{q}{k\lambda T_{c,ref}}I_{o,ref}\exp\left(\dfrac{q}{k\lambda T_{c,ref}}V_{oc,ref}\right) + \dfrac{1}{R_{sh}}} \tag{1.133}$$

The search algorithm is similar to that described above for the four-parameter model.

PV Section 3 : Module Operating Temperature

The TRNSYS model uses temperature data from the standard NOCT (Nominal Operating Cell Temperature) measurements to compute the module temperature T_c at each timestep. The NOCT temperature ($T_{c,NOCT}$) is the operating temperature of the module with a wind speed of 1 m/s, no electrical load, and a certain specified insolation and ambient temperature [Beckman and Duffie, 1991]. The values for insolation $G_{T,NOCT}$ and ambient temperature $T_{a,NOCT}$ are usually 800 W/m^2 and 20° C. TYPE 94 uses the NOCT data to determine the ratio of the module transmittance-reflectance product to the module loss coefficient:

$$\frac{\tau\alpha}{U_L} = \frac{\left(T_{c,NOCT} - T_{a,NOCT}\right)}{G_{T,NOCT}}$$

(1.134)

Assuming that this ratio is constant, the module temperature at any timestep is:

$$T_c = T_a + \frac{\left(1 - \dfrac{\eta_c}{\tau\alpha}\right)}{\left(\dfrac{G_T\tau\alpha}{U_L}\right)}$$

(1.135)

η_c is the convesion efficiency of the module, which varies with ambient conditions. $T_{c,NOCT}$, $T_{a,NOCT}$, and $G_{T,NOCT}$ are set in the IDF. $\tau\alpha$ may be either a constant or the a value calculated from an incidence angle correlation, as described below in PV Section 4.

PV Section 4: Incidence Angle Modifier Correlation

The TRNSYS PV model includes an optional "incidence angle modifier" routine. If this routine is used, an empirical correlation determines the transmittance-reflectance product ($\tau\alpha$) of the module at each timestep. This calculation is based on the module slope, and the angle of incidence and intensity of each radiation component (direct, diffuse, and ground-reflected). The tau-alpha product should be set to a negative value (between 0 and –1) to enable the incidence angle corrleation. In this case, the *magnitude* of pf the tau-alpha prduct equals $\tau\alpha$ at normal incidence. The tau-alpha product is set to a positive value (between 0 and 1) to disable the incidence modifier. If the incidence angle modifier is disabled, the specified $\tau\alpha$ will be used for all angles of incidence. For a given magnitude of tau-alpha, using the incidence angle modifier will always produce more a more conservative (and probably more accurate) estimate of system performance. For most locations, a given PV array will generate about 10% less energy over the course of a year when the incidence angle routine is enabled. $\tau\alpha$ at normal incidence is not usually included in the list of manufacturer's parameters, although 0.9 is usually a good estimate.

Whether or not the modifier is used, the radiation incident on the PV is always multiplied by $\tau\alpha$ to account for reflective losses before Eq. (1.117) is used to determine the photocurrent. The expression for the incidence angle modifier, taken from King et. al [1997] is:

$$IAM = 1 - \left(1.098 x 10^{-4}\right)\theta - \left(6.267 x 10^{-6}\right)\theta^2 + \left(6.583 x 10^{-7}\right)\theta^3 - \left(1.4272 x 10^{-8}\right)\theta^4$$

where

$$IAM \equiv \frac{\tau\alpha}{\tau\alpha_{normal}}$$

(1.136)

Here, θ is the angle of incidence in degrees, with $\theta = 0$ indicating normal incidence. The following figure plots *IAM* as a function of θ.
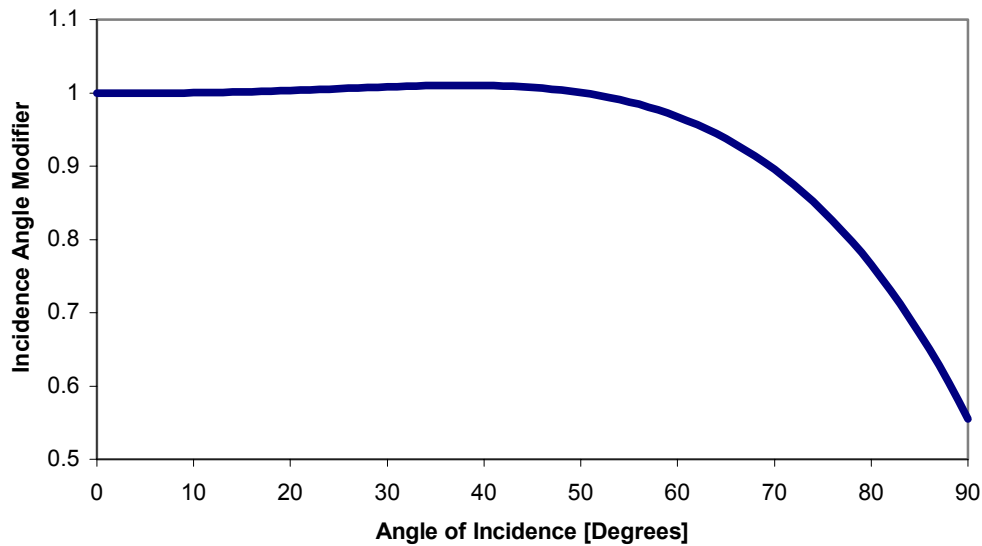
Figure 63. Incidence Angle Modifier of King et al [1997]

PV Section 5 : Multi-Array Modules

The electrical calculations discussed for the four-parameter and five-parameter PV models (**PV Sections 1** and **2**) deal only with a single module. The EnergyPlus/TRNSYS module may be used to simulate arrays with any number of modules. The IDF defines the number of modules in series (NS) and modules in parallel (NP) for the entire array. The total number of modules in the array is the product of NS and NP. When simulating a single module only, both NS and NP are set to 1. The single-module values for all currents and voltages discussed in PV Sections 1 and 2 are multiplied by NP or NS to find values for the entire array. This approach neglects module mismatch losses.

PV Section 6 : Convergence Issues for Various Applications

The EnergyPlys/TRNSYS PV module may be used in direct-coupled systems in which the PV array is connected directly to a load or is linked to a battery to provide daily energy storage. In both of these applications, system performance at each timestep depends on the point of intersection between the IV graphs of the photovoltaic array and the load or battery. Alternatively, the maximum power output of the module may be used in systems employing maximum power point tracking devices. One example of such an application is a grid-tied building-integrated PV system [Fry, 1999].

Many applications employ maximum power point tracking (MPPT) devices which force the PV array to always operate at the point of maximum power along its IV curve. MPPTs are generally included in all grid-interactive inverters. When an MPPT is being used, some arbitrary load voltage must be chosen and specified in the IDF. This voltage should be greater than zero and less than the open-circuit voltage of the array.

PV Section 7 : Inverter

For AC applications, photovoltaic systems include an inverter which converts their output DC to AC. The EnergyPlus TRNSYS PV module reads simple inverter efficiency and capacity values specified in the IDF and applies them to the PV power output, returning the minimum of the capacity or the output power times the inverter efficiency.

References

TRNSYS Reference Manual v. 15.2; Solar Energy Laboratory, University of Wisconsin - Madison, Madison, WI: 2000.

Duffie, John A. and William A. Beckman. *Solar Engineering of Thermal Processes*. New York: John Wiley & Sons, Inc., 1991.

Eckstein, Jürgen Helmut. *Detailed Modeling of Photovoltaic Components*. M. S. Thesis – Solar Energy Laboratory, University of Wisconsin, Madison: 1990.

Fry, Bryan*. Simulation of Grid-Tied Building Integrated Photovoltaic Systems.* M. S. Thesis – Solar Energy Laboratory, University of Wisconsin, Madison: 1999.

King, David L., Jay A. Kratochvil, and William E. Boyson. "Measuring the Solar Spectral and Angle-of-Incidence Effects on Photovoltaic Modules and Irradiance Sensors." *Proceedings of the 1994 IEEE Photovoltaics Specialists Conference*. Sept 30-Oct 3, 1997. pp. 1113-1116.

Townsend, Timothy U. *A Method for Estimating the Long-Term Performance of Direct-Coupled Photovoltaic Systems*. M. S. Thesis – Solar Energy Laboratory, University of Wisconsin, Madison: 1989.

.

Building Thermal Storage

Passive Trombe Wall

A passive Trombe wall is a passive solar wall designed for thermal storage and delivery. It consists of a thick wall (8" to 16") faced with a selective surface solar absorber, air gap, and high transmissivity glass pane. Trombe walls are usually South facing (in the Northern Hemisphere) for maximum sun exposure. An overhang above the wall is used to decrease exposure in the summer when the sun is high in the sky and heating is not required, yet still allows for full exposure in the winter when the sun is low in the sky and heating is desireable.

In EnergyPlus, there is no Trombe wall object per se; rather, it is composed of other existing EnergyPlus objects in the input file. This approach provides flexibility in specifying the various wall parameters and allows for the exploration of additional features such as natural convection ventilation through the Trombe wall, etc. On the other hand, this approach puts more of a burden on the user to be sure that all parts of the Trombe wall are correctly specified, otherwise unexpected results may be obtained.

To simulate the Trombe wall, a very narrow zone is coupled to the desired surface via an interzone partition. The depth of the zone corresponds to the size of the air space (usually ¾" to 6"). In most cases the Trombe zone will be a sealed zone with no ventilation or infiltration. The exterior wall of the Trombe zone contains a single or double-pane window. Optimally, the window covers nearly all of the wall area and has a very high transmissivity to allow the maximum amount of solar flux into the Trombe zone. The interior wall is usually constructed of very thick masonry materials with a solar absorber surface as the innermost layer of the wall. The absorber is a selective surface material with very high absorptivity and very low emissivity, e.g. copper with a special black surface treatment. It is important to make sure the SKY RADIANCE DISTRIBUTION is set to 1 (anisotropic) in the input file so that the majority of the solar flux is directed on the absorber surface and not just on the very small area of the Trombe zone floor. The Zone Inside Convection Algorithm for the Trombe zone should also be set to TrombeWall to correctly model the air space. As is the case for all interzone partitions, the wall construction of the adjoining zone must be the mirror image of the wall construction in the Trombe zone. Finally, an overhang is optionally attached to the Trombe zone to control the amount of seasonal sun exposure. Since all of the Trombe wall parameters are selected by the user in the input file, there is considerable freedom to experiment with different materials, sizes, and configurations.
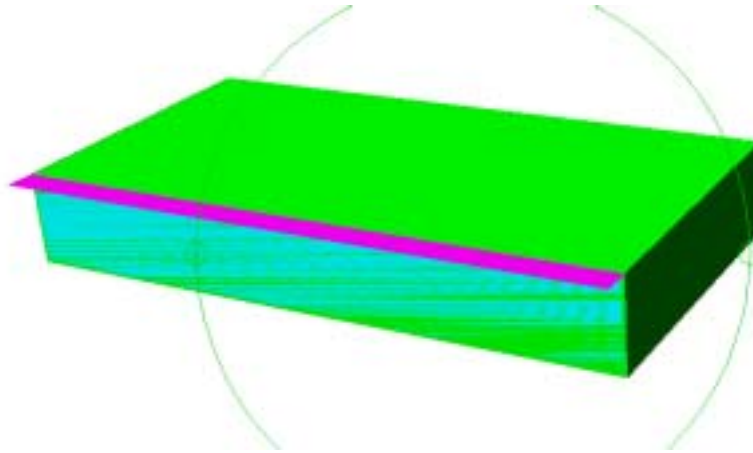
Figure 64. Building with Trombe Wall

Input File

An input file (PassiveTrombeWall.idf) is provided to demonstrate a sample Trombe wall implementation. In this file two separated fictional buildings are simulated for summer and winter design days in Zion, Utah. The buildings are identical in size and construction except that one has a Trombe wall and the other does not. The buildings have uncontrolled zones with no internal loads and heavy insulation. All floors use interzone partitions to disconnect them from the ground. The window on the Trombe zone is a 3 mm, low iron, single pane glazing with very high transmissivity (0.913 visible, 0.899 solar). The absorber surface is a Tabor solar absorber with an emittance of 0.05 and absorptance of 0.85.

Results

The resulting temperature profiles for winter and summer design days are plotted below.
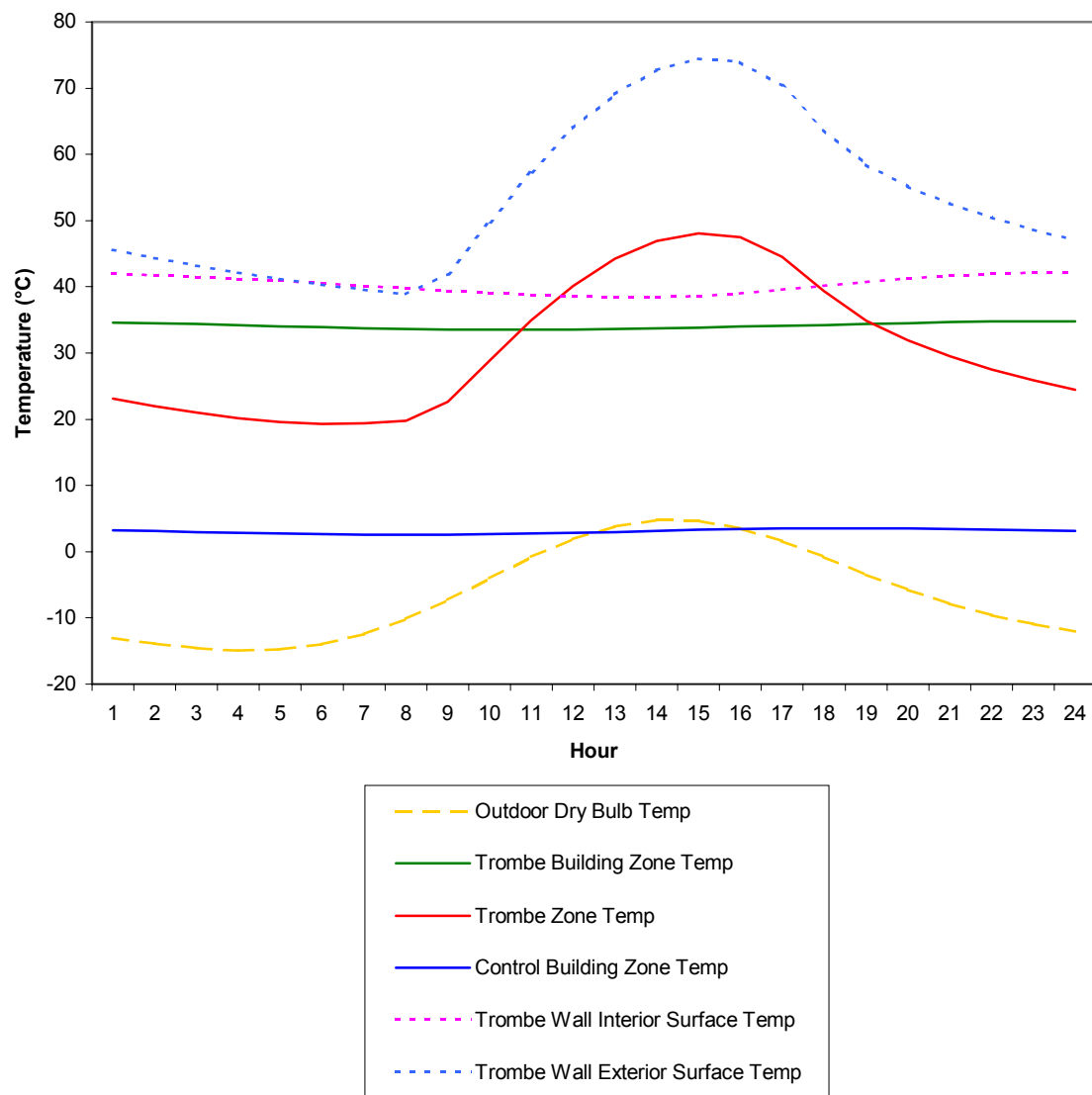
Figure 65. Passive Trombe Wall Winter
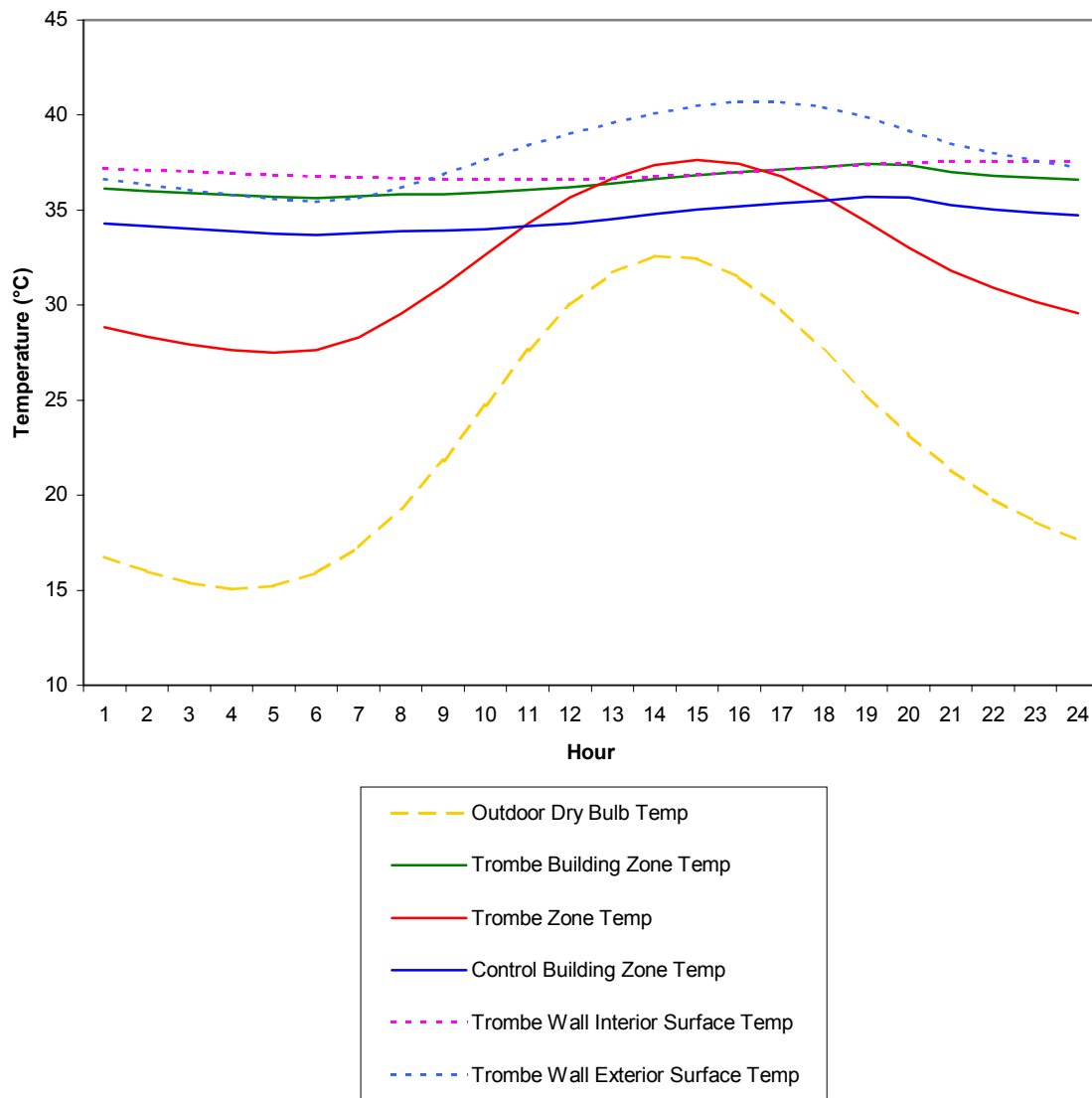
Figure 66. Passive Trombe Wall Summer

Active Trombe Wall

The active Trombe wall is the same as the passive Trombe wall with the addition of a simple fan system to circulate air between the Trombe zone and the main zone. The fan is scheduled to operate only during winter daylight hours to improve the heat transfer from the Trombe zone.

As with the passive Trombe wall, there is no EnergyPlus object for the active Trombe wall; it is simulated using a configuration of other EnergyPlus objects. Like the passive Trombe wall, the active Trombe wall uses a narrow zone coupled to the main zone with interzone partitions. However, the unique part of the active Trombe wall is that the Trombe zone is used to define a zone supply plenum object which allows the Trombe zone to be integrated into the air system. A constant volume fan is the main component of the air system. To make the zone connections, the Direct Air component is used.

Input File

An input file (ActiveTrombeWall.idf) is provided to demonstrate a sample active Trombe wall implementation. The building and Trombe wall in this file are identical to the ones described above for PassiveTrombeWall.idf. However, this input file adds a system in the form of a low flow rate (0.1 m^3/s) constant volume fan and the necessary duct connections. The fan is scheduled to operate October through March from 10 AM to 8 PM.

Results

The resulting temperature profile for the winter design day is plotted below. The plot for the summer design day is not shown because it is identical to Figure 66 above since the fan is not scheduled to operate in the summer.
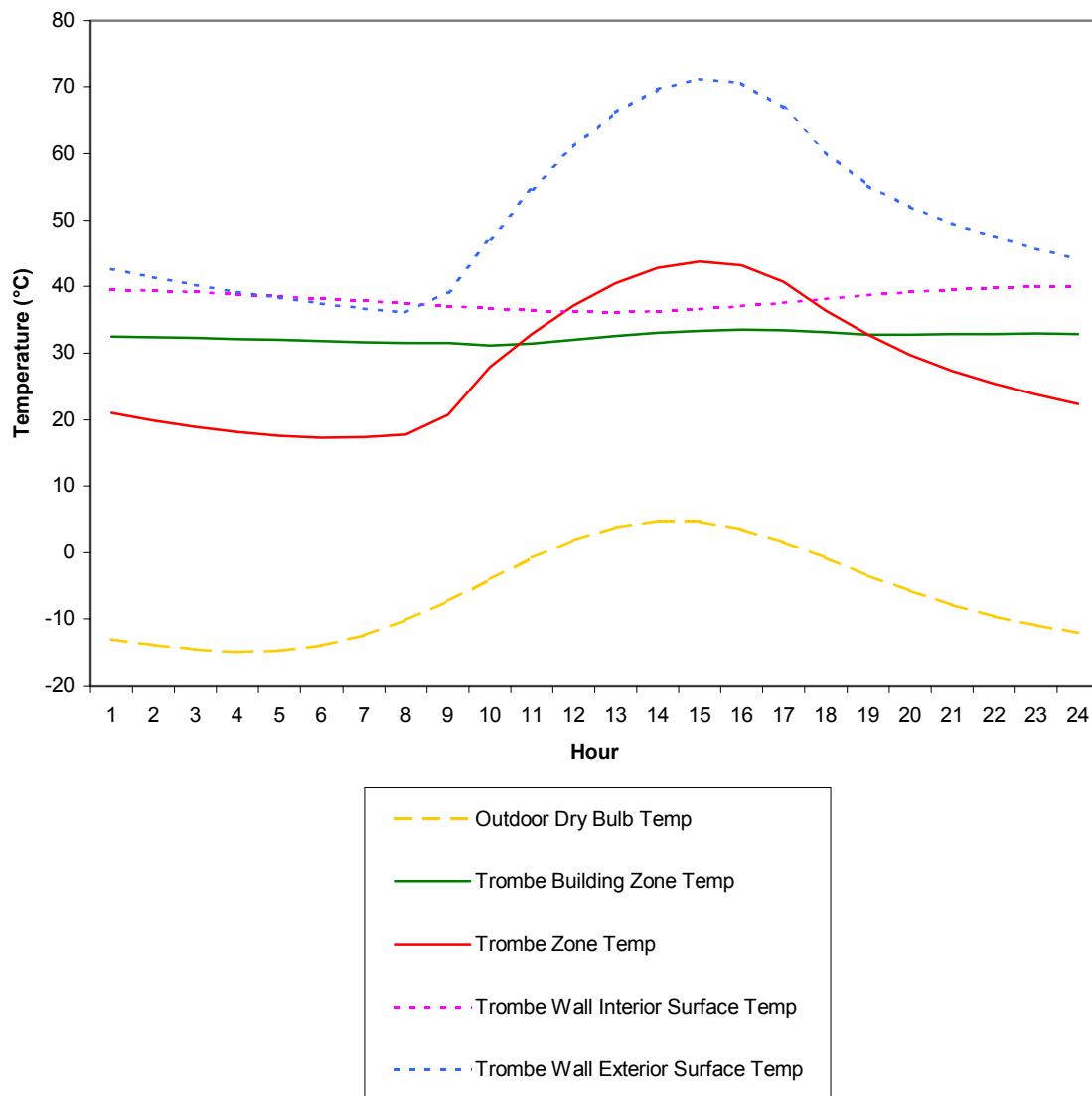
Figure 67. Active Trombe Wall Winter

Simulation Models

The following descriptions are grouped by "Heat Balance", "HVAC", and "Plant". With the integrated solution, these designations signify where the effects of these models have their first impacts.

Heat Balance:Internal Gains

Sources and Types of Gains

Internal heat gains from lights, people, and equipment of various types are often significant elements in the zone thermal balance. EnergyPlus allows the user to specify heat gains for several equipment types including people, lights, gas/electric equipment, and several other types. The total heat gain is comprised of convective, radiant and latent gains in various proportions from these sources. Convective gains are instantaneous additions of heat to the zone air. Radiant gains are distributed on the surfaces of the zone, where they are first absorbed and then released back into the room (with some fraction conducted through the surface) according to the surface heat balances. {See Surface Heat Balance Manager / Processes in this document}. Latent gains must be handled by ventilation or air conditioning equipment. Recommended heat gains are given by ASHRAE [1]. These recommendations include the sensible (convective plus radiative) and latent proportions. Sensible gains from equipment are primarily radiant. The user can specify the heat gains and proportions for any type of equipment. Determining the gains from lights, people and baseboard heat are slightly more complicated.

Heat Gain from Lights

Radiant gains from lights must be handled differently from other radiant gains for reasons described here (long wavelength description). The total radiant gains from lights must be divided into visible and thermal portions. For example, the total electric input to typical incandescent lights is converted to 10% visible radiation, 80% thermal radiation, and 10% convective gain. In contrast, the electric input to typical fluorescent lights is converted to 20% visible radiation, 20% thermal radiation, and 60% convective gain [2]. These percentage splits are under user control with the LIGHTS object.

Heat Gain from People

Heat is generated in the human body by oxidation at a rate called the metabolic rate (see Thermal Comfort discussion for more details). This heat is dissipated from the body surface and respiratory tract by a combination of radiation, convection, and evaporation. The relative proportions of sensible (radiation plus convection) and latent (evaporation) heat from people is a complex function of the metabolic rate and the environmental conditions. EnergyPlus uses a polynomial function to divide the total metabolic heat gain into sensible and latent portions. That function is based on a fit to data [3] at average adjusted metabolic rates of 350, 400, 450, 500, 750, 850, 1000 and 1450 Btu/h each at temperatures of 70, 75, 78, 80, 82 degrees Fahrenheit. Sensible gains of 0 at 96 F and sensible gains equal to the metabolic rate at 30 F were assumed in order to give reasonable values beyond the reported temperature range.

Average adjusted metabolic rate [3] is the metabolic rate to be applied to a mixed group of people with a typical percent composition based on the following factors:

Metabolic rate, adult female=Metabolic rate, adult male X 0.85

Metabolic rate, children = Metabolic rate, adult male X 0.75

The original data was in I-P (Inch-Pound) units, but the following correlation is in SI (Systems-International) units.

$$S = 6.461927 + .946892 \bullet M + .0000255737 \bullet M^2$$
$$+ 7.139322 \bullet T - .0627909 \bullet T \bullet M + .0000589172 \bullet T \bullet M^2$$
$$- .198550 \bullet T^2 + .000940018 \bullet T \bullet M - .00000149532 \bullet T^2 \bullet M^2$$

where
M=Metabolic Rate (W)
T=Air Temperature (C)
S=Sensible Gain (W)
Latent Gain is simply the total gain (metabolic rate) – sensible gain:

$$LatentGain = MetabolicRate - SensibleGain$$
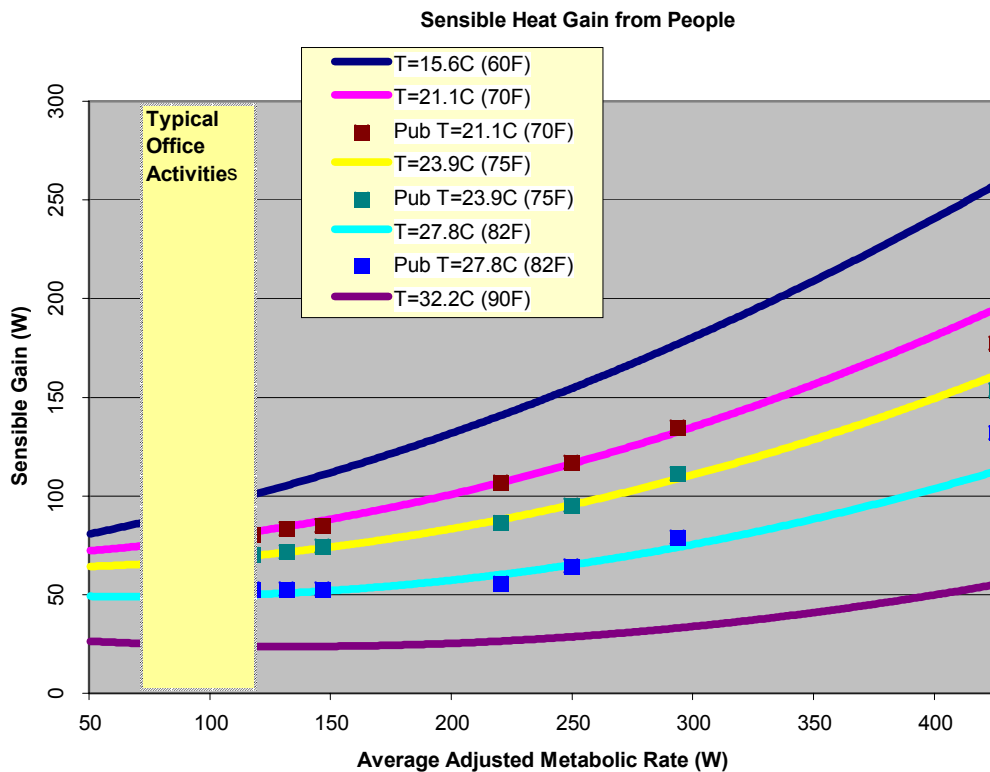
Figure 68. Sensible Heat Gain from People Correlation

The function for sensible gain calculation is compared to the original data points in the following figure. The radiant fraction of the sensible gain is a user input on the PEOPLE object.

Heat Gain from Baseboard Heat

Outdoor temperature controlled baseboard heat adds energy to the zone according a control profile as shown in the following figure. At TA = T2, the baseboard heat gain is Q2. For TA >

T2, there is no heat gain. For TA < T1, a maximum amount of energy, Q1, is added to the zone. There is proportional control between those two temperatures:

**Control of Baseboard Heating
(Outdoor Temperature controlled)**
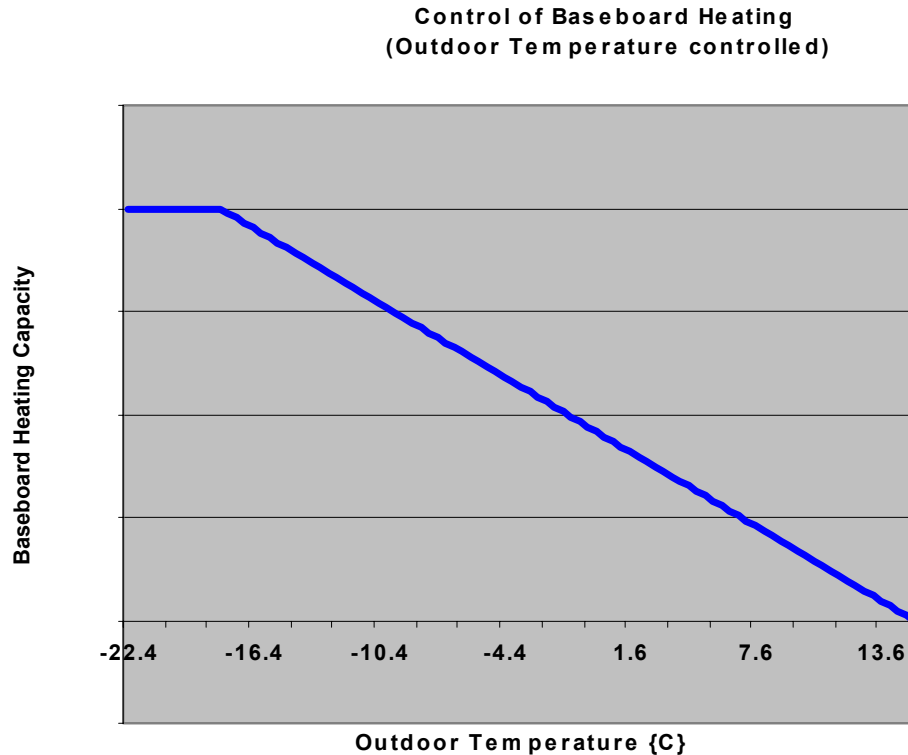
Figure 69. Control of Outdoor Temperature Controlled Baseboard Heat

$$Q = Q2 - \frac{(Q2 - Q1) \cdot (T2 - TA)}{(T2 - T1)}$$

Distribution of Radiant Gains

It is useful to consider the distribution of short wavelength (including visible) radiant energy separate from long wavelength (thermal) radiant energy because many materials have different optical properties at different wavelengths. An extreme example is glass which Is opaque to the long wavelengths and transparent to the short. Properties of materials vary across the entire spectrum of wavelengths. In EnergyPlus, all radiant interactions are represented in terms of only two wavelengths: "short" and "long". Short wavelength refers to the distribution given by a ~6000K black body source such as the sun. Long wavelengths refer to radiation from ~300K sources such as walls or people. There is negligible overlap between these two distributions. Some sources, such as lights, must be considered as emitting both long and short wavelength radiation in proportions that approximate their actual effects on room surfaces.

Long wavelength radiation from all internal sources, such as people, lights and equipment, is combined and then distributed over surfaces according to (see…)

Some fraction of the beam solar radiation transmitted into the zone is directly absorbed by the interior surfaces according to the solar distribution algorithm (see Solar Distribution) selected by the user. The beam radiation not directly absorbed, plus the diffuse sky and ground-reflected radiation, plus the short wavelength radiation from lights are combined and distributed over the surfaces of the zone according to:

$$QSI_i = QS_n \bullet \alpha_i / \sum_{i=1}^{NS} S_i \bullet (1 - \rho_i)$$

If all surfaces in the room are opaque, the radiation is distributed in proportion to the area*absorptance product of each surface. For surfaces which are transparent,

$$\rho_i = 1 - \alpha_i - \tau_i$$

That fraction of radiation represented by τ_i is lost from the zone.

The transmittance and absorptance of transparent surfaces (windows or glass doors) are calculated as in section Window Calculations Module(s) based on the optical properties of the window material layers. The total absorptance of the window is computed for the interior shading device, the inside surface, and the outside surface for diffuse solar radiation incident from outside the zone. Those absorptances are used for short wavelength radiation incident from inside the zone. In most cases, this should not cause significant error. When movable insulation covers the window, the radiation that would have been transmitted is absorbed at the outer surface of the window (thermally equal to the inside surface of the insulation).

References

1. ASHRAE Handbook – 2001 Fundamentals (ASHRAE, 2001), pp 29.8-29.13.
2. Handbook of Air Conditioning System Design (Carrier Air Conditioning Company, McGraw Hill, 1965), pp 1-99 to 1-100.
3. Handbook of Air Conditioning System Design (Carrier Air Conditioning Company, McGraw Hill, 1965), pp 1-100, Table 48.

Heat Balance:Thermal Comfort

The integration of a sophisticated building thermal analysis tool with thermal comfort models will allow us to perform an energy analysis on a zone and simultaneously determine if the environmental control strategy will be sufficient for the occupants to be thermally comfortable. This chapter is intended to provide background on thermal comfort, present an overview of state of the art thermal comfort models and present the mathematical models that have been incorporated into Energy Plus.

Background on Thermal Comfort Models

Nomenclature List of FORTRAN and Mathematical Variable Names

Table 24. General Nomenclature list for Thermal Comfort Models

Mathematical variable	Description	Units	Range	FORTRAN variable
A_{Du}	Dubois body surface area	m^2	-	-
H	Internal heat production rate of an occupant per unit area = M – W	W/m^2	-	IntHeatProd
I_{cl}	Thermal resistance of the clothing	clo	-	CloUnit
M	Metabolic rate per unit area	W/m^2	-	ActLevel

P_a	Water vapor pressure in ambient air	Torr	-	VapPress
T_a	Air temperature	°C	-	AirTemp
T_{cr}	Core or internal temperature	°C	-	CoreTemp
T_r	Mean radiant temperature	°C	-	RadTemp
T_{sk}	Skin temperature	°C	-	-
v	Relative air velocity	m/s	-	AirVel
W	The rate of heat loss due to the performance of work	W/m^2	-	WorkEff
w	Skin wettedness	-	-	-

Throughout the last few decades, researchers have been exploring the thermal, physiological and psychological response of people in their environment in order to develop mathematical models to predict these responses. Researchers have empirically debated building occupants' thermal responses to the combined thermal effect of the personal, environmental and physiological variables that influence the condition of thermal comfort.

There are two personal variables that influence the condition of thermal comfort: the thermal resistance of the clothing (I_{cl}), and the metabolic rate (H/A_{Du}). The thermal resistance of the clothing (I_{cl}) is measured in units of "clo." The 1985 ASHRAE Handbook of Fundamentals (3) suggests multiplying the summation of the individual clothing items clo value by a factor of 0.82 for clothing ensembles.

The metabolic rate (H/A_{Du}), is a measure of the internal heat production rate of an occupant (H) w/hr. in per unit of "Dubois" body surface area (A_{Du}) in units of m^2. The DuBois body surface area is given by :

$$A_{Du} = 0.202(weight)^{0.425}(height)^{0.725} \qquad\qquad (1.137)$$

Using this equation, an area of 1.8 m^2 represents the surface area of an average person of weight 70 kg. and height 1.73 m (7). The metabolic rate is measured in mets, where 1 met = 58.2 W/m^2.

The environmental variables that influence the conditions of thermal comfort include:

    (1) Air Temperature (T_a),

    (2) Mean Radiant Temperature (T_r),

    (3) Relative air velocity (v),

    (4) Water vapor pressure in ambient air (P_a)

The Air Temperature (T_a), a direct environmental index, is the dry-bulb temperature of the environment. The Mean Radiant Temperature (T_r) is a rationally derived environmental index defined as the uniform black-body temperature that would result in the same radiant energy exchange as in the actual environment. The Relative air velocity (v) a direct environmental index is a measure of the air motion obtainable via a hot wire or vane anemometers. The Water vapor pressure in ambient air (P_a) is a direct environmental index.

The physiological variables that influence the conditions of thermal comfort include:

    (1) Skin Temperature (T_{sk}),

    (2) Core or Internal Temperature (T_{cr}),

    (3) Sweat Rate,

    (4) Skin Wettedness (w),

(5) Thermal Conductance (K) between the core and skin.

Where the Skin Temperature (T_{sk}), the Core Temperature (T_{cr}) and the Sweat Rate are physiological indices. The Skin Wettedness (w) is a rationally derived physiological index defined as the ratio of the actual sweating rate to the maximum rate of sweating that would occur if the skin were completely wet.

One more consideration is important in dealing with thermal comfort - the effect of asymmetrical heating or cooling. This could occur when there is a draft or when there is a radiant flux incident on a person (which is what is of primary interest to us here). Fanger (5) noted that the human regulatory system is quite tolerant of asymmetrical radiant flux. A reasonable upper limit on the difference in mean radiant temperature (T_r) from one direction to the opposing direction is 15℃ (1). This limit is lower if there is a high air velocity in the zone.

Mathematical Models for Predicting Thermal Comfort

Many researchers have been exploring ways to predict the thermal sensation of people in their environment based on the personal, environmental and physiological variables that influence thermal comfort. From the research done, some mathematical models that simulate occupants' thermal response to their environment have been developed. Most thermal comfort prediction models use a seven or nine point thermal sensation scale, as in the following tables.

Table 25. Seven point Thermal Sensation Scale

Sensation	Description
3	hot
2	warm
1	slightly warm
0	neutral
-1	slightly cool
-2	cool
-3	cold

Table 26. Nine point Thermal Sensation Scale

Sensation Value	Description
4	very hot
3	hot
2	warm
1	slightly warm
0	neutral
-1	slightly cool
-2	cool
-3	cold
-4	very cold

The most notable models have been developed by P.O. Fanger (the Fanger Comfort Model), the J. B. Pierce Foundation (the Pierce Two-Node Model), and researchers at Kansas State University (the KSU Two-Node Model). Berglund (6) presents a detailed description of the theory behind these three models.

Note for all Thermal Comfort reporting: Though the published values for thermal comfort "vote" have a discrete scale (e.g. –3 to +3 or –4 to +4), the calculations in EnergyPlus are carried out on a continuous scale and, thus, reporting may be "off the scale" with specific conditions encountered in the space. This is not necessarily an error in EnergyPlus – rather a different approach that does not take the "limits" of the discrete scale values into account.

The main similarity of the three models is that all three apply an energy balance to a person and use the energy exchange mechanisms along with experimentally derived physiological parameters to predict the thermal sensation and the physiological response of a person due to their environment. The models differ somewhat in the physiological models that represent the human passive system (heat transfer through and from the body) and the human control system (the neural control of shivering, sweating and skin blood flow). The models also differ in the criteria used to predict thermal sensation.

Fanger comfort Model

Fanger's Comfort model was the first one developed. It was published first in 1967 (7) and then in 1972 (2), and helped set the stage for the other two models. The mathematical model developed by P.O. Fanger is probably the most well known of the three models and is the easiest to use because it has been put in both chart and graph form.

Fanger Model Nomenclature List

Table 27. Nomenclature list for Fanger model

Mathematical variable	Description	Units	Range	FORTRAN variable
A_{Du}	Dubois body surface area	m^2	-	BodySurfaceArea
C_{res}	The rate of dry respiratory heat loss	W/m^2	-	DryRespHeatLoss
E_{dif}	The rate of heat loss from the diffusion of water vapor through the skin	W/m^2	-	EvapHeatLossDiff
E_{res}	The rate of latent respiratory heat loss	W/m^2	-	LatRespHeatLoss
$E_{rsw,req}$	The rate of heat loss from the evaporation of regulatory sweating at the state of comfort	W/m^2	-	EvapHeatLossRegComf
E_{sk}	Total evaporative heat loss from skin	W/m^2		EvapHeatLoss
f_{cl}	The ratio of clothed body	-		CloBodyRat
f_{eff}	The fraction of surface effective for radiation (= 0.72)	-	-	RadSurfEff

H	Internal heat production rate of an occupant per unit area (= M – W)	W/m^2	-	IntHeatProd
h$_c$	Convective heat transfer coefficient	W/m^2°C	-	Hc
L	All the modes of energy loss from body	W/m^2	-	-
M	Metabolic rate per unit area	W/m^2	-	ActLevel
P$_a$	Water vapor pressure in ambient air	Torr	-	VapPress
PMV	Predicted Mean Vote	-	-4~4	PMV
P$_{sk}$	Saturated water vapor pressure at required skin temperature	Torr	-	SatSkinVapPress
Q$_c$	The rate of convective heat loss	W/m^2	-	ConvHeatLoss
Q$_{dry}$	Sensible heat flow from skin	W/m^2		DryHeatLoss
Q$_r$	The rate of radiative heat loss	W/m^2	-	RadHeatLoss
Q$_{res}$	The rate of respiratory heat loss	W/m^2	-	RespHeatLoss
T$_a$	Air temperature	$^\circ$C	-	AirTemp
T$_{cl}$	Clothing surface temperature	$^\circ$C	-	CloSurfTemp
T$_{cla}$	Clothing surface temperature (Absolute)	$^\circ$K	-	AbsCloSurfTemp
T$_{ra}$	Mean radiant temperature	$^\circ$K	-	AbsRadTemp
T$_{skr}$	Skin temperature required to achieve thermal comfort	$^\circ$C		SkinComfTemp
W	The rate of heat loss due to the performance of work	W/m^2	-	WorkEff
ε	The emissivity of clothing-skin surface	-	-	SkinEmiss
σ	The Stefan-Boltzman constant (= 5.67$\times$10^{-8})	W/m^{2}K^4	-	StefanBoltz

Description of the model and algorithm

Fanger developed the model based on the research he performed at Kansas State University and the Technical University of Denmark. Fanger used the seven-point form of a thermal sensation scale along with numerous experiments involving human subjects in various environments. He related the subjects in response to the variables, which influence the condition of thermal comfort. Fanger's model is based upon an energy analysis that takes into account all the modes of energy loss (L) from the body, including: the convection and radiant heat loss from the outer surface of the clothing, the heat loss by water vapor diffusion through the skin, the heat loss by evaporation of sweat from the skin surface, the latent and dry respiration heat loss and the heat transfer from the skin to the outer surface of the clothing. The model assumes that the person is thermally at steady state with his environment.

$$M = L \qquad\qquad\qquad \text{W/m}^2 \quad (1.138)$$

$$L = Q_{res} + Q_{dry} + E_{sk} + W \qquad\qquad\qquad \text{W/m}^2 \quad (1.139)$$

$$Q_{res} = E_{res} + C_{res} = 0.0023M(44 - P_a) + 0.0014M(34 - T_a) \quad \text{W/m}^2 \quad (1.140)$$

LatRespHeatLoss = 0.0023*ActLevel*(44. - VapPress)
DryRespHeatLoss = 0.0014*ActLevel*(34.- AirTemp)
RespHeatLoss = LatRespHeatLoss + DryRespHeatLoss

$$Q_c = h_c \times f_{cl}(T_{cl} - T_a) \qquad\qquad\qquad \text{W/m}^2 \quad (1.141)$$

$$Q_r = f_{eff} f_{cl} \varepsilon \sigma (T_{cla}{}^4 - T_{ra}{}^4) \qquad\qquad\qquad \text{W/m}^2 \quad (1.142)$$

$$Q_{dry} = Q_c + Q_r \qquad\qquad\qquad \text{W/m}^2 \quad (1.143)$$

ConvHeatLos = CloBodyRat*Hc*(CloSurfTemp - AirTemp)
RadHeatLoss = RadSurfEff*CloBodyRat*SkinEmiss*StefanBoltz &
                                *(AbsCloSurfTemp**4 - AbsRadTemp**4)
DryHeatLoss = ConvHeatLoss + RadHeatLoss

$$\text{For } H > 58.2, \ E_{rsw} = 0.42(H - 58.2) \qquad\qquad \text{W/m}^2 \quad (1.144)$$

$$\text{For } H \le 58.2, \ E_{rsw} = 0 \qquad\qquad\qquad \text{W/m}^2 \quad (1.145)$$

$$E_{diff} = 0.68 \times 0.61(P_{sk} - P_a) = 0.4148(P_{sk} - P_a) \qquad \text{W/m}^2 \quad (1.146)$$

$$E_{sk} = E_{rsw} + E_{diff} \qquad\qquad\qquad \text{W/m}^2 \quad (1.147)$$

EvapHeatLossRegComf = 0.42*(IntHeatProd - ActLevelConv)
EvapHeatLossRegComf = 0.0
EvapHeatLossDiff = 0.4148*(SkinComfVpress - VapPress)
EvapHeatLoss = EvapHeatLossRegComf + EvapHeatLossDiff
Where,
0.68 is the passive water vapor diffusion rate, (g/h·m²·Torr)
0.61 is the latent heat of water, (W·h/g)

P_{sk} is the saturated water vapor pressure at the skin temperature required to achieve the thermal comfort

$$P_{sk} = 1.92T_{skr} - 25.3$$ Torr   (1.148)

   SatSkinVapPress = 1.92*SkinTempComf - 25.3

$$T_{skr} = 35.7 - 0.028H$$ °C   (1.149)

   SkinTempComf = 35.7 - 0.028*IntHeatProd

By determining the skin temperature and evaporative sweat rate that a thermally comfortable person would have in a given set of conditions, the model calculates the energy loss (L). Then, using the thermal sensation votes from subjects at KSU and Denmark, a Predicted Mean Vote (PMV) thermal sensation scale is based on how the energy loss (L) deviates from the metabolic rate (M) in the following form:

$$PMV = (0.303e^{-0.036M} + 0.028)(H - L)$$ (1.150)

ThermSensTransCoef = 0.303*EXP(-0.036*ActLevel) + 0.028

PMV = ThermSensTransCoef*(IntHeatProd - EvapHeatLoss - RespHeatLoss - DryHeatLoss)

Pierce Two-Node Model

The Pierce Two-Node model was developed at the John B. Pierce Foundation at Yale University. The model has been continually expanding since its first publication in 1970 (8). The most recent version on the model appears in the 1986 ASHRAE Transactions (9).

Pierce Two-Node Model Nomenclature List

Table 28. Nomenclature list for Pierce Two-Node model

Mathematical variable	Description	Units	Range	FORTRAN variable
C_{dil}	Constant for skin blood flow			SkinBloodFlowConst
C_{res}	The rate of dry respiratory heat loss	W/m^2	-	DryRespHeatLoss
C_{sw}	Proportionality constant for sweat control	g/m^{2}hr		SweatContConst
DISC	Predicted discomfort vote	-	-5~5	DISC
E_{dif}	The rate of heat loss from the diffusion of water vapor through the skin	W/m^2	-	EvapHeatLossDiff
E_{max}	Maximum evaporative heat loss	W/m^2		EvapHeatLossMax
E_{sk}	Total evaporative heat loss from skin	W/m^2		EvapHeatLoss
E_{res}	The rate of latent respiratory heat loss	W/m^2	-	LatRespHeatLoss

E_{rsw}	The rate of heat loss from the evaporation of regulatory sweating	W/m^2	-	EvapHeatLossRegSweat
$E_{rsw,req}$	The rate of heat loss from the evaporation of regulatory sweating at the state of comfort	W/m^2		EvapHeatLossRegComf
ET*	Effective Temperature	$^{\circ}C$	-	ET
f_{cl}	The ratio of clothed body	-		CloBodyRat
f_{eff}	The fraction of surface effective for radiation (= 0.72)	-	-	RadSurfEff
H	Internal heat production rate of an occupant per unit area (= M – W)	W/m^2	-	IntHeatProd
h	Combined heat transfer coefficient	$W/m^{2\circ}C$		H
h_c	Convective heat transfer coefficient	$W/m^{2\circ}C$	-	Hc
h_e'	Combined evaporative heat transfer coefficient	$W/(m^2kPa)$		-
h_r	Radiant heat transfer coefficient	$W/m^{2\circ}C$	-	Hr
I_{cl}	Clothing insulation	$m^{2\circ}C/W$		-
L	All the modes of energy loss from body	W/m^2	-	-
L_{ET*}	All the modes of energy loss from body at ET*	W/m^2		-
L_{SET*}	All the modes of energy loss from body at SET*	W/m^2		-
M	Metabolic rate per unit area	W/m^2	-	ActLevel
M_{act}	Metabolic heat production due to activity	W/m^2		-
M_{shiv}	Metabolic heat production due to shivering	W/m^2		ShivResponse
P_a	Water vapor pressure in ambient air	Torr	-	VapPress
PMV*	Predicted Mean Vote modified by ET* or SET*	-	-4~4	PMVET PMVSET
P_{SET*}	Water vapor pressure at SET*	$^{\circ}C$		StdVapPressSET

P_{sk}	Saturated water vapor pressure at required skin temperature	Torr	-	SatSkinVapPress
Q_c	The rate of convective heat loss	W/m^2	-	ConvHeatLoss
Q_{crsk}	Heat flow from core to skin	W/m^2		HeatFlow
Q_{dry}	Sensible heat flow from skin	W/m^2		DryHeatLoss
Q_r	The rate of radiative heat loss	W/m^2	-	RadHeatLoss
Q_{res}	The rate of respiratory heat loss	W/m^2	-	RespHeatLoss
S_{cr}	Heat storage in core compartment	W/m^2		CoreheatStorage
SET*	Standard Effective Temperature	°C	-	SET
SIG_b	Thermal signal of body	°C		BodyThermSigCold BodyThermSigWarm
SIG_{cr}	Thermal signal of core	°C		CoreThermSigCold CoreThermSigWarm
SIG_{sk}	Thermal signal of skin	°C		SkinThermSigCold SkinThermSigWarm
SKBF	Skin blood flow	L/m^{2}hr		SkinBloodFlow
S_{sk}	Heat storage in skin compartment	W/m^2		SkinHeatStorage
S_{tr}	Constriction constant of skin blood flow for average person			Str
SW_{reg}	The rate of regulatory sweating	g/m^{2}hr		RegSweat
T_a	Air temperature	°C	-	AirTemp
T_b	Mean body temperature			AvgBodyTemp
T_{b-c}	Mean body temperature when DISC is zero (lower limit)	°C		AvgBodyTempLow
T_{b-h}	Mean body temperature when HSI is 100 (upper limit)	°C		AvgBodyTempHigh
T_{cl}	Clothing surface temperature	°C	-	CloSurfTemp
T_{cr}	Core or internal temperature	°C	-	CoreTemp
T_r	Mean radiant temperature	°C	-	RadTemp

TSENS	Thermal sensation vote	-	-5~5	TSENS
T_{sk}	Skin temperature	$^\circ$C		SkinTemp
W	The rate of heat loss due to the performance of work	W/m^2	-	WorkEff
w_{dif}	Skin wettedness due to diffusion trough the skin			SkinWetDiff
w_{rsw}	Skin wettedness due to regulatory sweating			SkinWetSweat
ε	The emissivity of clothing-skin surface	-	-	SkinEmiss
σ	The Stefan-Boltzman constant (= 5.67$\times$10^{-8})	W/m^{2}K^4	-	StefanBoltz

Description of the model and algorithm

The Pierce model thermally lumps the human body as two isothermal, concentric compartments, one representing the internal section or core (where all the metabolic heat is assumed to be generated and the skin comprising the other compartment). This allows the passive heat conduction from the core compartment to the skin to be accounted for. The boundary line between two compartments changes with respect to skin blood flow rate per unit skin surface area (SKBF in L/h•m^2) and is described by alpha – the fraction of total body mass attributed to the skin compartment (13).

$$\alpha = 0.0417737 + 0.7451832/(SKBF + 0.585417) \qquad (1.151)$$

SkinMassRat = 0.0417737 + 0.7451832/(SkinBloodFlow + 0.585417)

Furthermore, the model takes into account the deviations of the core, skin, and mean body temperature weighted by alpha from their respective set points. Thermoregulatory effector mechanisms (Regulatory sweating, skin blood flow, and shivering) are defined in terms of thermal signals from the core, skin and body (13).

$$SIG_{cr} = T_{cr} - 36.8 \qquad\qquad ^\circ\text{C} \qquad (1.152)$$

$$SIG_{sk} = T_{sk} - 33.7 \qquad\qquad ^\circ\text{C} \qquad (1.153)$$

$$SIG_{b} = T_{b} - 36.49 \qquad\qquad ^\circ\text{C} \qquad (1.154)$$

SkinThermSigWarm = SkinTemp - SkinTempSet
SkinThermSigCold = SkinTempSet - SkinTemp
CoreThermSigWarm = CoreTemp - CoreTempSet
CoreThermSigCold = CoreTempSet - CoreTemp
BodyThermSigWarm = AvgBodyTemp - AvgBodyTempSet
BodyThermSigCold = AvgBodyTempSet-AvgBodyTemp

$$SKBF = (6.3 + C_{dil} \times SIG_{cr})/(1 + S_{tr} \times (-SIG_{sk})) \qquad \text{L/hr•m}^2 \quad (1.155)$$

VasodilationFac = SkinBloodFlowConst*CoreWarmDelTemp
VasoconstrictFac = Str*SkinColdDelTemp
SkinBloodFlow = (6.3 + VasodilationFac)/(1. + VasoconstrictFac)

$$SW_{reg} = C_{sw}SIG_b e^{(SIG_{sk}/10.7)}$$ g/hr•m^2 (1.156)

RegSweat = SweatContConst*BodyWarmDelTemp*EXP(SkinWarmDelTemp/10.7)

$$M_{shiv} = 19.4(-SIG_{cr})(-SIG_{sk})$$ W/m^2 (1.157)

ShivResponse = 19.4*SkinThermSigCold*CoreThermSigCold

The latest version of the Pierce model (15) discusses the concepts of SET* and ET*. The Pierce model converts the actual environment into a "standard environment" at a Standard Effective Temperature, SET*. SET* is the dry-bulb temperature of a hypothetical environment at 50% relative humidity for subjects wearing clothing that would be standard for the given activity in the real environment. Furthermore, in this standard environment, the same physiological strain, i.e. the same skin temperature and skin wettedness and heat loss to the environment, would exist as in the real environment. The Pierce model also converts the actual environment into a environment at an Effective Temperature, ET*, that is the dry-bulb temperature of a hypothetical environment at 50% relative humidity and uniform temperature (Ta = MRT) where the subjects would experience the same physiological strain as in the real environment.

In the latest version of the model it is suggested that the classical Fanged PMV be modified by using ET* or SET* instead of the operative temperature. This gives a new index PMV* which is proposed for dry or humid environments. It is also suggested that PMV* is very responsive to the changes in vapor permeation efficiency of the occupants clothing.

$$M = M_{act} + M_{shiv}$$ W/m^2 (1.158)

ActLevel = ActLevel + ActShiv

$$L = Q_{res} + Q_{dry} + E_{sk} + W$$ W/m^2 (1.159)

$$Q_{res} = E_{res} + C_{res} = 0.0023M(44 - P_{a(torr)}) + 0.0014M(34 - T_a)$$
$$= 0.017251M(5.8662 - P_{a(kPa)}) + 0.0014M(34 - T_a)$$ W/m^2 (1.160)

LatRespHeatLoss = 0.017251*ActLevel*(5.8662 - VapPress)
DryRespHeatLoss = 0.0014*ActLevel*(34.- AirTemp)
RespHeatLoss = LatRespHeatLoss + DryRespHeatLoss

$$Q_c = h_c \times f_{cl}(T_{cl} - T_a)$$ W/m^2 (1.161)

$$Q_r = h_r \times f_{cl}(T_{cl} - T_r)$$ W/m^2 (1.162)

$$Q_{dry} = Q_c + Q_r$$ W/m^2 (1.163)

DryHeatLoss = CloBodyRat*(Hc*(CloSurfTemp - AirTemp) + Hr*(CloSurfTemp - RadTemp))

In Pierce model, the convective heat transfer coefficient, h_c, varies with the air velocity around body and metabolic rate. The model uses the maximum value of following equations.

$$h_c = 8.6 \times v^{0.53}$$ W/m^2°C (1.164)

$$h_c = 5.66(M/58.2 - 0.85)^{0.39}$$ W/m^2°C (1.165)

Hc = 8.6*AirVel**0.53

HcAct = 5.66*(ActMet - 0.85)**0.39

Also, in the model, the radiant heat transfer coefficient, h_r, is defined by following equation (13):

$$h_r = 4. \times f_{eff} \varepsilon \sigma \left((T_{cl} + T_r)/2 + 273.15 \right)^3 \qquad \text{W/m}^2 \text{°C} \quad (1.166)$$

Hr = 4.*RadSurfEff*StefanBoltz*((CloSurfTemp + RadTemp)/2. + TAbsConv)**3

In the Pierce model, T_{cl} is estimated by each iteration using following equation:

$$T_{cl} = (T_{sk}/I_{cl} + f_{cl}(h_c T_a - h_r T_r))/(1/I_{cl} + f_{cl}(h_c + h_r)) \qquad \text{°C} \qquad (1.167)$$

CloSurfTemp = (CloCond*SkinTemp + CloBodyRat*(Hc*AirTemp &
                        + Hr*RadTemp))/(CloCond + CloBodyRat*(Hc + Hr))

Total evaporative heat loss from the skin, E_{sk}, includes evaporation of water produced by regulatory sweating, E_{rsw}, and evaporation of water vapor that diffuses through the skin surface, E_{diff}.

$$E_{sk} = E_{rsw} + E_{diff} \qquad \text{W/m}^2 \qquad (1.168)$$

EvapHeatLoss = EvapHeatLossRegSweat + EvapHeatLossRegDiff

$$E_{rsw} = 0.68 \times SW_{reg} \qquad \text{W/m}^2 \qquad (1.169)$$

$$E_{diff} = w_{diff} \times E_{max} \qquad \text{W/m}^2 \qquad (1.170)$$

RegHeatLoss = 0.68*RegSweat
DiffHeatLoss = SkinWetDiff*MaxEvapHeatLoss
Where,
0.68 is the passive water vapor diffusion rate in g/h·m^2·Torr
and,

$$w_{diff} = 0.06(1 - w_{rsw}) \qquad (1.171)$$

$$E_{max} = h_e'(P_{sk} - P_a) \qquad \text{W/m}^2 \qquad (1.172)$$

$$w_{rsw} = E_{rsw}/E_{max} \qquad (1.173)$$

SkinWetDiff = (1.-SkinWetSweat)*.06
MaxEvapHeatLoss = (1./TotEvapHeatResist)*(SatSkinVapPress - VapPress)
SkinWetSweat = EvapHeatLossRegSweat/MaxEvapHeatLoss

The Pierce model has one additional heat flow term describing the heat transfer between the internal core compartment and the outer skin shell (13).

$$Q_{crsk} = (5.28 + 1.163 SKBF)(T_{cr} - T_{sk}) \qquad \text{W/m}^2 \qquad (1.174)$$

HeatFlow = (CoreTemp-SkinTemp)*(5.28 + 1.163*SkinBloodFlow)
Where
5.28 is the average body tissue conductance in W/m^2•°C
1.163 is the thermal capacity of blood in W•h/L•°C

Thus, individual heat balance equations for core and skin compartments are expressed using this term, Q_{c-s}. New temperatures of core, skin and body are calculated by each iteration from rates of heat storage in the core and skin.

$$S_{sk} = Q_{c-s} - Q_c - Q_r - E_{sk} \qquad \text{W/m}^2\text{°C} \quad (1.175)$$

SkinHeatStorage = HeatFlow - DryHeatLoss - EvapHeatLoss

$$S_{cr} = M - W - Q_{res} - Q_{c-s} \qquad \text{W/m}^2\text{°C} \quad (1.176)$$

CoreHeatStorage = IntHeatProd - RespHeatLoss - HeatFlow

Thus,

$$PMVET = (0.303e^{-0.036M} + 0.028)(H - L_{ET*}) \qquad (1.177)$$

$$PMVSET = (0.303e^{-0.036M} + 0.028)(H - L_{SET*}) \qquad (1.178)$$

ThermSensTransCoef = 0.303*EXP(-0.036*ActLevel) + 0.028
PMVET = ThermSensTransCoef*(IntHeatProd - EvapHeatLossDiff &
   - EvapHeatLossRegComf - RespHeatLoss - DryHeatLossET)
PMVSET = ThermSensTransCoef*(IntHeatProd - EvapHeatLossDiff &
   - EvapRegHeatLossReg Comf - RespHeatLoss - DryHeatLossSET)

Besides PMV*, the Pierce Two Node Model uses the indices TSENS and DISC as predictors of thermal comfort. Where TSENS is the classical index used by the Pierce foundation, and is a function of the mean body temperature. DISC is defined as the relative thermoregulatory strain that is needed to bring about a state of comfort and thermal equilibrium. DISC is a function of the heat stress and heat strain in hot environments and equal to TSENS in cold environments. In summary, the Pierce Model, for our purposes, uses four thermal comfort indices; PMVET-a function of ET*, PMVSET- a function of SET*, TSENS and DISC.

$$T_{b-c} = (0.185/58.2)(M - W) + 36.313 \qquad \text{°C} \qquad (1.179)$$

$$T_{b-h} = (0.359/58.2)(M - W) + 36.664 \qquad \text{°C} \qquad (1.180)$$

$$TSENS_c = 0.68175(T_b - T_{b-c}) \qquad\qquad T_b \leq T_{b-c} \quad (1.181)$$

$$TSENS_h = 4.7(T_b - T_{b-c})/(T_{b-h} - T_{b-c}) \qquad T_b > T_{b-c} \quad (1.182)$$

$$DISC = 5.(E_{rsw} - E_{rsw-comf})/(E_{max} - E_{rsw-comf} - E_{diff}) \qquad (1.183)$$

AvgBodyTempLow = (0.185/ActLevelConv)*IntHeatProd + 36.313
AvgBodyTempHigh = (0.359/ActLevelConv)*IntHeatProd + 36.664
TSENS = .68175*(AvgBodyTemp-AvgBodyTempLow)
TSENS = 4.7*(AvgBodyTemp - AvgBodyTempLow)/ &
     (AvgBodyTempHigh - AvgBodyTempLow)
DISC = 5.*(EvapHeatLossRegSweat - EvapHeatLossRegComf)/ &
     (MaxEvapHeatLoss - EvapHeatLossRegComf - DiffHeatLoss)

KSU Two-Node Model

The KSU two-node model, developed at Kansas State University, was published in 1977 (10). The KSU model is quite similar to that of the Pierce Foundation. The main difference between the two models is that the KSU model predicts thermal sensation (TSV) differently for warm and cold environment.

KSU Two Node Model Nomenclature List

Table 29. Nomenclature list for KSU Two-Node model

Mathematical variable	Description	Units	Range	FORTRAN variable
C_{cr}	Specific heat of body core	Whr/kg$^\circ$C		
C_{sk}	Specific heat of skin	Whr/kg$^\circ$C		
C_{res}	The rate of dry respiratory heat loss	W/m^2	-	DryRespHeatLoss
E_{dif}	The rate of heat loss from the diffusion of water vapor through the skin	W/m^2	-	EvapHeatLossDiff
E_{max}	Maximum evaporative heat loss	W/m^2		EvapHeatLossMax
E_{sk}	Total evaporative heat loss from skin	W/m^2		EvapHeatLoss
E_{sw}	Equivalent evaporation heat loss from the sweat secreted	W/m^2		EvapHeatLossSweat
$E_{sw.d}$	Sweat function for warm and dry skin	W/m^2		DrySweatRate
E_{res}	The rate of latent respiratory heat loss	W/m^2	-	LatRespHeatLoss
F_{cl}	The Burton thermal efficiency factor for clothing		-	CloThermEff
F_{pcl}	Permeation efficiency factor for clothing		-	CloPermeatEff
H	Internal heat production rate of an occupant per unit area = M - W	W/m^2	-	IntHeatProd
H	Combined heat transfer coefficient	W/m$^{2\circ}$C		H

h_c	Convective heat transfer coefficient	W/m^2°C	-	Hc
h_r	Radiant heat transfer coefficient	W/m^2°C	-	Hr
KS	Overall skin thermal conductance	W/m^2°C		ThermCndct
KS_o	Skin conductance at thermal neutrality	W/m^2°C		ThermCndctNeut
$KS_{(-4)}$	Skin conductance at thermal sensation very cold	W/m^2°C		ThermCndctMin
M	Metabolic rate per unit area	W/m^2	-	ActLevel
M_{shiv}	Metabolic heat production due to shivering	W/m^2		ShivResponse
P_a	Water vapor pressure in ambient air	Torr	-	VapPress
P_{sk}	Saturated water vapor pressure at required skin temperature	Torr	-	SatSkinVapPress
PT_{accl}	The pattern of acclimation			AcclPattern
Q_c	The rate of convective heat loss	W/m^2	-	ConvHeatLoss
Q_{dry}	Sensible heat flow from skin	W/m^2		DryHeatLoss
Q_r	The rate of radiative heat loss	W/m^2	-	RadHeatLoss
Q_{res}	The rate of respiratory heat loss	W/m^2	-	RespHeatLoss
RH	Relative humidity			RelHum
T_a	Air temperature	°C	-	AirTemp
T_{cr}	Core or internal temperature	°C	-	CoreTemp
T_o	Operative temperature	°C	-	OpTemp
T_r	Mean radiant temperature	°C	-	RadTemp
T_{sk}	Skin temperature	°C		SkinTemp
TSV	Thermal sensation vote		-4~4	TSV
V	Relative air velocity	m/s	-	AirVel

W	The rate of heat loss due to the performance of work	W/m^2	-	WorkEff
W	Skin wettedness	-	-	SkinWet
W$_{cr}$	Mass of body core per unit body surface	kg/m^2		-
w$_{rsw}$	Skin wettedness due to regulatory sweating			SkinWetSweat
w$_{rsw-o}$	Skin wettedness at thermal neutrality			SkinWetSweatNeut
W$_{sk}$	Mass of skin per unit body surface	kg/m^2		-

Description of the model and algorithm

The KSU two-node model is based on the changes that occur in the thermal conductance between the core and the skin temperature in cold environments, and in warm environments it is based on changes in the skin wettedness.

In this model metabolic heat production is generated in the core which exchanges energy with the environment by respiration and the skin exchanges energy by convection and radiation. In addition, body heat is dissipated through evaporation of sweat and/or water vapor diffusion through the skin. These principles are used in following passive system equations.

$$W_{cr}C_{cr}dT_{cr}/dt = M - W - Q_{res} - KS(T_{cr} - T_{sk}) \qquad \text{W/m}^2 \quad (1.184)$$

$$W_{sk}C_{sk}dT_{sk}/dt = KS(T_{cr} - T_{sk}) - Q_{dry} - E_{sk} \qquad \text{W/m}^2 \quad (1.185)$$

Where

$$Q_{res} = E_{res} + C_{res} = 0.0023M(44 - P_{a(torr)}) + 0.0014M(34 - T_a) \qquad \text{W/m}^2$$
$$(1.186)$$

LatRespHeatLoss = 0.0023*ActLevelTot*(44. - VapPress)
DryRespHeatLoss = 0.0014*ActLevelTot*(34. - AirTemp)
RespHeatLoss = LatRespHeatLoss + DryRespHeatLoss

$$Q_{dry} = Q_c + Q_r = h\ f_{cl}F_{cl}(T_{sk} - T_o) \qquad \text{W/m}^2 \quad (1.187)$$

DryHeatLoss = H*CloBodyRat*CloThermEff*(SkinTemp - OpTemp)

$$h = h_c + h_r \qquad\qquad\qquad \text{W/m}^{2}°\text{C} \ (1.188)$$

$$h_c = 8.3\sqrt{v} \qquad\qquad\qquad \text{W/m}^{2}°\text{C} \ (1.189)$$

$$h_r = 3.87 + 0.031T_r \qquad\qquad\qquad \text{W/m}^{2}°\text{C} \ (1.190)$$

H = Hc + Hr
Hc = 8.3*SQRT(AirVel)

Hr = 3.87 + 0.031*RadTemp

$$T_o = (h_c T_a + h_r T_r)/(h_c + h_r) \qquad\qquad °C \qquad (1.191)$$

OpTemp = (Hc*AirTemp + Hr*RadTemp)/H

and

For $E_{sw} \le E_{max}$, $E_{sk} = E_{sw} + (1 - w_{rsw})E_{diff}$ $\qquad$ W/m^2 $\quad$ (1.192)

For $E_{sw} > E_{max}$, $E_{sk} = E_{max}$ $\qquad\qquad$ W/m^2 $\quad$ (1.193)

$$E_{diff} = 0.408(P_{sk} - P_a) \qquad\qquad W/m^2 \quad (1.194)$$

$$E_{max} = 2.2 h_c F_{pcl}(P_{sk} - P_a) \qquad\qquad W/m^2 \quad (1.195)$$

EvapHeatLoss   =   SkinWetSweat*EvapHeatLossMax+(1.   -
SkinWetSweat)*EvapHeatLossDiff

SkinWetSweat = EvapHeatLossDrySweat/EvapHeatLossMax

EvapHeatLossDiff = 0.408*(SkinVapPress - VapPress)

EvapHeatLossMax = 2.2*Hc*(SkinVapPress - VapPress)*CloPermeatEff

Here, control signals, based on set point temperatures in the skin and core, are introduced into passive system equations and these equations are integrated numerically for small time increments or small increments in core and skin temperature. The control signals modulate the thermoregulatory mechanism and regulate the peripheral blood flow, the sweat rate, and the increase of metabolic heat by active muscle shivering. The development of the controlling functions of skin conductance (KS), sweat rate (E_{sw}), and shivering (M_{shiv}) is based on their correlation with the deviations in skin and core temperatures from their set points.

$$KS = 5.3 + [6.75 + 42.45(T_{cr} - 36.98) + 8.15(T_{cr} - 35.15)^{0.8}(T_{sk} - 33.8)]$$
$$/[1.0 + 0.4(32.1 - T_{sk})] \qquad (1.196)$$

SkinCndctDilation = 42.45*CoreSignalWarmMax &

$\qquad$ + 8.15*CoreSignalSkinSens**0.8*SkinSignalWarmMax

SkinCndctConstriction = 1.0 + 0.4*SkinSignalColdMax

ThermCndct = 5.3+(6.75+SkinCndctDilation)/SkinCndctConstriction

$$E_{sw} = \phi \times [260(T_{cr} - 36.9) + 26(T_{sk} - 33.8)]\exp[(T_{sk} - 33.8)/8.5]$$
$$/[1.0 + 0.05(33.37 - T_{sk})^{2.4}] \qquad (1.197)$$

WeighFac = 260.+70.*AcclPattern

SweatCtrlFac = 1. + 0.05*SkinSignalSweatColdMax**2.4

DrySweatRate = ((WeighFac*CoreSignalSweatMax &

$\qquad$ + 0.1*WeighFac*SkinSignalSweatMax) &

$\qquad$ *EXP(SkinSignalSweatMax/8.5))/SweatCtrlFac

Where

$$\phi = 1.0 \qquad\qquad\qquad w \le 0.4 \quad (1.198)$$

$$\phi = 0.5 + 0.5\exp[-5.6(w-0.4)] \qquad\qquad w > 0.4 \ (1.199)$$

SweatSuppFac = 1.

SweatSuppFac = 0.5 + 0.5*EXP(-5.6*SkinWetSignal)

$$M_{shiv} = 20(36.9 - T_{cr})(32.5 - T_{sk}) + 5(32.5 - T_{sk}) \qquad \text{W/m}^2 \quad (1.200)$$

ShivResponse = 20.*CoreSignalShivMax*SkinSignalShivMax + 5.*SkinSignalShivMax

In KSU model, two new parameters are introduced and used in correlating thermal sensations with their associated physiological responses. In stead of correlating warm thermal sensations with skin wettedness, it is here correlated with a wettedness factor defined by

$$\varepsilon_{wsw} = (w_{rsw} - w_{rsw-o})/(1.0 - w_{rsw-o}) \qquad\qquad (1.201)$$

SkinWetFac = (SkinWetSweat - SkinWetNeut)/(1. - SkinWetNeut)

Where

$$w_{wsw} = E_{sw}/E_{max}$$

$$w_{wsw-o} = 0.2 + 0.4\{1.0 - \exp[-0.6(H/58.2-1.0)]\}$$

SkinWetSweat = DrySweatRate/EvapHeatLossMax

SkinWetNeut = 0.02 + 0.4*(1.-EXP(-0.6*(IntHeatProdMetMax - 1.)))

and instead of correlating cold thermal sensation with the skin temperature, it is here correlated with a factor identified as vasoconstriction factor defined by

$$\varepsilon_{vc} = (KS_o - KS)/(KS_o - KS_{(-4)}) \qquad\qquad (1.202)$$

VasoconstrictFac = (ThermCndctNeut - ThermCndct) &
          /(ThermCndctNeut - ThermCndctMin)

Thus, TSV in the cold is a function of a vasoconstriction factor (ε_{vc}) as:

$$TSV = -1.46 \times \varepsilon_{vc} + 3.75 \times \varepsilon_{vc}^{\ 2} - 6.17 \times \varepsilon_{vc}^{\ 3} \qquad\qquad (1.203)$$

TSV = -1.46153*VasoconstrictFac + 3.74721*VasoconstrictFac**2 &
          - 6.168856*VasoconstrictFac**3

and for the warm environments, TSV is defined as:

$$TSV = [5.0 - 6.56(RH - 0.5)] \times \varepsilon_{wsw} \qquad\qquad (1.204)$$

TSV = (5. - 6.56*(RelHum - 0.50))*SkinWetFac

The KSU model's TSV was developed from experimental conditions in all temperature ranges and from clo levels between .05 clo to 0.7 clo and from activities levels of 1 to 6 mets (6).

MRT Calculation

There are three options to calculate mean radiant temperature in the thermal comfort models. One is the zone averaged MRT, another is the surface weighted MRT, and the other is angle factor MRT. The zone averaged MRT is calculated on the assumption that a person is in the center of a space, whereas the surface weighted MRT is calculated in consideration of the surface that a person is closest to, and the angle factor MRT is calculated based on angle factors between a person and the different surfaces in a space. Here, the surface weighted

MRT is the average temperature of the selected surface and zone averaged MRT and is intended to represent conditions in the limit as a person gets closer and closer to a particular surface. In that limit, half of the person's radiant field will be dominated by that surface and the other half will be exposed to the rest of the zone. Note that the surface weighted MRT is only an approximation. The angle factor MRT is the mean temperature of the surrounding surface temperatures weighted according to the magnitude of the respective angle factors and allows the user to more accurately predict thermal comfort at a particular location within a space.

Table 30. Nomenclature and variable list for MRT calculation

Mathematical variable	Description	Units	Range	FORTRAN variable
T_r	Mean radiant temperature	°C	-	RadTemp
$T_{r\text{-}avg}$	Zone averaged radiant temperature	°C	-	ZoneRadTemp
T_{surf}	Surface temperature	°C	-	SurfaceTemp
F_{surf}	Angle factor between person and surface	-	0~1	AngleFactor

Description of the model and algorithm

The zone averaged MRT is calculated without weighting any surface temperature of the space.

$$T_r = T_{r-avg}$$

RadTemp = MRT(ZoneNum)

The surface weighted MRT is the average temperature of the zone averaged MRT and the temperature of the surface that a person is closest to.

$$T_r = (T_{r-avg} + T_{surf})/2$$

ZoneRadTemp = MRT(ZoneNum)

SurfaceTemp = GetSurfaceTemp(People(PeopleNum)%SurfacePtr)

RadTemp = (ZoneRadTemp + SurfaceTemp)/2.0

The angle factor MRT is the mean value of surrounding surface temperatures weighted by the size of the respective angle factors between a person and each surface.

$$T_r = T_{surf-1}F_{surf-1} + T_{surf-2}F_{surf-2} + ... + T_{surf-n}F_{surf-n}$$

SurfTempAngleFacSummed = SurfTempAngleFacSummed &

      + SurfaceTemp * AngleFactorList(AngleFacNum)%AngleFactor(SurfNum)

RadTemp = SurfTempAngleFacSummed

References

1. ASHRAE, "High Intensity Infrared Radiant Heating", 1984 system Handbook, American Society of Heating, Refrigerating and Air Conditioning Engineers, Atlanta, GA, Chapter 18, 1984.

2. Fanger, P.O., Thermal Comfort-Analysis and Applications in Environmental Engineering, Danish Technical Press, Copenhagen, 1970.

3. ASHRAE, "Physiological Principles for Comfort and Health," 1985 Fundamental Handbook, American Society of Heating, Refrigerating and Air Conditioning Engineers, Atlanta, GA, Chapter 8, 1985.

4. Du Bois, D. and E.F., "A Formula to Estimate Approximate Surface Area, if Height and Weight are Known", Archives of internal Medicine, Vol.17, 1916.

5. Fanger, P.O., "Radiation and Discomfort", ASHRAE Journal. February 1986.

6. Berglund, Larry, "Mathematical Models for Predicting the Thermal Comfort Response of Building Occupants", ASHRAE Trans., Vol.84, 1978.

7. Fanger P.O., "Calculation of Thermal Comfort: Introduction of a Basic Comfort Equation", ASHRE Trans., Vol.73, Pt 2, 1967.

8. Gagge, A.P., Stolwijk, J. A. J., Nishi, Y., "An Effective Temperature Scale Based on a Simple Model of Human Physiological Regulatory Response", ASHRAE Trans., Vol.70, Pt 1, 1970.

9. Gagge, A.P., Fobelets, A.P., Berglund, L. G., "A Standard Predictive Index of Human Response to the Thermal Environment", ASHRAE Trans., Vol.92, Pt 2, 1986.

10. Azer, N.Z., Hsu, S., "The prediction of Thermal Sensation from Simple model of Human Physiological Regulatory Response", ASHRAE Trans., Vol.83, Pt 1, 1977.

11. Hsu, S., "A Thermoregulatory Model for Heat Acclimation and Some of its Application", Ph. D. Dissertation, Kansas State University, 1977.

12. ISO., "Determination of the PMV and PPD Indices and Specification of the Conditions for Thermal Comfort", DIS 7730, Moderate Thermal Environment, 1983.

13. Doherty, T.J., Arens, E., "Evaluation of the Physiological Bases of Thermal Comfort Models", ASHRAE Trans., Vol.94, Pt 1, 1988.

14. ASHRAE, "Physiological Principles and Thermal Comfort", 1993 ASHRAE Handbook-Fundamentals, American Society of Heating, Refrigerating and Air Conditioning Engineers, Atlanta, GA, Chapter 8, 1993.

15. Fountain, Marc.E., Huizenga, Charlie, "A Thermal Sensation Prediction Tool for Use by the Profession", ASHRAE Trans., Vol.103, Pt 2, 1997.

16. Int-Hout, D., "Thermal Comfort Calculation / A Computer Model", ASHRAE Trans., Vol.96, Pt 1, 1990.

Radiant System Models

Low Temperature Radiant System Model

Low temperature radiant heating and cooling systems appear, on the surface, to be relatively simple systems. The system circulates hot or cold fluid through tubes embedded in a wall, ceiling, or floor or runs current through electric resistance wires embedded in a surface or a panel. Energy is thus either added to or removed from the space, and zone occupants are conditioned by both radiation exchange with the system and convection from the surrounding air that is also affected by the system. Unless specifically required for indoor air quality considerations, fans, ductwork, dampers, etc. are not needed.

Despite the relative simplicity of the low temperature radiant systems, the integration of such a system within an energy analysis program requires one to overcome several challenges. First, for systems with significant thermal mass, the conduction transfer function method for modeling transient conduction must be extended to include embedded heat sources or sinks. Second, one must integrate this formulation within an energy analysis program like EnergyPlus. Finally, one must overcome the fact that the radiant system is both a zone heat balance element and a conditioning system. Each of these issues will be addressed in the next several subsections.

One Dimensional Heat Transfer Through Multilayered Slabs

One of the most important forms of heat transfer in energy analysis is heat conduction through building elements such as walls, floors, and roofs. While some thermally lightweight structures can be approximated by steady state heat conduction, a method that applies to all structures must account for the presence of thermal mass within the building elements. Transient one dimensional heat conduction through a homogeneous layer with constant thermal properties such as the one shown in Figure 70 is governed by the following equation:

$$\frac{\partial^2 T}{\partial x^2} = \frac{1}{\alpha}\frac{\partial T}{\partial t} \qquad\qquad (1.205)$$

where: T is the temperature as a function of position and time,

x is the position,

t is the time,

$\alpha = \dfrac{k}{\rho c_p}$ is the thermal diffusivity of the layer material,

k is its thermal conductivity,

ρ is its density, and

c_p is its specific heat.

This equation is typically coupled with Fourier's law of conduction that relates the heat flux at any position and time to temperature as follows:

$$q''(x,t) = -k\frac{\partial T(x,t)}{\partial x} \qquad\qquad (1.206)$$

$T_1(0,t)$ $T_2(x_1,t)$

$q''_1(0,t)$ $q''_2(x_1,t)$

$x = 0$ $x = x_1$
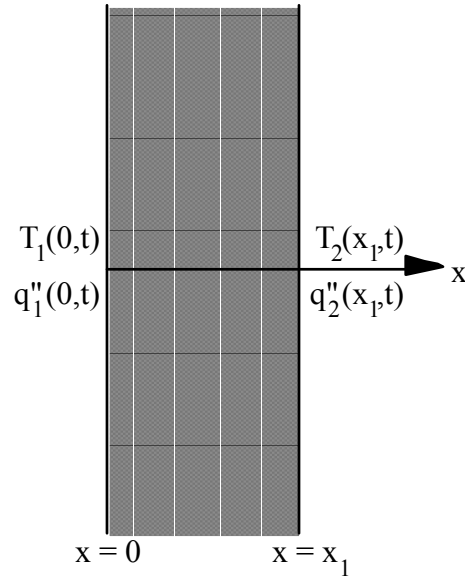
Figure 70. Single Layered Building Element

While analytical solutions exist for the single homogeneous layer shown in Figure 70, the solution becomes extremely tedious for the multiple layered slab shown in Figure 71.

$T_1(0,t)$ $T_2(x_1,t)$ $T_3(x_2,t)$ $T_4(x_3,t)$ $T_5(x_4,t)$ $T_n(x_{n-1},t)$ $T_{n+1}(x_n,t)$

$q''_1(0,t)$ $q''_2(x_1,t)$ $q''_3(x_2,t)$ $q''_4(x_3,t)$ $q''_5(x_4,t)$ $q''_n(x_{n-1},t)$ $q''_{n+1}(x_n,t)$

$x = 0$ $x = x_1$ $x = x_2$ $x = x_3$ $x = x_4$ $x = x_{n-1}$ $x = x_n$
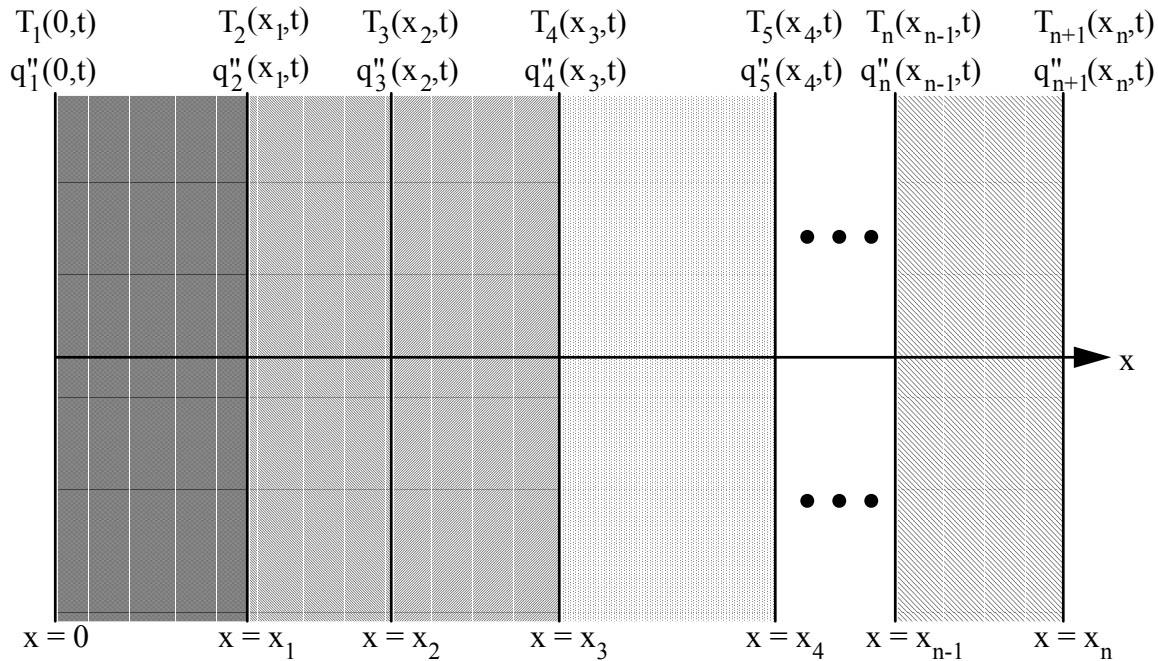
Figure 71. Multilayered Building Element

Time Series Solutions: Conduction Transfer Functions

Equations (1.205) and (1.206) can be solved numerically in a variety of ways. As mentioned in the previous section, other models have used control theory and numerical methods such as finite difference and finite element. However, each of these methods have drawbacks which render them inappropriate for use within an energy analysis program which requires both accuracy and efficiency from the simulation.

Another possible modeling method is a time series solution. Several of the detailed energy analysis programs such as EnergyPlus use a time series solution to transient heat conduction. The most basic time series solution is the response factor equation which relates the flux at one surface of an element to an infinite series of temperature histories at both sides as shown by:

$$q''_{i,t} = \sum_{m=1}^{\infty} X_m T_{i,t-m+1} - \sum_{m=1}^{\infty} Y_m T_{o,t-m+1} \qquad (1.207)$$

where q" is heat flux, T is temperature, i signifies the inside of the building element, o signifies the outside of the building element, and t represents the current time step.

While in most cases the terms in the series decay fairly rapidly, the infinite number of terms needed for an exact response factor solution makes it less than desirable. Fortunately, the similarity of higher order terms can be used to replace them with flux history terms. The new solution contains elements that are called conduction transfer functions (CTFs). The basic form of a conduction transfer function solution is shown by the following equation:

$$q''_{i,t} = \sum_{m=1}^{M} X_m T_{i,t-m+1} - \sum_{m=1}^{M} Y_m T_{o,t-m+1} + \sum_{m=1}^{k} F_m q''_{i,t-m} \qquad (1.208)$$

where k is the order of the conduction transfer functions, M is a finite number defined by the order of the conduction transfer functions, and X, Y, and F are the conduction transfer functions. This equation states that the heat flux at the interior surface of any generic building element for which the assumption of one dimensional conduction heat transfer is valid is linearly related to the current and some of the previous temperatures at both the interior and exterior surface as well as some of the previous flux values at the interior surface. A similar equation holds for the heat flux at the exterior surface.

The final CTF solution form reveals why it is so elegant and powerful. With a single, relatively simple equation, the conduction heat transfer through an element can be calculated. The coefficients (CTFs) in the equation are constants that only need to be determined once. The only storage of data required is the CTFs themselves and a limited number of temperature and flux terms. The formulation is valid for any surface type and does not require the calculation or storage of element interior temperatures.

As the next several sections will detail, there are two main methods for calculating conduction transfer functions: the Laplace Transform method and the State Space method. Both methods are well suited for the main focus of this research, the extension of conduction transfer functions to include heat sources or sinks.

Laplace Transform Formulation

The traditional method for calculating conduction transfer functions is described in detail by Hittle (1981).   Beginning with the transient one dimensional heat conduction equation {Equation (1.205)} and Fourier's law of conduction {Equation (1.206)}, the Laplace transform method is used to convert the governing equations into the s-domain for a single layer such as the one shown in Figure 70.

$$\frac{d^2 T(x,s)}{dx^2} = \frac{s}{\alpha} T(x,s) \qquad (1.209)$$

$$q''(x,s) = -k \frac{dT(x,s)}{dx} \qquad (1.210)$$

The transformed equations are solved and then put in matrix form as shown below:

$$
\begin{bmatrix} T_1(s) \\ q_1(s) \end{bmatrix} = \begin{bmatrix} A_1(s) & B_1(s) \\ C_1(s) & D_1(s) \end{bmatrix} \begin{bmatrix} T_2(s) \\ q_2(s) \end{bmatrix}
$$
(1.211)

where: $T_1(s)$, $T_2(s)$, $q_1(s)$, and $q_2(s)$ are the temperature and flux terms in the Laplace domain,

$$A_1(s) = \cosh\left(\ell_1\sqrt{s/\alpha_1}\right),$$

$$B_1(s) = \left(1/k_1\sqrt{s/\alpha_1}\right)\sinh\left(\ell_1\sqrt{s/\alpha_1}\right),$$

$$C_1(s) = k_1\sqrt{s/\alpha_1}\,\sinh\left(\ell_1\sqrt{s/\alpha_1}\right),$$

$$D_1(s) = \cosh\left(\ell_1\sqrt{s/\alpha_1}\right),$$

k_1 is the thermal conductivity of the layer,

α_1 is the thermal diffusivity of the layer, and

ℓ_1 is the thickness of the layer.

The 2 x 2 matrix consisting of $A_1(s)$, $B_1(s)$, $C_1(s)$, and $D_1(s)$ is called the transmission matrix and contains all of the thermophysical properties of the layer necessary to calculate transient conduction heat transfer through it. It can easily be shown that a second layer could be characterized in a similar way as:

$$
\begin{bmatrix} T_2(s) \\ q_2(s) \end{bmatrix} = \begin{bmatrix} A_2(s) & B_2(s) \\ C_2(s) & D_2(s) \end{bmatrix} \begin{bmatrix} T_3(s) \\ q_3(s) \end{bmatrix}
$$
(1.212)

where $A_2(s)$, $B_2(s)$, $C_2(s)$, and $D_2(s)$ are calculated using the properties of the second layer. This can be substituted into Equation (1.211) to provide insight how the extension to multilayered slabs is achieved.

$$
\begin{bmatrix} T_1(s) \\ q_1(s) \end{bmatrix} = \begin{bmatrix} A_1(s) & B_1(s) \\ C_1(s) & D_1(s) \end{bmatrix} \begin{bmatrix} A_2(s) & B_2(s) \\ C_2(s) & D_2(s) \end{bmatrix} \begin{bmatrix} T_3(s) \\ q_3(s) \end{bmatrix}
$$
(1.213)

Thus, for a multilayered element as shown in Figure 71, each separate layer has a transmission matrix of $A_i(s)$, $B_i(s)$, $C_i(s)$, and $D_i(s)$ associated with it. The form of the matrix equation for the multilayered element is the same as the equation for a single layer:

$$
\begin{bmatrix} T_1(s) \\ q_1(s) \end{bmatrix} = \begin{bmatrix} A(s) & B(s) \\ C(s) & D(s) \end{bmatrix} \begin{bmatrix} T_{n+1}(s) \\ q_{n+1}(s) \end{bmatrix}
$$
(1.214)

but the transmission matrix is replaced by:

$$
\begin{bmatrix} A(s) & B(s) \\ C(s) & D(s) \end{bmatrix} = \begin{bmatrix} A_1(s) & B_1(s) \\ C_1(s) & D_1(s) \end{bmatrix} \begin{bmatrix} A_2(s) & B_2(s) \\ C_2(s) & D_2(s) \end{bmatrix} \cdots \begin{bmatrix} A_n(s) & B_n(s) \\ C_n(s) & D_n(s) \end{bmatrix} \tag{1.215}
$$

Equation (1.214) is typically rearranged as follows:

$$
\begin{bmatrix} q_1(s) \\ q_{n+1}(s) \end{bmatrix} = \begin{bmatrix} \dfrac{D(s)}{B(s)} & \dfrac{-1}{B(s)} \\ \dfrac{1}{B(s)} & \dfrac{-A(s)}{B(s)} \end{bmatrix} \begin{bmatrix} T_1(s) \\ T_{n+1}(s) \end{bmatrix} \tag{1.216}
$$

which relates the flux at either surface of the element to the temperature histories at both surfaces. When the temperature histories are formulated as triangular pulses made up of simple ramp functions, the roots of this equation can be found and result in response factors. The response factors can be simplified as described above through the introduction of flux history terms to form conduction transfer functions. A simplified method of finding the roots of the Laplace domain equations is described by Hittle and Bishop (1983) and is used by the current version of BLAST.

State Space Formulation

Recently, another method of finding conduction transfer functions starting from a state space representation has begun receiving increased attention (Ceylan and Myers 1980; Seem 1987; Ouyang and Haghighat 1991). The basic state space system is defined by the following linear matrix equations:

$$
\frac{d[x]}{dt} = [A][x] + [B][u] \tag{1.217}
$$

$$
[y] = [C][x] + [D][u] \tag{1.218}
$$

where x is a vector of state variables, u is a vector of inputs, y is the output vector, t is time, and A, B, C, and D are coefficient matrices. Through the use of matrix algebra, the vector of state variables (x) can be eliminated from the system of equations, and the output vector (y) can be related directly to the input vector (u) and time histories of the input and output vectors.

This formulation can be used to solve the transient heat conduction equation by enforcing a finite difference grid over the various layers in the building element being analyzed. In this case, the state variables are the nodal temperatures, the environmental temperatures (interior and exterior) are the inputs, and the resulting heat fluxes at both surfaces are the outputs. Thus, the state space representation with finite difference variables would take the following form:

$$
\frac{d\begin{bmatrix} T_1 \\ \vdots \\ T_n \end{bmatrix}}{dt} = [A] \begin{bmatrix} T_1 \\ \vdots \\ T_n \end{bmatrix} + [B] \begin{bmatrix} T_i \\ T_o \end{bmatrix} \tag{1.219}
$$

$$\begin{bmatrix} q_i'' \\ q_o'' \end{bmatrix} = \begin{bmatrix} C \end{bmatrix} \begin{bmatrix} T_1 \\ \vdots \\ T_n \end{bmatrix} + \begin{bmatrix} D \end{bmatrix} \begin{bmatrix} T_i \\ T_o \end{bmatrix} \qquad (1.220)$$

where T_1, T_2, ..., T_{n-1}, T_n are the finite difference nodal temperatures, n is the number of nodes, T_i and T_o are the interior and exterior environmental temperatures, and q_i'' and q_o'' are the heat fluxes (desired output).

Seem (1987) shows that for a simple one layer slab with two interior nodes as in Figure 72 and convection at both sides the resulting finite difference equations are given by:

$$C\frac{dT_1}{dt} = hA(T_o - T_1) + \frac{T_2 - T_1}{R} \qquad (1.221)$$

$$C\frac{dT_2}{dt} = hA(T_i - T_2) + \frac{T_1 - T_2}{R} \qquad (1.222)$$

$$q_i'' = A(T_i - T_2) \qquad (1.223)$$

$$q_o'' = A(T_1 - T_o) \qquad (1.224)$$

where: $R = \dfrac{\ell}{kA}$,

$C = \dfrac{\rho c_p \ell A}{2}$, and

A is the area of the surface exposed to the environmental temperatures.
In matrix format:

$$\begin{bmatrix} \dfrac{dT_1}{dt} \\ \dfrac{dT_2}{dt} \end{bmatrix} = \begin{bmatrix} \dfrac{-1}{RC} - \dfrac{hA}{C} & \dfrac{1}{RC} \\ \dfrac{1}{RC} & \dfrac{-1}{RC} - \dfrac{hA}{C} \end{bmatrix} \begin{bmatrix} T_1 \\ T_2 \end{bmatrix} + \begin{bmatrix} \dfrac{hA}{C} & 0 \\ 0 & \dfrac{hA}{C} \end{bmatrix} \begin{bmatrix} T_o \\ T_i \end{bmatrix} \qquad (1.225)$$

$$\begin{bmatrix} q_1'' \\ q_2'' \end{bmatrix} = \begin{bmatrix} 0 & -h \\ h & 0 \end{bmatrix} \begin{bmatrix} T_1 \\ T_2 \end{bmatrix} + \begin{bmatrix} 0 & h \\ -h & 0 \end{bmatrix} \begin{bmatrix} T_o \\ T_i \end{bmatrix} \qquad (1.226)$$
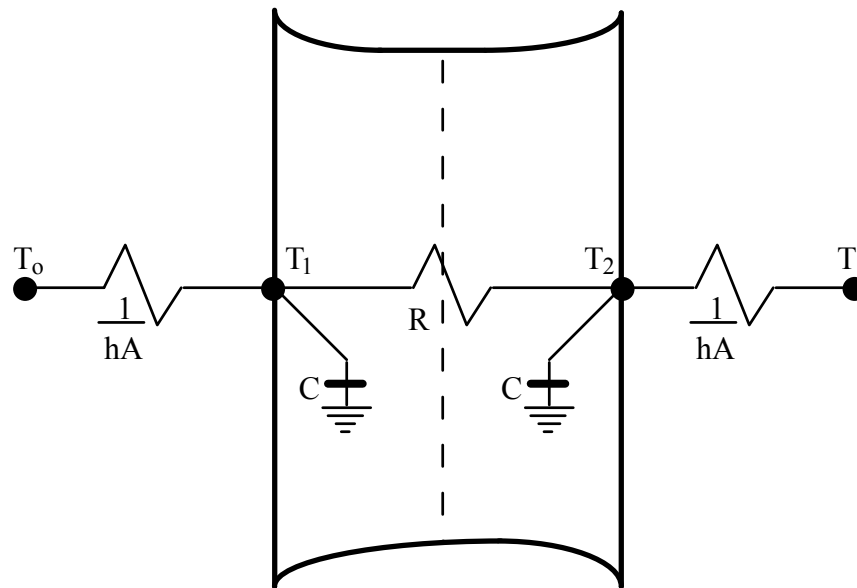
Figure 72. Two Node State Space Example

The important aspect of the state space technique is that through the use of relatively simple matrix algebra the state space variables (nodal temperatures) can be eliminated to arrive at a matrix equation that gives the outputs (heat fluxes) as a function of the inputs (environmental temperatures) only. This eliminates the need to solve for roots in the Laplace domain. In addition, the resulting matrix form has more physical meaning than complex functions required by the Laplace transform method. The current version of EnergyPlus uses the state space method for computing CTFs.

The accuracy of the state space method of calculating CTFs has been addressed in the literature. Ceylan and Myers (1980) compared the response predicted by the state space method to various other solution techniques including an analytical solution. Their results showed that for an adequate number of nodes the state space method computed a heat flux at the surface of a simple one layer slab within 1% of the analytical solution. Ouyang and Haghighat (1991) made a direct comparison between the Laplace and state space methods. For a wall composed of insulation between two layers of concrete, they found almost no difference in the response factors calculated by each method.

Extension of Time Series Solutions to Include Heat Sources and Obtain Internal Temperatures

Laplace Transform Formulation

Degiovanni (1988) proposed two methodologies for including sources or sinks in the Laplace Transform Formulation. The first method shows how a source that varies as a function of time and location can be incorporated. The resulting equations involve some fairly complicated terms including spatial derivatives.

The second method that will be analyzed in more detail involves the addition of a source or sink at the interface between two layers. The derivation of the necessary equations is begun by analyzing the simple two layer element shown in Figure 73.
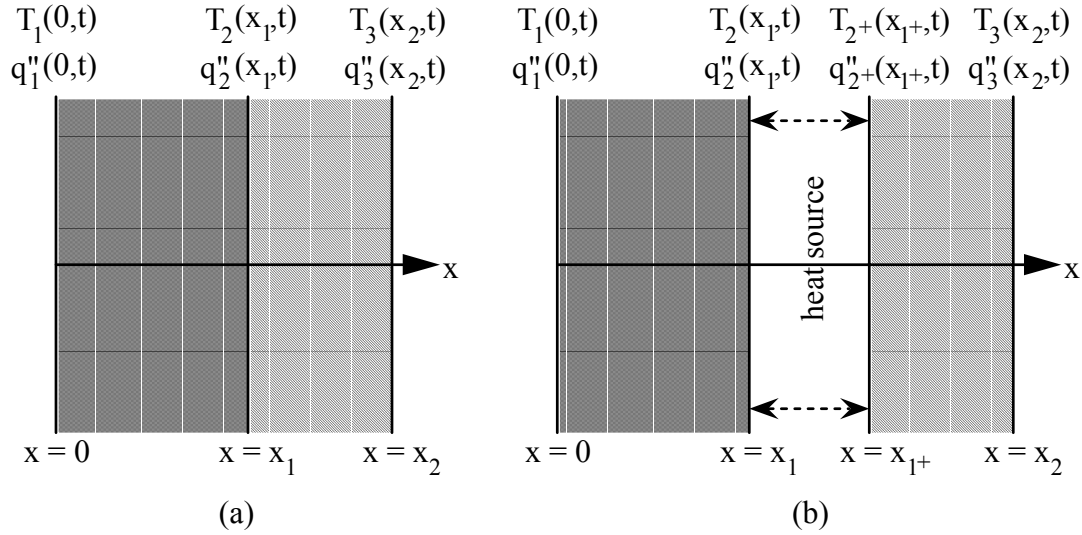
Figure 73. Two Layer Example for Deriving the Laplace Transform Extension to Include Sources and Sinks

For the first layer, it was determined that in the Laplace domain

$$\begin{bmatrix} T_1(s) \\ q_1(s) \end{bmatrix} = \begin{bmatrix} A_1(s) & B_1(s) \\ C_1(s) & D_1(s) \end{bmatrix} \begin{bmatrix} T_2(s) \\ q_2(s) \end{bmatrix}$$

(1.227)

For the second layer:

$$\begin{bmatrix} T_2(s) \\ q_2(s) \end{bmatrix} = \begin{bmatrix} A_2(s) & B_2(s) \\ C_2(s) & D_2(s) \end{bmatrix} \begin{bmatrix} T_3(s) \\ q_3(s) \end{bmatrix}$$

(1.228)

To link the two layers and include the heat source between them, the following substitution is made:

$$\begin{bmatrix} T_2(s) \\ q_2(s) \end{bmatrix} = \begin{bmatrix} T_{2+}(s) \\ q_{2+}(s) \end{bmatrix} + \begin{bmatrix} 0 \\ q_{source}(s) \end{bmatrix}$$

(1.229)

which results in:

$$\begin{bmatrix} T_1(s) \\ q_1(s) \end{bmatrix} = \begin{bmatrix} A_1(s) & B_1(s) \\ C_1(s) & D_1(s) \end{bmatrix} \left\{ \begin{bmatrix} T_{2+}(s) \\ q_{2+}(s) \end{bmatrix} + \begin{bmatrix} 0 \\ q_{source}(s) \end{bmatrix} \right\}$$

(1.230)

$$\begin{bmatrix} T_1(s) \\ q_1(s) \end{bmatrix} = \begin{bmatrix} A_1(s) & B_1(s) \\ C_1(s) & D_1(s) \end{bmatrix} \left\{ \begin{bmatrix} A_2(s) & B_2(s) \\ C_2(s) & D_2(s) \end{bmatrix} \begin{bmatrix} T_3(s) \\ q_3(s) \end{bmatrix} + \begin{bmatrix} 0 \\ q_{source}(s) \end{bmatrix} \right\}$$

(1.231)

$$\begin{bmatrix} T_1(s) \\ q_1(s) \end{bmatrix} = \begin{bmatrix} A_1(s) & B_1(s) \\ C_1(s) & D_1(s) \end{bmatrix}\begin{bmatrix} A_2(s) & B_2(s) \\ C_2(s) & D_2(s) \end{bmatrix}\begin{bmatrix} T_3(s) \\ q_3(s) \end{bmatrix} + \begin{bmatrix} A_1(s) & B_1(s) \\ C_1(s) & D_1(s) \end{bmatrix}\begin{bmatrix} 0 \\ q_{source}(s) \end{bmatrix}$$

(1.232)

While Degiovanni concludes with this formula, some insight into what the generic equation for an element that has n layers might look like is gained by working with Equation (1.232). If a layer is added to the left of the first layer, the entire right hand side of Equation (1.232) is multiplied by the transmission matrix of the new layer. Conversely, if a layer is added to the right of the second layer in Figure 73, the vector containing the Laplace transform of the temperature and heat flux at interface 3 is replaced by the product of the transmission matrix of the new layer and the vector for temperature and heat flux at the next interface, and the term dealing with the heat source is not affected. The general equation for a building element with n layers and m layers between the left hand surface and the heat source can be derived as:

$$\begin{bmatrix} T_1(s) \\ q_1(s) \end{bmatrix} = \left(\prod_{i=1}^{n}\begin{bmatrix} A_i(s) & B_i(s) \\ C_i(s) & D_i(s) \end{bmatrix}\right)\begin{bmatrix} T_{n+1}(s) \\ q_{n+1}(s) \end{bmatrix} + \left(\prod_{i=1}^{m}\begin{bmatrix} A_i(s) & B_i(s) \\ C_i(s) & D_i(s) \end{bmatrix}\right)\begin{bmatrix} 0 \\ q_{source}(s) \end{bmatrix}$$

(1.233)

or in more compact form:

$$\begin{bmatrix} T_1(s) \\ q_1(s) \end{bmatrix} = \begin{bmatrix} A(s) & B(s) \\ C(s) & D(s) \end{bmatrix}\begin{bmatrix} T_{n+1}(s) \\ q_{n+1}(s) \end{bmatrix} + \begin{bmatrix} a(s) & b(s) \\ c(s) & d(s) \end{bmatrix}\begin{bmatrix} 0 \\ q_{source}(s) \end{bmatrix}$$

(1.234)

where:
$$\begin{bmatrix} A(s) & B(s) \\ C(s) & D(s) \end{bmatrix} = \prod_{i=1}^{n}\begin{bmatrix} A_i(s) & B_i(s) \\ C_i(s) & D_i(s) \end{bmatrix}$$
and

$$\begin{bmatrix} a(s) & b(s) \\ c(s) & d(s) \end{bmatrix} = \prod_{i=1}^{m}\begin{bmatrix} A_i(s) & B_i(s) \\ C_i(s) & D_i(s) \end{bmatrix}.$$

Next, Equation (1.234) must be rearranged to match the form of Equation (1.216), which relates the heat flux at both sides of the element to the temperature at each side. The matrix equation that is obtained shows that:

$$\begin{bmatrix} q_1(s) \\ q_{n+1}(s) \end{bmatrix} = \begin{bmatrix} \dfrac{D(s)}{B(s)} & \dfrac{-1}{B(s)} \\ \dfrac{1}{B(s)} & \dfrac{-A(s)}{B(s)} \end{bmatrix}\begin{bmatrix} T_1(s) \\ T_{n+1}(s) \end{bmatrix} + \begin{bmatrix} d(s) - \dfrac{D(s)b(s)}{B(s)} \\ \dfrac{b(s)}{B(s)} \end{bmatrix}\begin{bmatrix} q_{source}(s) \end{bmatrix}$$ (1.235)

This equation bears a striking resemblance to Equation (1.216). If the source term in Equation (1.235) is dropped, then the equation is identical to Equation (1.216). This result conforms with the superposition principle which was used to develop the conduction transfer functions from the summation of a series of triangular pulses or ramp sets. Now, the effect of the heat source is simply added to the response to the temperature inputs.

While Equation (1.235) is correct for any single or multilayered element, the first term in the heat source transmission matrix does not appear to match the compactness of the other terms in the matrix equation. It can be shown (see Strand 1995: equations 32 through 42

which detail this derivation) that the heat source transmission term for a two layer problem reduces to

$$
\begin{bmatrix} q_1(s) \\ q_3(s) \end{bmatrix} = \begin{bmatrix} \dfrac{D(s)}{B(s)} & \dfrac{-1}{B(s)} \\[2mm] \dfrac{1}{B(s)} & \dfrac{-A(s)}{B(s)} \end{bmatrix} \begin{bmatrix} T_1(s) \\ T_3(s) \end{bmatrix} + \begin{bmatrix} \dfrac{B_2(s)}{B(s)} \\[2mm] \dfrac{B_1(s)}{B(s)} \end{bmatrix} \begin{bmatrix} q_{source}(s) \end{bmatrix} \qquad (1.236)
$$

If this is extended to a slab with n layers and a source between the m and m+1 layers, the general matrix equation for obtaining heat source transfer functions using the Laplace transform method is:

$$
\begin{bmatrix} q_1(s) \\ q_{n+1}(s) \end{bmatrix} = \begin{bmatrix} \dfrac{D(s)}{B(s)} & \dfrac{-1}{B(s)} \\[2mm] \dfrac{1}{B(s)} & \dfrac{-A(s)}{B(s)} \end{bmatrix} \begin{bmatrix} T_1(s) \\ T_{n+1}(s) \end{bmatrix} + \begin{bmatrix} \dfrac{\bar{b}(s)}{B(s)} \\[2mm] \dfrac{b(s)}{B(s)} \end{bmatrix} \begin{bmatrix} q_{source}(s) \end{bmatrix} \qquad (1.237)
$$

where: $\begin{bmatrix} A(s) & B(s) \\ C(s) & D(s) \end{bmatrix} = \prod_{i=1}^{n} \begin{bmatrix} A_i(s) & B_i(s) \\ C_i(s) & D_i(s) \end{bmatrix}$,

$\begin{bmatrix} a(s) & b(s) \\ c(s) & d(s) \end{bmatrix} = \prod_{i=1}^{m} \begin{bmatrix} A_i(s) & B_i(s) \\ C_i(s) & D_i(s) \end{bmatrix}$, and

$\begin{bmatrix} \bar{a}(s) & \bar{b}(s) \\ \bar{c}(s) & \bar{d}(s) \end{bmatrix} = \prod_{i=m+1}^{n} \begin{bmatrix} A_i(s) & B_i(s) \\ C_i(s) & D_i(s) \end{bmatrix}$.

At first glance, the terms in the heat source transmission matrix may appear to be reversed. It is expected that only the layers to the left of the source will affect $q_1(s)$, but the presence of $\bar{b}(s)$ in the element multiplied by $q_{source}(s)$ to obtain $q_1(s)$ seems to be contradictory. In fact, the entire term, $\bar{b}(s)/B(s)$, must be analyzed to determine the effect of $q_{source}(s)$ on $q_1(s)$. In essence, the appearance of $\bar{b}(s)$ removes the effects of the layers to the right of the source from B(s) leaving only the influence of the layers to the left of the source. The form displayed by Equation (1.237) is, however, extremely convenient because the terms in the heat source transmission matrix have the same denominators, and thus roots, as the terms in the temperature transmission matrix. Thus, the same roots that are calculated for the CTFs can be used for the QTFs, saving a considerable amount of computer time during the calculation of the transfer functions.

Once Equation (1.237) is inverted from the Laplace domain back into the time domain, the combined CTF–QTF solution takes the following form:

$$
q''_{i,t} = \sum_{m=1}^{M} X_m T_{i,t-m+1} - \sum_{m=1}^{M} Y_m T_{o,t-m+1} + \sum_{m=1}^{k} F_m q''_{i,t-m} + \sum_{m=1}^{M} W_m q_{source,t-m+1} \qquad (1.238)
$$

This relation is identical to Equation (1.210) except for the presence of the QTF series that takes the heat source or sink into account.

State Space Formulation

The two node example introduced by Seem (1987) can be utilized to examine the extension of the state space method to include heat sources or sinks. Figure 74 shows the simple two node network with a heat source added at node 1.

The nodal equations for the finite difference network shown in Figure 74 are:

$$C\frac{dT_1}{dt} = hA\left(T_o - T_1\right) + \frac{T_2 - T_1}{R} + q_{source}A \tag{1.239}$$

$$C\frac{dT_2}{dt} = hA\left(T_i - T_2\right) + \frac{T_1 - T_2}{R} \tag{1.240}$$

$$q_i'' = A\left(T_i - T_2\right) \tag{1.241}$$

$$q_o'' = A\left(T_1 - T_o\right) \tag{1.242}$$
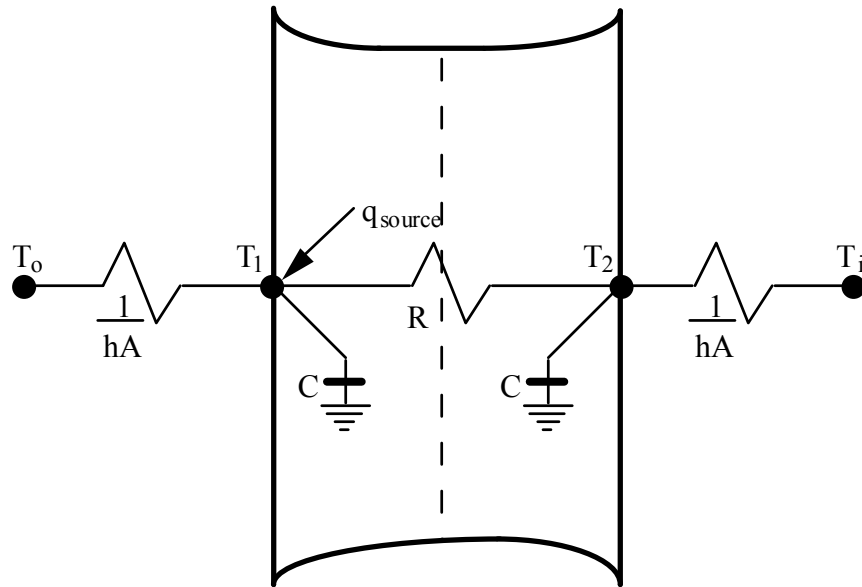
Figure 74. Two Node State Space Example with a Heat Source

In obtaining the matrix equivalent for this set of equations, it should be noted that the source term is not a constant but rather an input that varies with time. Thus, it must be grouped with the environmental temperatures as inputs. The resulting matrix equations take the following form:

$$\begin{bmatrix} \dfrac{dT_1}{dt} \\ \dfrac{dT_2}{dt} \end{bmatrix} = \begin{bmatrix} \dfrac{-1}{RC} - \dfrac{hA}{C} & \dfrac{1}{RC} \\ \dfrac{1}{RC} & \dfrac{-1}{RC} - \dfrac{hA}{C} \end{bmatrix} \begin{bmatrix} T_1 \\ T_2 \end{bmatrix} + \begin{bmatrix} \dfrac{hA}{C} & 0 & \dfrac{A}{C} \\ 0 & \dfrac{hA}{C} & 0 \end{bmatrix} \begin{bmatrix} T_o \\ T_i \\ q_{source} \end{bmatrix} \tag{1.243}$$

$$\begin{bmatrix} q_1'' \\ q_2'' \end{bmatrix} = \begin{bmatrix} 0 & -h \\ h & 0 \end{bmatrix} \begin{bmatrix} T_1 \\ T_2 \end{bmatrix} + \begin{bmatrix} 0 & h & 0 \\ -h & 0 & 0 \end{bmatrix} \begin{bmatrix} T_o \\ T_i \\ q_{source} \end{bmatrix} \qquad (1.244)$$

Equation (1.244) appears to suggest that the source term has no direct effect on the heat flux at either side of the element because its coefficients are zero. This is not the case. Equation (1.244) only relates variables that have a direct influence on heat flux. So, while T_i has no direct influence on q_o'', it does have an indirect influence through the nodal network. The same would hold for the influence of q_{source}.

If this analysis is extended to a finite difference network with n nodes, the corresponding matrix equations can be shown to be:

$$\frac{d \begin{bmatrix} T_1 \\ \vdots \\ T_n \end{bmatrix}}{dt} = \begin{bmatrix} A \end{bmatrix} \begin{bmatrix} T_1 \\ \vdots \\ T_n \end{bmatrix} + \begin{bmatrix} B \end{bmatrix} \begin{bmatrix} T_o \\ T_i \\ q_{source} \end{bmatrix} \qquad (1.245)$$

$$\begin{bmatrix} q_i'' \\ q_o'' \end{bmatrix} = \begin{bmatrix} C \end{bmatrix} \begin{bmatrix} T_1 \\ \vdots \\ T_n \end{bmatrix} + \begin{bmatrix} D \end{bmatrix} \begin{bmatrix} T_o \\ T_i \\ q_{source} \end{bmatrix} \qquad (1.246)$$

The influence of the heat source is also confirmed by the final solution form, which is identical to the Laplace transform result shown in Equation (1.238). As with the Laplace solution method, the state space method results in a set of QTFs that relate the heat source at the current time step and several previous time steps to the current heat flux at the surface of the element.

Other similarities between the two solution methods are evident. It is interesting to note that as with the Laplace method there is no alteration of the CTFs calculated by the state space method. Thus, the principle of superposition is still valid. Furthermore, the introduction of the source term did not substantially increase the computing effort required to calculate the additional transfer functions. In the Laplace method, this was shown by the common roots, B(s), shared by both the CTFs and the QTFs. In the state space method, it can be noted that the A matrices in Equations (1.225) and (1.243) are identical. Since the state space method requires the inversion and the exponentiation of the A matrix only, the additional QTF terms will not require a substantial amount of additional computing time for their calculation.

Determination of Internal Temperatures

One aspect of low temperature radiant systems that has not been addressed to this point is the appropriateness of specifying the effect of the system on slab response via a heat source term. For a heating system that employs electrical resistance heating, the use of a heat source as the input variable is logical. The heat produced by such a system can easily be related to the current passing through the heating wire. However, for a hydronic heating or cooling system, the known quantity is not heat but rather the temperature of the water being sent to the building element.

The use of a temperature to simulate the presence of a heating or cooling system presents one major obstacle. When fluid is not being circulated, there is no readily available temperature value available for use as an input variable.

In a hydronic system, a link between the fluid temperature being sent to the slab and the heat delivered to the slab exist. The most effective way of relating these two variables is to consider the slab to be a heat exchanger. Using heat exchanger relationships, an equation could then be formulated to obtain the heat delivered to the slab based on the inlet fluid temperature.

Most heat exchangers are used to thermally link two fluids. In the case of a hydronic radiant system, there is only one fluid and a stationary solid. Presumably, if the inlet fluid temperature, the system geometry, and the solid temperature are known, then the outlet temperature and thus the heat transfer to the building element can be computed. This leads to an interesting question: what is the solid temperature?

By definition, for one dimensional conduction heat transfer, the solid temperature is the temperature of the building element at the depth where the hydronic loop is located. Typically, this temperature is not known because it is not needed. The goal of both methods of calculating CTFs was the elimination of internal temperatures that were not needed for the simulation. For a hydronic system, it is necessary to extract this information to solve for the heat source term. Two methods of accomplishing this are described below.

Returning to the two layer example shown in Figure 73, it can be shown that the final solution form in the time domain for the slab with a source at the interface between the two layers is:

$$q''_{1,t} = \sum_{m=1}^{M} X_{k,m} T_{1,t-m+1} - \sum_{m=1}^{M} Y_{k,m} T_{3,t-m+1} + \sum_{m=1}^{k} F_m q''_{1,t-m} + \sum_{m=1}^{M} W_m q_{source,t-m+1} \qquad (1.247)$$

A similar equation could be written for the response of the first layer in absence of any source term and is given by:

$$q''_{1,t} = \sum_{m=1}^{M} x_{k,m} T_{1,t-m+1} - \sum_{m=1}^{M} y_{k,m} T_{2,t-m+1} + \sum_{m=1}^{k} f_m q''_{1,t-m} \qquad (1.248)$$

While the current temperature at the interface is not known, presumably the previous values of this parameter will be known. In addition, the temperatures and the flux histories at surface 1 are also know. The unknowns in Equation (1.248) are the current heat flux at surface 1 and the temperature at surface 2. However, Equation (1.247) does define the current value of the heat flux at surface 1 based on temperature, heat flux, and heat source histories. Thus, if this value is used in Equation (1.248), the only remaining unknown in this equation is the current temperature at surface 2, the surface where the heat source or sink is present. Rearranging Equation (1.248) provides an equation from which the temperature at the source location may be calculated:

$$T_{2,t} = \sum_{m=1}^{M} \bar{X}_{k,m} T_{1,t-m+1} - \sum_{m=1}^{M-1} \bar{Y}_{k,m} T_{2,t-m} + \sum_{m=1}^{k+1} \bar{F}_m q''_{1,t-m+1} \qquad (1.249)$$

where the new coefficients are obtained from the standard conduction transfer functions for the first layer via the following equations:

$$\bar{X}_{k,m} = \frac{x_{k,m}}{y_1} \quad \left(m = 1, \cdots, M \right) \qquad (1.250)$$

$$\bar{Y}_{k,m} = \frac{y_{k,m+1}}{y_1} \quad \left(m = 1, \cdots, M-1 \right) \qquad (1.251)$$

$$\bar{F}_1 = \frac{1}{y_1} \qquad\qquad (1.252)$$

$$\bar{F}_m = \frac{f_{m-1}}{y_1} \quad (m = 2, \cdots, k+1) \qquad\qquad (1.253)$$

This system for backing out an internal temperature through the use of a second, rearranged CTF equation is valid regardless of whether the Laplace transform or state space method is utilized to calculate the CTFs and QTFs. The state space method, however, offers a more direct method of obtaining an internal temperature through its definition as an additional output variable.

Consider again the state space example shown in Figure 74. Two output variables were defined for this example: q_i'' and q_o''. The temperature of the node where the source is present can also be defined as an output variable through the identity equation:

$$T_1 = T_1 \qquad\qquad (1.254)$$

When this equation for T$_1$ is added to Equations (1.252) and (1.253), the resulting output matrix equation for the heat flux at both surfaces and the internal temperature is:

$$\begin{bmatrix} q_i'' \\ q_o'' \\ T_1 \end{bmatrix} = \begin{bmatrix} 0 & -h \\ h & 0 \\ 1 & 0 \end{bmatrix} \begin{bmatrix} T_1 \\ T_2 \end{bmatrix} + \begin{bmatrix} 0 & h & 0 \\ -h & 0 & 0 \\ 0 & 0 & 0 \end{bmatrix} \begin{bmatrix} T_i \\ T_o \\ q_{source} \end{bmatrix} \qquad\qquad (1.255)$$

The only difference between this relation and Equation (1.244) is the presence of T$_1$ on both the right and left hand side of the equation. The dual role of T$_1$ as a state variable and an output parameter may seem to contradict the goal of the state space method of eliminating the state variables. However, due to the flexibility of the formulation, nodal temperatures can be extracted in the same manner that any other output quantity would be obtained. For an element with n layers, Equation (1.255) becomes:

$$\begin{bmatrix} q_i'' \\ q_o'' \\ T_s \end{bmatrix} = [C] \begin{bmatrix} T_1 \\ \vdots \\ T_n \end{bmatrix} + [D] \begin{bmatrix} T_i \\ T_o \\ q_{source} \end{bmatrix} \qquad\qquad (1.256)$$

where T$_S$ is the temperature of the node where the heat source or sink is present. The transfer function equation for the calculation of T$_S$ that results from Equation (1.256) is identical in form to Equation (1.238):

$$T_{s,t} = \sum_{m=1}^{M} x_{k,m} T_{i,t-m+1} - \sum_{m=1}^{M} y_{k,m} T_{o,t-m+1} + \sum_{m=1}^{k} f_m T_{s,t-m} + \sum_{m=1}^{M} w_m q_{source,t-m+1} \qquad (1.257)$$

Instead of the flux at either side of the element characterized as a function of temperature, flux, and source history terms, the temperature at the source location is related to source and temperature histories including histories of T$_S$. The validity of these internal temperature

calculation methods as well as heat source transfer functions in general will be discussed in the next chapter.

Low Temperature Radiant System Controls

The use of this equation allows the low temperature radiant system to be handled like any other surface within the heat balance framework. Heat balances at the inside and outside surfaces take on the same form as other surfaces, and the participation of the radiant system in the radiation balance within the space and thermal comfort models is automatically included. Thus, the radiant system model is fully integrated into the heat balance, and any improvements that are made in areas such as convection coefficients, shading models, etc. are immediately available to the radiant system as part of the overall heat balance solution.

Once the transient nature of the system is accounted for, one must then turn to the next difficult issue: controls. Controls are problematic for almost any simulation program. The problem is not whether something can be simulated because typically a simulation program offers the ability to experiment with many different control strategies. Rather, the problem is typically the diversity of controls that are implemented and keeping the controls that can be simulated up to date. In this area, the new model within EnergyPlus should be seen as a first attempt at modeling basic low temperature radiant systems and not as the definition of all radiant systems. Plans call for the addition of other control strategies in future versions of the program.

As a result, controls for low temperature radiant systems within the initial version of EnergyPlus are fairly simple though there is some flexibility through the use of schedules. The program user is allowed to define a setpoint temperature as well as a throttling range through which the system varies the flow rate of water (or current) to the system from zero to the user defined maximum flow rate. The flow rate is varied linearly with the flow reaching 50% of the maximum when the controlling temperature reaches the setpoint temperature. Setpoint temperatures can be varied on an hourly basis throughout the year if desired. The controlling temperature can be the mean air temperature, the mean radiant temperature, or the operative temperature of the zone, and this choice is also left to the user's discretion. Since flow rate is varied, there is no explicit control on the inlet water temperature or mixing to achieve some inlet water temperature in a hydronic system. However, the user does have the ability to specify on an hourly basis through a schedule the temperature of the water that would be supplied to the radiant system.

Graphical descriptions of the controls for the low temperature radiant system model in EnergyPlus are shown in Figure 75 for a hydronic system. In a system that uses electric resistance heating, the power or heat addition to the system varies in a manner similar to mass flow rate variation shown in Figure 75.
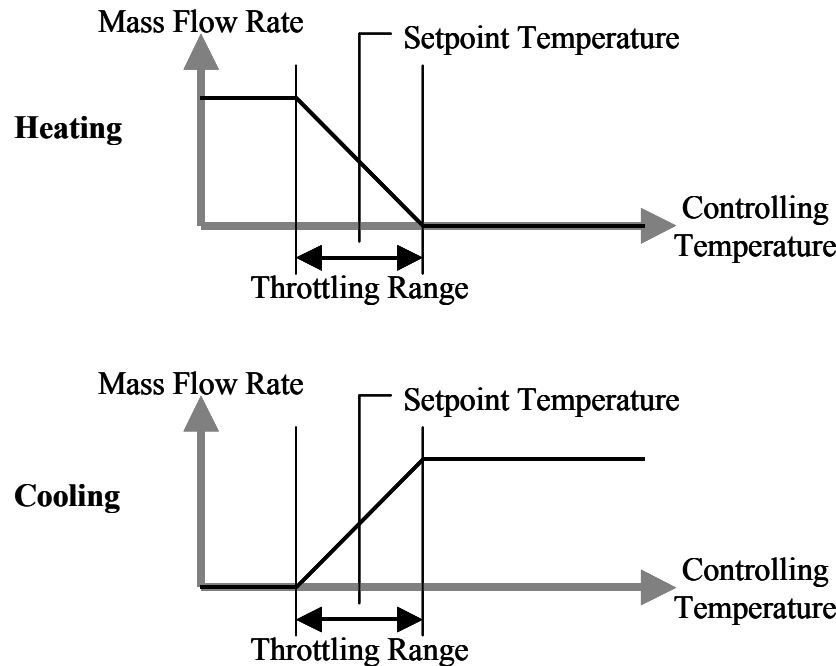
Figure 75. Low Temperature Radiant System Controls

One remaining challenge is the merging of the low temperature radiant system model with an integrated building simulation program. In the past, most simulation programs have simulated the building envelope, the space conditioning systems, and the central plant equipment in three separate steps. While this had some advantages and was partly due to a lack of computing capacity, the large drawback for this arrangement is that there is no feedback from the space conditioning system or central plant response to the building conditions. Thus, if the system or plant was undersized, it was reported as an "unmet load" and does not affect the temperatures experienced within the building.   IBLAST, a predecessor (Taylor 1991) to EnergyPlus, resolved this issue by integrating all three major components of a building simulation and thus allowing feedback between the equipment and the building envelope.

This integration was not a trivial task and required that the systems be simulated at shorter time steps in some cases to maintain solution stability. In essence, the system simulation will shorten its time step whenever it senses that conditions are changing too rapidly. While this is effective in maintaining solution stability, it can present problems for a radiant system. The radiant system has either a direct or an indirect impact on the surfaces within a building. So, it must be simulated with the building envelope. Yet, it is also a space conditioning system that must act on the space like any other system and thus must also be simulated at the system time step, which can be less than the building time step and can also vary within EnergyPlus.

This issue was handled using a multi-step approach. In EnergyPlus, the heat balance is always simulated first. When this happens, the radiant system is temporarily shut-off to find how the building would respond if there was no heat source/sink. Then, as the system and plant are simulated at multiple shorter time steps, the radiant system is allowed to operate per the controls specified by the user. Flow rate is allowed to vary at each system time step, and the radiant system model is simulated at each time step as if the current flow rate was being used throughout the entire zone time step. This means that each time the heat source/sink in the radiant system is varied during the system simulation the zone heat balance must be recomputed to see what the reaction of the rest of the zone is to this change in the conditions of one (or more) of the surfaces.

In reality, this is not physically correct because each change in the flow rate throughout the system simulation will have an impact on the system time steps remaining before the heat balance is simulated during the next zone time step. Yet, other approaches to solving the mismatch between the system and the zone response of radiant systems are not feasible. One could force the system to run at the same time step as the zone, but this could result in instabilities in other types of systems that might be present in the simulation. On the other hand, one could try to force the zone to run at the shorter time steps of the system, but this could lead to instability within the heat balance due to limits on the precision of the conduction transfer function coefficients.

Despite the fact that the simulation algorithm described above may either over- or under-predict system response dependent on how the system has been controlled in previous system time steps, it is reasonable to expect that the effect of these variations will balance out over time even though it might lead to slightly inaccurate results at any particular system time step. The long-term approach is also in view in the final simulation step at each zone time step. After the system has simulated through enough system time steps to equal a zone time step, the radiant system will rerun the heat balance using the average heat source/sink over all of the system time steps during the past zone time step. This maintains the conservation of energy within the heat balance simulation over the zone time steps and defines more appropriate temperature and flux histories at each surface that are critical to the success of a conduction transfer function based solution. A graphical picture of this somewhat complex multiple step simulation is shown in the figure below.
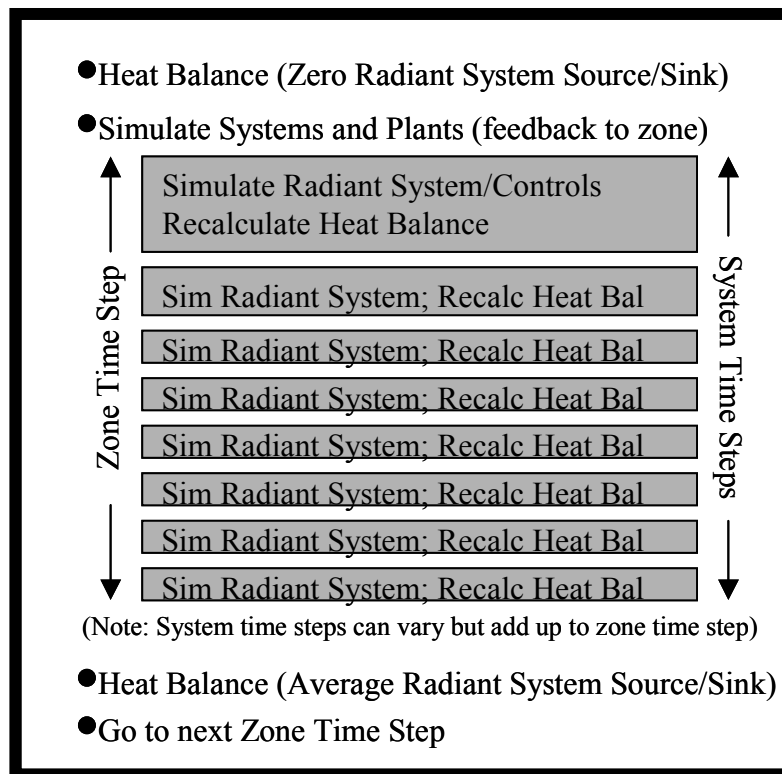
Figure 76. Resolution of Radiant System Response at Varying Time Steps

Heat Exchanger Formulation for Hydronic Systems

As has been mentioned previously, the actual heat transferred between the building element and the hydronic loop is related to the temperature of the building element at the source location as well as the water system inlet and outlet temperatures. In EnergyPlus, it is assumed that the inlet temperature to the slab (defined by a user schedule and the plant simulation) and the mass flow rate (determined by the control algorithm) are known and that

the remaining parameters must be calculated. However, the heat balance equations require the heat transferred to the building element from the water loop in order to calculate the heat transferred from the element to the building environment.

Even though systems defined by this model can vary somewhat, the same characteristic link between the system variables exist. For modeling purposes, the overall water/slab system can be thought of as a heat exchanger. While in principle there are two alternative heat exchanger methodologies, it is more convenient to use the effectiveness-NTU method in this case.

Several assumptions will be incorporated into the heat exchanger analysis. It is assumed that the building element that contains the hydronic loop is stationary and that its temperature along the length of the tubing is constant. The latter part of this assumption stems from assumptions made in both the one and two dimensional heat source transfer function derivations. In either case, the source was added at a single node that was characterized by a single temperature. For consistency, this assumption must be made again in the heat exchanger analysis. Another assumption for the current EnergyPlus model is that the fluid in the tubing is water. Additionally, it is assumed that the thermal properties of the water do not vary significantly over the length of the tubing and that the water flows at a constant flow rate. Finally, the temperature at the inside surface of the water tubing is assumed to be equal to the temperature at the source location. In other words, it is assumed that the water tubing itself has no appreciable effect on the heat transfer process being modeled.

Using these assumptions and the effectiveness-NTU heat exchanger algorithm, several equations can be defined which establish the relationship between the heat source and the water temperatures. First, a heat balance on the water loop results in:

$$q = \left(\dot{m} c_p \right)_{water} \left(T_{wi} - T_{wo} \right) \tag{1.258}$$

where q is the energy transferred between the water loop and the building element, $\dot{m}$ is the mass flow rate of the water, c_p is the specific heat of the water, T_{wi} is the inlet water temperature, and T_{wo} is the outlet water temperature.

The maximum amount of heat transfer that is possible according to the Second Law of Thermodynamics is:

$$q_{max} = \left(\dot{m} c_p \right)_{water} \left(T_{wi} - T_s \right) \tag{1.259}$$

where q_{max} is the maximum amount of energy transfer that is possible and T_s is the temperature at the source location.

The effectiveness of the heat exchanger, ε, is defined as the ratio of the actual energy transfer to the maximum possible, or:

$$\varepsilon \equiv \frac{q}{q_{max}} \tag{1.260}$$

For a heat exchanger where one fluid is stationary, the effectiveness can be related to NTU, the number of transfer units, by the following equation (Incropera and DeWitt 1985):

$$\varepsilon = 1 - e^{-NTU} \tag{1.261}$$

where NTU is defined by:

$$NTU \equiv \frac{UA}{\left(\dot{m}c_p\right)_{water}} \tag{1.262}$$

Since the water tubes were assumed to have no effect on the heat transfer process, the only term present in the overall heat transfer coefficient, UA, is a convection term. Thus, the equation for UA is:

$$UA = h\left(\pi DL\right) \tag{1.263}$$

where h is the convection coefficient, D is the interior tube diameter, and L is the total length of the tube.

The convection coefficient can be obtained from internal flow correlations that relate the Nusselt dimensionless number to other flow properties. For laminar flow in a tube of constant surface temperature, the Nusselt number is defined by:

$$Nu_D = \frac{hD}{k} = 3.66 \tag{1.264}$$

where k is the thermal conductivity of the water.

For turbulent internal flow, the Colburn equation can be used to define the Nusselt number:

$$Nu_D = \frac{hD}{k} = 0.023 \, \mathrm{Re}_D^{4/5} \, \mathrm{Pr}^{1/3} \tag{1.265}$$

where Pr is the Prandtl number of water and Re_D is the Reynolds number which is defined by:

$$\mathrm{Re}_D = \frac{4\dot{m}}{\pi \mu D} \tag{1.266}$$

The parameter μ is the absolute viscosity of water. For internal pipe flow, the flow is assumed to be turbulent for $\mathrm{Re}_D \geq 2300$.

Knowledge of the flow conditions allows Equations (1.260) through (1.266) to be calculated. This essentially eliminates ε as an unknown in Equation (1.259). The controls and the plant define the water mass flow rate and the inlet water temperature, leaving two equations (Equations (1.258) and (1.259)) and three unknowns. The third equation that can be used in conjunction with Equations (1.258) and (1.259) is Equation (1.257), which is the CTF/QTF equation for the temperature at the source location.

Knowing the inlet water temperature and water mass flow rate, the calculation procedure is somewhat involved and requires, in addition to Equations (1.257), (1.258), and (1.259), the use of a modified form of Equation (1.238). Equation (1.238) is the standard conduction transfer function formula for a building element with an embedded source/sink of heat. In EnergyPlus, the surface flux on the left hand side of the equation is replaced with a surface heat balance:

$$\begin{bmatrix} Surface \\ Heat \\ Balance \end{bmatrix} = \sum_{m=1}^{M} X_{k,m} T_{1,t-m+1} - \sum_{m=1}^{M} Y_{k,m} T_{3,t-m+1} + \sum_{m=1}^{k} F_m q''_{1,t-m} + \sum_{m=1}^{M} W_m q_{source,t-m+1} \tag{1.267}$$

The surface heat balance includes terms for incident solar energy, radiation heat transfer from internal heat sources such as lights and electrical equipment, radiation between surfaces using Hottel's Gray Interchange concept, and convection to the surrounding air. The presence of the surface temperature in the heat balance does not pose any problems since Equation (1.267) will be rearranged to solve for this temperature. Since the radiation heat balance is dependent on conditions at the other surfaces, an iteration loop is required to provide a more accurate estimate of the radiative exchange within the building. This is not the case with the mean air temperature. An assumption of the heat balance is that the mean temperature of the surrounding air is equal to the final air temperature of the previous time step. Using this estimate in the heat balance avoids a second iterative loop around the radiative iteration loop.

Thus, the terms of the heat balance on the left hand side of the equation have been set with the only unknown quantity being T_i, the inside surface temperature at the current time step. On the right hand side of Equation (1.267), most of the terms are already defined since they depend on known values from previous time steps (temperature, flux, and source histories). The only terms which are not defined are the inside surface temperature (T_i), outside surface temperature (T_o), and internal heat source/sink (q_{source}) of the current time step.

The outside surface temperature will depend on the type of environment to which it is exposed. For example, if the surface is a slab on grade floor, the outside surface temperature is defined as ground temperature and does not require an outside surface heat balance. If the element is an interior surface which has both surfaces exposed to the same air space, the outside surface temperature is redefined to be equal to the inside surface temperature. In cases where the outside surface temperature is not simply defined such as a surface exposed to the exterior environment, a heat balance similar to Equation (1.267) is required to define the outside surface temperature. However, to again avoid iteration, the heat balance equation for the outside surface assumes that conditions at the inside surface were the same as the previous time step. In most cases, since the influence of the current inside surface temperature on the outside surface temperature is very small, this is a valid assumption. In cases were the inside surface temperature has a significant effect, an approximate inside surface heat balance which defines the inside surface temperature is used. This approximate inside balance uses mean air and radiant temperatures from the previous time step.

At this point in the simulation algorithm then, all of the terms in Equation (1.267) have been defined except the value at the current time step of the inside surface temperature and the heat source/sink. Thus, Equation (1.267) can be rewritten in a simpler form:

$$T_{i,t} = C_1 + C_2 q_{source,t} \qquad (1.268)$$

where the variable C_1 includes surface heat balance and past history terms as well as the influence of the current outside temperature. The term C_2 will depend on the heat source transfer function term and the coefficients of terms linked directly to $T_{i,t}$.

Equation (1.257), which was the CTF/QTF equation for the temperature at the source location, can be simplified in a similar manner. Grouping the temperature and source history terms which are known quantities together with the effect of the outside surface temperature which is defined as described above, the original equation

$$T_{s,t} = \sum_{m=1}^{M} x_{k,m} T_{i,t-m+1} - \sum_{m=1}^{M} y_{k,m} T_{o,t-m+1} + \sum_{m=1}^{k} f_m T_{s,t-m} + \sum_{m=1}^{M} w_m q_{source,t-m+1} \qquad (1.257)$$

can be reduced to:

$$T_s = C_3 + C_4 q_{source,t} + C_5 T_{i,t} \qquad (1.269)$$

where C_3 includes all of the history terms and the effect of the current outside temperature, C_4 is the heat source transfer function for the current time step, and C_5 is the conduction transfer function for the inside surface temperature at the current time step.

Substituting Equation (1.268) into Equation (1.269) and noting that $q_{source,t}$ is the same quantity as q in Equations (1.258) and (1.259) results in:

$$T_s = C_3 + C_4 q + C_5 \left(C_1 + C_2 q \right) \qquad (1.270)$$

When this equation is combined with Equation (1.259), the heat source, which results from a known water inlet temperature, can be shown to be:

$$q = \frac{T_{wi} - C_3 - C_1 C_5}{\dfrac{1}{\varepsilon \left(\dot{m} c_p \right)_{water}} + C_4 + C_2 C_5} \qquad (1.271)$$

With both q and T_{wi} known, it is a trivial matter to calculate T_{wo} and T_S from Equations (1.268) and (1.269), respectively. Even though the coefficients in Equation (1.271) are fairly complex, the final equation relating the heat source directly to inlet water temperature is compact and does not require any iteration. As with flux control, once the heat source/sink is defined, the inside surface heat balance can be performed to determine the surface temperatures.

It should be noted that Equations (1.268) through (1.271) are a slight simplification of the actual implementation in EnergyPlus. The development shown above follows the heat balance conventions that assume previous values of the inside temperature to calculate the outside temperature. This, in reality, is not necessary and since the radiant system can be significantly influenced by the delay that such an assumption might cause, the initial implementation of radiant systems in EnergyPlus used a development (shown below) that does not lag either the inside or the outside surface temperature. In effect, we can establish three basic equations for the temperature at the inside and outside surface as well as at the location of the heat source/sink:

$$T_{inside} = C_a + C_b T_{outside} + C_C q'' \qquad (1.272)$$

$$T_{outside} = C_d + C_e T_{inside} + C_f q'' \qquad (1.273)$$

$$T_{source} = C_g + C_h q'' + C_i T_{inside} + C_j T_{outside} \qquad (1.274)$$

where: T_{inside} is the temperature at the inside surface

$T_{outside}$ is the temperature at the outside surface

T_{source} is the temperature within the radiant system at the location of the source/sink

C_a is all of the other terms in the inside heat balance (solar, LW exchange, conduction history terms, etc.)

C_b is the current cross CTF term

C_c is the QTF inside term for the current heat source/sink

C_d is all of the other terms in the outside heat balance (solar, LW exchange, conduction history terms, etc.)

C_e is the current cross CTF term (should be equal to Cb)

C_f is the QTF outside term for the current heat source/sink

C_g is the summation of all temperature and source history terms at the source/sink location

C_h is the QTF term at the source/sink location for the current heat source/sink

C_i is the CTF inside term for the current inside surface temperature

C_j is the CTF outside term for the current outside surface temperature

Equations (1.272) and (1.273) above can be solved to remove the other surface temperature. Substituting the new equations for T_{inside} and $T_{outside}$ as a function of C and q" into the equation for Tsource and simplifying results in the following equation:

$$T_{source} = C_k + C_l q''$$
<div align="right">(1.275)</div>

where:
$$C_k = C_g + \frac{C_i(C_a + C_b C_d) + C_j(C_d + C_e C_a)}{1 - C_e C_b}$$

$$C_l = C_h + \frac{C_i(C_c + C_b C_f) + C_j(C_f + C_e C_c)}{1 - C_e C_b}$$

Combining this with heat exchanger analysis as shown above, we eventually arrive at the following equation to relate the flux to the slab to the water inlet temperature and mass flow rate:

$$q'' = \frac{T_{water,in} - C_k}{\dfrac{C_l}{A} + \dfrac{1}{\varepsilon (\dot{m} c_p)_{water}}}$$
<div align="right">(1.276)</div>

which includes all of the inside and outside heat balance terms ("hidden" in the C_k and C_l coefficients). Once the flux to the slab is known, the remaining terms of interest (outlet water temperature, inside and outside surface temperatures, etc.) can be calculated using the relatively simpler equations shown above.

High Temperature Radiant Heater Model

The high temperature radiant heater model is intended to encapsulate an entire class of heating devices that seek to heat the occupants within a zone by direct radiation. This encompasses a wide variety of heaters including both gas-fired and electric. In most cases, the heater appears much like a lamp or a tube that is suspended from the ceiling of a space, and the surface temperatures are high enough that the heaters must be a safe distance away from the occupied portion of the space for safety concerns.

In EnergyPlus, the high temperature radiant heater model allows the user a reasonable amount of flexibility. Rather than specifying an exact location for the radiant heater(s), the user is allowed to specify the percentage of heat leaving the heater as radiation and then on which surfaces this radiation is incident. In addition, the user is also allowed the ability to define what fraction of radiation leaving the heater is incident directly on a person within the zone for thermal comfort purposes. This amount of heat is then used in the thermal comfort models as shown in Equation 84, which is similar in form to the equation promoted by Fanger (1970). The input parameters for the high temperature radiant heater model are shown in Table 1.

$$T_{radiant} = \left[\left(T_{MRT}^4 \right) + \left(\frac{Q_{heater \rightarrow person}}{\sigma A_{person}} \right) \right]^{0.25} \tag{1.277}$$

```
HIGH TEMP RADIANT SYSTEM,! Program keyword for high temp. radiant heaters
  Zone 1 Radiant Heater, ! Zone name
  Radiant Operation,      ! Availability schedule
  SHOP ZONE,              ! Zone name (name of zone system is serving)
  10000,                  ! maximum power input (in Watts)
  GAS,                    ! type of heater (either gas or electric)
  0.85,                   ! combustion efficiency (ignored for elec. heaters)
  0.75,                   ! fraction radiant
  0.05,                   ! fraction latent
  0.05,                   ! fraction lost
  OPERATIVE,              ! temperature control type (MAT, MRT also possible)
  2.0 ,                   ! heating throttling range (in C)
  Heating Setpoints,      ! schedule of heating setpoint temperatures
  0.05,                   ! fraction of radiant energy to people
  Zn001:Flr001, 0.75,     ! surface/fraction of radiant energy incident on it
  Zn001:Wall001, 0.05,    ! surface/fraction of radiant energy incident on it
  Zn001:Wall002, 0.05,    ! surface/fraction of radiant energy incident on it
  Zn001:Wall003, 0.05,    ! surface/fraction of radiant energy incident on it
  Zn001:Wall004, 0.05;    ! surface/fraction of radiant energy incident on it
```

Figure 77. Input Description for High Temperature Radiant Heaters

The input for the high temperature radiant heater has two additive relationships that are assumed. First, the fractions of radiant, convective, latent, and lost heat must sum to unity. The user is required to enter the fractions radiant, latent, and lost with the remainder assumed to be convective energy. The fraction latent is added to the latent energy balance and will affect moisture levels within the zone. The fraction lost is assumed to have no impact on the energy balance of the zone and is assumed to be lost or vented to the exterior environment.

The second additive relationship is within the distribution of the radiant fraction. This energy is distributed to people and to the surfaces within the zone. The sum of all of these distribution fractions (the last six lines of input shown in Figure 77) must sum to unity. Note that each high temperature radiant heater is allowed to distribute energy to up to 20 surfaces and that radiant energy placed on a surface using these distribution fractions is assumed to be completely absorbed. Thus, the distribution fractions should also take into account any differences in long wavelength absorptivity among the surfaces.

Several things should be noted about the fraction of heat that is radiated directly to people. This parameter is somewhat sensitive and will have a direct impact on the thermal comfort models. This is exactly the intent of the high temperature radiant heaters; however, one must use caution when determining this fraction since overestimation of this number might lead to predictions of thermal comfort where in fact it does not exist. In addition, this fraction of radiant energy to people does not have a direct impact on any of the surface heat balances. The thermal comfort energy balance is completely separate from and has no bearing on the zone air or the surface heat balances. Thus, in order to not "lose" this amount of energy from the perspective of the zone air or the surface heat balances, the model assumes that any radiation from the high temperature radiant heater that is incident directly on people is accounted for in the thermal comfort model using Equation (1.277) but is also assumed to be added to the zone air heat balance via convection from people to the surrounding air. This guarantees that the people within the space feel the direct radiative effect of the heaters and that this quantity of energy is not "lost" within the heat balance routines.

Many of the control and integration aspects of the high temperature radiant system model in EnergyPlus are very similar to the low temperature radiant system model. The controls are the same as shown in "Figure 75. Low Temperature Radiant System Controls" where the

amount of heat generated by the radiant heater varies as a function of the difference between the controlling and the setpoint temperatures. As with the low temperature radiant system, the controlling temperature is allowed to be the mean air, the mean radiant, or the operative temperature, and the setpoint temperature is allowed to vary hourly based on a user defined schedule. Also, since the high temperature radiant heater has a direct impact on the surfaces within a zone, the surface heat balances are recalculated to determine an approximate response to the radiation from the heater. A final "average" heat balance calculation is done after all of the system time steps have been simulated to maintain continuity within the surface heat balances. The algorithm shown in "Figure 76. Resolution of Radiant System Response at Varying Time Steps is also used for high temperature radiant heaters.

References

Ceylan, H.T. and G.E. Myers. 1980. Long-time solutions to heat conduction transients with time-dependent inputs. ASME Journal of Heat Transfer, Volume 102, Number 1, pp. 115-120.

Degiovanni, A. 1988. Conduction dans un "mur" multicouche avec sources: extension de la notion de quadripole. International Journal of Heat and Mass Transfer, Volume 31, Number 3, pp. 553-557.

Fanger, P.O., Thermal Comfort-Analysis and Applications in Environmental Engineering, Danish Technical Press, Copenhagen, 1970.

Hittle, D.C. 1981. Calculating building heating and cooling loads using the frequency response of multilayered slabs. Ph.D. Thesis, Department of Mechanical and Industrial Engineering, University of Illinois at Urbana-Champaign and Technical Manuscript E-169, United States Army Construction Engineering Research Laboratory, Champaign, IL.

Hittle, D.C. and R. Bishop. 1983. An improved root-finding procedure for use in calculating transient heat flow through multilayered slabs. International Journal of Heat and Mass Transfer, Volume 26, Number 11, pp. 1685-1693.

Hottel, H.C. and A.F. Sarofim, Radiative Transfer, McGraw-Hill, New York, 1967.

Incropera, F.P. and D.P. DeWitt. 1985. Introduction to Heat Transfer. New York: John Wiley & Sons.

Lawrie, L.K., W.F. Buhl, D.E. Fisher, R.J. Liesen, R.K. Strand, and F.W. Winkelmann, "EnergyPlus Input Output Reference", Draft Publication, Lawrence Berkeley National Laboratories, Berkeley, CA, 2001.

Lee, J. and R.K. Strand, "An Analysis of the Effect of the Building Envelope on Thermal Comfort using the EnergyPlus Program", submitted for publication in the proceedings of the 2001 ACSA (Association of Collegiate Schools of Architecture) Technology Conference, Austin, TX.

Liesen, R.J. and C.O. Pedersen, "An Evaluation of Inside Surface Heat Balance Models for Cooling Load Calculations", ASHRAE Transactions, Volume 103, Part 2, 1997.

Maloney, D., "Development of a radiant heater model and the incorporation of thermal comfort considerations into the BLAST energy analysis program", M.S. thesis, University of Illinois at Urbana-Champaign, Department of Mechanical and Industrial Engineering, 1987.

McClellan, T.M. and C.O. Pedersen, "Investigation of Outside Heat Balance Models for Use in a Heat Balance Cooling Load Calculation Procedure", ASHRAE Transactions, Volume 103, Part 2, 1997.

Pedersen, C.O., D.E. Fisher, and R.J. Liesen, "Development of a Heat Balance Procedure for Cooling Loads", ASHRAE Transactions, Volume 103, Part 2, 1997.

Pedersen, C.O., D.E. Fisher, J.D. Spitler, and R.J. Liesen, Cooling and Heating Load Calculation Principles, ASHRAE, 1998.

Seem, J.E. 1987. Modeling of heat transfer in buildings. Ph.D. Thesis, University of Wisconsin-Madison.

Strand, R.K., and C.O. Pedersen, "Analytical verification of heat source transfer functions", First Joint Conference of International Simulation Societies, Zürich, Switzerland, 1994.

Strand, R.K., "Heat source transfer functions and their application to low temperature radiant heating systems", Ph.D. dissertation, University of Illinois at Urbana-Champaign, Department of Mechanical and Industrial Engineering, 1995.

Strand, R.K. and C.O. Pedersen, "Implementation of a Radiant Heating and Cooling Model into an Integrated Building Energy Analysis Program", ASHRAE Transactions, Volume 103, Part 1, 1997.

Strand, R.K. and C.O. Pedersen, "Modularization and Simulation Techniques for Heat Balance Based Energy and Load Calculation Programs: the Experience of the ASHRAE LOADS Toolkit and EnergyPlus", International Building Performance Simulation Association, Conference Proceedings of Building Simulation 2001, Rio de Janeiro, Brazil, 2001.

Taylor, R.D., C.O. Pedersen, D. Fisher, R. Liesen, and L. Lawrie, "Impact of simultaneous simulation of building and mechanical systems in heat balance based energy analysis programs on system response and control", International Building Performance Simulation Association, Conference Proceedings of Building Simulation 1991, Nice, France, 1991.

HVAC Models

Furnace : BlowThru : HeatOnly or HeatCool

Overview

The EnergyPlus blowthru furnace is a "virtual" component that consists of an ON-OFF fan component and a GAS or ELECTRIC heating coil component. If the HeatCool version is selected, then a DX cooling coil is also modeled as part of the system as shown in Figure 78 below. For the HeatCool version, an optional reheat coil may also be modeled for controlling high zone humidity levels and the furnace's configuration when specifying this option is shown in Figure 79 below.
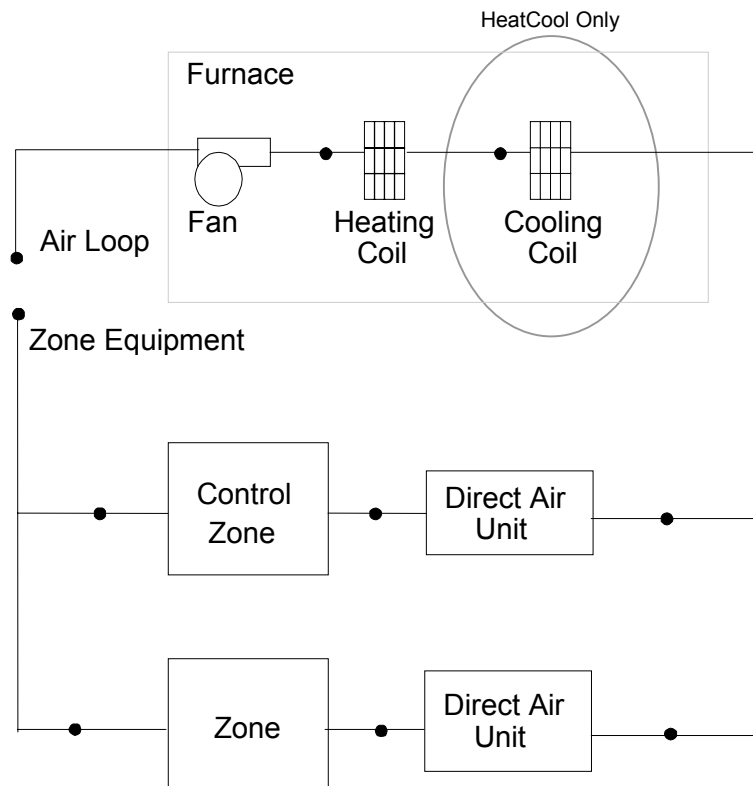
Figure 78. Schematic of the EnergyPlus Blowthru Furnace

While the furnace may be configured to serve multiple zones, system operation is controlled by a thermostat located in a single "control" zone. One of the key input parameters for the furnace component is the fraction of the total system volumetric air flow that goes through the controlling zone. The furnace module scales the calculated load for the control zone upward based on this fraction to determine the total load to be met by the furnace. The module then proceeds to calculate the required part-load ratio for the system coil and the supply air fan to meet this total load. The heating or cooling capacity delivered by the furnace is distributed to all of the zones served by this system via the direct air units that supply air to each zone.

The furnace component is able to model supply air fan operation in two modes: cycling fan – cycling coil (i.e., AUTO fan) and continuous fan – cycling coil (i.e., fan ON). The fan operation mode specified for the furnace must be similarly specified for the DX cooling coil if the HeatCool system is being modeled (see the IO Reference Manual for details). The heating

coil does not require fan operation mode as an input for either the HeatOnly or HeatCool configurations.

The only output variables reported by the furnace object are the fan part-load ratio and the compressor part-load ratio (HeatCool only). The fan part-load ratio is defined as the actual air mass flow rate through the system for the time step divided by the design mass flow rate specified for the furnace ($\dot{m}_{actual}/\dot{m}_{design}$). For the HeatCool version, the compressor part-load ratio is reported as the ratio of the actual cooling load to the full-load sensible capacity (see Eqn. (1.287)). Reporting of other variables of interest for the furnace (heating rate, cooling rate, energy consumption, etc.) is done by the individual system components (fan, heating coil and DX cooling coil).

Model Description

As described previously, the furnace is a "virtual" component consisting of a fan, heating coil and, for the HeatCool version, a cooling coil with an optional reheat coil. The sole purpose of the furnace model is to properly coordinate the operation of the various system components. The following sections describe the flow of information within the model for both the HeatOnly and HeatCool configurations, as well as the differences between cycling and continuous supply air fan operation. The last section describes the optional control of high zone humidity with a reheat coil for the HeatCool configuration.

HeatOnly Configuration

The HeatOnly configuration consists of an ON-OFF fan and an electric or gas heating coil. When the model is first called during an EnergyPlus simulation, all of the input data specified for each furnace in the input data file are read into data structures for use throughout the remainder of the simulation.

For each simulation time step when the performance of a heat-only furnace is being modeled, the first step is to retrieve the heating load required to meet the thermostat setpoint for the "control" zone (see Figure 78. Schematic of the EnergyPlus Blowthru Furnace). See the section "Summary of Predictor-Corrector Procedure" elsewhere in this document for more details regarding load calculations. Since the furnace may be specified to serve several zones but controlled based on the load calculated for the "control" zone, the total heating load to be met by the furnace is determined from the following equation:

$$Furnace\ Heating\ Load = \frac{Control\ Zone\ Heating\ Load}{Control\ Zone\ Air\ Flow\ Fraction} \qquad (1.278)$$

If the system is scheduled to operate for this simulation time step and a heating load exists, the model calculates the desired temperature exiting the heating coil. For the case with cycling supply air fan operation, the desired exiting air temperature is calculated as follows:

$$Temp\ Out\ Heating\ Coil_{cyc\ fan} = T_{inlet} + \frac{Design\ Heating\ Capacity + Full\ Load\ Fan\ Heat}{\left(c_{p,air}\right)\left(Design\ Mass\ Flow\ Rate\right)}$$

$$(1.279)$$

where

T_{inlet} = Dry-bulb temperature of air entering the furnace, °C

Design Heating Capacity = furnace heating capacity specified in the input data file, W

Full Load Fan Heat = heat added to the air stream from the supply air fan when operating at full-load conditions, W

$c_{p,air}$ = specific heat of entering air at T_{inlet} and humidity ratio ω_{inlet}, J/kg-°C

Design Mass Flow Rate = design volumetric air flow rate specified in the input data file converted to mass flow, kg/s

For the case of continuous supply air fan operation, the desired exiting air temperature is calculated slightly differently:

$$Temp\,Out\,Heating\,Coil_{cont\,fan} = MAT_{control\,zone} + \frac{Furnace\,Heating\,Load}{\left(c_{p,air}\right)\left(Mass\,Flow\,Rate\right)} \quad (1.280)$$

where

$MAT_{control\,zone}$ = Mean air dry-bulb temperature for the control zone, °C

Mass Flow Rate = mass flow rate through the furnace, kg/s

The different methods for calculating the desired exiting air temperature are due to the EnergyPlus methodology for modeling component performance. The EnergyPlus methodology for determining the impact that HVAC equipment has on an air stream is to calculate the mass flow rate and air properties (e.g., enthalpy, dry-bulb temperature, humidity ratio) exiting the equipment. These exiting conditions are passed along as inlet conditions to the next component model in the air stream. Eventually the flow rate and properties of the air being supplied to the conditioned zone are used in the zone energy balance to determine the resulting zone air temperature and humidity ratio.

With this methodology, the determination of the desired exiting air temperature for the two different supply air fan operation modes is slightly different. For the case of cycling fan/cycling coil, the conditions of the air leaving the heating coil are the steady-state values based on the design heater capacity, full load fan heat and the design air mass flow rate. For the case of continuous fan/cycling coil, the air mass flow rate is constant and the air temperature leaving the heating coil is calculated as the average dry-bulb temperature during the system simulation time step.

The increase in air temperature required to meet the heating load in the control zone is then calculated as follows:

$$\Delta T = MIN\left(Design\,Max\,Outlet\,Temp, Temp\,Out\,Heating\,Coil\right) - MAT_{control\,zone} \quad (1.281)$$

where

Design max outlet temp = the maximum supply air temperature specified for the furnace, °C

For the case of continuous fan operation, the mass flow rate through the system remains constant when it is scheduled to operate. For the case of cycling fan/cycling coil, the model calculates the average air mass flow rate through the furnace:

$$\dot{m}_{cyc\,fan} = \frac{Furnace\,Heating\,Load}{\left(c_{p,air}\right)\left(\Delta T\right)} \quad (1.282)$$

Based on the mass flow rate through the system from the above calculations, and the conditions of the air entering the furnace supply air fan, the model calculates the performance of the ON-OFF fan to determine the conditions of the air exiting the fan. The supply air fan motor adds a portion or all of its heat to the air stream depending on the input parameters specified for the fan. With the exiting air temperature from the fan now known, the remaining heating load to be met by the heating coil is calculated:

$$Heating\,Coil\,Load = \dot{m}\left(c_{p,air}\right)\left(Temp\,Out\,Heating\,Coil - T_{fan,out}\right) \quad (1.283)$$

The model then passes the calculated load for the heating coil to the heating coil model to determine the properties of the air leaving the heating coil and the energy required to meet the heating coil load.

For the case where the furnace is scheduled to operate with continuous supply air fan operation, but no heating load is required to meet the set point temperature in the control zone, the supply air fan model is still called to determine the fan exiting air conditions. The heating coil model is also called, but for the case with no heating load the heating coil model simply passes the inlet air conditions and mass flow rate from its inlet node to its outlet node. The air exiting the heating coil is then sent to the direct air units for distribution to each zone served by the furnace, where the zone heat balance is performed to determine the resulting zone air conditions.

HeatCool Configuration

The HeatCool configuration consists of an ON-OFF fan, an electric or gas heating coil, and a DX cooling coil. For the cases where a heating load is calculated for the control zone or no heating/cooling load is calculated for the control zone, the model follows the exact same computational steps as described in the HeatOnly Configuration section above. If a cooling load is calculated by EnergyPlus for the control zone, then the calculation procedure is slightly different and the methodology for this case is described here.

If EnergyPlus determines that the furnace must supply cooling to the control zone to meet the zone air temperature set point, then the model computes the total sensible cooling load to be met by the furnace based on the control zone sensible cooling load and the fraction of the furnace air flow that goes through the control zone.

$$Furnace\,Cooling\,Load = \frac{Control\,Zone\,Cooling\,Load}{Control\,Zone\,Air\,Flow\,Fraction} \qquad (1.284)$$

The model then calculates the furnace's sensible cooling energy rate delivered to the zones being served when the system runs at full-load conditions and when the DX cooling coil is OFF. If the supply air fan cycles with the compressor, then the sensible cooling energy rate is zero when the cooling coil is OFF. However if the fan is configured to run continuously regardless of coil operation, then the sensible cooling energy rate will not be zero when the cooling coil is OFF. Calculating the sensible cooling energy rate involves modeling the supply air fan (and associated fan heat), the heating coil (simply to pass the air properties and mass flow rate from its inlet node to its outlet node) and the DX cooling coil. For each of these cases (full load and DX cooling coil OFF), the sensible cooling energy rate delivered by the furnace is calculated as follows:

$$Full\,Cool\,Output = \left(Mass\,Flow\,Rate_{full\,load}\right)\left(h_{out,\,full\,load} - h_{control\,zone}\right)_{HR\min} \quad (1.285)$$

$$No\,Cool\,Output = \left(Mass\,Flow\,Rate_{coil\,off}\right)\left(h_{out,\,coil\,off} - h_{control\,zone}\right)_{HR\min} \quad (1.286)$$

where

$Mass\,Flow\,Rate_{full\,load}$ = air mass flow rate through furnace at full-load conditions, kg/s

$h_{out,\,full\,load}$ = enthalpy of air exiting the furnace at full-load conditions, J/kg

$h_{control\,zone}$ = enthalpy of air leaving the control zone (where thermostat is located), J/kg

HR_{min} = enthalpies evaluated at a constant humidity ratio, the minimum humidity ratio of the heat pump exiting air or the air leaving the control zone

$Mass\,Flow\,Rate_{coil\,off}$ = air mass flow rate through the furnace with the cooling coil OFF, kg/s

$h_{out,\,coil\,off}$ = enthalpy of air exiting the furnace with the cooling coil OFF, J/kg

With the calculated sensible cooling energy rates and the total sensible cooling load to be met by the system, the part-load ratio for the furnace is estimated.

$$PartLoadRatio = MAX\left(0.0, \frac{ABS\left(FurnaceCoolingLoad - NoCoolOutput\right)}{ABS\left(FullCoolOutput - NoCoolOutput\right)}\right) \quad (1.287)$$

Since the part-load performance of the DX cooling coil is frequently non-linear (Ref: DX Cooling Coil Model), and the supply air fan heat varies based on cooling coil operation for the case of cycling fan/cycling coil (AUTO fan), the final part-load ratio for the cooling coil compressor and fan are determined through iterative calculations (successive modeling of the cooling coil and fan) until the furnace's cooling output matches the cooling load to be met within the cooling convergence tolerance that is specified. The furnace exiting air conditions and energy consumption are calculated and reported by the individual component models (on/off fan and DX cooling coil).

If the furnace has been specified with cycling fan/cycling coil (AUTO fan), then the furnace's design air mass flow rate is multiplied by PartLoadRatio to determine the average air mass flow rate for the system simulation time step. The air conditions at nodes downstream of the cooling coil represent the full-load (steady-state) values when the coil is operating. If the supply air fan is specified to run continuously (fan ON), then the air mass flow rate remains at the furnace's design air mass flow rate. In this case, the air conditions at nodes downstream of the cooling coil are calculated as the average conditions over the simulation time step (i.e., the weighted average of full-load conditions when the coil is operating and inlet air conditions when the coil is OFF).

High Humidity Control with HeatCool Configuration

An optional reheat coil can be specified with the HeatCool configuration to allow the furnace to control high zone humidity levels. The specific configuration of the blowthru HeatCool Furnace with high humidity control option is shown in Figure 79. The system is controlled to keep the relative humidity in the control zone from exceeding the set point specified in the object ZONE CONTROL:HUMIDISTAT. This option is only available with a fan operating mode of ContFanCycCoil (fan ON continuously).

The model first calculates the PartLoadRatio required to meet the sensible cooling load as described above (see Eqn. (1.287)) to maintain the dry-bulb temperature set point in the control zone. If a moisture (latent) load exists because the control zone humidity has exceeded the set point, the total moisture load to be met by the heatcool furnace (*SystemMoistureLoad*) is calculated based on the control zone moisture load and the control zone air flow fraction. The model then calculates the LatentPartLoadRatio required to meet the humidistat set point.

$$SystemMoistureLoad = \frac{Control\,Zone\,Moisture\,Load}{Control\,Zone\,Air\,Flow\,Fraction} \quad (1.288)$$

$$LatentPartLoadRatio = MAX\left(0.0, \frac{ABS\left(SystemMoistureLoad - NoLatentOutput\right)}{ABS\left(FullLatentOutput - NoLatentOutput\right)}\right) \quad (1.289)$$

where

FullLatentOutput   = the furnace's latent cooling energy rate at full-load conditions, W

NoLatentOutput   = the furnace's latent cooling energy rate with the cooling coil OFF, W

The model uses the greater of the two part-load ratios, PartLoadRatio or LatentPartLoadRatio, to determine the operating part-load ratio of the furnace's DX cooling

coil. As previously described, iterations are performed to converge on the solution within the specified cooling convergence tolerance.
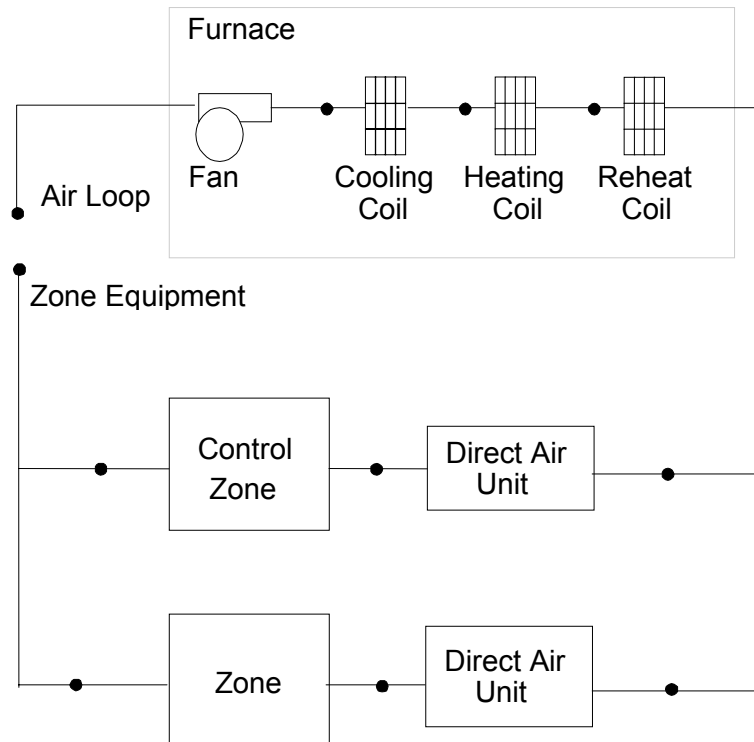
Figure 79. Schematic for Blow Thru Furnace with High Humidity Control

If the model determines that the LatentPartLoadRatio is to be used as the operating part-load ratio of the furnace's cooling coil, the reheat coil is used to offset the excess sensible capacity provided by the unit. The model first checks to see if a sensible cooling load or sensible heating load exists for the current simulation time step. If a sensible cooling load exists, the model calculates the difference between the actual sensible cooling energy rate delivered by the unit (with LatentPartLoadRatio) and the sensible cooling load to be met. In this case, the reheat coil is used to meet the excess sensible cooling energy provided by the DX cooling coil. If a heating load exists, the reheat coil is used to offset the entire sensible cooling energy rate of the DX cooling coil (to meet the humidistat set point) and the heating coil is used to meet the entire heating load as described in the HeatOnly configuration section above. As with the fan, DX cooling coil, and heating coil, report variables associated with reheat coil performance (e.g., heating coil energy, heating coil rate, heating coil gas or electric consumption, heating coil runtime fraction, etc.) are managed in the reheat (heating) coil object.

UnitarySystem : BlowThru : HeatOnly or HeatCool

The Unitary System models are identical to the equivalently named Furnace models. Please reference the previous section for details.

Air Loop:UnitarySystem : HeatPump : AirToAir

Overview

The EnergyPlus air-to-air heat pump is a "virtual" component that consists of an ON-OFF fan component, a DX cooling coil, a DX heating coil, and a gas or electric supplemental heating

coil. The specific configuration of the blowthru heat pump is shown in the following figure. For a drawthru heat pump, the fan is located between the DX heating coil and the supplemental heating coil.
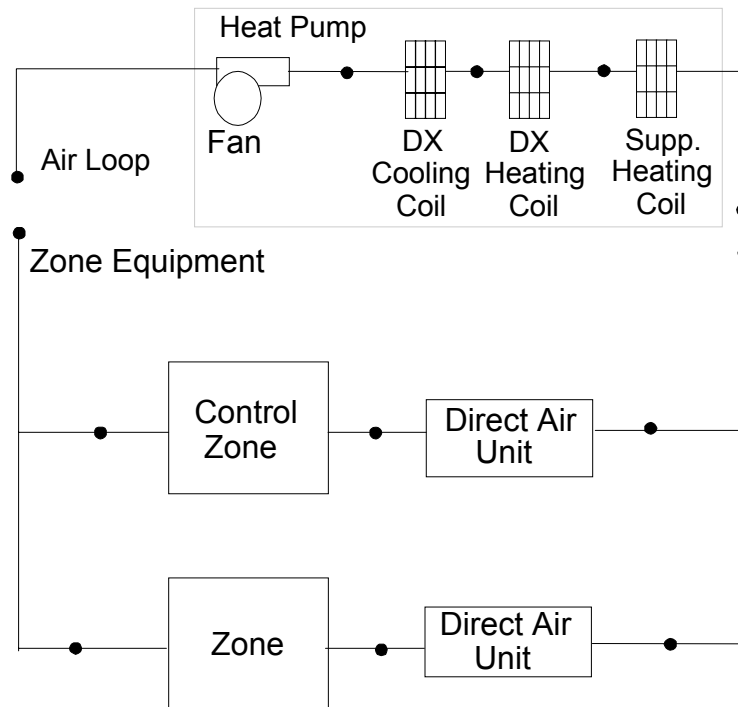
Figure 80. Schematic of a Blowthru Air-to-Air Heat Pump

While the heat pump may be configured to serve multiple zones, system operation is controlled by a thermostat located in a single "control" zone. One of the key input parameters for the heat pump component is the fraction of the total system volumetric airflow that goes through the controlling zone. The heat pump module scales the calculated load for the control zone upward based on this fraction to determine the total load to be met by the heat pump. The module then proceeds to calculate the required part-load ratio for the system coil and the supply air fan to meet this total load. The heating or cooling capacity delivered by the heat pump is distributed to all of the zones served by this system via the direct air units that supply air to each zone.

The heat pump component is able to model supply air fan operation in two modes: cycling fan – cycling coil (i.e., AUTO fan) and continuous fan – cycling coil (i.e., fan ON). The fan operation mode specified for the heat pump must be similarly specified for the DX cooling and DX heating coils being modeled (see the IO Reference Manual for details).

The output variables reported by the heat pump object are fan part-load ratio and compressor part-load ratio. Fan part-load ratio is defined as the actual air mass flow rate through the system for the time step divided by the design mass flow rate specified for the heat pump ($\dot{m}_{actual}/\dot{m}_{design}$). Compressor part-load ratio is the actual load for the time step divided by the full-load sensible capacity (see Eqn. (1.293) or Eqn.(1.297)). Reporting of other variables of interest for the heat pump (heating rate, cooling rate, energy consumption, etc.) is done by the individual system components (fan, DX cooling coil, DX heating coil, and supplemental heating coil).

Model Description

As described previously, the heat pump is a "virtual" component consisting of a fan, DX cooling coil, DX heating coil and a supplemental heating coil. The sole purpose of the heat pump model is to properly coordinate the operation of the various system components. The following sections describe the flow of information within the model, as well as the differences between cycling and continuous supply air fan operation.

Cooling Operation

If EnergyPlus determines that the heat pump must supply cooling to the control zone to meet the zone air temperature set point, then the heat pump model computes the total sensible cooling load to be delivered to the zones being served based on the control zone sensible cooling load and the fraction of the heat pump air flow that goes through the control zone.

$$Heat\,Pump\,Cooling\,Load = \frac{Control\,Zone\,Cooling\,Load}{Control\,Zone\,Air\,Flow\,Fraction} \qquad (1.290)$$

The model then calculates the heat pump's sensible cooling energy rate delivered to the zones being served when the system runs at full-load conditions and when the DX cooling coil is OFF. If the supply air fan cycles with the compressor, then the sensible cooling energy rate is zero when the cooling coil is OFF. However if the fan is configured to run continuously regardless of coil operation, then the sensible cooling energy rate will not be zero when the cooling coil is OFF. Calculating the sensible cooling energy rate involves modeling the supply air fan (and associated fan heat) and the DX cooling coil. The DX heating coil and the supplemental heating coil are also modeled, but only to pass the air properties and mass flow rate from their inlet nodes to their outlet nodes. For each of these cases (full load and DX cooling coil OFF), the sensible cooling energy rate delivered by the heat pump is calculated as follows:

$$Full\,Cool\,Output = \left(Mass\,Flow\,Rate_{full\,load}\right)\left(h_{out,\,full\,load} - h_{control\,zone}\right)_{HR\min} \qquad (1.291)$$

$$No\,Cool\,Output = \left(Mass\,Flow\,Rate_{coil\,off}\right)\left(h_{out,coil\,off} - h_{control\,zone}\right)_{HR\min} \qquad (1.292)$$

where

$Mass\,Flow\,Rate_{full\,load}$ = air mass flow rate through heat pump at full-load conditions, kg/s

$h_{out,\,full\,load}$ = enthalpy of air exiting the heat pump at full-load conditions, J/kg

$h_{control\,zone}$ = enthalpy of air leaving the control zone (where thermostat is located), J/kg

HR_{min} = enthalpies evaluated at a constant humidity ratio, the minimum humidity ratio of the heat pump exiting air or the air leaving the control zone

$Mass\,Flow\,Rate_{coil\,off}$ = air mass flow rate through the heat pump with the cooling coil OFF, kg/s

$h_{out,coil\,off}$ = enthalpy of air exiting the heat pump with the cooling coil OFF, J/kg

With the calculated sensible cooling energy rates and the total sensible cooling load to be met by the system, the part-load ratio for the heat pump is estimated.

$$PartLoadRatio = MAX \left(0.0, \frac{ABS \left(Heat\ Pump\ Cooling\ Load - NoCoolOutput \right)}{ABS \left(FullCoolOutput - NoCoolOutput \right)} \right)$$

(1.293)

Since the part-load performance of the DX cooling coil is frequently non-linear (Ref: DX Cooling Coil Model), and the supply air fan heat varies based on cooling coil operation for the case of cycling fan/cycling coil (AUTO fan), the final part-load ratio for the cooling coil compressor and fan are determined through iterative calculations (successive modeling of the cooling coil and fan) until the heat pump's cooling output matches the cooling load to be met within the cooling convergence tolerance that is specified. The heat pump exiting air conditions and energy consumption are calculated and reported by the individual component models (on/off fan and DX cooling coil).

If the heat pump has been specified with cycling fan/cycling coil (AUTO fan), then the heat pump's design air mass flow rate is multiplied by PartLoadRatio to determine the average air mass flow rate for the system simulation time step. The air conditions at nodes downstream of the cooling coil represent the full-load (steady-state) values when the coil is operating. If the supply air fan is specified to run continuously (fan ON), then the air mass flow rate remains at the heat pump's design air mass flow rate. In this case, the air conditions at nodes downstream of the cooling coil are calculated as the average conditions over the simulation time step (i.e., the weighted average of full-load conditions when the coil is operating and inlet air conditions when the coil is OFF).

Heating Operation

Calculations for heating operation are similar to those for cooling operation in most respects. However, due to the inclusion of a supplemental heating coil, additional calculations are necessary to properly meet the total heating load for the zones being served.

If EnergyPlus determines that the heat pump must supply heating to the control zone to meet the zone air temperature set point, then the heat pump model computes the total sensible heating load to be delivered to the zones being served based on the control zone sensible heating load and the control zone airflow fraction.

$$Heat\ Pump\ Heating\ Load = \frac{Control\ Zone\ Heating\ Load}{Control\ Zone\ Air\ Flow\ Fraction}$$

(1.294)

The model then calculates the heat pump's sensible heating energy rate delivered to the zones being served when the system runs at full-load conditions and when the DX heating coil is OFF (without supplemental heater operation in either case). If the supply air fan cycles with the compressor, then the sensible heating energy rate is zero when the compressor is OFF. However if the fan is configured to run continuously regardless of coil operation, then the sensible heating energy rate will not be zero when the compressor is OFF. Calculating the sensible heating energy rate involves modeling the supply air fan (and associated fan heat), the DX cooling coil (simply to pass the air properties and mass flow rate from its inlet node to its outlet node), the DX heating coil, and the supplemental heating coil (simply to pass the air properties and mass flow rate from its inlet node to its outlet node). For each of these cases (full load and DX heating coil OFF, without supplemental heater operation in either case), the sensible heating energy rate delivered by the heat pump is calculated as follows:

$$Full\ Heat\ Output = \left(Mass\ Flow\ Rate_{full\ load} \right) \left(h_{out,full\ load} - h_{control\ zone} \right)_{HR\min}$$

(1.295)

$$No\ Heat\ Output = \left(Mass\ Flow\ Rate_{coil\ off}\right)\left(h_{out,coil\ off} - h_{control\ zone}\right)_{HR\min}$$

(1.296)

where

$Mass\ Flow\ Rate_{full\ load}$ = air mass flow rate through heat pump at full-load conditions, kg/s

$h_{out,\ full\ load}$ = enthalpy of air exiting the heat pump at full-load conditions, J/kg

$h_{control\ zone}$ = enthalpy of air leaving the control zone (where thermostat is located), J/kg

HR_{min} = enthalpies evaluated at a constant humidity ratio, the minimum humidity ratio of the heat pump exiting air or the air leaving the control zone

$Mass\ Flow\ Rate_{coil\ off}$ = air mass flow rate through the heat pump with the heating coil OFF, kg/s

$h_{out,\ coil\ off}$ = enthalpy of air exiting the heat pump with the heating coil OFF, J/kg

With the calculated sensible heating energy rates and the total sensible heating load to be met by the system, the part-load ratio for the heat pump is estimated.

$$PartLoadRatio = MAX\left(0.0, \frac{ABS\left(Heat\ Pump\ Heating\ Load - NoHeatOutput\right)}{ABS\left(FullHeatOutput - NoHeatOutput\right)}\right)$$

(1.297)

Since the part-load performance of the DX heating coil is frequently non-linear (Ref: DX Heating Coil Model), and the supply air fan heat varies based on heating coil operation for the case of cycling fan/cycling coil (AUTO fan), the final part-load ratio for the heating coil compressor and fan are determined through iterative calculations (successive modeling of the heating coil and fan) until the heat pump's heating output matches the heating load to be met within the heating convergence tolerance that is specified. The heat pump exiting air conditions and energy consumption are calculated and reported by the individual component models (on/off fan and DX heating coil).

If the heat pump's DX heating coil output at full load is insufficient to meet the entire heating load, PartLoadRatio is set equal to 1.0 (compressor and fan are not cycling) and the remaining heating load is passed to the supplemental heating coil. If the heat pump model determines that the outdoor air temperature is below the minimum outdoor air temperature for compressor operation (Ref: DX Heating Coil Model), the compressor is turned off and the entire heating load is passed to the supplemental gas or electric heating coil.

If the heat pump has been specified with cycling fan/cycling coil (AUTO fan), then the heat pump's design air mass flow rate is multiplied by PartLoadRatio to determine the average air mass flow rate for the system simulation time step. The air conditions at nodes downstream of the heating coils represent the full-load (steady-state) values when the coils are operating. If the supply air fan is specified to run continuously (fan ON), then the air mass flow rate remains at the heat pump's design air mass flow rate. In this case, the air conditions at nodes downstream of the heating coils are calculated as the average conditions over the simulation time step (i.e., the weighted average of full-load conditions when the coils are operating and inlet air conditions when the coils are OFF).

Coil Models

Detailed Cooling Coil

In order to provide this simulation capability, a coil model that predicts changes in air and water flow variables across the coil based on the coil geometry is required. A greatly simplified schematic of enthalpy and temperature conditions in a counterflow cooling/dehumidifying coil is shown in the following schematic figure. In addition, the

variables required to model a cooling/dehumidifying coils and their definitions are extensively listed in "Table 31. Coil Geometry and flow variables for coils". The input required to model the coil includes a complete geometric description that, in most cases, should be derivable from specific manufacturer's data. The coil simulation model is essentially the one presented by Elmahdy and Mitalas (1977) and implemented in HVACSIM+ (Clark, 1985), a modular program also designed for energy analysis of building systems. The model solves the equations for the dry and wet sections of the coil using log mean temperature and log mean enthalpy differences between the liquid and the air streams. Elmahdy and Mitalas state that crossflow counterflow coils with at four rows or more are approximated well by this model. This does not constitute a major limitation since cooling and dehumidifying coils typically have more than four rows.
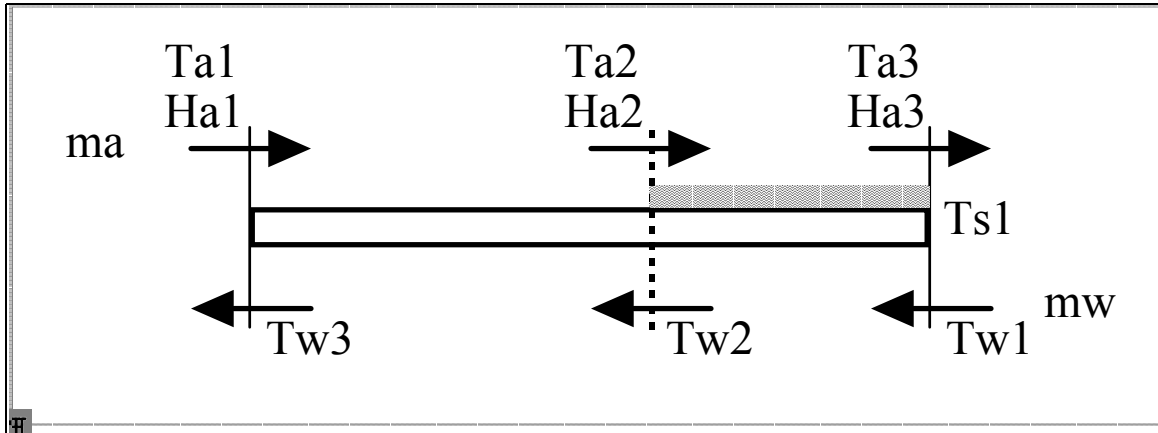
Figure 81. Simplified Schematic of Cooling/Dehumidifying Coil

Heat Transfer and Energy Balance

The cooling coil may be completely dry, completely wet with condensation, or it may have wet and dry sections. The actual condition of the coil surface depends on the humidity and temperature of the air passing over the coil and the coil surface temperature. The partly wet-partly dry case represents the most general scenario for the coil surface conditions. The all dry and all wet cases can be considered as limiting solutions of the wet or dry areas respectively going to zero. In the general case, equations are written for both the dry and wet regions of the coil. For each region the heat transfer rate from air to water may be defined by the rate of enthalpy change in the air and in the water. The rates must balance between each medium for energy to be conserved. Equations (1.298) through (1.301) express the energy balance between the water and the air for the case of dry and wet coils respectively. Equations (1.302) and (1.303) represent the heat transfer rate between water and air based on the actual performance of the coil. The UA parameter can be calculated from the parameters in the following table.

Table 31. Coil Geometry and flow variables for coils

A	area	LMHD	log mean enthalpy difference
A	air, air side	LMTD	log mean temperature difference
aa, bb	coeff. in enthalpy approximation	$\dot{m}$	mass flow rate
C1, C2	coeff. in air side film coeff.	mf	metal and fouling
Cp	specific heat	μ	viscosity
D	diameter, effective diameter	o	outside (air side)
Dhdr	hydraulic diameter on air side	Pr	Prandtl number
D	dry region	$\dot{Q}$	heat transfer rate

δ	thickness	R	overall thermal resistance
Δ	spacing	Re	Reynolds number
F	heat transfer film coefficient	ρ	ratio of diameters
Fai	variable in fin eff. calculation	s	surface, outside of metal
fin, fins	air side fin geometry	St	Stanton number
H	enthalpy	T	temperature
η	efficiency	tube	water tube
I0()	mod Bessel fn, 1st kind, ord 0	UAdry	dry heat xfer coeff. * dry area
I1()	mod Bessel fn, 1st kind, ord 1	UcAw	wet heat xfer coeff. * wet area
K0()	mod Bessel fn, 2nd kind, ord 0	ub, ue	variables in fin eff. calculation
K1()	mod Bessel fn, 2nd kind, ord 1	V	average velocity
I	inside (water side)	w	water, water side, or wet region
K1	variable in sol'n form of eq.	wa	humidity ratio
K	thermal conductivity	Z	variables in sol'n form of eq.
L	length	1, 2, 3	positions (see diagram)

Equations (1.298) through (1.303) represent two sets of three equations with 7 unknowns: $\dot{Q}_d$, $T_{a,1}$, $T_{a,2}$, $T_{w,2}$, $T_{w,3}$, $\dot{m}_a$, $\dot{m}_w$. However, normally at least four of these variables are specified, for example: inlet water temperature, outlet air temperature, water flow rate, air flow rate, so that the system of equations is effectively closed.

$$\dot{Q}_d = m_a Cp_a \left(T_{a,1} - T_{a,2} \right) \tag{1.298}$$

$$\dot{Q}_d = m_w Cp_w \left(T_{w,3} - T_{w,2} \right) \tag{1.299}$$

$$\dot{Q}_d = \left(UA_{dry} \right) \left(LMTD \right) \tag{1.300}$$

$$\dot{Q}_w = m_a \left(H_{a,2} - H_{a,3} \right) \tag{1.301}$$

$$\dot{Q}_w = m_w Cp_w \left(T_{w,2} - T_{w,1} \right) \tag{1.302}$$

$$\dot{Q}_w = \left(U_c A_w \right) \left(LMHD \right) \tag{1.303}$$

In order to manipulate these equations, the log mean temperature and enthalpy differences are expanded as shown in Equations (1.304) and (1.305). Finally, a linear approximation of the enthalpy of saturated air over the range of surface temperature is made using Equation (1.306). Note that in Equation (1.305) H_w refers to the enthalpy of saturated air at the water temperature.

$$LMTD = \frac{\left(T_{a,1} - T_{w,3} \right) - \left(T_{a,2} - T_{w,2} \right)}{\ln \dfrac{T_{a,1} - T_{w,3}}{T_{a,2} - T_{w,2}}} \tag{1.304}$$

$$LMHD = \frac{\left(H_{a,2} - H_{w,2}\right) - \left(H_{a,3} - H_{w,1}\right)}{\ln \dfrac{H_{a,2} - H_{w,2}}{H_{a,3} - H_{w,1}}} \tag{1.305}$$

$$H_w = aa + bb\, T_w \tag{1.306}$$

Equation (1.307) is derived from the above equations and is used to solve for the coil conditions when all of the inlet conditions are given as input. Operating in this manner, the coil does not have a controlled outlet air temperature.

$$T_{w,2} = \frac{(1-Z)\left(H_{a,1} - aa - K1\, Cp_a\, T_{a,1}\right) + Z\, T_{w,1}\left(bb - \dfrac{m_w Cp_w}{m_a}\right)}{bb - Z\dfrac{m_w Cp_w}{m_a} - (1-Z)\, K1\, Cp_a} \tag{1.307}$$

An alternative solution method is to define the coil leaving air temperature as an input with a variable water flow rate. In this case Equations (1.308) and (1.309) are more convenient. Equations (1.310) through (1.312) define terms that are used to simplify Equations (1.307), (1.308) and (1.309).

$$T_{w,2} = \frac{(1-Z)\left(H_{a,3} - aa\right) + T_{w,1}\left(\dfrac{m_w Cp_w}{m_a} - bb\, Z\right)}{\dfrac{m_w Cp_w}{m_a} - bb} \tag{1.308}$$

$$T_{w,2} = \frac{(Z_d - 1)\, T_{a1} Cp_a + T_{w,3}\left(Cp_a - Z_d \dfrac{m_w Cp_w}{m_a}\right)}{Z_d\left(Cp_a - \dfrac{m_w Cp_w}{m_a}\right)} \tag{1.309}$$

$$Z = \exp\left(U_c A_w \left(\frac{1}{m_a} - \frac{bb}{m_w Cp_w}\right)\right) \tag{1.310}$$

$$K1 = \frac{Z_d - 1}{Z_d - \dfrac{m_a Cp_a}{m_w Cp_w}} \tag{1.311}$$

$$Z_d = \exp\left(U_c A_{dry}\left(\frac{1}{m_a Cp_a} - \frac{1}{m_w Cp_w}\right)\right) \tag{1.312}$$

Underlying Correlations, Properties, and Assumptions

Overall heat transfer coefficients are calculated from the specified coil geometry and by using empirical correlations from fluid mechanics and heat transfer. For the water side, Equation (1.313) gives the film heat transfer coefficient in SI units:

$$f_i = 1.429 \left(1 + 0.0146\, T_w\right) V_w^{0.8} D_i^{-0.2} \tag{1.313}$$

This is valid for Reynolds numbers greater than 3100 based on water flow velocity and pipe inside diameter and is given in Elmahdy and Mitalas (1977) as recommended in the standard issued by the Air-Conditioning and Refrigeration Institute (1972) for air-cooling coils. The definition of overall inside thermal resistance follows directly as shown in Equation(1.314).

$$R_i = \frac{1}{f_i A_i} \tag{1.314}$$

Equation (1.315) gives the film coefficient for the air side. Another form of the same equation is Equation (1.316), which is familiar from the data presented in Kays and London (1984). For coil sections that have a wet surface due to condensation, the air side film coefficient is modified according to Equation (1.317). The correction term, a function of air Reynolds number, is valid for Reynolds numbers between 400 and 1500. The coefficients in Equation (1.315) and (1.316) are calculated by Equations (1.318) and (1.319) that are functions of the coil geometry. Elmahdy (1977) explains the modifier for the wet surface and coefficients for the film coefficient. Equations (1.320) through (1.323) show definitions and values of common parameters and properties.

$$f_o = C_1 Re_a^{C_2} \frac{m_a}{A_{a\_min\_flow}} Cp_a Pr_a^{2/3} \tag{1.315}$$

$$C_1 Re_a^{C_2} = St_a Pr_a^{2/3} \tag{1.316}$$

$$f_{o,w} = f_o \left(1.425 - 5.1 \times 10^{-4} Re_a + 2.63 \times 10^{-7} Re_a^2\right) \tag{1.317}$$

$$C_1 = 0.159 \left(\frac{\delta_{fin}}{D_{hdr}}\right)^{-0.065} \left(\frac{\delta_{fin}}{L_{fin}}\right)^{0.141} \tag{1.318}$$

$$C_2 = -0.323 \left(\frac{\Delta_{fins}}{L_{fin}}\right)^{0.049} \left(\frac{D_{fin}}{\Delta_{tube\_rows}}\right)^{0.549} \left(\frac{\delta_{fin}}{\Delta_{fins}}\right)^{-0.028} \tag{1.319}$$

$$D_{hdr} = \frac{4 A_{a\_min\_flow} \delta_{coil}}{A_{s\_total}} \tag{1.320}$$

$$Re_a = \frac{4 \delta_{coil} \left(1 + w_a\right) m_a}{A_{s\_total} \mu_a} \tag{1.321}$$

$$Pr_a = 0.733 \tag{1.322}$$

$$\mu_a = 1.846 \times 10^{-5} \tag{1.323}$$

The film coefficients above act on the extended surface of the air side, that is the area of the fins and the tubes. Therefore, the fin efficiency must also be considered in calculating the overall thermal resistance on the outside. Gardner (1945) gives the derivation of Equation (1.324), used as a curve fit to find the fin efficiency as a function of film coefficient. This equation is based on circular fins of constant thickness. To model a coil with flat fins, an effective diameter -- that of circular fins with the same fin area -- is used. Equations (1.325) through (1.328) define variables used in Equation (1.324). The overall efficiency of the surface is shown by Equation (1.329). Note that the efficiency is found by the same equations for the wet surface using the wet surface film coefficient.

$$\eta_{fin} = \frac{-2\rho}{fai(1+\rho)} \left[\frac{I_1(u_b)K_1(u_e) - K_1(u_b)I_1(u_e)}{I_0(u_b)K_1(u_e) + K_0(u_b)I_1(u_e)} \right] \tag{1.324}$$

$$fai = \frac{(D_{fin} - D_{tube})}{2} \sqrt{\frac{2f_o}{k_{fin}\delta_{fin}}} \tag{1.325}$$

$$\rho = \frac{D_{tube}}{D_{fin}} \tag{1.326}$$

$$u_e = \frac{fai}{1-\rho} \tag{1.327}$$

$$u_b = u_e\rho \tag{1.328}$$

$$\eta_o = 1 - (1-\eta_{fin})\frac{A_{fins}}{A_{s\_total}} \tag{1.329}$$

The definition of overall outside thermal resistance is given in Equation (1.330) as a function of fin efficiency and film coefficient. For a wet coil surface the resistance must be defined differently because the heat transfer equations are based on enthalpy rather than temperature differences, as shown in Equation (1.331).

$$R_o = \frac{1}{f_o\eta_o A_{s,total}} \tag{1.330}$$

$$R_{o,w} = \frac{Cp_a/bb}{f_{o,w}\eta_{o,w}A_{s,total}} \tag{1.331}$$

Equation (1.332) gives the last two overall components of thermal resistance. They represent the metal tube wall and internal fouling. The fouling factor, due to deposits of dirt

and corrosion of the tube inside surfaces, is assumed to be 5×10^{-5} m$^2 \cdot$K/W. All components of thermal resistance are added in series to produce the overall heat transfer coefficients shown in Equations (1.333) and (1.334).

$$R_{mf} = \frac{\delta_{tube}}{k_{tube} A_i} + \frac{Fl}{A_i} \qquad (1.332)$$

$$UA_{dry} = \frac{A_{dry}}{A_{s,total}} \left[\frac{1}{R_i + R_{mf} + R_o} \right] \qquad (1.333)$$

$$U_c A_w = \frac{A_w}{A_{s,total}} \left[\frac{1/bb}{R_i + R_{mf} + R_{o,w}} \right] \qquad (1.334)$$

Solution Method of Model

The complicated equations derived above were implemented in a successive substitution solution procedure to calculate the coil performance based on the input parameters. The MODSIM implementation of a cooling coil, the TYPE12 subroutine, was the motivation for this approach; the method used there has been retained with modifications for the uncontrolled coil model. Clark (1985) contains notes about the MODSIM routine.

In the general case, the cooling coil is only partially wet. For an uncontrolled coil, Equation (1.307) is used to find the water temperature at the boundary. Several simple equations in the loop adjust the boundary point until the dry surface temperature at the boundary is equal to the dew point of the inlet air. For the controlled coil, Equations (1.308) and (1.309) give two calculations of the boundary temperature, and the water flow rate and boundary position are adjusted until the two equations agree.

Special cases occur when the coil is all wet or all dry. The coil is solved as if it were all wet before the general case is attempted. If the wet surface temperatures at the coil inlet and outlet are both below the dew point, no further solution is required. However, to ensure a continuous solution as flow variables are changed, when the surface is all dry or when it is wet with only the dry surface equations yielding a surface temperature below the dew point at the water outlet, the general solution is used to calculate the unknowns. In the solution of the controlled coil the outlet air enthalpy, given some resulting dehumidification, must correspond to the enthalpy at the specified outlet air temperature.

Application of Cooling Coil Model to Heating Coils

The implementation of detailed heating coil models in IBLAST was another important aspect of the system/plant integration. The same kind of loops exist to provide hot water to the heating coils from the boilers as exist to supply the cooling coils with chilled water from the chillers. Some simplifications can be made, however, since the enthalpy change of the air flowing over a heating coil is entirely sensible. There is no condensation in a heating coil. In order to allow heating and cooling coils to be specified using the same geometric parameters, a heating coil simulation was developed from the cooling coil model described above by eliminating the wet surface analysis.

In addition, it was concluded that, since much simpler and less computationally expensive heating coil simulations are possible, an option was provided in IBLAST for a heating coil design using only the UA value of the coil, the product of heat transfer coefficient and coil area. This model was largely based on the TYPE10 subroutine implemented in MODSIM. The equations used to model the performance of the TYPE10 heating coil are as follows:

$$T_{a,out} = T_{a,in} + \left(T_{w,in} - T_{ain}\right)\varepsilon\left(\frac{\min\left(C_{p,a}\dot{m}_a, C_{p,w}\dot{m}_w\right)}{C_{p,a}\dot{m}_a}\right)$$

$$T_{w,out} = T_{w,in} - \left(T_{a,out} - T_{ain}\right)\left(\frac{C_{p,a}\dot{m}_a}{C_{p,w}\dot{m}_w}\right)$$

(1.335)

where the coil effectiveness is given by:

$$\varepsilon = 1 - \exp\left(\frac{\left\{\exp\left[-\left(\frac{\min\left\{C_{p,a}\dot{m}_a, C_{p,w}\dot{m}_w\right\}}{\max\left\{C_{p,a}\dot{m}_a, C_{p,w}\dot{m}_w\right\}}\right)\left\{NTU\right\}^{0.78}\right]-1\right\}}{\left(\frac{\min\left\{C_{p,a}\dot{m}_a, C_{p,w}\dot{m}_w\right\}}{\max\left\{C_{p,a}\dot{m}_a, C_{p,w}\dot{m}_w\right\}}\right)\left\{NTU\right\}^{-.22}}\right)$$

(1.336)

The parameter NTU is the number of transfer units and is defined as a function of the UA value of the coil as follows:

$$NTU = \frac{UA}{\min\left(C_{p,a}\dot{m}_a, C_{p,w}\dot{m}_w\right)}$$

(1.337)

DX Heating Coil Model

Overview

This model (object name Coil:DX:HeatingEmpirical) simulates the performance of an air-to-air direct expansion (DX) heating system. The model uses performance information at rated conditions along with curve fits for variations in total capacity, energy input ratio and part-load fraction to determine the performance of the unit at part-load conditions (DOE 1982). Adjustment factors are applied to total capacity and input power to account for frost formation on the outdoor coil.

This model simulates the thermal performance of the indoor DX heating coil, and the power consumption of the outdoor unit (compressors and fans). The performance of the indoor supply air fan varies widely from system to system depending on control strategy (e.g., constant fan vs. AUTO fan, constant air volume vs. variable air volume, etc.), fan type, fan motor efficiency and pressure losses through the air distribution system. Therefore, this DX system model does not account for the thermal effects or electric power consumption of the indoor supply air fan. EnergyPlus contains separate models for simulating the performance of various indoor fan configurations, and these models can be easily linked with the DX system model described here to simulate the entire DX system being considered (e.g., see Unitary System:HeatPump:AirToAir).

Model Inputs

The user must input the total heating capacity, coefficient of performance (COP) and the volumetric airflow rate across the heating coil at rated conditions. The capacity and COP inputs should be "gross" values, excluding any thermal or energy impacts due to the indoor supply air fan. The rating condition is considered to be outdoor air at 8.33C dry bulb and 6.11C wet bulb temperatures (i.e., air entering the outdoor coil), with air entering the indoor DX heating coil at 21.11C dry bulb and 15.55C wet bulb temperatures. The rated volumetric

air flow across the DX heating coil should be between 0.00004699 m^3/s and 0.00006041 m^3/s per watt of rated total heating capacity (350 – 450 cfm/ton).

Depending on the defrost strategy that is selected, the user must also input up to six performance curves that describe the change in total heating capacity and efficiency at part-load conditions, and efficiency during reverse-cycle defrosting:

1. The total heating capacity modifier curve (function of temperature) is a quadratic or cubic curve with a single independent variable: outdoor air dry-bulb temperature. The output of this curve is multiplied by the rated total heating capacity to give the total heating capacity at specific temperature operating conditions (i.e., at an outdoor air temperature different from the rating point temperature).

$$TotCapTempModFac = a + b\left(T_{db,o}\right) + c\left(T_{db,o}\right)^2 \qquad (1.338)$$

or

$$TotCapTempModFac = a + b\left(T_{db,o}\right) + c\left(T_{db,o}\right)^2 + d\left(T_{db,o}\right)^3 \qquad (1.339)$$

where

$T_{db,o}$ = dry-bulb temperature of the air entering the outdoor coil, °C

2. The total heating capacity modifier curve (function of flow fraction) is a quadratic or cubic curve with the independent variable being the ratio of the actual air flow rate across the heating coil to the rated air flow rate (i.e., fraction of full load flow). The output of this curve is multiplied by the rated total heating capacity and the total heating capacity modifier curve (function of temperature) to give the total heating capacity at the specific temperature and air flow conditions at which the coil is operating.

$$TotCapFlowModFac = a + b\left(ff\right) + c\left(ff\right)^2 \qquad (1.340)$$

or

$$TotCapFlowModFac = a + b\left(ff\right) + c\left(ff\right)^2 + d\left(ff\right)^3 \qquad (1.341)$$

where

$$ff = flow\ fraction = \left(\frac{Actual\ air\ mass\ flow\ rate}{Rated\ air\ mass\ flow\ rate}\right)$$

Note: The actual volumetric airflow rate through the heating coil for any simulation time step where the DX unit is operating should be between 0.00003356 m^3/s and .00006713 m^3/s per watt of rated total heating capacity (250 - 500 cfm/ton). The simulation will issue a warning message if this airflow range is exceeded.

3. The energy input ratio (EIR) modifier curve (function of temperature) is a quadratic or cubic curve with the independent variable being the outdoor air dry-bulb temperature. The output of this curve is multiplied by the rated EIR (inverse of the rated COP) to give the EIR at specific temperature operating conditions (i.e., at an outdoor air dry-bulb temperature different from the rating point temperature).

$$EIRTempModFac = a + b\left(T_{db,o}\right) + c\left(T_{db,o}\right)^2 \qquad (1.342)$$

or

$$EIRTempModFac = a + b\left(T_{db,o}\right) + c\left(T_{db,o}\right)^2 + d\left(T_{db,o}\right)^3 \qquad (1.343)$$

4. The energy input ratio (EIR) modifier curve (function of flow fraction) is a quadratic or cubic curve with the independent variable being the ratio of the actual air flow rate across the heating coil to the rated air flow rate (i.e., fraction of full load flow). The output of this curve is multiplied by the rated EIR (inverse of the rated COP) and the EIR modifier curve (function of temperature) to give the EIR at the specific temperature and air flow conditions at which the coil is operating.

$$EIRFlowModFac = a + b\left(ff\right) + c\left(ff\right)^2 \qquad (1.344)$$

or

$$EIRFlowModFac = a + b\left(ff\right) + c\left(ff\right)^2 + d\left(ff\right)^3 \qquad (1.345)$$

5. The part-load fraction correlation (function of part-load ratio) is a quadratic or cubic curve with the independent variable being part-load ratio (sensible heating load / steady-state heating capacity). The output of this curve is used in combination with the rated EIR and EIR modifier curves to give the "effective" EIR for a given simulation time step. The part-load fraction (PLF) correlation accounts for efficiency losses due to compressor cycling.

$$PartLoadFrac = PLF = a + b\left(PLR\right) + c\left(PLR\right)^2 \qquad (1.346)$$

or

$$PartLoadFrac = a + b\left(PLR\right) + c\left(PLR\right)^2 + d\left(PLR\right)^3 \qquad (1.347)$$

where

$$PLR = part\text{-}load\ ratio = \left(\frac{sensible\ heating\ load}{steady\text{-}state\ sensible\ heating\ capacity}\right)$$

The part-load fraction correlation should be normalized to a value of 1.0 when the part load ratio equals 1.0 (i.e., no efficiency losses when the compressor(s) run continuously for the simulation time step). For PLR values between 0 and 1 (0 <= PLR < 1), the following rules apply:

   PLF >= 0.7   and   PLF >= PLR

If PLF < 0.7 a warning message is issued, the program resets the PLF value to 0.7, and the simulation proceeds. The runtime fraction of the coil is defined a PLR/PLF. If PLF < PLR, then a warning message is issued and the runtime fraction of the coil is limited to 1.0.

A typical part load fraction correlation for a conventional, single-speed DX heating coil (e.g., residential heat pump) would be:

   PLF = 0.75 + 0.25(PLR)

6. The defrost energy input ratio (EIR) modifier curve (function of temperature) is a bi-quadratic curve with two independent variables: outdoor air dry-bulb temperature and the

heating coil entering air wet-bulb temperature. The output of this curve is multiplied by the heating coil capacity and the fractional defrost time period to give the defrost power at the specific temperatures at which the coil is operating. This curve is only required when a reverse-cycle defrost strategy is specified.

$$DefrostEIRTempModFac = a + b\left(T_{wb,i}\right) + c\left(T_{wb,i}\right)^2 + d\left(T_{db,o}\right) + e\left(T_{db,o}\right)^2 + f\left(T_{wb,i}\right)\left(T_{db,o}\right) \qquad (1.348)$$

where

$T_{wb,i}$ = wet-bulb temperature of the air entering the indoor heating coil, °C

$T_{db,o}$ = dry-bulb temperature of the air entering the outdoor coil, °C

All six curves are accessed through EnergyPlus' built-in performance curve equation manager (curve:quadratic, curve:cubic and curve:biquadratic). It is not imperative that the user utilize all coefficients shown in the preceding equations {(1.338) through (1.348)} in items (1) through (6) if their performance equation has fewer terms (e.g., if the user's PartLoadFrac performance curve is linear instead of quadratic or cubic, simply enter the appropriate values for the coefficients a and b, and set the remaining coefficients to zero).

The next input item for the HeatingEmpirical DX coil is the supply air fan operation mode. Either the supply air fan runs continuously while the DX coil cycles on/off, or the fan and coil cycle on/off together. The next two inputs define the minimum outdoor dry-bulb temperature that the heat pump compressor will operate and the maximum outdoor dry-bulb temperature for defrost operation. Crankcase heater capacity and crankcase heater cutout temperature are entered in the following two inputs. The final four inputs cover the type of defrost strategy (reverse-cycle or resistive), defrost control (timed or on-demand), the fractional defrost time period (timed defrost control only), and the resistive defrost heater capacity if a resistive defrost strategy is selected.

Model Description

The general flow of the model is as follows:

1) If the outdoor air dry-bulb temperature is below the specified minimum temperature for compressor operation or the DX heating coil is not scheduled to operate, simply pass through the heating coil inlet air conditions as the coil outlet conditions, set power and heating rates equal to zero, and set crankcase heater power equal to the crankcase heater capacity value specified by the input file.

2) If the outdoor air dry-bulb temperature is above the specified minimum temperature for compressor operation and the DX heating coil is scheduled to operate, then:

    a. If the outdoor dry-bulb temperature is below the specified maximum outdoor dry-bulb temperature for defrost operation, calculate a heating capacity multiplier, input power multiplier and fractional defrost time period depending on the defrost strategy and defrost control type specified for the heating coil.

    b. Using the rated heating capacity and COP, the part-load curves specified for the DX heating coil, the defrost multipliers calculated above (if applicable), and the part-load ratio that is being requested of the heating coil, determine the following: heating coil exiting air conditions (dry-bulb temperature, humidity ratio and enthalpy), total DX coil heating rate, electric power during heating (compressors and outdoor fans), electric power during defrost, and crankcase heater power.

The following paragraphs give a detailed description of the model calculations that are performed when the DX heating coil is operating (i.e., scenario # 2 above).

Frost Adjustment Factors

Frost formation on the outdoor coil, and the need to periodically defrost this coil, has a significant impact on heating capacity and energy use by the DX heating system. If the

outdoor air dry-bulb temperature is below the specified maximum temperature for defrost operation, then the model calculates adjustment factors for heating capacity and input power due to frost formation, and the fractional defrost time period, depending on the defrost strategy and defrost control type specified for the heating coil. This method of accounting for the impacts of frosting/defrost was taken from the model used in DOE-2.1E (ESTSC 2001, Miller and Jaster 1985).

The model first estimates the outdoor coil temperature according to a linear empirical relationship with outdoor air dry-bulb temperature as the independent variable.

$$T_{coil,out} = 0.82 T_{db,o} - 8.589 \tag{1.349}$$

The difference between the outdoor air humidity ratio (from the weather file) and the saturated air humidity ratio at the estimated outdoor coil temperature is then calculated, and this value is used as an indication of frost formation on the outdoor coil.

$$\Delta\omega_{coil,out} = MAX \left[1.0E-6, \ \omega_{outdoor} - \omega_{sat} \left(T_{coil,out}, \text{OutBaroPress} \right) \right] \tag{1.350}$$

Frost formation on the outdoor coil must be periodically removed. The portion of the simulation time step that the coil is being defrosted is either entered by the user (for timed defrost) or is calculated by the model (for on-demand defrost) using an empirical equation and $\Delta\omega_{coil,out}$. Adjustment factors to total heating coil capacity and input power due to frost formation on the outdoor coil are also calculated by empirical models with $\Delta\omega_{coil,out}$ or fractional defrost time period as the independent variable. The defrost time period fraction and adjustment factors due to frost formation on the outdoor coil vary depending on the defrost control type as shown below.

Timed Defrost:

$$Fractional\ Defrost\ Time = time\ period\ specified\ by\ user = t_{frac,defrost} \tag{1.351}$$

$$Heating\ Capacity\ Multiplier = 0.909 - 107.33 \left(\Delta\omega_{coil,out} \right) \tag{1.352}$$

$$Input\ Power\ Multiplier = 0.9 - 36.45 \left(\Delta\omega_{coil,out} \right) \tag{1.353}$$

On-Demand Defrost:

$$Fractional\ Defrost\ Time = \frac{1}{1 + \left(\dfrac{0.01446}{\Delta\omega_{coil,out}} \right)} = t_{frac,defrost} \tag{1.354}$$

$$Heating\ Capacity\ Multiplier = 0.875 \left(1 - t_{frac,defrost} \right) \tag{1.355}$$

$$Input\ Power\ Multiplier = 0.954 \left(1 - t_{frac,defrost} \right) \tag{1.356}$$

If the outdoor air dry-bulb temperature is <u>above</u> the specified maximum temperature for defrost operation, the fractional defrost time period is set to zero and the heating capacity/input power multipliers are set to unity.

Defrost Operation

If the fractional defrost time period is greater than zero for the simulation time step, then the model calculates the electrical power used during defrost. The method for calculating defrost power varies based on the defrost strategy specified (i.e., reverse-cycle or resistive). In the case of reverse-cycle defrost, the additional heating load due to defrost (indoor cooling during defrost) is also calculated so that it may be added to the existing heating load when calculating input power for the compressor(s) and outdoor coil fan(s).

Reverse-Cycle:

$$Q_{defrost} = 0.01 \left(t_{frac,defrost} \right) \left(7.222 - T_{db,o} \right) \left(\frac{Q_{total,rated}}{1.01667} \right) \tag{1.357}$$

$$P_{defrost} = DefrostEIRTempModFac \left(\frac{Q_{total,rated}}{1.01667} \right) t_{frac,defrost} \tag{1.358}$$

Resistive:

$$Q_{defrost} = 0.0 \tag{1.359}$$

$$P_{defrost} = \left(Q_{cap,defrost} \right) \left(t_{frac,defrost} \right) \tag{1.360}$$

where:

$Q_{defrost}$ = additional indoor heating load due to reverse-cycle defrost (*W*)

$Q_{total,rated}$ = total full-load heating capacity of the coil at rated conditions (W)

$P_{defrost}$ = average defrost power for the simulation time step (W)

$Q_{cap,defrost}$ = capacity of the resistive defrost heating element (W)

$DefrostEIRTempModFac$ = energy input ratio modifier curve applicable during defrost

Heating Operation

For any simulation time step, the total heating capacity of the DX unit is calculated as follows:

$$Q_{total} = Q_{total,\,rated} \left(TotCapTempModFac \right) \left(TotCapFlowModFac \right) \tag{1.361}$$

If the outdoor air dry-bulb temperature is below the maximum temperature for defrost operation, then the total heating capacity is further adjusted due to outdoor coil frost formation based on the results of Equation (1.361) and Equation (1.352) or (1.355).

$$Q_{total} = Q_{total} \left(HeatingCapacityMultiplier \right) \tag{1.362}$$

In a similar fashion, the electrical power draw by the DX unit (compressors plus outdoor coil fans) for any simulation time step is calculated. For a reverse-cycle defrost strategy, the additional heating load ($Q_{defrost}$) generated during defrost operation is added to the heating load being requested by adjusting the part-load ratio. If a resistive defrost strategy is selected, $Q_{defrost}$ = 0. The part-load fraction correlation for the heating coil (user input,

Equation (1.346) or (1.347)) is used in the calculation of electrical power draw to account for efficiency losses due to compressor cycling.

$$PLR = MIN\left(1.0, PLR + \left(\frac{Q_{defrost}}{Q_{total}}\right)\right)$$ (1.363)

$$PartLoadFrac = a + b\left(PLR\right) + c\left(PLR\right)^2 + d\left(PLR\right)^3$$ (1.347)

$$P_{heating} = \frac{\left(Q_{total}\right)\left(EIR\right)\left(PLR\right)}{PartLoadFrac} \times InputPowerMultiplier$$ (1.364)

where

$P_{heating}$ = average compressor and outdoor fan power for the simulation time step(W)

Q_{total} = total heating capacity W, Eqn. (1.362)

$$EIR = Energy\ input\ ratio = \left(\frac{1}{COP_{rated}}\right)\left(EIRTempModFac\right)\left(EIRFlowModFac\right)$$

COP_{rated} = coefficient of performance at rated conditions (user input)

$InputPowerMultiplier$ = power adjustment due to frost if applicable -Eqn. (1.353) or (1.356)

The crankcase heater is assumed to operate when the heating coil's compressor is OFF, and the average crankcase heater power for the simulation time step is calculated as follows:

$$P_{crankcase} = Q_{cap,crankcase}\left(1 - RTF\right)$$ (1.365)

$$RTF = \left(\frac{PLR}{PartLoadFrac}\right) = runtime\ fraction\ of\ the\ heating\ coil$$ (1.366)

where

$P_{crankcase}$ = average crankcase heater power for the simulation time step (W)

$Q_{cap,crankcase}$ = crankcase heater capacity (W)

The properties of the air leaving the heating coil at full-load operation are calculated using the following equations:

$$h_{outlet} = h_{inlet} + \frac{Q_{total}}{\dot{m}}$$ (1.367)

$$\omega_{outlet} = \omega_{inlet}$$ (1.368)

$$T_{db,outlet} = PSYTHW\left(h_{outlet}, \omega_{outlet}\right)$$ (1.369)

where

h_{outlet} = enthalpy of the air leaving the heating coil (J/kg)

ω_{outlet} = leaving air humidity ratio (kg/kg)

$T_{db,outlet}$ = leaving air dry-bulb temperature (°C)

$PSYTHW$ = EnergyPlus psychrometric function, returns dry-bulb temp given enthalpy and humidity ratio

Supply Air Fan Control: Cycling vs. Continuous

One of the inputs to the DX coil model is the supply air fan operation mode: cycling fan, cycling compressor (CycFanCycComp) or continuous fan, cycling compressor (ContFanCycComp). The first operation mode is frequently referred to as "AUTO fan", where the compressor(s) and supply air fan operate in unison to meet the zone heating load, and cycle off together when the heating load has been met. The second operation mode is often referred to as "fan ON", where the compressor(s) cycle on and off to meet the zone heating load but the supply air fan operates continuously regardless of compressor operation.

The EnergyPlus methodology for determining the impact that HVAC equipment has on an air stream is to calculate the mass flow rate and air properties (e.g., enthalpy, dry-bulb temperature, humidity ratio) exiting the equipment. These exiting conditions are passed along as inlet conditions to the next component model in the air stream. Eventually the flow rate and properties of the air being supplied to the conditioned zone are used in the zone energy balance to determine the resulting zone air temperature and humidity ratio.

With this methodology, the determination of the air mass flow rate and air properties for the two different supply air fan operation modes is slightly different. For the case of cycling fan/cycling compressor, the conditions of the air leaving the heating coil are the steady-state values calculated using equations (1.367), (1.368) and (1.369) above. However the air mass flow rate passed along to the next component (and eventually to the conditioned zone) is the average air mass flow rate for the system simulation time step (determined by the heating system; see Unitary System:HeatPump:AirToAir). For this fan control type, the heating coil part-load fraction (Equation (1.346) or (1.347)) is also passed to Fan:Simple:OnOff (if used) to properly calculate the supply air fan power and associated fan heat.

For the case of continuous fan/cycling compressor, the air mass flow rate is constant. However, the air properties leaving the heating coil are calculated as the average conditions during the system simulation time step. The model assumes that the exiting air conditions are the steady-state values calculated using equations (1.367), (1.368) and (1.369) above when the compressor(s) operate. For the remainder of the system simulation time step, it is assumed that the air exiting the DX coil has the same properties as the air entering the coil. For this supply air fan operating strategy, the leaving air properties are calculated as follows:

$$h_{outlet,ContFanCycComp} = h_{outlet}(PLR) + h_{inlet}(1 - PLR) \qquad (1.370)$$

$$\omega_{outlet,ContFanCycComp} = \omega_{outlet}(PLR) + \omega_{inlet}(1 - PLR) \qquad (1.371)$$

$$T_{db,outlet,ContFanCycComp} = PSYTHW(h_{outlet,ContFanCycComp}, \ \omega_{outlet,ContFanCycComp}) \quad (1.372)$$

References

DOE. 1982. *DOE-2 engineers manual*, version 2.1A. LBL-11353. Berkeley, CA: Lawrence Berkeley National Laboratory.

ESTSC. 2001. DOE-2.1E Version 110 (source code). Oak Ridge, TN: Energy Science and Technology Software Center.

Miller, R.L. and Jaster, H. 1985. Performance of Air-Source Heat Pumps. EM-4226. Palo Alto, CA: Electric Power Research Institute.

DX Cooling Coil Model

Overview

The object (Coil:DX:CoolingBypassFactorEmpirical) model simulates the performance of an air-cooled, direct expansion (DX) air conditioner. The model uses performance information at rated conditions along with curve fits for variations in total capacity, energy input ratio and part-load fraction to determine the performance of the unit at part-load conditions (Henderson et al. 1992, ASHRAE 1993). Sensible/latent capacity splits are determined by the rated sensible heat ratio (SHR) and the apparatus dew point (ADP)/bypass factor (BF) approach. This approach is analogous to the NTU-effectiveness calculations used for sensible-only heat exchanger calculations, extended to a cooling and dehumidifying coil.

This model simulates the thermal performance of the DX cooling coil and the power consumption of the outdoor condensing unit (compressors and condenser fans). The performance of the indoor fan varies widely from system to system depending on control strategy (e.g., constant fan vs. AUTO fan, constant air volume vs. variable air volume, etc.), fan type, fan motor efficiency and pressure losses through the air distribution system. Therefore, this DX system model does not account for the thermal effects or electric power consumption of the indoor fan. EnergyPlus contains separate models for simulating the performance of various indoor fan configurations, and these models can be easily linked with the DX system model described here to simulate the entire DX air conditioner being considered (e.g., see Furnace:HeatCool, Unitary System:HeatCool, Air Conditioner:Window or UnitarySystem:HeatPump).

Model Description

The user must input the total cooling capacity, sensible heat ratio (SHR), coefficient of performance (COP) and the volumetric air flow rate across the cooling coil at rated conditions. The capacity, SHR and COP inputs should be "gross" values, excluding any thermal or energy impacts due to the indoor supply air fan. The rated condition is considered to be 35C outdoor dry-bulb temperature (i.e., air entering the air-cooled condenser), with air entering the DX cooling coil at 26.7C dry bulb and 19.4C wet bulb. The rated volumetric air flow should be between 0.00004699 m^3/s and 0.00006041 m^3/s per watt of rated total cooling capacity (350 – 450 cfm/ton).

The user must also input five performance curves that describe the change in total cooling capacity and efficiency at part-load conditions:

1) Total Cooling Capacity Modifier Curve (function of temperature)

2) Total Cooling Capacity Modifier Curve (function of flow fraction)

3) Energy input ratio (EIR) modifier curve (function of temperature)

4) Energy input ratio (EIR) modifier curve (function of flow fraction)

5) Part load fraction correlation (function of part load ratio)

■ The total cooling capacity modifier curve (function of temperature) is a biquadratic curve with two independent variables: wet-bulb temperature of the air entering the cooling coil, and dry-bulb temperature of the air entering the air-cooled condenser. The output of this curve is multiplied by the rated total cooling capacity to give the total cooling capacity at the specific entering air temperatures at which the DX coil unit is operating (i.e., at temperatures different from the rating point temperatures).

$$TotCapTempModFac = a + b\left(T_{wb,i}\right) + c\left(T_{wb,i}\right)^2 + d\left(T_{db,o}\right) + e\left(T_{db,o}\right)^2 + f\left(T_{wb,i}\right)\left(T_{db,o}\right) \quad (1.373)$$

where

$T_{wb,i}$ = wet-bulb temperature of the air entering the cooling coil, °C

$T_{db,o}$ = dry-bulb temperature of the air entering the air-cooled condenser, °C

■ The total cooling capacity modifier curve (function of flow fraction) is a quadratic curve with the independent variable being the ratio of the actual air flow rate across the cooling coil to the rated air flow rate (i.e., fraction of full load flow). The output of this curve is multiplied by the rated total cooling capacity and the total cooling capacity modifier curve (function of temperature) to give the total cooling capacity at the specific temperature and air flow conditions at which the DX unit is operating.

$$TotCapFlowModFac = a + b\left(ff\right) + c\left(ff\right)^2 \qquad\qquad (1.374)$$

where

$$ff = flow\ fraction = \left(\frac{Actual\ air\ mass\ flow\ rate}{Rated\ air\ mass\ flow\ rate}\right)$$

Note: The actual volumetric air flow rate through the cooling coil for any simulation time step where the DX unit is operating must be between 0.00003356 m^3/s and .00006713 m^3/s per watt of rated total cooling capacity (250 - 500 cfm/ton). The simulation will issue a warning message if this air flow range is exceeded.

■ The energy input ratio (EIR) modifier curve (function of temperature) is a biquadratic curve with two independent variables: wetbulb temperature of the air entering the cooling coil, and drybulb temperature of the air entering the air-cooled condenser. The output of this curve is multiplied by the rated EIR (inverse of the rated COP) to give the EIR at the specific entering air temperatures at which the DX coil unit is operating (i.e., at temperatures different from the rating point temperatures).

$$EIRTempModFac = a + b\left(T_{wb,i}\right) + c\left(T_{wb,i}\right)^2 + d\left(T_{db,o}\right) + e\left(T_{db,o}\right)^2 + f\left(T_{wb,i}\right)\left(T_{db,o}\right) \qquad (1.375)$$

where

$T_{wb,i}$ = wet-bulb temperature of the air entering the cooling coil, °C

$T_{db,o}$ = dry-bulb temperature of the air entering the air-cooled condenser, °C

■ The energy input ratio (EIR) modifier curve (function of flow fraction) is a quadratic curve with the independent variable being the ratio of the actual air flow rate across the cooling coil to the rated air flow rate (i.e., fraction of full load flow). The output of this curve is multiplied by the rated EIR (inverse of the rated COP) and the EIR modifier curve (function of temperature) to give the EIR at the specific temperature and air flow conditions at which the DX unit is operating.

$$EIRFlowModFac = a + b\left(ff\right) + c\left(ff\right)^2 \qquad\qquad (1.376)$$

where

$$ff = flow\ fraction = \left(\frac{Actual\ air\ mass\ flow\ rate}{Rated\ air\ mass\ flow\ rate}\right)$$

■ ■ The part load fraction correlation (function of part load ratio) is a quadratic or a cubic curve with the independent variable being part load ratio (sensible cooling load / steady-state sensible cooling capacity). The output of this curve is used in combination with the rated EIR and EIR modifier curves to give the "effective" EIR for a given simulation time step. The part load fraction (PLF) correlation accounts for efficiency losses due to compressor cycling.

$$PartLoadFrac = PLF = a + b(PLR) + c(PLR)^2 \qquad (1.377)$$

or

$$PartLoadFrac = a + b(PLR) + c(PLR)^2 + d(PLR)^3 \qquad (1.378)$$

where

$$PLR = part\text{-}load\,ratio = \left(\frac{sensible\,cooling\,load}{steady\text{-}state\,sensible\,cooling\,capacity} \right)$$

The part-load fraction correlation should be normalized to a value of 1.0 when the part load ratio equals 1.0 (i.e., no efficiency losses when the compressor(s) run continuously for the simulation time step). For PLR values between 0 and 1 (0 <= PLR < 1), the following rules apply:

   PLF >= 0.7   and   PLF >= PLR

If PLF < 0.7 a warning message is issued, the program resets the PLF value to 0.7, and the simulation proceeds. The runtime fraction of the coil is defined a PLR/PLF. If PLF < PLR, then a warning message is issued and the runtime fraction of the coil is limited to 1.0.

A typical part load fraction correlation for a conventional, single-speed DX cooling coil (e.g., residential unit) would be:

           PLF = 0.75 + 0.25(PLR)

All five part-load curves are accessed through EnergyPlus' built-in performance curve equation manager (curve:quadratic, curve:cubic and curve:biquadratic). It is not imperative that the user utilize all coefficients shown in equations (1.373) through (1.377) if their performance equation has fewer terms (e.g., if the user's PartLoadFrac performance curve is linear instead of quadratic, simply enter the values for a and b, and set coefficient c equal to zero).

For any simulation time step, the total (gross) cooling capacity of the DX unit is calculated as follows:

$$Q_{total} = Q_{total,\,rated}(TotCapTempModFac)(TotCapFlowModFac) \qquad (1.379)$$

In a similar fashion, the electrical power consumed by the DX unit (compressors plus outdoor condenser fans) for any simulation time step is calculated using the following equation:

$$Power = \frac{(Q_{total})(EIR)(PLR)}{PartLoadFrac} \qquad (1.380)$$

where

Q_{total} = Total cooling capacity, W -- ref. equation (1.379)

$$EIR = Energy\ input\ ratio = \left(\frac{1}{COP_{rated}}\right)(EIRTempModFac)(EIRFlowModFac)$$

COP_{rated} = Coefficient of performance at rated conditions (user input)

In addition to calculating the total cooling capacity provided by the DX air conditioner, it is important to properly determine the break down of total cooling capacity into its sensible (temperature) and latent (dehumidification) components. The model computes the sensible/latent split using the rated SHR and the ADP/BF approach (Carrier et al. 1959). When the DX coil model is initially called during an EnergyPlus simulation, the rated total capacity and rated SHR are used to calculate the coil bypass factor (BF) at rated conditions. The rated total capacity and rated SHR are first used to determine the ratio of change in air humidity ratio to air dry-bulb temperature:

$$SlopeRated = \left(\frac{\omega_{in} - \omega_{out}}{T_{db,in} - T_{db,out}}\right)_{rated} \tag{1.381}$$

where

ω_{in} = humidity ratio of the air entering the cooling coil at rated conditions, kg/kg

ω_{out} = humidity ratio of the air leaving the cooling coil at rated conditions, kg/kg

$T_{db,in}$ = dry-bulb temperature of the air entering the cooling coil at rated conditions, °C

$T_{db,out}$ = dry-bulb temperature of the air leaving the cooling coil at rated conditions, °C

Along with the rated entering air conditions, the algorithm then searches along the saturation curve of the psychrometric chart until the slope of the line between the point on the saturation curve and the inlet air conditions matches *SlopeRated*. Once this point, the apparatus dew point, is found on the saturation curve the coil bypass factor at rated conditions is calculated as follows:

$$BF_{rated} = \frac{h_{out,rated} - h_{ADP}}{h_{in,rated} - h_{ADP}} \tag{1.382}$$

where

$h_{out,rated}$ = enthalpy of the air leaving the cooling coil at rated conditions, J/kg

$h_{in,rated}$ = enthalpy of the air entering the cooling coil at rated conditions, J/kg

h_{ADP} = enthalpy of saturated air at the coil apparatus dew point, J/kg

The coil bypass factor is analogous to the "ineffectiveness" (1-ε) of a heat exchanger, and can be described in terms of the number of transfer of unit (NTU).

$$BF = e^{-NTU} = e^{-\left(\frac{UA}{c_p}\right)/\dot{m}} = e^{-Ao/\dot{m}} \tag{1.383}$$

For a given coil geometry, the bypass factor is only a function of mass flow rate. The model calculates the parameter A_o in equation (1.383) based on BF_{rated} and the rated air mass flow rate. With A_o known, the coil BF can be determined for non-rated air flow rates.

For each simulation time step when the DX air conditioner operates to meet a cooling load, the total cooling capacity at the actual operating conditions is calculated using equation (1.379) and the coil bypass factor is calculated based on equation (1.383). The coil bypass

factor is used to calculate the operating sensible heat ratio (SHR) of the cooling coil using equations (1.384) and (1.385).

$$h_{ADP} = h_{in} - \frac{(Q_{total} / \dot{m})}{1 - BF} \tag{1.384}$$

$$SHR = Minimum\left(\left(\frac{h_{Tin, wADP} - h_{ADP}}{h_{in} - h_{ADP}}\right), 1\right) \tag{1.385}$$

where

h_{in} = enthalpy of the air entering the cooling coil, J/kg

h_{ADP} = enthalpy of air at the apparatus dew point condition, J/kg

$h_{Tin, wADP}$ = enthalpy of air at the entering coil dry-bulb temperature and humidity ratio at ADP, J/kg

$\dot{m}$ = air mass flow rate, kg/s

With the SHR for the coil at the current operating conditions, the properties of the air leaving the cooling coil are calculated using the following equations:

$$h_{out} = h_{in} - \frac{Q_{total}}{\dot{m}} \tag{1.386}$$

$$h_{Tin, \omega out} = h_{in} - (1 - SHR)(h_{in} - h_{out}) \tag{1.387}$$

$$\omega_{out} = PSYWTH(T_{in}, h_{Tin, \omega out}) \tag{1.388}$$

$$T_{db, out} = PSYTHW(h_{out}, \omega_{out}) \tag{1.389}$$

where

h_{out} = enthalpy of the air leaving the cooling coil, J/kg

$h_{Tin, \omega out}$ = enthalpy of air at the entering coil dry-bulb temperature and leaving air humidity ratio, J/kg

ω_{out} = leaving air humidity ratio, kg/kg

$T_{db, out}$ = leaving air dry-bulb temperature, °C

PSYWTH = EnergyPlus psychrometric function, returns humidity ratio given dry-bulb temp and enthalpy

PSYTHW = EnergyPlus psychrometric function, returns dry-bulb temp given enthalpy and humidity ratio

Dry Coil Conditions

If the model determines that the cooling coil is dry ($\omega_{in} < \omega_{ADP}$), then equations (1.379) and (1.380) are invalid since they are functions of entering wet-bulb temperature. Under dry-coil conditions, coil performance is a function of dry-bulb temperature rather than wet-bulb temperature. In this case, the model recalculates the performance of the DX cooling unit using the calculation procedure described above but with $\omega_{in} = \omega_{dry}$, where ω_{dry} is the inlet air humidity ratio at the coil dry-out point (SHR = 1.0).

Supply Air Fan Control: Cycling vs. Continuous

One of the inputs to the DX coil model is the supply air fan operation mode: cycling fan, cycling compressor (CycFanCycComp) or continuous fan, cycling compressor (ContFanCycComp). The first operation mode is frequently referred to as "AUTO fan", where the compressor(s) and supply air fan operate in unison to meet the zone cooling load, and cycle off together when the cooling load has been met. The second operation mode is often referred to as "fan ON", where the compressor(s) cycle on and off to meet the zone cooling load but the supply air fan operates continuously regardless of compressor operation.

The EnergyPlus methodology for determining the impact that HVAC equipment has on an air stream is to calculate the mass flow rate and air properties (e.g., enthalpy, dry-bulb temperature, humidity ratio) exiting the equipment. These exiting conditions are passed along as inlet conditions to the next component model in the air stream. Eventually the flow rate and properties of the air being supplied to the conditioned zone are used in the zone energy balance to determine the resulting zone air temperature and humidity ratio.

With this methodology, the determination of the air mass flow rate and air properties for the two different supply air fan operation modes is slightly different. For the case of cycling fan/cycling compressor, the conditions of the air leaving the cooling coil are the steady-state values calculated using equations (1.386), (1.388) and (1.389) above. However the air mass flow rate passed along to the next component (and eventually to the conditioned zone) is the average air mass flow rate for the system simulation time step (determined by the cooling system; see Air Conditioner:Window, Furnace:HeatCool, Unitary System:HeatCool or UnitarySystem:HeatPump).

For the case of continuous fan/cycling compressor, the air mass flow rate is constant. However, the air properties leaving the cooling coil are calculated as the average conditions during the system simulation time step. The model assumes that the exiting air conditions are the steady-state values calculated using equations (1.386), (1.388) and (1.389) above when the compressor(s) operate. For the remainder of the system simulation time step, it is assumed that the air exiting the DX coil has the same properties as the air entering the coil. For this supply air fan operating strategy, the leaving air properties are calculated as follows:

$$h_{out, ContFanCycComp} = h_{out}(PLR) + h_{in}(1 - PLR) \qquad (1.390)$$

$$\omega_{out, ContFanCycComp} = \omega_{out}(PLR) + \omega_{in}(1 - PLR) \qquad (1.391)$$

$$T_{db, out, ContFanCycComp} = PSYTHW(h_{out, ContFanCycComp}, \ \omega_{out, ContFanCycComp}) \qquad (1.392)$$

References

ASHRAE. 1993. HVAC2 Toolkit: A Toolkit for Secondary HVAC System Energy Calculation. Atlanta: American Society of Heating, Refrigerating and Air-Conditioning Engineers, Inc.

Carrier, W.H., R.E. Cherne, W.A. Grant, and W.H. Roberts. 1959. *Modern air conditioning, heating and ventilating*, 3d ed. New York: Pitman Publishing Corporation.

Henderson, H.I. Jr., K. Rengarajan, and D.B. Shirey III. 1992. The impact of comfort control on air conditioner energy use in humid climates. *ASHRAE Transactions* 98(2): 104-113.

Humidifier:Steam:Electrical

Overview

Humidifiers are components that add moisture to the supply air stream. They fall into 2 broad categories: spray type humidifiers which act like direct evaporative coolers, cooling the supply air as well as humidifying it; and dry steam humidifiers, which humidify the supply air stream while causing almost no change to the supply air stream temperature. The EnergyPlus

electric steam humidifier uses electrical energy to convert ordinary tap water to steam which it then injects into the supply air stream by means of a blower fan. The actual unit might be an electrode-type humidifier or a resistance-type humidifier.

The electric steam humidifier model is based on moisture and enthalpy balance equations plus standard psychrometric relationships. The approach is similar to that taken in the ASHRAE HVAC 2 Toolkit, page 4-112 (ASHRAE 1993). EnergyPlus contains its own module of psychrometric routines; the psychrometric theory and relations are given in the 2001 edition of ASHRAE Fundamentals, Chapter 6 (ASHRAE 2001). The model contains both an ideal controller and the component. The control model assumes that there is a minimum humidity set point on the component air outlet node. This set point is established by a set point manager described elsewhere.

Model

The component model is a forward model: its inputs are its inlet conditions; its outputs are its outlet conditions and its energy consumption. The inputs are the temperature, humidity ratio, and mass flow rate of the inlet air stream, which are known; and the water addition rate (kg/s) which is determined by the controller.

Controller

The controller first decides whether the humidifier is on or off. For the humidifier to be on:

1. the humidifier schedule value must be nonzero;
2. the inlet air mass flow must be greater than zero;
3. the inlet air humidity ratio must be less than the minimum humidity ratio set point.

If the humidifier is off, the water addition rate is set to zero. If the humidifier is on, the water addition rate needed to meet the humidity set point is calculated.

$$\dot{m}_a \cdot w_{in} + \dot{m}_{w,add,needed} = \dot{m}_a \cdot w_{set} \qquad\qquad (1.393)$$

where

$\dot{m}_a$ = the air mass flow rate [kg/s]

w_{in} = the inlet air humidity ratio [kg/kg]

$\dot{m}_{w,add,needed}$ = water addition rate needed to meet the set point [kg/s]

w_{set} = the humidity ratio set point [kg/kg]

Equation (1.393) is the moisture balance equation for the component. It is solved for $\dot{m}_{w,add,needed}$ (the other variables are known) which is passed to the humidifier component model as its desired inlet water addition rate.

Component

The inputs to the component model are the air inlet conditions and mass flow rate and the water addition rate set by the controller. The outputs are the air outlet conditions. First the desired water addition rate is checked against component capacity.

$$\dot{m}_{w,add,needed,\max} = Min(\dot{m}_{w,add}, Cap_{nom})$$

where

Cap_{nom} = the humidifier nominal capacity [kg/s], a user input.

If $\dot{m}_{w,add,needed,\max}$ is zero, the outlet conditions are set to the inlet conditions and the water addition rate is set to zero. If the humidifier is scheduled on the component power consumption is set to the standby power consumption: $W_{hum} = W_{stby}$. Otherwise W_{hum} = 0.

If $\dot{m}_{w,add,needed,\max}$ > 0, then the moisture and enthalpy balance equations

$$\dot{m}_a \cdot w_{in} + \dot{m}_w = \dot{m}_a \cdot w_{out}$$

$$\dot{m}_a \cdot h_{in} + \dot{m}_w \cdot h_w = \dot{m}_a \cdot h_{out}$$

with $\dot{m}_w$ set equal to $\dot{m}_{w,add,needed,\max}$ are solved for w_{out} and h_{out}. Here

$\dot{m}_a$ = the air mass flow rate [kg/s]

w_{in} = the inlet air humidity ratio [kg/kg]

$\dot{m}_w$ = the inlet water addition rate [kg/s]

w_{out} = the outlet air humidity ratio [kg/kg]

h_{in} = the inlet air specific enthalpy [J/kg]

h_w = the steam specific enthalpy = 2676125. [J/kg] at 100 ^{o}C

h_{out} = the outlet air specific enthalpy [J/kg]

The outlet temperature is obtained from

$$T_{out} = PSYTHW(h_{out}, w_{out})$$

where

T_{out} = outlet air temperature [^{o}C],

$PSYTHW(h_{out}, w_{out})$ is an EnergyPlus psychrometric function.

The humidity ratio at saturation at the outlet temperature is

$$w_{out,sat} = PSYWTR(T_{out}, 1.0, P_{atmo})$$

where

P_{atmo} = the barometric pressure [Pa],

1.0 is the relative humidity at saturation,

$PSYWTR$ is an EnergyPlus psychrometric function.

IF $w_{out} \le w_{out,sat}$ then the outlet condition is below the saturation curve and the desired moisture addition rate can be met. $\dot{m}_{w,add}$ is set to $\dot{m}_{w,add,needed,\max}$ and the calculation of outlet conditions is done. But if $w_{out} > w_{out,sat}$ then it is assumed that this condition will be detected and the steam addition rate throttled back to bring the outlet conditions back to the saturation condition. We need to find the point where the line drawn between state 1 (inlet) and state 2 (our desired outlet) crosses the saturation curve. This will be the new outlet condition. Rather than iterate to obtain this point, we find it approximately by solving for the

point where 2 lines cross: the first drawn from state 1 to state 2, the second from T_1, $w_{1,sat}$ to

T_2, $w_{2,sat}$; where

T_1 is the inlet temperature [°C],

$w_{1,sat}$ is the humidity ratio at saturation at temperature T_1 [kg/kg],

T_2 is the desired outlet temperature [°C],

$w_{2,sat}$ is the humidity ratio at saturation at temperature T_2 [kg/kg].

The 2 lines are given by the equations:

$$w = w_1 + ((w_2 - w_1)/(T_2 - T_1)) \cdot T$$

$$w = w_{1,sat} + ((w_{2,sat} - w_{1,sat})/(T_2 - T_1)) \cdot T$$

Solving for the point (state 3) where the lines cross:

$$w_3 = w_1 + ((w_2 - w_1) \cdot (w_{1,sat} - w_1))/(w_2 - w_{2,sat} + w_{1,sat} - w_1)$$

$$T_3 = (w_3 - w_1) \cdot ((T_2 - T_1)/(w_2 - w_1))$$

This point isn't quite on the saturation curve since we made a linear approximation of the curve, but the temperature should be very close to the correct outlet temperature. We will use this temperature as the outlet temperature and move to the saturation curve for the outlet humidity and enthalpy. Thus we set $T_{out} = T_3$ and

$$w_{out} = PSYWTR(T_{out}, 1.0, P_{atmo})$$

$$h_{out} = PSYHTW(T_{out}, w_{out})$$

where $PSYHTW$ is an EnergyPlus psychrometric function. The water addition rate is set to

$$\dot{m}_{w,add} = \dot{m}_a \cdot (w_{out} - w_{in})$$

We now have the outlet conditions and the adjusted steam addition rate for the case where the desired outlet humidity results in an outlet state above the saturation curve.

Finally, the electricity consumption is given by

$$W_{hum} = (\dot{m}_{w,add}/Cap_{nom}) \cdot W_{nom} + W_{fan} + W_{stby}$$

where

W_{fan} = nominal fan power [W], a user input,

W_{stby} = standby power [W], a user input.

and the water consumption rate is

$$\dot{V}_{cons} = \dot{m}_{w,add} / \rho_w$$

where

$\dot{V}_{cons}$ = the water consumption rate [m^3],

ρ_w = water density (998.2 kg/m^3).

References

ASHRAE 1993. HVAC 2 Toolkit: A Toolkit for Secondary HVAC System Energy Calculations. Atlanta: American Society of Heating, Refrigerating and Air-Conditioning Engineers, Inc.

ASHRAE 2001. 2001 ASHRAE Handbook Fundamentals. Atlanta: American Society of Heating, Refrigerating and Air-Conditioning Engineers, Inc.

Plant:Boiler:Simple

The EnergyPlus boiler model is "simple" in the sense that it requires the user to supply the theoretical boiler efficiency. The combustion process is not considered in the model. The model is independent of the fuel type, which is input by the user for energy accounting purposes only.

The model is based the following three equations

$$OperatingPartLoadRatio = \frac{BoilerLoad}{BoilerNomCapacity} \tag{1.394}$$

$$TheoreticalFuelUse = \frac{BoilerLoad}{BoilerEfficiency} \tag{1.395}$$

$$FuelUsed = \frac{TheoreticalFuelUsed}{C1 + C2 * OperatingPartLoadRatio + C3 * OperatingPartLoadRatio^2} \tag{1.396}$$

A constant efficiency boiler is specified by setting C1=1, C2=0, and C3=0.

Plant:Load Distribution

Summary of Load Distribution Schemes

Two load distribution schemes are employed in EnergyPlus.

The figure "Load Distribution Scheme" shows plant loop operation procedure with load distribution.

DistributeLoad calls Plant Components in order to figure out component's minimum, optimal, and maximum part load ratio. Plant Components calls CalcCompCapacity for the calculation of component loads. Once DistributeLoad computes components' loads, each plant component calculates its mass flow rate based on its own load.
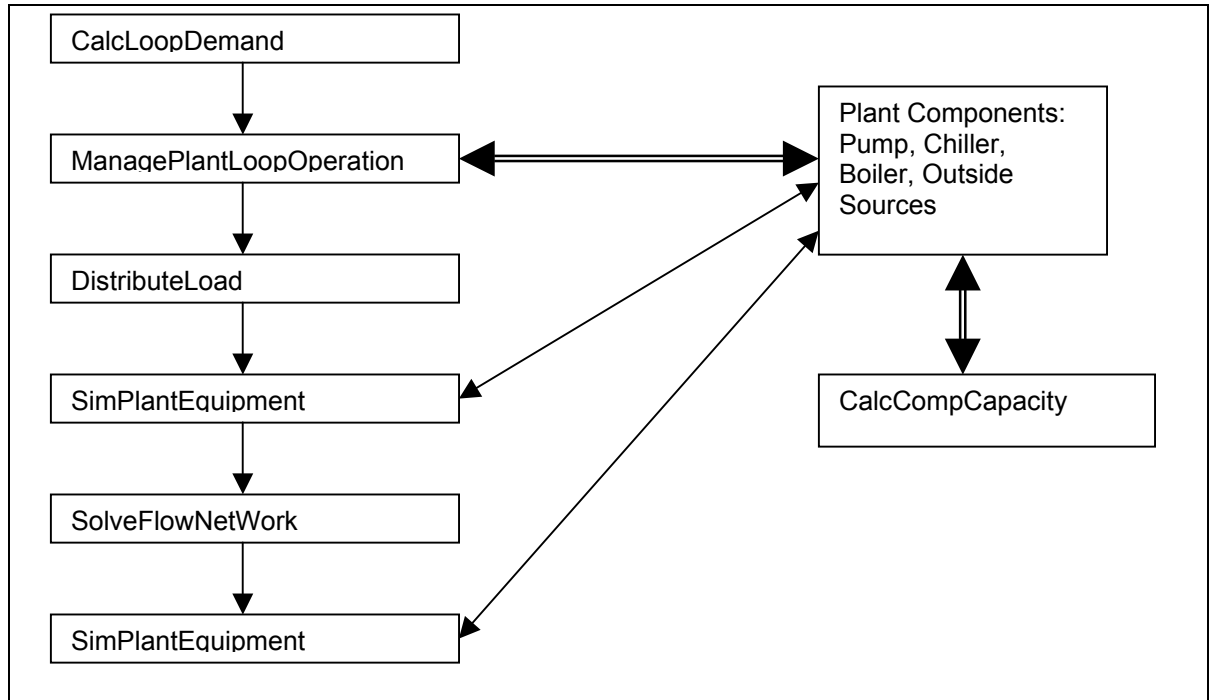
Figure 82. Load Distribution Scheme

Load distribution consists of two steps:

1)   Fill components up to optimum PRL level sequentially, if possible.

2)   If we have remaining loop demand (RLD), fill components to the maximum PRL level sequentially.

Step 2 may result in unmet demand since the remaining loop demand is less than the minimum capacity of a component. In order to avoid this problem, two schemes are devised.

For the component that has mininimum capacity > RLD,

Load Distribution Scheme 1 ("Optimal")

1)   Fill the component to a minimum PLR level.

2)   Reset all other component loads to zero.

3)   Re-compute RLD.

4)   Redistribute remaining load to the reset components.

Load Distribution Scheme 2 ("Overloading")

1)   Fill the component to a minimum PRL level.

2)   This component has FlowLock =2.

3)   Disregard RLD. Plant loop will overcool.

FlowLock is an integer variable with values of either 0,1, or 2. If FlowLock = 0, then each component can request a desired flow rate. If FlowLock =1, then the flow resolver has locked down the branch flow rates at specified levels to maintain continuity. If FlowLock=2, the flowrate for the component is set by the the load distribution scheme under scheme 2 above.

Since scheme 1 is trying to reach component's optimal PRL level, it will be called 'Optimal Operation', and since scheme 2 enforces a component to have minimum capacity by adding a certain amount of load, it will be called 'Overloading Operation'.

The designation for the load distribution scheme is added to the 'Plant Loop' object (ref Input Output Reference). The keys "Optimal" or "Overloading" designate the field. Thus, IDF input

file should have an appropriate key representing the operation scheme both under 'Chilled Water Loop' and 'Hot Water Loop'.

Plant:WaterHeater:Simple

The Hot Water Heater/storage tank component performs three functions as follows:

> Allow for scheduling of domestic hot water use.

> Provide a hot water source for plant loop equipment.

> Provide a hot water storage tank for heat recovery and solar heating loops.

It is modeled as a storage tank with three inputs and outputs as shown in the following figure. Cold "make-up" water replaces hot water demand imposed on the tank by the building hot water use schedule. Simple heat exchanger models connect the tank to both the plant supply side loop and the heat recovery loop. Basic inputs to the model are shown below.

- Heating Capacity [W]
- Heating Efficiency
- Tank Volume [L]
- Set Point Temperature [C]
- Heat Loss Coefficient (UA)
- Cold Water Supply Temperature [C]

The user has the option of connecting scheduled hot water use. This scheduled water will not be recycled to the tank. This is accomplished with a defined hourly flow rate schedule for the hot water demand. Additionally, the user will have the option of connecting a Hot Water Source (Heat Recovery) Loop and a Hot Water Use Loop to the water heater component. In this way, the water heater can be plugged into any combination of these loops. In order for the heat recovery and hot water loops to operate, pumps will need to be added, so that water can be circulated whenever the component is operating.

The hot water heater algorithm assumes that the tank starts at its set point temperature and that the water is well mixed. The algorithm performs an energy balance, determines the new tank temperature, and supplies water to the schedule and/or hot water loops. The temperature of the tank is monitored; so that max and min flow rates are not necessary. In this way, all components will get the requested hot water, but tank temperature will approach the make-up water temperature as demand exceeds tank heating capacity.

The hot water heater algorithm converges on the heat balance solution using a simple successive substitution scheme.
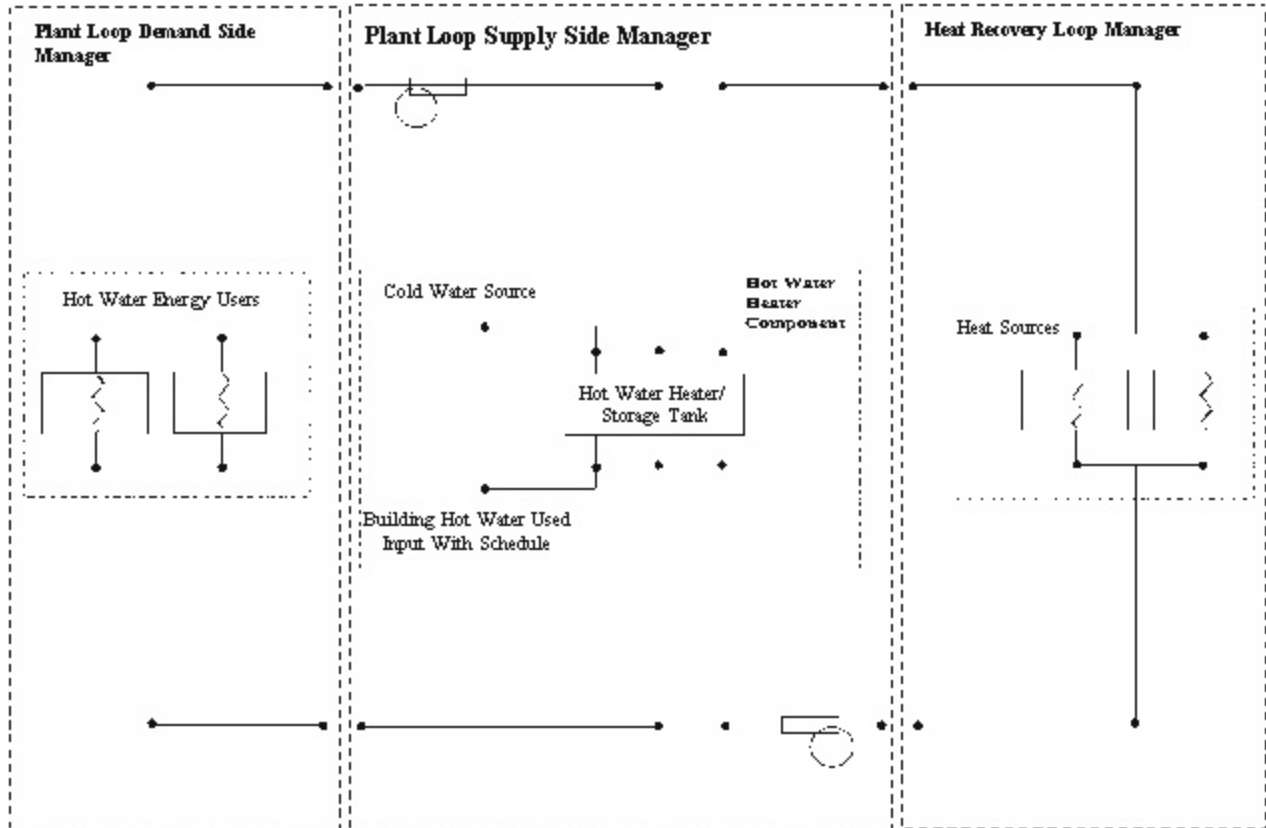
Figure 83. Hot Water Heater in Plant Loop Context

Plant: Condenser Loop: Cooling Towers

Overview

The EnergyPlus cooling tower model is based on Merkel's theory (Merkel 1925), which is also the basis for the tower model included in ASHRAE's HVAC1 Toolkit for primary HVAC system energy calculations (ASHRAE 1999, Bourdouxhe et al. 1994). Cooling tower performance is modeled using effectiveness-NTU relationships for counterflow heat exchangers. The model can be used to simulate the performance of both single speed and two speed mechanical-draft cooling towers. The model will also account for tower performance in the "free convection" regime, when the tower fan is off but the water pump remains on. For part-load operation, the model assumes a simple linear interpolation between two steady-state regimes without accounting for any cycling losses.

Model Description

Based on Merkel's theory, the steady-state total heat transfer between the air and water entering the tower can be defined by the following equation:

$$d\dot{Q}_{total} = \frac{UdA}{c_p}\left(h_s - h_a\right) \tag{1.397}$$

where

h_s = enthalpy of saturated air at the wetted-surface temperature, J/kg

h_a = enthalpy of air in the free stream, J/kg

c_p = specific heat of moist air, J/kg-^{o}C

U = cooling tower overall heat transfer coefficient, W/m^2-^{o}C

A = heat transfer surface area, m^2

Equation (1.397) is based on several assumptions:

- air and water vapor behave as ideal gases
- the effect of water evaporation is neglected
- fan heat is neglected
- the interfacial air film is assumed to be saturated
- the Lewis number is equal to 1

In this model, it is also assumed that the moist air enthalpy is solely a function of the wet-bulb temperature and that the moist air can be treated as an equivalent ideal gas with its mean specific heat defined by the following equation:

$$\overline{c}_{pe} = \frac{\Delta h}{\Delta T_{wb}} \tag{1.398}$$

where

Δh = enthalpy difference between the air entering and leaving the tower, J/kg

ΔT_{wb} = wet-bulb temperature difference between the air entering and leaving the tower, ^{o}C

Since the liquid side conductance is much greater than the gas side conductance, the wetted-surface temperature is assumed to be equal to the water temperature. Based on this assumption and equations (1.397) and (1.398), the expression for total heat transfer becomes:

$$d\dot{Q}_{total} = U_e dA \left(T_w - T_{wb} \right) \tag{1.399}$$

where

$$U_e = \frac{U \, \overline{c}_{pe}}{c_p}$$

T_{wb} = wet-bulb temperature of the air, ^{o}C

T_w = temperature of the water, ^{o}C

An energy balance on the water and air sides of the air/water interface yields the following equations:

$$d\dot{Q}_{total} = \dot{m}_w c_{pw} \, dT_w \tag{1.400}$$

$$d\dot{Q}_{total} = \dot{m}_a \overline{c}_{pe} \, dT_{wb} \tag{1.401}$$

where

$\dot{m}_w$ = mass flow rate of water, kg/s

$\dot{m}_a$ = mass flow rate of air, kg/s

Assuming that the heat capacity rate ($\dot{m}c_p$) for the cooling tower water is less than that for the air, the effectiveness of the cooling tower can be defined by analogy to the effectiveness of a simple heat exchanger:

$$\varepsilon = \frac{T_{Win} - T_{Wout}}{T_{Win} - T_{wbin}}$$

(1.402)

where

ε = heat exchanger effectiveness

T_{win} = inlet water temperature, $^{\circ}$C

T_{wout} = outlet water temperature, $^{\circ}$C

T_{wbin} = wet-bulb temperature of the inlet air, $^{\circ}$C

Combining equations (1.399), (1.400), and (1.401) and integrating over the entire heat transfer surface area, and combining the result with equation (1.402) provides the following expression for cooling tower effectiveness:

$$\varepsilon = \frac{1 - \exp\left\{-NTU\left[1 - \left(\dot{C}_w / \dot{C}_a\right)\right]\right\}}{1 - \left(\dot{C}_w / \dot{C}_a\right)\exp\left\{-NTU\left[1 - \left(\dot{C}_w / \dot{C}_a\right)\right]\right\}}$$

(1.403)

where

$$\dot{C}_w = \dot{m}_w c_{pw} \text{ and } \dot{C}_a = \dot{m}_a \overline{c}_{pe}$$

$$NTU = Number\ of\ Transfer\ Units = \frac{UA_e}{\dot{C}_w}$$

This equation is identical to the expression for effectiveness of an indirect contact (i.e., fluids separated by a solid wall) counterflow heat exchanger (Incropera and DeWitt 1981). Therefore, the cooling tower can be modeled, in the steady-state regime, by an equivalent counterflow heat exchanger as shown in the following figure.
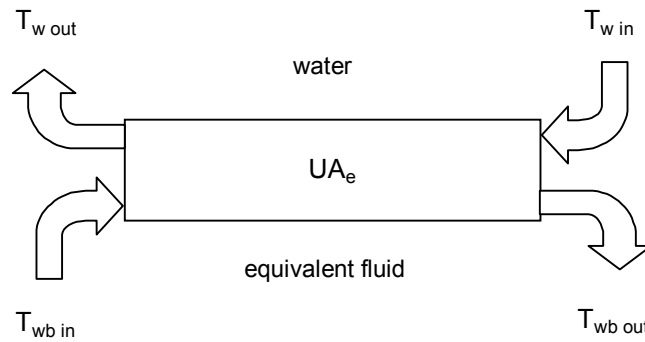
Figure 84. Cooling Tower Schematic

The first fluid is water and the second fluid is an equivalent fluid entering the heat exchanger at temperature T_{wbin} and specific heat $\overline{c}_{pe}$. The heat exchanger is characterized by a single parameter, its overall heat transfer coefficient-area product UA_e. The actual cooling tower heat transfer coefficient-area product is related to UA_e by the following expression:

$$UA = UA_e \frac{c_p}{\overline{c}_{pe}}$$

(1.404)

This heat transfer coefficient-area product is assumed to be a function of the air mass flow rate only and can be estimated from laboratory test results or manufacturers' catalog data.

Method for Calculating Steady-State Exiting Water Temperature

The objective of the cooling tower model is to predict the exiting water temperature and the fan power required to meet the exiting water set point temperature. Since only the inlet air and inlet water temperatures are known at any simulation time step, an iterative procedure is required to determine the exiting fluid temperatures using the equations defined in the previous section. In the case of the EnergyPlus model, the iterations are performed to determine the exiting wet-bulb temperature of the air. The exiting water temperature is then calculated based on an energy balance that assumes that the energy absorbed by the air is equivalent to the energy removed from the water. The procedure for calculating the steady-state, exiting air wet-bulb temperature is outlined below.

As explained previously, it is assumed that the moist air enthalpy can be defined by the wet-bulb temperature alone. Therefore, the first step in the procedure is to calculate the enthalpy of moist air entering the cooling tower based on the ambient wet-bulb temperature from the weather file. Since an iterative solution is required, a first guess of the outlet air wet-bulb temperature is then made and the enthalpy of this estimated outlet air wet-bulb temperature is calculated. Based on these inlet and outlet air conditions, the mean specific heat of the air is calculated based on equation (1.398), repeated here:

$$\overline{c}_{pe} = \frac{\Delta h}{\Delta T_{wb}}$$

With the overall heat transfer coefficient-area product for the cooling tower entered by the user, the effective heat transfer coefficient-area product is calculated by rearranging equation (1.404):

$$UA_e = UA \frac{\overline{c}_{pe}}{c_p}$$

With $\overline{c}_{pe}$ and UA_e known, the effectiveness of the heat exchanger is then calculated:

$$\varepsilon = \frac{1 - \exp\left\{-NTU\left[1 - \left(\dot{C}_{min}/\dot{C}_{max}\right)\right]\right\}}{1 - \left(\dot{C}_{min}/\dot{C}_{max}\right)\exp\left\{-NTU\left[1 - \left(\dot{C}_{min}/\dot{C}_{max}\right)\right]\right\}}$$

where

$$\dot{C}_{min} = Minimum\,(\dot{C}_{w}, \dot{C}_{a}) \text{ and } \dot{C}_{max} = Maximum\,(\dot{C}_{w}, \dot{C}_{a})$$

$$\dot{C}_{w} = \dot{m}_w c_{pw} \text{ and } \dot{C}_{a} = \dot{m}_a \overline{c}_{pe}$$

$$NTU = Number\,of\,Transfer\,Units = \frac{UA_e}{\dot{C}_{min}}$$

The heat transfer rate is then calculated as follows:

$$\dot{Q}_{total} = \varepsilon \, \dot{C}_{min} \left(T_{win} - T_{wbin} \right)$$

The outlet air wet-bulb temperature is then recalculated:

$$T_{wbout} = T_{wbin} + \frac{\dot{Q}_{total}}{\dot{C}_a}$$

The iterative process of calculating T_{wbout} continues until convergence is reached.

Finally, the outlet water temperature is calculated as follows:

$$T_{wout} = T_{win} + \frac{\dot{Q}_{total}}{\dot{C}_w}$$

Calculating the Actual Exiting Water Temperature and Fan Power

The previous section describes the methodology used for calculating the steady-state temperature of the water leaving the cooling tower. This methodology is used to calculate the exiting water temperature in the free convection regime (water pump on, tower fan off) and with the tower fan operating (including low and high fan speed for the two-speed tower). The exiting water temperature calculations use the fluid flow rates (water and air) and the UA-values entered by the user for each regime.

The cooling tower model seeks to maintain the temperature of the water exiting the cooling tower at (or below) a set point. The set point schedule is defined by the field "Loop Temperature Setpoint Schedule Name" for the CONDENSER LOOP object. The model first checks to determine the impact of "free convection", if specified by the user, on the tower exiting water temperature. If free convection is not specified by the user, then the exiting water temperature is initially set equal to the entering tower water temperature. If the user specifies "free convection" and the steady-state exiting water temperature based on "free convection" is at or below the set point, then the tower fan is not turned on.

If the exiting water temperature remains above the set point after "free convection" is modeled, then the tower fan is turned on to reduce the exiting water temperature to the set point. The model assumes that part-load operation is represented by a simple linear interpolation between two steady-state regimes (e.g., tower fan on for the entire simulation time step and tower fan off for the entire simulation time step). Cyclic losses are not taken into account.

The fraction of time that the tower fan must operate is calculated based on the following equation:

$$\omega = \frac{T_{set} - T_{wout,\,off}}{T_{wout,\,on} - T_{wout,\,off}} \tag{1.405}$$

where

T_{set} = exiting water set point temperature, ^{o}C

$T_{wout,\,off}$ = exiting water temperature with tower fan off, ^{o}C

$T_{wout,\,on}$ = exiting water temperature with tower fan on, ^{o}C

The average fan power for the simulation time step is calculated by multiplying ω by the steady-state fan power specified by the user.

The calculation method for the two-speed tower is similar to that for the single-speed tower example described above. The model first checks to see if "free convection" is specified and if the resulting exiting water temperature is below the set point temperature. If not, then the model calculates the steady-state exiting water temperature with the tower fan at low speed. If the exiting water temperature at low fan speed is below the set point temperature, then the average fan power is calculated based on the result of equation (1.405) and the steady-state, low speed fan power specified by the user. If low-speed fan operation is unable to reduce the exiting water temperature below the set point, then the tower fan is increased to its high speed and the steady-state exiting water temperature is calculated. If this temperature is below the set point, then a modified version of equation (1.405) is used to calculate runtime at high fan speed:

$$\omega = \frac{T_{set} - T_{wout,\,low}}{T_{wout,\,high} - T_{wout,\,low}}$$

(1.406)

where

T_{set} = exiting water set point temperature, ^{o}C

$T_{wout,\,low}$ = exiting water temperature with tower fan at low speed, ^{o}C

$T_{wout,\,high}$ = exiting water temperature with tower fan at high speed, ^{o}C

The average fan power for the simulation time step is calculated for the two-speed cooling tower as follows:

$$Power_{fan,\,avg} = \omega\,(Power_{fan,\,high}) + (1 - \omega)(Power_{fan,\,low})$$

(1.407)

References

ASHRAE 1999. HVAC1 Toolkit: A Toolkit for Primary HVAC System Energy Calculations. Atlanta: American Society of Heating, Refrigerating and Air-Conditioning Engineers, Inc.

Bourdouxhe, J.P., M. Grodent, J. Lebrun and C. Silva. 1994. Cooling tower model developed in a toolkit for primary HVAC system energy calculation: part 1. Proceedings of the fourth international conference on system simulation in buildings, Liege (Belgium), December 5-7, 1994.

Clark, D.R., HVACSIM+ Building Systems and Equipment Simulation Program Reference Manual, Pub. No. NBSIR 84-2996, National Bureau of Standards, U.S. Department of Commerce, January, 1985

Elmahdy, A.H., Analytical and Experimental Multi-Row Finned-Tube Heat Exchanger Performance During Cooling and Dehumidifying Processes , Ph.D. Thesis, Carleton University, Ottawa, Canada, December, 1975.

Elmahdy, A.H., and Mitalas, G.P., "A Simple Model for Cooling and Dehumidifying Coils for Use in Calculating Energy Requirements for Buildings," ASHRAE Transactions , 1977 , Vol. 83, Part 2, pp. 103-117.

Incropera, F.P. and D.P. DeWitt. 1981. Fundamentals of Heat Transfer. New York: John Wiley & Sons.

Merkel, F. 1925. Verduftungskuhlung. VDI Forschungarbeiten, No 275, Berlin.

Special Modules/Reporting

Report Pollution Calculations

Currently when a new building technology is evaluated the energy difference from a baseline building is compared to the alternatives and then the life cycle cost is performed to determine the suitability of the alternative. There are times when the lowest energy cost alternative is not necessarily the cleanest or has the lowest environmental impact. Adding an algorithm to calculate the pollution produced for the design alternatives gives the designer another consideration to evaluate for a more optimal and sustainable design. The program calculates the amount of six different pollutants: CO, CO_2, NO_x, SO_2, Particulate Matter (PM), and Hydrocarbons (HC) for on-site and off-site energy production. To calculate the kilograms [kg] of pollution for gas, oil, coal, etc. consumption are multiplied by the average value of pollution produced by the combustion of gas, oil, coal, etc. For electrical energy, the regional characteristics (by state) of how electricity is produced are used to adjust the pollution coefficients. If you have done your own pollution calculations for your site and equipment, then the custom coefficients can be entered directly into the program. The default pollution coefficients and are based on the REEP model and assumptions [1].

Energy Savings

The EnergyPlus model outputs energy as on-site fossil fuels and purchased electricity, which is derived from a variety of sources including gas, oil, coal, hydroelectric, nuclear, etc. With purchased electricity, only the fossil fuels of interest are used when calculating pollution rates. The primary pollutants associated with fossil fuel combustion are: Sulfur Dioxide (SO_2), Nitrogen Oxides (NO_x), Carbon Monoxide (CO), Carbon Dioxide (CO_2), Particulate Matter (PM), and Hydrocarbons (HC). The energy calculated by the EnergyPlus program is then converted into the amount of pollution produced. From a baseline building, alternative energy and pollution saving technologies can be explored, and the energy and pollution savings can be calculated.

On-Site Fossil Fuel Pollution Estimates

Using the AP-42 [2] developed by the United States Environmental Protection Agency (EPA) in conjunction with the assumptions listed below, pollution coefficient estimates for fossil fuel energy savings were developed. Table 32 shows the final controlled pollution estimates by fossil fuel type. Gas, oil, and coal consumed can be directly converted into kgs of pollutants using these default or custom user coefficients. The gasoline and propane coefficients do not have a default set of coefficients and need custom coefficients supplied by the user. In addition all coefficients can be modified to suit any situation.

Table 32. Pollution Coefficients by Fossil Fuel Type

Pollutant	Gas	Residual Oil	Distillate Oil	Coal
	kg/J	kg/J	kg/J	kg/J
CO_2	4.94410970E-08	7.30868390E-08	7.30868390E-08	8.59845165E-08
SO_2	2.53654324E-13	4.49987069E-10	2.37668512E-10	1.26586405E-09
NO_x	5.88993938E-11	1.57639713E-10	6.05524461E-11	2.51074788E-10
CO	1.46173678E-11	1.43293197E-11	1.51380040E-11	8.96646538E-11
HC	2.49355098E-13	3.66852939E-12	1.75408414E-13	1.79277717E-12
PM	1.28976775E-12	3.72613902E-11	6.05545957E-12	1.28976775E-11

The assumptions which are used in the calculation of the pollution coefficients are:

- Coal purchased is assumed to be Bituminous.
- Coal was also assumed to have a Sulfur content of 1.81 %.
- All residual oil was assumed to have a sulfur content of 1.0 %, while distillate oil was assumed to have a sulfur content of 0.5 %.
- Natural gas was assumed to have 3 lbs of PM/10^6 ft^3 of gas.
- When performing calculations from the AP-42, the assumption was to utilize Industrial Boilers for oil and gas, while spreader stoker boilers were assumed for all coal.
- The oil pollution rates are a weighted average of rates from residual (27%) and distillate (73%) based on the REEP model [1].
- Control Technologies (Baghouses or Electrostatic Precipitators) exist for Coal Fired Boilers and reduce PM emissions to 0.03 lbs/MBtu [1].

Off-Site Electric Energy Pollution Estimates

While fossil fuels combusted on-site are straightforward in estimating pollution savings, off-site electricity is more challenging. How the electricity is produced, i.e., from gas, oil, coal, nuclear, or hydroelectric, is a critical issue when estimating pollution rates. In order to improve the accuracy state averages were used [1] and Table 35 gives the values for all states, including Washington DC and Puerto Rico. Efficiency of electricity production was assumed to be 28.5%, which includes transmission losses, in plant use and combustion losses [1]. Utility sized boilers were assumed rather than the industrial sized boilers used in on-site fossil fuel algorithms. Table 33 shows the estimated pollution rates of the fossil fuels used in generating electricity.

Table 33. Pollution Coefficients for Purchased Electricity Derived From Gas, Oil, or Coal

Pollutant	Gas	Oil	Coal
	kg/J	kg/J	kg/J
SO_2	Regional	regional	regional
NO_x	8.59845165E-11	1.28976775E-10	3.00945808E-10
CO	1.68005147E-11	1.42626817E-11	1.24075657E-11
CO_2	4.94410970E-08	7.30868390E-08	8.59845165E-08
PM	1.25967317E-12	4.29922582E-11	4.29922582E-11
HC	7.14101409E-13	2.96646582E-12	2.06792762E-12

EPA Green Lights provides regional sulfur dioxide estimates, which are aggregations of state pollution emission factors. Table 34 shows the regional sulfur dioxide estimates and their respective states.

Table 34. Green Lights Regional SO_2 Estimates

Region	SO_2 (lbs/MBtu)	States in Region
1	1.11117791E-09	CT, MA, ME, NH, RI, VT
2	9.44496921E-10	NJ, NY, PR, VI
3	2.27785882E-09	DC, DE, MD, PA, VA, WV
4	1.91674534E-09	AL, FL, GA, KY, MS, NC, SC, TN
5	2.88900667E-09	IL, IN, MI, MN, OH, WI
6	6.11134951E-10	AR, LA, NM, OK, TX
7	2.36120791E-09	IA, KS, MO, NE
8	9.16706725E-10	CO, MT, ND, SD, UT, WY

Region	SO$_2$ (lbs/MBtu)	States in Region
9	3.05567475E-10	AZ, CA, HI, NV
10	1.38895089E-10	AK, ID, OR, WA

The percent of an energy source for the electric production for that state is shown below in Table 35. These percentages are used in conjunction with the pollution coefficients to produce the off-site pollution.

Table 35. Electric Production in Percent by Energy Source

State	Coal Fired	Petrol. Fired	Nat. Gas. Fired	Hydro Elect	Nuclear	Other	State	Coal Fired	Petrol. Fired	Nat. Gas. Fired	Hydro Elect	Nuclear	Other
AK	0.07	0.09	0.61	0.23	0	0	MT	0.67	0	0	0.33	0	0
AL	0.68	0	0	0.11	0.21	0	NC	0.66	0	0	0.07	0.27	0
AR	0.53	0	0.08	0.09	0.3	0	ND	0.94	0	0	0.06	0	0
AZ	0.49	0	0.05	0.1	0.36	0	NE	0.55	0	0.01	0.05	0.39	0
CA	0	0	0.48	0.16	0.29	0.07	NH	0.23	0.1	0.54	0.07	0.06	0
CO	0.94	0	0.01	0.05	0	0	NJ	0.17	0.03	0.11	0	0.69	0
CT	0.09	0.21	0.01	0.01	0.66	0.02	NM	0.91	0	0.08	0.01	0	0
DC	0	1	0	0	0	0	NV	0.77	0.01	0.12	0.1	0	0
DE	0.61	0.29	0.1	0	0	0	NY	0.22	0.16	0.18	0.23	0.21	0
FL	0.45	0.22	0.14	0	0.19	0	OH	0.89	0	0	0	0.11	0
GA	0.64	0	0	0.05	0.31	0	OK	0.6	0	0.33	0.07	0	0
HI	0	1	0	0	0	0	OR	0.1	0	0	0.76	0.14	0
IA	0.85	0	0.01	0.03	0.11	0	PA	0.62	0.01	0	0.01	0.36	0
ID	0	0	0	1	0	0	PR	0	1	0	0	0	0
IL	0.4	0	0.01	0	0.59	0	RI	0	0.67	0.33	0	0	0
IN	0.98	0	0.01	0.01	0	0	SC	0.33	0	0	0.03	0.64	0
KS	0.7	0	0.04	0	0.26	0	SD	0.41	0	0	0.59	0	0
KY	0.95	0	0	0.05	0	0	TN	0.68	0	0	0.12	0.2	0
LA	0.35	0.01	0.46	0	0.18	0	TX	0.49	0	0.39	0.01	0.11	0
MA	0.33	0.4	0.12	0	0.15	0	UT	0.95	0	0.02	0.02	0	0.01
MD	0.6	0.07	0.02	0.05	0.26	0	VA	0.46	0.03	0.02	0.01	0.48	0
ME	0	0.16	0	0.21	0.63	0	VT	0	0	0.03	0.17	0.79	0.01
MI	0.75	0.01	0.01	0.01	0.22	0	WA	0.12	0	0.01	0.81	0.06	0
MN	0.62	0.02	0.01	0.02	0.32	0.01	WI	0.71	0	0	0.05	0.24	0
MO	0.84	0	0	0.02	0.14	0	WV	0.99	0	0	0.01	0	0
MS	0.39	0.02	0.21	0	0.38	0	WY	0.98	0	0	0.02	0	0

Assumptions for Off-Site electricity Production:

■ Residual oil is assumed in all electricity oil pollution rates.

■ Natural gas was assumed to have 3 lbs of PM/10^6 ft^3 of gas.

■ When performing calculations from the AP-42, electric utilities were assumed to utilize Utility Boilers for oil and gas, while a dry bottom, pulverized coal fired boiler was assumed for all coal burning..

■ Federal Guidelines which apply to PM, SO_2, and NO_x were used as emission factors.

The electrical energy was assumed to be divided equally between the different fossil fuels, nuclear, hydroelectric and others as per the state percentage breakdowns for electricity production. In reality this is not true, since in many cases coal is used to meet the base demand and gas is used in meeting peak demands. Theoretically, gas could dominate the fuel savings on a design day. Thus, due to its lower emission rates, pollution produced could be lower. Also in reality the exact location of the electricity production is not known. At any given time the electric energy could be purchased off of the utility grid and its actual origin is not known. Due to the scope, this complexity was not addressed. For our purpose, the pollution coefficients are adequate for the model to determine average comparisons. Table 36 shows the pollution coefficients that are used by default, listed by state.

Table 36. Pollution Coefficients State by State for Electric Energy Produced Off-Site; All Coefficients are in [kg/J]

State	CO_2	SO_2	NO_x	CO	Hydro Carbon	Part Matter
AK	1.5002149E-07	1.3757523E-10	2.9664658E-10	4.2992258E-11	4.2992258E-12	2.5795355E-11
AL	2.0515476E-07	1.9174547E-09	7.1797071E-10	3.0094581E-11	4.2992258E-12	1.0318142E-10
AR	1.7679706E-07	6.1049007E-10	5.9329316E-10	3.0094581E-11	4.2992258E-12	8.1685291E-11
AZ	1.5650902E-07	3.0524503E-10	5.3310400E-10	2.5795355E-11	4.2992258E-12	7.3086839E-11
CA	8.1534818E-08	3.0524503E-10	1.4187445E-10	2.5795355E-11	0.0000000E+00	0.0000000E+00
CO	2.8533102E-07	9.1573510E-10	9.9742039E-10	4.2992258E-11	8.5984516E-12	1.4187445E-10
CT	8.2742900E-08	1.1092003E-09	1.9346516E-10	1.2897677E-11	4.2992258E-12	4.7291484E-11
DC	2.5644452E-07	2.2785897E-09	4.5141871E-10	5.1590710E-11	8.5984516E-12	1.5047290E-10
DE	2.7575234E-07	2.2785897E-09	8.0395523E-10	4.7291484E-11	8.5984516E-12	1.3757523E-10
FL	2.1948838E-07	1.9174547E-09	6.2768697E-10	3.8693032E-11	4.2992258E-12	1.0318142E-10
GA	1.9610489E-07	1.9174547E-09	6.8787613E-10	3.0094581E-11	4.2992258E-12	9.8882194E-11
HI	2.5644452E-07	3.0524503E-10	4.5141871E-10	5.1590710E-11	8.5984516E-12	1.5047290E-10
IA	2.5817982E-07	2.3612208E-09	9.0055883E-10	3.7575234E-11	6.1908852E-12	1.2824591E-10
ID	0.0000000E+00	1.3757523E-10	0.0000000E+00	0.0000000E+00	0.0000000E+00	0.0000000E+00
IL	1.2241616E-07	2.8890798E-09	4.2562336E-10	1.7196903E-11	4.2992258E-12	6.0189162E-11
IN	2.9739895E-07	2.8890798E-09	1.0361134E-09	4.2992258E-11	8.5984516E-12	1.4617368E-10
KS	2.1812982E-07	2.3602750E-09	7.5236452E-10	3.4393807E-11	4.2992258E-12	1.0748065E-10
KY	2.8661649E-07	1.9174547E-09	1.0017196E-09	4.2992258E-11	8.5984516E-12	1.4187445E-10
LA	1.8795785E-07	6.1049007E-10	5.1160787E-10	4.2992258E-11	4.2992258E-12	5.5889936E-11
MA	2.2295785E-07	1.1092003E-09	5.6749781E-10	4.2992258E-11	8.5984516E-12	1.1177987E-10
MD	2.0244195E-07	2.2785897E-09	6.7067923E-10	3.0094581E-11	4.2992258E-12	1.0318142E-10
ME	4.1031811E-08	1.1092003E-09	7.3086839E-11	8.5984516E-12	0.0000000E+00	2.5795355E-11
MI	2.3057608E-07	2.8890798E-09	7.9965600E-10	3.4393807E-11	4.2992258E-12	1.1607910E-10
MN	1.9693472E-07	2.8889938E-09	6.7730004E-10	2.9019774E-11	4.8151329E-12	9.8108333E-11
MO	2.5041103E-07	2.3612208E-09	8.7644018E-10	3.6113497E-11	6.0189162E-12	1.2519346E-10
MS	1.5620377E-07	1.9174547E-09	4.7291484E-10	3.0094581E-11	4.2992258E-12	6.0189162E-11
MT	2.0214100E-07	9.1573510E-10	7.0937226E-10	3.0094581E-11	4.2992258E-12	1.0318142E-10
NC	1.9912294E-07	1.9174547E-09	6.9647458E-10	3.0094581E-11	4.2992258E-12	9.8882194E-11
ND	2.8359843E-07	9.1573510E-10	9.9312117E-10	4.2992258E-11	8.5984516E-12	1.4187445E-10
NE	1.6766981E-07	2.3602750E-09	5.8469471E-10	2.5795355E-11	4.2992258E-12	8.1685291E-11
NH	9.5035505E-08	1.1092003E-09	2.8813411E-10	1.5004298E-11	2.7085123E-12	4.9785035E-11
NJ	7.8065342E-08	9.4582968E-10	2.2785897E-10	1.7196903E-11	0.0000000E+00	3.0094581E-11
NM	2.8842646E-07	6.1049007E-10	9.8452271E-10	4.2992258E-11	8.5984516E-12	1.3757523E-10

State	CO_2	SO_2	NO_x	CO	Hydro Carbon	Part Matter
NV	2.5870591E-07	3.0524503E-10	8.6414439E-10	4.2992258E-11	4.2992258E-12	1.2037832E-10
NY	1.3863284E-07	9.4582968E-10	3.6113497E-10	3.0094581E-11	4.2992258E-12	6.0189162E-11
OH	2.6851245E-07	2.8890798E-09	9.4153046E-10	3.8693032E-11	8.5984516E-12	1.3327600E-10
OK	2.3826739E-07	6.1049007E-10	7.3516762E-10	4.7291484E-11	4.2992258E-12	9.0283742E-11
OR	2.7153007E-08	1.3890799E-10	9.5055883E-11	3.9122955E-12	6.4488387E-13	1.3585554E-11
PA	1.8961735E-07	2.2785897E-09	6.5778155E-10	2.5795355E-11	4.2992258E-12	9.4582968E-11
PR	2.5644504E-07	9.4449692E-10	4.5253651E-10	5.0042989E-11	1.0404126E-11	1.5085983E-10
RI	2.2906705E-07	1.1092003E-09	4.0412723E-10	5.1590710E-11	8.5984516E-12	1.0318142E-10
SC	9.9561472E-08	1.9174547E-09	3.4823729E-10	1.2897677E-11	4.2992258E-12	5.1590710E-11
SD	1.2369733E-07	9.1573510E-10	4.3422181E-10	1.7196903E-11	4.2992258E-12	6.0189162E-11
TN	2.0214100E-07	1.9174547E-09	7.0937226E-10	3.0094581E-11	4.2992258E-12	1.0318142E-10
TX	2.1549010E-07	6.1049007E-10	6.3628542E-10	4.2992258E-11	4.2992258E-12	7.7386065E-11
UT	2.9309972E-07	9.1573510E-10	1.0189165E-09	4.2992258E-11	8.5984516E-12	1.4617368E-10
VA	1.4994410E-07	2.2785897E-09	5.0730865E-10	2.1496129E-11	4.2992258E-12	7.3086839E-11
VT	5.2043418E-09	1.1092003E-09	9.0713665E-12	1.7626826E-12	8.5984516E-14	1.2897677E-13
WA	3.4922611E-08	1.3757523E-10	1.2037832E-10	4.2992258E-12	0.0000000E+00	1.7196903E-11
WI	2.1420703E-07	2.8889938E-09	7.4974199E-10	3.0911434E-11	5.1590710E-12	1.0709372E-10
WV	2.9868304E-07	2.2785897E-09	1.0453998E-09	4.3121235E-11	7.1797071E-12	1.4935511E-10
WY	2.9566636E-07	9.1573510E-10	1.0361134E-09	4.2992258E-11	8.5984516E-12	1.4617368E-10

Carbon Equivalent

The Intergovernmental Panel on Climate Change has studied the effects on the relative radiative forcing effects of various greenhouse gases. This effect has been called the Global Warming Potential (GWP) and is talked about in terms of Carbon Equivalent. This equivalent is based on a factor of 1.0 for carbon dioxide. This group of gases includes carbon dioxide, nitrous oxide, halocarbon emission, hydrofluorocarbons (HFC's), perfluorocarbons (PFC's), chlorofluorocarbons (CFC's), etc. From stationary combustion sources used in electric production for the heating and cooling of buildings, the only gases of concern are carbon dioxide, carbon monoxide, and nitrous oxide. Carbon monoxide is produced in combustion and its lifetime is relatively short and normally reacts to produce carbon dioxide, but it can't be ignored since it is produced in incomplete combustion and the carbon remains to interact as CO_2. Carbon dioxide and nitrous oxide are first calculated to determine their carbon equivalent and then multiplied by their GWP on a 100 year time frame. The Carbon Equivalents of the following gases have been determined and used in the program are shown in Table 37.

Table 37. Carbon Equivalents

Gas	Carbon Equivalent
CO_2	0.2727
CO	0.4286
NO_x	83.2

The carbon equivalents are shown in the output of the program along with the individual gas pollutants.

References

[1] "Pollution Reduction Through Energy Conservation, REEP Model", Peter G. Stroot, Robert J. Nemeth, & Donald F. Fournier, from USACERL

[2] "AP-42 Compilation of Air Pollutant Emission Factors Volume I: Stationary Point and Area Sources", Supplement D September 1991

[3] 40CFR Chapter 1, Subpart D, Paragraph 60.40, 1990

[4] "Atmospheric Pollution Prediction in a Building Energy Simulation Program", Richard J. Liesen Ph. D., BLAST Support Office, University of Illinois, April, 1997